



The  
University  
Of  
Sheffield.

## **Musculoskeletal Models to Aid in Clinical Decision-Making in Children with Cerebral Palsy**

**Claude Fiifi Hayford**

A thesis submitted in partial fulfilment of the requirements for the degree of  
Doctor of Philosophy

INSIGNEO Institute for in silico Medicine  
Department of Mechanical Engineering  
Faculty of Engineering  
The University of Sheffield

January 2022



## Summary

Clinical decision-making benefits from having accurate and complete information to make objective and justified treatment and surgical intervention recommendations as well as ensuring higher likelihoods of positive outcomes for patients. In Cerebral Palsy (CP), a neurological condition causing movement disability in children, 3D clinical gait analysis provides an important diagnostic and evaluation tool to achieve this to a large extent. It is somewhat limited with regards to certain surgical interventions, particularly when they are complex and involve information that cannot be obtained directly or without the use of invasive measurements. The advent of musculoskeletal (MSK) models have shown that this additional information such as muscle-tendon lengths, moment arms, muscle forces and joint contact forces, can be obtained, while permitting interrogative analysis as well. Although efforts have been made to verify the accuracy and reliability of MSK modelling with regards to the current measures obtained from clinical gait analysis, these methods have not seen much uptake. The general aim of this thesis was therefore to investigate the suitability and use of MSK models to quantify and predict longitudinal changes and surgical intervention outcomes in children with cerebral palsy using an example case of the Femoral Derotation Osteotomy (FDO) and thereby make a case for their use in supporting the clinical decision-making process.

The results from this work showed that generic MSK models can perform as well as currently employed techniques in estimating longitudinal changes over time of clinical measures and outcomes after surgical intervention of FDO. Potential predictors of positive outcome after the FDO from muscle-tendon lengths that are usually not included in the clinical decision-making process were also identified, lending support to the available literature on the utility of musculoskeletal models use in this manner and for clinical gait analysis. Additionally, the results discussed showed that the accuracy of outputs from the generic model can be improved with minimal personalisation although additional work is required to achieve improvements in aspects related to the muscle-tendon parameters.

Future work will be targeted at investigating and validating the identified muscles with predictive value for FDO outcomes as well as improving the personalisation of the bone and muscle-tendon properties using less time and cost intensive techniques such as ultrasound.

## **Acknowledgements**

I would like to thank my supervisors, Professor Claudia Mazzà and Ms. Emma Pratt for the opportunity granted me to pursue this project, for the academic and professional guidance and ultimately for the support and encouragement over the past three and a half years of this PhD. I also wish to acknowledge my colleagues, both past and present from the MSK and IMSB group at INSIGNEO, especially Erica, Bart, Lorenza, Kirsty, Tecla, Eloise, Will, Alex and Linda. Thank you for being my community. Also, to the team at the Sheffield Children's Hospital Gait Analysis Laboratory.

Finally, to my family and friends for the unflinching belief, encouragement and support.

This experience would not have been possible without a scholarship nomination from the University of Ghana and funding from the Commonwealth Scholarship Commission and the University of Sheffield.

# Publications

## Refereed Journals

### In Print

1. **C.F. Hayford**, E. Montefiori, E. Pratt, C. Mazzà, "Predicting Longitudinal Changes in Joint Contact Forces in a Juvenile Population: Scaled Generic Versus Subject-Specific Musculoskeletal Models", *CMBBE* (2020) doi: 10.1080/10255842.2020.1783659
2. **C. F. Hayford**, E. Pratt, J. P. Cashman, O. G. Evans, and C. Mazzà, "Effectiveness of Global Optimisation and Direct Kinematics in Predicting Surgical Outcome in Children with Cerebral Palsy," *Life*, vol. 11, no. 12, p. 1306, 2021, doi:10.3390/life11121306
3. E. Montefiori, **C. F. Hayford**, and C. Mazzà, "Variations of lower-limb joint kinematics associated with the use of different ankle joint models," *Journal of Biomechanics*, vol. 136, p. 111072, 2022/05/01/ 2022, doi: <https://doi.org/10.1016/j.jbiomech.2022.111072>

### In Preparation

1. **C. F. Hayford**, E. Pratt, J. P. Cashman, O. G. Evans, and C. Mazzà, "The role of pre-surgery muscle-tendon lengths on the outcome of Femoral Derotation Osteotomy".

## Conference abstracts

### Oral presentations

1. **C.F. Hayford**, E. Montefiori, E. Pratt, C. Mazzà, "Suitability of Scaled Generic Musculoskeletal Models in Predicting Longitudinal Changes in Joint Contact Forces in Children with Juvenile Idiopathic Arthritis," *CompBioMed* 2019, September (2019)
2. **C.F. Hayford**, E. Montefiori, E. Pratt, C. Mazzà, "Evaluation of a Scaled Generic Musculoskeletal Model for Estimating Joint Reactions during Normal Gait in Children," *BioMedEng19*, Imperial College, September (2019) – Received a Versus Arthritis Travel Award
3. **C.F. Hayford**, E. Pratt, J.P. Cashman, O.G. Evans, C. Mazzà, Towards Musculoskeletal Model Use in the Clinic: Assessing the Kinematics-based Clinical GPS Measure in Cerebral Palsy, *BioMedEng2021*, September 2021.

### Poster presentations

1. **C.F. Hayford**, E. Montefiori, E. Pratt, C. Mazzà, "Evaluation of a Scaled Generic Musculoskeletal Model for Estimating Joint Reactions during Normal Gait in Children, *Insigneo Showcase* 2019, Sheffield, (2019)
2. **C.F. Hayford**, E. Pratt, C. Mazzà, Musculoskeletal Models for Assessing Surgical Indications and Outcomes in Cerebral Palsy, *XXVIII Congress of the International Society of Biomechanics*, July 2021.
3. **C.F. Hayford**, E. Pratt, J.P. Cashman, O.G. Evans, C. Mazzà, Predicting Clinical Judgement of Surgical Outcome in Cerebral Palsy using a Gait Profile Score Computed from Multibody Optimisation Kinematics, *Virtual ESMAC* 2021, September 2021.

# Table of Contents

Summary.....	iii
Acknowledgements.....	iv
Publications.....	v
Table of Contents.....	vi
Nomenclature.....	xi
List of Tables.....	xii
Table of Figures .....	xiii
Declaration .....	xvii
1. Overview.....	1
1.1 Introduction .....	2
1.2 Thesis outline.....	3
1.3 References.....	5
2 Background .....	8
2.1 Cerebral Palsy.....	9
2.1.1 Anatomical and Functional Classifications of CP .....	9
2.1.2 Treatment Options.....	10
2.2 Femoral Anteversion and Excessive Internal Rotation Gait.....	11
2.2.1 Clinical Assessment of Excessive Femoral Anteversion .....	12
2.3 Femoral Derotation Osteotomies.....	14
2.3.1 Outcome Measures of FDO and Recurrence of IHR.....	15
2.3.2 Risk factors for recurrence after FDO .....	15
2.4 Clinical Gait Analysis.....	16
2.4.1 Instrumented CGA.....	16
2.5 Musculoskeletal Modelling.....	18

2.5.1	Generic Musculoskeletal Models .....	20
2.5.2	Subject-Specific Musculoskeletal Models .....	20
2.5.3	Biomechanical model simulation.....	21
2.5.4	Inverse Dynamics .....	22
2.5.5	Static Optimisation.....	23
2.5.6	Joint Reaction Analysis.....	24
2.5.7	Musculoskeletal Modelling and Simulation in CP.....	25
2.6	Aim and objectives.....	26
2.7	References.....	29
3	Effect of lower limb marker set on musculoskeletal model predictions of joint kinematics in a juvenile population.....	39
3.1	Summary.....	40
3.2	Introduction .....	40
3.3	Methods.....	42
3.3.1	Participants and data collection.....	42
3.3.2	Scaled generic kinematic skeletal model.....	42
3.3.3	Image-based kinematic skeletal model.....	43
3.3.4	Simulation and data analysis.....	43
3.4	Results.....	45
3.5	Discussion .....	52
3.6	Conclusion.....	54
3.7	References.....	55
4	Effectiveness of global optimisation and direct kinematics in predicting surgical outcome in children with cerebral palsy.....	59
4.1	Abstract.....	61
4.2	Introduction .....	61

4.3	Methods.....	63
4.3.1	Data description.....	63
4.3.2	Calculation of the joint kinematics.....	64
4.3.3	Data analysis.....	65
4.3.4	Results.....	67
4.4	Discussion.....	71
4.5	Conclusion.....	74
4.6	References.....	75
5	Role of pre-surgery muscle-tendon lengths on the outcome of femoral derotation osteotomy.....	79
5.1	Introduction.....	80
5.2	Methods.....	82
5.2.1	Data and statistical analysis.....	82
5.3	Results.....	85
5.4	Discussion.....	88
5.5	Conclusion.....	90
5.6	References.....	91
6	Predicting longitudinal changes in joint contact forces in a juvenile population: scaled generic versus subject-specific musculoskeletal models.....	95
6.1	Abstract.....	97
6.2	Introduction.....	97
6.3	Materials and methods.....	98
6.3.1	Data collection.....	98
6.3.2	Modelling approaches.....	99
6.3.3	Differences between Gen and SubS models.....	100
6.3.4	Consistency in longitudinal predictions.....	101



6.4	Results.....	102
6.5	Discussion .....	106
6.6	Conclusion .....	109
6.7	Acknowledgements .....	109
6.8	References.....	110
7	Effects of statistical shape modelling-based personalisation of musculoskeletal models on muscle-tendon length and moment arm length estimates during gait.....	114
7.1	Summary.....	115
7.2	Introduction .....	115
7.3	Materials and methods.....	116
7.3.1	Participants.....	116
7.3.2	Motion capture and magnetic resonance imaging .....	117
7.3.3	Musculoskeletal modelling.....	117
7.3.4	Data processing.....	119
7.3.5	Data and statistical analysis.....	120
7.4	Results.....	121
7.4.1	Bone geometry similarity .....	121
7.4.2	Segment length and inter-HJC.....	121
7.4.3	Muscle attachments' location.....	122
7.4.4	Muscle-tendon length and moment arm length.....	124
7.4.5	Joint kinematics.....	127
7.5	Discussion .....	130
7.6	Conclusion .....	132
7.7	References.....	133
8	General discussion .....	136

8.1	Summary .....	137
8.2	Discussion .....	138
8.3	Limitations .....	140
8.4	Future work.....	141
8.5	Conclusion .....	142
8.6	References.....	143
Appendix 1 - Chapter 4 supplemental material .....		147
Appendix 2 - Chapter 5 supplemental material .....		151
Appendix 3 - Chapter 6 supplemental material .....		154
Appendix 4 - Chapter 7 supplemental material .....		157

## Nomenclature

CP	Cerebral Palsy
FDO	Femoral Derotation Osteotomy
GMFCS	Gross Motor Function Classification System
CGA	Clinical Gait Analysis
MSK	Musculoskeletal
IK	Inverse Kinematics
ID	Inverse Dynamics
JIA	Juvenile Idiopathic Arthritis
GPS	Gait Profile Score
GVS	Gait Variable Score
MRI	Magnetic Resonance Imaging
PiG	PlugIn Gait
BW	Body Weight
JCF	Joint Contact Force
MTL	Muscle-tendon Length
RMSD	Root Mean Square Difference
R <sup>2</sup>	Coefficient of determination
SEMLS	Single Event Multi Level Surgery
TD	Typically Developed
KAD	Knee Alignment Device
SSM	Statistical Shape Model

## List of Tables

Table 3.1 Summary of markers used in static pose estimation and inverse kinematics. .....	44
Table 3.2 Correlation between static pose estimates between generic and MR model for the four marker pipelines.....	46
Table 4.1 Anthropometric details for the TD cohort subgroups.....	64
Table 5.1 Post-surgery change in $MTL_{max}$ (mean (SD)) for RS and NR groups.....	87
Table 6.1 Inter-model analysis of gait waveform profile at M0 and M12.....	103
Table 6.2 Inter-model differences in participant estimates at M0 .....	105
Table 6.3 Inter-model differences in participant estimates at M12 .....	105
Table 6.4 Agreement in longitudinal changes (M12 - M0) in selected metrics between Gen and SubS predictions of JCF for each of 11 participants. ....	106
Table 7.1 Comparison of $MTL_{max}$ and average MAL between MRb, SGn and SMb for muscles with hip ab/adduction function.....	126
Table 7.2 Maximum absolute difference (Mean (SD)) in MAL between estimates from SMb and SGn with respect to MRb. ....	128

## Table of Figures

Figure 2.1 Illustration of excessive femoral anteversion (B) and intoeing of the lower extremity (C). Image adapted from <https://clinicalgate.com/hip-5/>.....12

Figure 2.2 Trochanteric Prominence Angle Test (A, Image adapted from [30]) and an illustration of the midpoint of hip rotation passive range of motion measurement (B, Image adapted from [32]). .....13

Figure 2.3 Definition of the Plug-In Gait Model from experimental marker trajectories .....17

Figure 2.4 Schematic of the Hill-type model of the muscle-tendon unit adapted from [69] showing a contractile element (CE) and two passive elastic elements (DE and SE). LMT- muscle-tendon length, LM – muscle fibre length, LT – tendon length,  $\alpha$  – muscle pennation angle. .... 19

Figure 3.1 Inter-model comparison of static pose angles for the four marker sets. \*\*\*p < 0.01 .....46

Figure 3.2 RMSD between MRI-based and Gen models for all four marker set configurations. Horizontal bars indicate significant difference between marker pipelines ..... 47

Figure 3.3 Mean root mean square differences for the comparison of joint kinematics between M1 and three other marker sets (M2, M3, and M4) for the MRI-based and scaled generic models..... 47

Figure 3.4 Kinematic waveform comparison between MR and Generic models for the M1 marker set. Black bars indicate significant difference between the two model estimates..... 48

Figure 3.5 Kinematic waveform comparison between MR and Generic models for the M2 marker set. Black bars indicate significant difference between the two model estimates.....49

Figure 3.6 Kinematic waveform comparison between MR and Generic models for the M3 marker set. Black bars indicate significant difference between the two model estimates.....49

Figure 3.7 Kinematic waveform comparison between MR and Generic models for the M4 pipeline. Black bars indicate significant difference between the two model estimates..... 50

Figure 3.8 Kinematic curves showing differences due to markers used in IK for the generic model. Black bars indicate statistical significance between marker pipelines. ....51

Figure 3.9 Kinematic curves showing differences due to markers used in IK for the MRI model. Black bars indicate statistical significance between marker pipelines .....51

Figure 4.1 Flowchart showing workflow of analysis .....64

Figure 4.2 Box plot of knee flexion axis corrections estimated from the KAD and applied to mGen for the TD and CP participants. p-values indicate significant differences as highlighted by a post-hoc Dunn’s multiple comparison test comparing TD, CP pre and CP post..... 68

Figure 4.3 Mean joint kinematic waveforms for 68 limbs from 34 TD participants estimated with PiG and mGen models. Shaded bands indicate 1SD with significant difference shown by bottom black bars..... 68

Figure 4.4 Distribution of RMSD of joint kinematics between PiG and mGen models for TD participants. Bars represent median and interquartile range. Dotted line at 5° represents clinically acceptable threshold of data error [29]. .....69

Figure 4.5 Correlation between the GPS estimated with PiG and mGen for all subject limbs and observations. ....70

Figure 4.6 Bland-Altman plot of changes in GPS estimated by PiG and mGen. Solid and dotted lines represent the mean difference and limits of agreement, respectively....70

Figure 4.7 Agreement of clinical classification of CP participants after surgery with PiG and mGen-based classification from GPS values for 41 limbs analysed. The boxes represent the three cases where there was a difference (values within box) between model predictions of outcome with similar coloured arrows pointing to the prediction from mGen and PiG..... 71

Figure 5.1 Classification of muscles as long or short with respect to the controls (TD). Maximum MTL achieved over the gait cycle (A). Colour scale indicating the magnitude of deviation of a CP group muscle from the TD maximum values (B).....83

Figure 5.2 Correlation between generic (Gen) and subject-specific (MR) estimates of  $MTL_{max}$  for each segment per muscle and as the average of muscle segment values.84

Figure 5.3 Example of muscle-tendon lengths over the gait cycle for a CP participant before and after FDO-SEMLS .....85

Figure 5.4 Heatmap showing classification of CP cohort hip ab/adductor muscles as longer or shorter than TD before and after FDO-SEMLS. Muscle abbreviations are adductor brevis (add.brev), adductor longus (add.long), adductor magnus (add.mag), gluteus medius (glut.med), gluteus minimus (glut.min), gracilis (grac), pectoralis (pect), quadratus femoris (quad.fem) and sartorius (sar). FA18 had no 3D data for post-intervention (grey)..... 86

Figure 5.5  $MTL_{max}$  distribution and comparison between RS and NR groups of the CP cohort at pre- and post- FDO-SEMLS. Blue bands indicate statistically significant differences between pre and post lengths for the RS group. \*Significant difference between RS and NR pre-surgery.....87

Figure 5.6 Pre/post-surgery comparison of  $MTL_{max}$  values for RS group who had only the FDO. Plots for NR not shown due to low sample size (n=2). Blue bands indicate statistically significant differences between pre and post  $MTL_{max}$ ..... 88

Figure 6.1 Comparison between Gen (red) and SubS (blue) model estimations of joint contact forces at observations M0 and M12. Black bars indicate region of gait cycle with significant statistical difference between the two models at  $P < 0.01$ . .....102

Figure 6.2 Boxplot distribution of P1 and P2 JCF estimates for scaled generic and subject-specific models at two observations, M0 and M12. \* indicates significant difference at  $P < 0.05$ .....104

Figure 6.3 Boxplot distribution of overall joint loading estimates calculated as area under BW-normalised JCF curve. AUC expressed as  $BW * \%Gait\ Cycle$  (BW.%c) .....104

Figure 7.1 Joint scans for SMb model generation. Green shaded regions indicate the bone sections selected from the complete MRI image and used. .... 119

Figure 7.2 Body segment similarity between MR and SM derived bone geometries. . 121

Figure 7.3 Comparison of the femur length and inter-HJC measurements between SMb, SGn and MRb..... 122

Figure 7.4 Example of MRb, SMB and SGn bone geometries for one participant model. Models were aligned at the pelvis origin ..... 123

Figure 7.5 Anterior, lateral and posterior views of aligned SMB, SGn and MRb models of a participant highlighting bone and muscle geometry differences ..... 123

Figure 7.6 Difference in 3D location of origin and insertion points for hip adductors in SGn and SMb with respect to MRb. .... 124

Figure 7.7 MTL differences between models for hip ab/adduction muscles..... 127



## **Declaration**

*I, Claude Fiifi Hayford, confirm that the Thesis is my own work. I am aware of the University's Guidance on the Use of Unfair Means (<http://www.sheffield.ac.uk/ssid/unfair-means>). This work has not previously been presented for an award at this, or any other, university and constitutes my own research while enrolled as a PhD student between September 2018 and December 2021. Aspects of the work presented were supported by the UK EPSRC (Multisim project. Grant number: EP/K03877X/1).*

# 1. Overview

## 1.1 Introduction

Movement forms an integral aspect of human life and when this is curtailed either by accident or pathology, the quality of life of the individual is affected. Such is the case in Cerebral Palsy (CP), a group of disorders affecting movement and coordination that arises from a non-progressive injury to the developing brain [1]. CP is estimated to occur in 2 out of every 1000 live births [2]. The injury to the brain affects motor control, muscle tone and function which can lead to musculoskeletal deformities. These issues, together, contribute to the development of an abnormal gait.

A common abnormal gait feature presenting in individuals with CP is an internal rotation gait [3]. This internal rotation gait is characterised by transverse plane gait deviations such as internal hip rotation, a medial orientation of the knee and/or long axis of the foot (in-toeing) with respect to the direction of travel [4]. The internal rotation gait may be caused by an excessive femoral anteversion (defined by an excessively anteriorly angled femoral head and neck) or torsions within the long bones of the lower limb [5]. As with most pathologies, different strategies exist to attempt to restore movement functionality, ranging from invasive approaches such as surgery or less intrusive mechanisms such as physiotherapy [6]. In the case of the excessive femoral anteversion, a surgical intervention known as a Femoral Derotation Osteotomy is the preferred standard [7, 8]. To understand and quantify these gait deviations, different clinical measures and tools are used, enabling an objective analysis and basis for making the clinical decisions for treatment. Clinical gait analysis provides a means for understanding and quantifying the effect of human movement disorders and any interventions that may be applied [9].

Although outcomes of the FDO are generally reported to be positive, there are also reports of negative outcomes and recurrence of the internal rotation gait [10-14]. What predisposes individuals with CP to not benefiting from the intervention is however unclear although a number of studies point to certain risk factors that can be used in aid the decision-making process [15, 16]. That notwithstanding, these factors are based primarily on clinical measures and outputs from gait analysis (kinematics and kinetics). Other information that could be informative such as the functioning of the muscles (muscle length, moment arms and generated forces) and joint loads are however not easy to measure experimentally or would require invasive processes to measure.

In recent times, computational modelling and simulation have been developed that permit the use of data from gait analysis to investigate these variables not easily accessible to the clinician [17]. In CP, these models and simulation outputs have been used to understand factors that contribute to the abnormal gait [18, 19], the influence of the abnormal gait on joint loading [20, 21], as well as to optimise and interrogate the

effect of treatment options [22-24]. The insights gained from the use of these computational methods bode well for the application of these methods to the issue of outcomes after FDO and potentially help with the identification of persons most likely to benefit from this intervention.

The general aim of this thesis was therefore to investigate the ability of musculoskeletal models to estimate changes in clinical measures after intervention and to identify potential indicators for these interventions to aid in the clinical decision-making process using retrospective data of children with CP.

## **1.2 Thesis outline**

This exploration of the subject matter in this thesis is organised into eight chapters, each providing insights of different aspects of the challenge of using musculoskeletal models to aid in clinical decision-making and predicting outcome after FDO, as summarised below.

Chapter 1 is an overview of the thesis and how it is structured.

Chapter 2 provides a review of the literature, giving the clinical context and justification as well as the theoretical background on which the methods applied in this thesis are based. It also situates the research in the larger context of clinical decision-making and the need to improve outcomes. The aim and objectives of the thesis are also specified.

Chapter 3 focusses on the joint kinematics estimated by the musculoskeletal models and the influence of experimental and modelling choices on simulation outputs. It examines the influence of number of markers on estimates of joint angles and the sensitivity of kinematic outputs to marker set and choice of skeletal model type, that is generic or subject-specific model.

In Chapter 4, the application of a generic musculoskeletal model to determine outcomes of FDO in children with CP is reported. It describes the use of a global optimisation-based estimate of a clinical measure to determine surgical outcomes and how this compares to the performance of the traditional approach used in clinical settings. This is based on the published paper: "Effectiveness of global optimisation and direct kinematics in predicting surgical outcome in children with cerebral palsy" [25].

Chapter 5 follows on from the results of the previous chapter to extend the analysis to identifying the potential role of pre-surgical muscle-tendon lengths on predicting the outcomes of the FDO.

Chapter 6 also based on a published paper [26], "Predicting longitudinal changes in joint contact forces in a juvenile population: scaled generic versus subject-specific musculoskeletal models", examines the utility of generic models in estimating

longitudinal changes in gait and the trade-offs compared to using a model with increased subject-specific details.

Chapter 7 reports on preliminary work, based on insights from the previous chapters, exploring the gains to be had with moving from a generic model to a fully subject-specific model with the intention of testing the limits of how much subject specificity is required to achieve good enough estimates of biomechanical parameters for use in the clinical decision-making process.

Chapter 8 provides a summary of the studies undertaken as part of this thesis as well as discussing the implications for the use of musculoskeletal models in the clinical decision-making process.

### 1.3 References

- [1] M. Bax *et al.*, "Proposed definition and classification of cerebral palsy, April 2005," *Dev Med Child Neurol*, vol. 47, no. 8, pp. 571-6, Aug 2005, doi: 10.1017/s001216220500112x.
- [2] M. Oskoui, F. Coutinho, J. Dykeman, N. Jette, and T. Pringsheim, "An update on the prevalence of cerebral palsy: a systematic review and meta-analysis," *Dev Med Child Neurol*, vol. 55, no. 6, pp. 509-19, Jun 2013, doi: 10.1111/dmcn.12080.
- [3] T. A. L. Wren, S. Rethlefsen, and R. M. Kay, "Prevalence of Specific Gait Abnormalities in Children With Cerebral Palsy: Influence of Cerebral Palsy Subtype, Age, and Previous Surgery," *Journal of Pediatric Orthopaedics*, vol. 25, no. 1, pp. 79-83, 2005. [Online]. Available: [https://journals.lww.com/pedorthopaedics/Fulltext/2005/01000/Prevalence\\_of\\_Specific\\_Gait\\_Abnormalities\\_in.18.aspx](https://journals.lww.com/pedorthopaedics/Fulltext/2005/01000/Prevalence_of_Specific_Gait_Abnormalities_in.18.aspx).
- [4] S. Ounpuu, P. DeLuca, R. Davis, and M. Romness, "Long-term effects of femoral derotation osteotomies: an evaluation using three-dimensional gait analysis," (in eng), *J Pediatr Orthop*, vol. 22, no. 2, pp. 139-45, Mar-Apr 2002.
- [5] S. A. Rethlefsen, B. S. Healy, T. A. Wren, D. L. Skaggs, and R. M. Kay, "Causes of intoeing gait in children with cerebral palsy," (in eng), *J Bone Joint Surg Am*, vol. 88, no. 10, pp. 2175-80, Oct 2006, doi: 10.2106/jbjs.E.01280.
- [6] J. R. Gage, M. H. Schwartz, S. E. Koop, and T. F. Novacheck, *The Identification and Treatment of Gait Problems in Cerebral Palsy*. Wiley, 2009.
- [7] T. Dreher, S. Wolf, F. Braatz, D. Patikas, and L. Doderlein, "Internal rotation gait in spastic diplegia--critical considerations for the femoral derotation osteotomy," *Gait & posture*, vol. 26, no. 1, pp. 25-31, Jun 2007, doi: 10.1016/j.gaitpost.2006.07.018.
- [8] M. Pirpiris, A. Trivett, R. Baker, J. Rodda, G. R. Nattrass, and H. K. Graham, "Femoral derotation osteotomy in spastic diplegia. Proximal or distal?," (in eng), *The Journal of bone and joint surgery. British volume*, vol. 85, no. 2, pp. 265-72, Mar 2003, doi: 10.1302/0301-620x.85b2.13342.
- [9] S. Armand, G. Decoulon, and A. Bonnefoy-Mazure, "Gait analysis in children with cerebral palsy," *EFORT Open Rev*, vol. 1, no. 12, pp. 448-460, Dec 2016, doi: 10.1302/2058-5241.1.000052.
- [10] C. Church *et al.*, "Persistence and Recurrence Following Femoral Derotational Osteotomy in Ambulatory Children With Cerebral Palsy," *J Pediatr Orthop*, vol. 37, no. 7, pp. 447-453, Oct/Nov 2017, doi: 10.1097/BPO.0000000000000701.
- [11] E. Boyer, T. F. Novacheck, A. Rozumalski, and M. H. Schwartz, "Long-term changes in femoral anteversion and hip rotation following femoral derotational osteotomy in children with cerebral palsy," *Gait & posture*, vol. 50, pp. 223-228, Oct 2016, doi: 10.1016/j.gaitpost.2016.09.004.
- [12] H. Kim, M. Aiona, and M. Sussman, "Recurrence after femoral derotational osteotomy in cerebral palsy," *J Pediatr Orthop*, vol. 25, no. 6, pp. 739-43, Nov-Dec 2005, doi: 10.1097/01.bpo.0000173304.34172.06.

- [13] M. Niklasch, M. C. Klotz, S. I. Wolf, and T. Dreher, "Long-term development of overcorrection after femoral derotation osteotomy in children with cerebral palsy," *Gait & posture*, vol. 61, pp. 183-187, Mar 2018, doi: 10.1016/j.gaitpost.2018.01.012.
- [14] R. O'Sullivan and D. Kiernan, "Recurrent internal hip rotation gait in cerebral palsy: Case reports of two patients," *HRB Open Res*, vol. 1, no. 28, p. 28, 2018, doi: 10.12688/hrbopenres.12893.2.
- [15] M. Niklasch *et al.*, "Factors associated with recurrence after femoral derotation osteotomy in cerebral palsy," *Gait & posture*, vol. 42, no. 4, pp. 460-5, Oct 2015, doi: 10.1016/j.gaitpost.2015.07.059.
- [16] M. H. Schwartz, A. Rozumalski, and T. F. Novacheck, "Femoral derotational osteotomy: surgical indications and outcomes in children with cerebral palsy," *Gait & posture*, vol. 39, no. 2, pp. 778-83, Feb 2014, doi: 10.1016/j.gaitpost.2013.10.016.
- [17] M. Wesseling, E. C. Ranz, and I. Jonkers, "Objectifying Treatment Outcomes Using Musculoskeletal Modelling-Based Simulations of Motion," in *Handbook of Human Motion*, B. Müller *et al.* Eds. Cham: Springer International Publishing, 2018, ch. Chapter 52-1, pp. 1-25.
- [18] A. S. Arnold, A. V. Komattu, and S. L. Delp, "Internal rotation gait: a compensatory mechanism to restore abduction capacity decreased by bone deformity," (in eng), *Dev Med Child Neurol*, vol. 39, no. 1, pp. 40-4, Jan 1997, doi: 10.1111/j.1469-8749.1997.tb08202.x.
- [19] S. L. Delp, A. S. Arnold, R. A. Speers, and C. A. Moore, "Hamstrings and psoas lengths during normal and crouch gait: Implications for muscle-tendon surgery," *Journal of Orthopaedic Research*, vol. 14, no. 1, pp. 144-151, 1996, doi: <https://doi.org/10.1002/jor.1100140123>.
- [20] A. Carriero *et al.*, "Influence of altered gait patterns on the hip joint contact forces," (in English), *Comput Method Biomech*, vol. 17, no. 4, pp. 352-9, Mar 12 2014, doi: 10.1080/10255842.2012.683575.
- [21] K. M. Steele, M. S. Demers, M. H. Schwartz, and S. L. Delp, "Compressive tibiofemoral force during crouch gait," (in English), *Gait & posture*, vol. 35, no. 4, pp. 556-60, Apr 2012, doi: 10.1016/j.gaitpost.2011.11.023.
- [22] A. S. Arnold, M. Q. Liu, M. H. Schwartz, S. Ounpuu, L. S. Dias, and S. L. Delp, "Do the hamstrings operate at increased muscle-tendon lengths and velocities after surgical lengthening?" *J Biomech*, vol. 39, no. 8, pp. 1498-506, 2006, doi: 10.1016/j.jbiomech.2005.03.026.
- [23] A. Rajagopal, Ł. Kidziński, A. S. McGlaughlin, J. L. Hicks, S. L. Delp, and M. H. Schwartz, "Pre-operative gastrocnemius lengths in gait predict outcomes following gastrocnemius lengthening surgery in children with cerebral palsy," *PLOS ONE*, vol. 15, no. 6, p. e0233706, 2020, doi: 10.1371/journal.pone.0233706.
- [24] F. De Groote *et al.*, "SimCP: A Simulation Platform to Predict Gait Performance Following Orthopedic Intervention in Children with Cerebral Palsy," Cham, 2019:

Springer International Publishing, in *Wearable Robotics: Challenges and Trends*, pp. 267-270.

- [25] C. F. Hayford, E. Pratt, J. P. Cashman, O. G. Evans, and C. Mazza, "Effectiveness of Global Optimisation and Direct Kinematics in Predicting Surgical Outcome in Children with Cerebral Palsy," *Life (Basel)*, vol. 11, no. 12, p. 1306, Nov 27 2021, doi: 10.3390/life11121306.
- [26] C. F. Hayford, E. Montefiori, E. Pratt, and C. Mazza, "Predicting longitudinal changes in joint contact forces in a juvenile population: scaled generic versus subject-specific musculoskeletal models," *Comput Method Biomec*, pp. 1-12, Jun 26 2020, doi: 10.1080/10255842.2020.1783659.



## 2 Background

## **2.1 Cerebral Palsy**

Cerebral Palsy (CP) is a term used to refer to a group of disorders that affect movement and posture. It is the commonest physical disability in childhood with an estimated prevalence of 2.11 per 1000 live births [1]. The literature abounds with several different causes but allude to a non-progressive injury to the brain of the infant before, during and immediately after birth. The initial injury to the child does not change but its effect on the musculoskeletal system can be progressive with the growth of the child. The motor function deficits associated with the disorder are usually identified within the first 18 months of the child's life [2]. When the cause was before or during birth, it is known as congenital CP. However, when the cause of the disorder occurs 28 days after birth it is referred to as acquired CP. CP is usually characterised by deficiencies in motor movement, cognitive development and speech ability.

### **2.1.1 Anatomical and Functional Classifications of CP**

While CP is the general name used to refer to this disorder, there exists a spectrum of severity of the condition ranging from very mild to extremely debilitating. Children affected by CP exhibit a range of abilities with some requiring very little assistance in activities of daily living and some others incapable of doing anything on their own. Clinically, CP has been categorised into distinct groups based on the qualities of the patient. It is however important to note that the condition is a spectrum and thus a patient classified into a particular group may still exhibit characteristics of another group, although to a different degree. The currently used classifications are mainly based on anatomy of the condition in terms of the part of the body affected or on its effect on the function of the patient.

There are three main classes based on the anatomical classification of CP. These anatomical classifications specify the nature of the condition that leads to its observed features. They are namely ataxic, dyskinetic and spastic CP. Ataxic CP is defined by the lack of balance and coordination in the affected part of the patient. Dyskinetic CP is characterised by the lack of neuromuscular control, and spastic CP, the most common form of CP with 70-80% of all cases [3], the tightening of muscle. Patients can have a combination of features from the three groups and this is referred to as mixed CP. Under these classifications can be found subcategories that are based on the part of the body affected namely monoplegia, hemiplegia, diplegia and quadriplegia. Monoplegia is the case where the condition affects any single limb of the patient. This could be the left lower limb or the right upper limb. In diplegia, any two symmetrical limbs are affected such as the two upper limbs or the two lower limbs. The side of the

body affected by the condition is the basis on which a patient may be classified as having hemiplegic CP. In quadriplegia, all four limbs of the patient are affected.

The functional classification of CP is based on the patient's ability to perform different specified activities, the level of independence/support required and the extent of ambulation. This classification is known as the Gross Motor Function Classification System (GMFCS) [4] and this puts CP patients into five classes; I, II, III, IV and V. Those in the last two classes have no ambulatory capacity and rely on assist devices and physical support to perform any activities. Further details of the functional classes can be found in [4].

The above descriptions and classifications of CP highlight the different possible combinations of features a patient can present, secondary to the primary injury. There is therefore a wide range of impairment and levels of severity that must be objectively assessed by the physician, making it an important point to be able to tailor treatment as much as possible for each patient for best outcomes.

### **2.1.2 Treatment Options**

Cerebral Palsy is a condition that cannot be cured but only managed to improve the quality of life of the patient. Depending on the severity and manifestation of neuromuscular control deficit, different treatment options are proffered with physical therapy the most common. The aim of most physical therapy is to improve range of motion, muscle strength, balance and coordination of the patient's limbs [5, 6]. As standalone or in conjunction with the physical therapy, medications and the use of orthotics may also be prescribed to alleviate the pain and some of the symptoms associated with the disorder [5]. A common pharmacologic intervention used to facilitate muscle stretching by decreasing the muscle spasticity in persons with CP are Botulinum toxin injections [7, 8].

In certain instances where indications warrant, surgery may be performed although the frequency of surgery may be influenced by severity or institutional treatment practices [9, 10]. One study reports up to 90% of adults with CP having undergone at least one surgery over a 5-year period [11]. Surgical interventions comprise both bone and soft tissue surgeries to address bony deformities and contractures, respectively. These surgical interventions are often undertaken in one session in what is termed a single event multi-level surgery (SEMLS) to reduce hospital attendance for surgical intervention and rehabilitation episodes [12, 13]. Surgical interventions include selective dorsal rhizotomy (to reduce spasticity in muscle [14]), derotation osteotomies (to correct rotational deformities in long bones and lever-arm dysfunction [15, 16]), muscle lengthening, tendon transfers and joint stabilisations (to

facilitate satisfactory joint positioning without restrictions during gait [5]). One of these bony corrections, the femoral derotation osteotomy, would be the focus of this thesis.

The challenge with all these however is the fact that the type and combination of interventions given can be subjective depending on the knowledge and experience of the treating physician [17] with no standardized protocols for determining which surgeries a patient should receive [18]. Additionally, and in the context of SEMLS, there is the issue of confounding, where for example a correction of a rotational deformity of a bone can influence the effect of a muscle lengthening, thereby producing an overall deleterious effect on the biomechanical function of the patient. While advances have been made to help improve clinical decision making such as the use of clinical gait analysis which helps to highlight the gait deviations that should be targeted for treatment [19, 20], there is still room for improvement. For instance, knowledge of muscle length and velocity during dynamic activity would be useful information to guide decision-making with regards to muscle lengthening [5, 21, 22], however this is not currently obtained from traditional gait analysis.

## **2.2 Femoral Anteversion and Excessive Internal Rotation Gait**

Muscle imbalances such as abnormal muscle tone account for most of the musculoskeletal deformities that are associated with cerebral palsy. These muscle imbalances arising from either increased muscle activity or spasticity modify the normal mechanical forces that are exerted on bony geometries and lead to the deformation of the skeletal structures as the individual grows [23] especially when not corrected early on. Excessive femoral anteversion is one of such common deformities in children with cerebral palsy [24] that arises with a more anteriorly angled femoral head and neck than normal. The normal anteversion which defines the angle between the plane that divides the femoral neck symmetrically and the plane that runs parallel to the femoral shaft and divides both lateral and medial knee condyles has a normative value of 15-20° [25]. An increase from this normative range is what is termed excessive anteversion (Figure 2.1). The excessive anteversion results in a lever arm dysfunction which in this case is a reduction in the moment arms of the hip abductors in the frontal plane leading to the development of an abnormal gait [26].

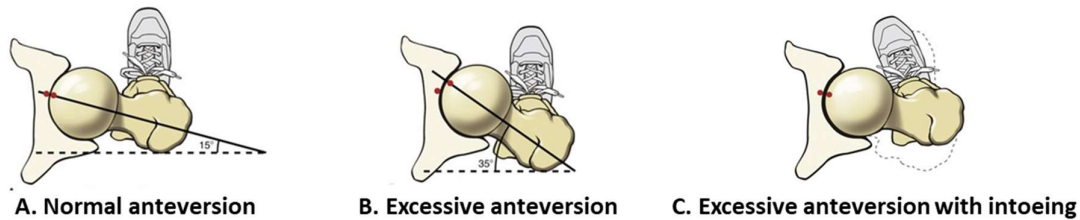


**Figure 2.1 Illustration of excessive femoral anteversion (B) and intoeing of the lower extremity (C). Image adapted from <https://clinicalgate.com/hip-5/>**

The development of an abnormal gait seeks to restore the moment capacity of affected muscles. This abnormal gait is observed as an internal rotation gait (IRG) characterised by an excessive internal hip rotation (IHR) during the stance phase of gait and intoeing of the lower extremity as shown in Figure 2.1 above. The intoeing can lead to tripping and clumsiness during physical activity and in the long term, pathology such as hip joint arthrosis and patella instability [27].

While excessive femoral anteversion of as high as  $40^\circ$  can be present in typically developing children [24], this is expected to resolve to normal as they grow up and is not attributed to muscle imbalances. In a study by Arnold, et al. [28] which sought to test the hypothesis that internal rotation gait is a mechanism to compensate for the increased femoral anteversion, an increased internal hip rotation angle was shown to restore the moment arms of the gluteus medius and therefore its abduction capacity. In addition, muscle abduction capacities were shown to be influenced by valgus deformities (increased femoral neck and shaft angles measured in the frontal plane) that are present. Following from this hypothesis, it is expected that restoring the moment arm of the hip abductors by correcting the increased femoral anteversion would restore the abduction moments and correct the occurrence of the internal rotation gait. Other bony deformities have also been attributed as the cause of internal rotation gait, such as femoral or tibial torsions. To correct these deformities, derotation osteotomies are utilised with the femoral derotation osteotomy the standard intervention for femoral anteversion and internal hip rotation [26, 29].

### **2.2.1 Clinical Assessment of Excessive Femoral Anteversion**

The accurate and reliable assessment of the degree of femoral anteversion forms the basis for the prescription of a corrective intervention. A number of techniques and measures are used in the measurement and determination of an excessive femoral anteversion in the clinical setting. These are namely the Trochanteric Prominence Angle Test (TPAT), Foot Progression Angle in stance and midpoint of hip rotation Passive Range of Motion (PROM).

The TPAT involves placing the patient in a prone position and knee in 90° of flexion. The hip is externally rotated until the neck of the femur lies in a plane parallel to the horizontal plane with the trochanter in a position of maximum lateral prominence [30, 31]. The angle between the tibia and the true vertical represents the degree of femoral anteversion.

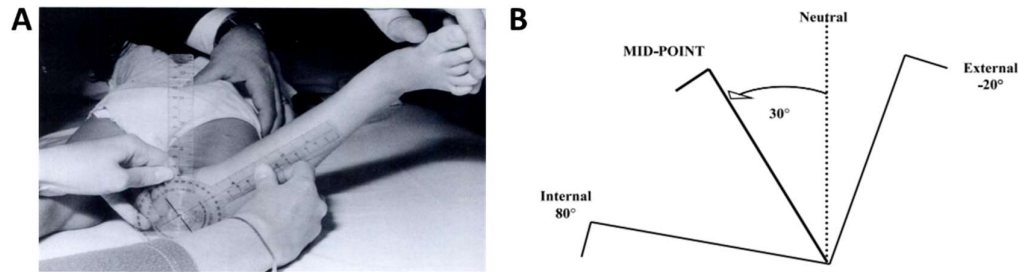


**Figure 2.2 Trochanteric Prominence Angle Test (A, Image adapted from [30]) and an illustration of the midpoint of hip rotation passive range of motion measurement (B, Image adapted from [32]).**

The midpoint of hip rotation PROM (Figure 2.2) is the sum of the maximum lateral hip rotation and the maximum medial hip rotation divided by two. To determine this, the patient is made to lie prone with the hip extended and the knees flexed at 90°. The hip is internally rotated by the examiner and a goniometer used to measure the angle between the tibia and true vertical as the passive range of hip internal rotation. Similarly, the hip is externally rotated, and the measurement of passive range of hip external rotation taken. An abnormal femoral anteversion is also concluded from this measurement when the Internal rotation exceeds the external rotation by more than 30° [25].

The clinical midpoint of hip rotation range of motion has been suggested to not sufficiently inform on the functional alignment of the distal femur during gait, leading to an over- or under-correction [33] after an intervention. The midpoint of hip PROM measurement is also affected by muscle spasticity as is present in CP and this is overcome using the TPAT which focusses on the maximum lateral placement of the trochanteric prominence.

The TPAT and midpoint of passive hip rotation methods are static measurements. To estimate the femoral anteversion dynamically, gait analysis is employed to define the hip rotation in stance. The midpoint of hip PROM has been shown to be a good indicator of the hip rotation in stance during gait in cerebral palsy [32] although low correlations are generally reported between static and dynamic measures of anteversion [34, 35]. That notwithstanding, in the absence of imaging data, these

dynamic and static measures have been used as fair indications of the degree of femoral anteversion and for determining extent of derotation [25, 30, 33] and could be explored as surrogate measures of outcome for the work in this thesis. Details on gait analysis are discussed in a subsequent section.

The foot progression angle, the second functional measure of the degree of anteversion, is the angle between the direction of travel of the patient and the long axis of the foot. The foot progression angle shows significant improvements following the femoral derotation osteotomy and forms a component in the assessment of gait quality outcomes after surgery [36, 37]. The mean normative value for this measure in children is 10° of external rotation [38].

### **2.3 Femoral Derotation Osteotomies**

Femoral Derotation Osteotomy (FDO) is one of the available surgical interventions that is used to help improve the ambulation of certain categories of CP patients. The FDO is usually performed as part of a Single Event Multi Level Surgery (SEMLS) to correct bony and soft-tissue issues. FDO is usually indicated when there is a persistent and excessive anteversion of the femur of the patient from the normal of about 15° [39], in addition to a passive internal hip rotation exceeding 50° [33]. The increased anteversion leads to an insufficiency in hip abductor strength and thus during ambulation, the hip is internally rotated to compensate. In individuals manifesting just excessive anteversion, it is also suggested that FDO not be carried out as this could rather lead to a deterioration of the gait in terms of an excessive external rotation and increased foot progression angle [39].

Several strategies exist in performing the FDO with some preferring the surgery be done at the proximal (intertrochanteric) or distal (supracondylar) end of the femur. A recent study however indicates no significant differences in outcomes for the two options of location in children [16] although the proximal FDO had marginally better outcomes in adults [40]. Other factors that have been suggested to impact the outcome of the FDO have been the posture of the patient during the surgery, with the prone posture suggested as having better outcomes than the supine posture [41]. The same authors go on to recommend the intraoperative measurement of the anteversion angle. Differences of 5-10° have been reported to exist between values of anteversion measured using the clinical TPAT and those measured intraoperatively [42] and this can impact the amount of correction effected.

### **2.3.1 Outcome Measures of FDO and Recurrence of IHR**

The aim of the Femoral Derotation Osteotomy is to reduce the internal hip rotation during gait. The primary outcome measures used to evaluate the success of an FDO to correct excessive femoral anteversion are mainly transverse plane kinematics. These include the mean hip rotation and mean pelvic rotation in stance during gait and the foot progression angle [43-45]. More general quantifications of gait abnormality used are the Gait Deviation Index [46] and Gait Profile Score [47].

Overall, FDO has been shown to have excellent outcomes in the short term with corrections observed in gait abnormalities that existed prior to the intervention [48]. The improvements include a decreased anteversion, increased hip abductor moment, decreased internal rotation gait as well as foot progression angles [40, 49-51]. The situation is however not so clear for the long-term (>3-5 years) improvements with a number of studies reporting a recurrence of the internally rotated gait pattern in patients [52, 53]. Other studies also point to the maintenance of the corrective effect several years after the intervention [41]. In pre-pubic children especially, this recurrence is more pronounced due to the occurrence of the growth spurt in puberty [54].

### **2.3.2 Risk factors for recurrence after FDO**

With the reported recurrence of IHR after FDO, a number of studies have investigated the potential cause or predicating factors for a recurrence. These studies have mainly been retrospective in nature, using gait data captured as part of treatment planning and evaluation after the intervention. From the outcomes of these studies, a number of risk factors for potential recurrence were identified but none of these studies was able to identify outcome measures for predicting positive responders from non-responders.

Niklasch, et al. [54] investigated outcomes in a group of children with CP one and greater than five years after an FDO intervention and found that preoperative younger age at intervention, reduced hip joint impulse, increased plantarflexion and internal foot progression angle could be associated with recurrence. Young age (<10 years) was also identified by Kim, et al. [55] as a predisposing factor. Church, et al. [52] identified in their study, lower gait velocity and high levels of spasticity preoperatively as a characteristic of children who experienced recurrence compared to those who maintained correction after the FDO in the long term. Very little literature exists on the use of these measures and impact on recurrence rates. Overcorrection is one approach to tackle the risk of recurrence however there is the attendant risk of deterioration (an increase in external rotation) [56].



Irrespective of the potential benefits of these measures, the FDO is usually performed as part of a battery of procedures correcting other structural or functional deviations such as lengthening of muscles around the hip among others. As previously mentioned, an excessive anteversion modifies the moment arms of the muscles effecting motion about the hip and a restoration of the moment arm should restore the motion capacity assuming the muscle force capacity is normal. The studies that investigated predictive factors however do not consider the contribution of muscles forces and lengths. Including such information could further reduce the number of concomitant surgeries prescribed for a patient. In addition, even with knowledge of these factors contributing to recurrence of an internal rotation gait, preoperative prediction of children who are most likely to suffer recurrence is not possible [56].

## **2.4 Clinical Gait Analysis**

Clinical gait analysis (CGA) has become an assessment standard in the diagnosis and treatment of most movement/ambulatory disorders, especially in cases of cerebral palsy [6]. CGA is a process of observing and quantifying human locomotion. This may be through clinical assessments of function or the use of instrumented systems to assess the kinematics, kinetics and muscle activity associated with a movement [57].

### **2.4.1 Instrumented CGA**

Instrumented CGA utilises motion capture using a set of cameras and markers as well as force plates embedded in the floor to track the movement of the patient as they walk or perform an activity of interest. The three-dimensional motion capture process involves the use of a stereophotogrammetric system that comprises a set of cameras that record the trajectories of reflective markers placed on specific anatomical or informative landmarks on the individual's body as they perform the task of interest. To assist with understanding the kinetics of the movement, one or more force plates may be used to capture the forces the body exerts on the ground and vice versa, what are termed the ground reaction forces. The marker trajectories and ground reaction forces are subsequently used to determine the joint kinematics, moments and powers associated with the movement.

To reconstruct and calculate the joint kinematics from the marker trajectories, CGA utilises a biomechanical model and a computational approach known as direct kinematics. The biomechanical model provides a description of the body segments, the joints that interface these segments as well as any constraints. The commonly used biomechanical model in instrumented gait analysis is the Plug-In Gait (PiG) Model (Vicon, UK), a popular implementation of the so called conventional gait model proposed by Davis, et al. [58] and Kadaba, et al. [59]. The PiG model defines a minimal

set of markers from which the different anatomical segments and their reference frames are determined. This model represents each joint as a spherical ball-and-socket joint, permitting three degrees of rotational freedom. Based on this definition and the assumption that the experimental skin surface markers are rigidly fixed to the underlying bone, the direct kinematics approach estimates the location and orientation of these body segments in three-dimensional space. The joint kinematics are calculated as the Cardan angles between defined segments which are adjacent [60]. Joint moments are subsequently determined using the estimated joint kinematics in an inverse dynamic operation. Inverse dynamics is a process of defining the kinetics responsible for the motion with the known kinematics. Outputs of inverse dynamics produced by gait analysis are net of all forces acting across a joint.

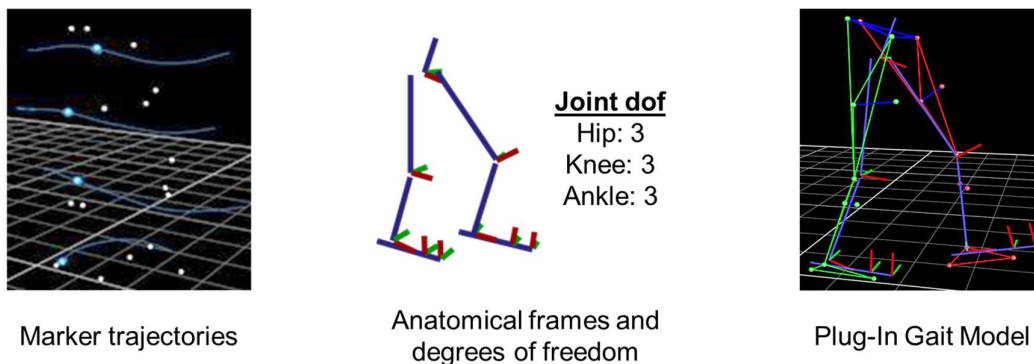


**Figure 2.3 Definition of the Plug-In Gait Model from experimental marker trajectories**

The output from gait analysis together with the clinical assessment are used to determine the level of deviation from normal of the gait of the patient and can inform the decision of the treating physician on the choice of intervention and/or degree of intervention. It also provides an avenue for the care team to quantify the degree of improvement or deterioration in condition with pre- and post-analysis. Gait analysis is used to estimate the foot progression angle in addition to other kinematic variables such as joint angles and net joint moments. Deviation of parameters from data acquired of typically developing children is used in quantifying abnormal gait patterns.

While the joint angles and moments allow for the description of the movement and an understanding of what the muscle groups are doing at any point in the gait cycle, they are not focussed on investigating deeper how individual muscles are contributing to the motion (muscle lengthening, moment arms and forces) and how these translate to loading of the joints. An alternative model that provides a means to probe these details are musculoskeletal models.

## 2.5 Musculoskeletal Modelling

Musculoskeletal models are mathematical representations of the human body that permit the simulation and analysis of human movement to measure and estimate additional quantities of interest such as muscle forces and joint reaction forces. The development of these models also permits for the investigation of “what if” scenarios and provides a means for clinically meaningful insights that may not be available through other means. MSK modelling also has benefits of being non-invasive with minimised subject risk and financial cost. The current challenge with the use of musculoskeletal modelling in the clinical setting include the expertise required to generate and simulate these models [61]. Secondly, there is the need for increased validation to increase trust in these models and their simulation outputs [62, 63].

Musculoskeletal modelling involves the formulation of the musculoskeletal system as a collection of rigid bodies, an idealisation, connected by joints with movement about these joints achieved by force producing actuators representing muscles. The assumption of bone segments as rigid bodies with movement permitted only at the joints allows the application of the principles of rigid multibody dynamics in the solution of the formulation [64]. It should be noted however that this assumption of infinite mechanical stiffness may not be realistic to the problem being analysed when large loads are involved especially when values of deformations exceed the limits of observation of the experimental methods or in instances when interest is in these deformations as in the case of injury from impact which is not a critical consideration in this application. Secondly, the joints are idealised as frictionless with kinematic constraints imposed. This reduction to frictionless joints is acceptable on the basis that human synovial joints have a low coefficient of friction, which when converted to friction loads could be considered negligible compared to other internal and external loads acting.

The path of muscles that actuate movement are represented in the musculoskeletal model as a line segment or set of line segments that run from each muscle’s origin to insertion. To approximate physiological features such as overlapping muscles, muscles wrapping around bone geometries or tendon sheaths, wrapping surfaces or via points may be introduced [65]. The accurate representation of the muscle-tendon geometry is important as it allows to determine muscle-tendon length and velocities, moment arms and ultimately muscle force at different positions of the body during movement. Inaccuracies in their definition have been shown to affect estimates of muscle forces and joint contact forces [66-68]. The commonly used representation of muscle function used is the Hill-type model (Figure 2.4) where the muscle sarcomere unit is represented as an elastic element in series with a parallel combination of an active

contractile element and elastic damping element [69]. The series elastic element represents the tendon, whereas the parallel combination of contractile element and elastic element represents the muscle fibres and all passive structures in and around the muscle, respectively. To permit estimation of muscle forces from the musculoskeletal model, muscle-tendon parameters (maximum isometric force, optimal fibre length, muscle pennation angle, tendon slack length and contraction velocity) and the dynamics that govern their force generation function (force-length-velocity relationship and activation dynamics) must be defined [70]. These muscle parameters may be obtained from the literature and cadaveric experiments [71, 72] or estimated from imaging modalities such as ultrasound and magnetic resonance imaging [73, 74].

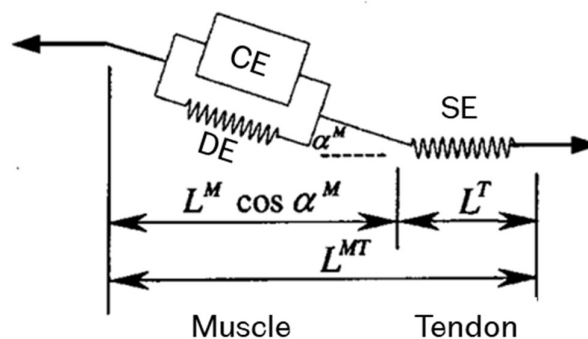


**Figure 2.4 Schematic of the Hill-type model of the muscle-tendon unit adapted from [69] showing a contractile element (CE) and two passive elastic elements (DE and SE).  $L^{MT}$  - muscle-tendon length,  $L^M$  - muscle fibre length,  $L^T$  - tendon length,  $\alpha$  - muscle pennation angle.**

The rigid body formulation permits the relation of the movement (kinematics) to the forces (kinetics) using the equations of motion. The relation between the two quantities thus enables the calculation of one entity with knowledge of the other. Two main approaches of estimating these quantities are possible namely the inverse dynamics and the forward dynamics approaches [75, 76]. Inverse dynamics uses knowledge of the movement and ground reaction forces to calculate the net moments about each joint and subsequently muscle forces at each instant in time. When muscle excitations or joint torques are known or can be assumed, the forward dynamics approach can then be used to estimate the movement. This report however limits the discussion to the inverse dynamics approach, which has been shown to be computationally efficient and more robust to measurement errors [77]. Secondly, given as this was a retrospective study, availability of the inputs (muscle activations in the form of electromyography) for forward dynamics was not assured.

### **2.5.1 Generic Musculoskeletal Models**

Most generic models are based on measurement data from cadaveric specimens [65, 78]. Body segments geometries of these models are defined from images of an average adult person which are subsequently scaled to match individual anthropometry during use. The resulting model generally referred to as a scaled generic model, is a replica of the original model, with segment lengths, inertial properties and muscle-tendon length-related parameters modified to reflect the anthropometry of the subject of interest.

Muscle and tendon units in these models are simplified to line segments with defined origin and insertion points. Due to the different types of muscles present in the human body, with some spanning multiple joints or having multiple points of attachment, some muscles in the models are represented with multiple line segments with different attachment points to provide an equivalent representation. In addition, wrapping surfaces or via points may be introduced to prevent the modelled muscle from penetrating the bone segment during some range of motions as is present in vivo [65, 79].

These models are straightforward to use and provide meaningful and general understanding of phenomena of interest [80] but are challenged in their applicability and uptake in the clinical setting for the treatment of patients. This challenge stems from the sources of data used in the construction of these models. The cadaveric specimens whose measurements are used are usually of healthy and unimpaired adults which has been reported to affect simulations and estimates for subjects from different parts of the population such as children or those with anatomical deformities. Common generic models available in the literature for analysing human movement include the lower limb gait2392 model by Delp, et al. [65], its modified version by Arnold, et al. [81] that accounts for knee rotation and ab-adduction as well as the model by Hamner, et al. [82] for running. Most of the work in this thesis is based on the gait2392 generic model.

### **2.5.2 Subject-Specific Musculoskeletal Models**

Image-based subject-specific models are similar to generic musculoskeletal models in terms of their composition. The main difference is that subject-specific models embed a lot more detail of the subject in the model using information from imaging modalities such as Magnetic Resonance Imaging (MRI) and Computed Tomography (CT) [83]. The details obtained from these images include specific bone geometries which capture deformities or subject bone segment peculiarities, muscle origin and insertion locations and paths as well as orientation of joint axes.

Images from the MRI or CT are segmented to obtain the body segment bone geometries and properties. To estimate body segment properties from the segmented images, densities of bone and soft tissue from literature are assigned and together with the volume and shape of each segment, inertial properties can be determined. Joint parameters of the model can be determined by fitting articular surfaces with geometric shapes [84]. For instance, the knee and ankle joint can be modelled as a hinge joint and their centres and axes of rotation determined by fitting cylinders to the condyles and malleoli, respectively.

In addition to personalised bone geometries, muscle segmentations can also be obtained from the images and can thus be used to further personalise the model in terms of their origins and insertions on the bone surfaces as well as their paths. Aside the geometrical features required to define a representative model, other parameters that are intrinsic to physiological function are required to be defined to enable accuracy of musculoskeletal modelling outputs. These include muscle properties such as the maximum isometric force, tendon slack length, optimal fibre length, pennation angle and contraction velocity. Segmentations of muscles from imaging such as MRI can be used to obtain muscle volumes and lengths, from which the muscle physiological cross-sectional area (PCSA) can be calculated [73]. The maximum isometric force of a muscle can then be derived from the PCSA due to their proportionality [85-87]. In CP, the maximum isometric force is especially important as patients generally have weaker muscle strength [88, 89] and thus using generic adult values may not be appropriate. Different approaches have also been used including scaling by subject mass [90], mass and individual muscle-tendon lengths [91] or dynamometer-informed approaches [92]. Results comparing these different methods when applied to CP children however showed not too different estimates of maximum muscle force during gait although muscle activations were different [92]. Additionally, although the method of determining the maximum isometric force does not significantly affect the muscle and joint contact forces generated [93, 94], it could influence the success of the model simulation as reported by Modenese, et al. [86].

### **2.5.3 Biomechanical model simulation**

Different software applications such as SIMM [95], Anybody [96] and OpenSim [97] have been developed for running simulations of musculoskeletal models. These platforms enable the solution of the complex equations of motion for these multibody systems. OpenSim was however used in this thesis due to its availability as an open-source software with extensive documentation and high use in musculoskeletal modelling research. The OpenSim simulation pipeline includes inverse kinematics, inverse

dynamics, static optimisation, and joint reaction analysis. These are detailed in the sections below.

### Inverse Kinematics

Inverse Kinematics (IK) also referred to as global optimisation is a computational method to estimate a set of generalised coordinates of segments in the musculoskeletal model using a least squares minimization algorithm to match modelled and experimental marker positions [98].

The least squares problem solved by IK is given as:

$$\min_{\vec{q}} \left[ \sum_{i \in mk} \omega_i \|x_i^{exp} - x_i(\vec{q})\|^2 + \sum_{j \in UC} \omega_j (q_j^{exp} - q_j)^2 \right]$$

**Equation 2.1**

where  $\vec{q}$  is the solution of generalised coordinates,  $x_i^{exp}$ ,  $x_i(\vec{q})$  are the experimental and virtual model positions, respectively of marker  $i$ ,  $\omega$  are specified weights,  $q_j^{exp}$  is the experimental value of coordinate  $j$  and  $mk$  and  $UC$  refer to marker set and unprescribed coordinates, respectively.

Applied to a static trial, the joint angles define the static pose of the model. The output of the inverse kinematics method in dynamic tasks is a set of generalised coordinates ( $\vec{q}$ ) that describe the location and orientation of the body segments of the system at any instant in time. By differentiating the generalised coordinates over time once and twice, the change in configuration of the system can be obtained as generalised velocities ( $\dot{\vec{q}}$ ) and accelerations ( $\ddot{\vec{q}}$ ), respectively. These generalised velocities and accelerations are both linear and angular.

### 2.5.4 Inverse Dynamics

Inverse dynamics is a method for estimating net moments about each joint in the model. The method uses calculated joint kinematics output from inverse kinematics and the ground reaction forces collected during experimental trials. Joint moments are calculated recursively by isolating body segments from distal to proximal and applying the Newton-Euler equations of motion. The joint moments estimated in this manner do not discriminate the contribution of individual muscles to the observed movement.

Solving by inverse dynamics involves solving the instantaneous equilibrium equation (Equation 2.2) for the joint torques  $\vec{T}(t)$  with knowledge of the model inertial properties, kinematics and external forces acting.

$$M(\vec{q})\ddot{\vec{q}}(t) = \vec{T}(t) + \vec{C}(\vec{q}(t), \dot{\vec{q}}(t)) + \vec{G}(\vec{q}(t)) + \vec{E}(\vec{q}(t), \dot{\vec{q}}(t))$$

**Equation 2.2**

where  $M$  is a square mass matrix dependent on the number of degrees of freedom of the model,  $\vec{T}$  is a vector of forces and moments acting at the joints/coordinates,  $\vec{C}$ , the centrifugal forces,  $\vec{G}$ , gravitational forces and  $\vec{E}$ , any external forces acting.

### 2.5.5 Static Optimisation

Muscles in the human body function redundantly to produce any motion and static optimisation provides a means to quantify the contribution of individual muscles to the net joint torque produced. The generalised torques estimated at the joints are a function of the product of the force exerted by each muscle and the muscle moment arm at each instant of time. The muscle forces must therefore satisfy the equilibrium condition of:

$$\vec{T}(t) = B(\vec{q})\vec{F}^M(t)$$

**Equation 2.3**

where  $\vec{T}$  are the estimated torques,  $B$ , a matrix of muscle moment arms and  $\vec{F}^M$ , a vector of muscle forces. Given an  $n$  degrees of freedom model with  $m$  actuating muscles,  $B$  is an  $n \times m$  matrix.

Given that the number of muscles associated with a joint can be more than the number of degrees of freedom of the joint, the formulation of the solution becomes underdetermined, and a large space of possible muscle force solutions can produce the net joint torques. This is referred to as the muscle load sharing problem [99].

The force generated by a muscle can be expressed in terms of the maximal force the muscle can generate ( $\vec{F}_{max}^M$ ). Given that the level of activation of a muscle directly impacts on the force generated, the relation between  $\vec{F}^M$  and muscle activation ( $\vec{a}^M$ ) can be expressed as:

$$\vec{F}^M(t) = \vec{a}^M(t)\vec{F}_{max}^M$$

**Equation 2.4**

The muscle load sharing problem is therefore solved as an optimisation problem based on how muscles are believed to function physiologically. Static optimisation is one method used in solving the problem by minimizing some performance criterion represented as an objective function and subject to some constraint [100]. A performance criterion most frequently used in gait is the muscle activations where a solution is to find the muscle activations that minimize the sum of muscle activations



squared [101] (Equation 2.5) and matches/produces the joint torques estimated as the inverse dynamic solution. The load sharing problem can thus be solved mathematically with Equation 2.3 subject to:

$$\vec{0} \leq \vec{F}^M \leq \vec{F}_{max}^M(t)$$

while minimising:

$$J(\vec{a}^M) = \sum_{i=1}^m (a_i(t))^p$$

**Equation 2.5**

where  $J$  is the objective function,  $m$  is the number of muscles,  $\vec{a}^M$  is the activation (defined as  $0 \leq a \leq 1$ ),  $p$  is a user-defined constant that is commonly set to 2 for gait [101, 102].

By this, static optimisation determines the best set of muscle forces that minimize the sum of muscle activations. Static optimisation however does not account for the muscle activation and contraction dynamics which affects its consistency with muscle physiology [103]. A study comparing the static optimisation and dynamic optimisation methods for estimating muscle forces during normal walking however concluded on no significant differences between estimates made by the two [101], an observation that may not hold for other motor tasks. Although the dynamic optimisation approach is more computationally intensive to solve, other studies have also found that it estimates values that have closer agreement with electromyography measurements [104, 105].

### 2.5.6 Joint Reaction Analysis

Joint reaction analysis is a process for estimating the joint contact forces (JCFs) acting at joints defined in the musculoskeletal model. Knowledge of these JCFs can inform the prescription of rehabilitation protocols for patients or the prediction of fracture in different loading conditions and movement activities. Muscle forces acting around a joint are the main contributors to joint contact forces in addition to external forces and inertial forces arising from segments. By applying force equilibrium conditions to each segment starting from distal, location of ground reaction forces, to proximal iteratively, the JCFs can be estimated. The general formulation of the JCF calculation is shown in Equation 2.6 as described by Steele, et al. [106].

$$\vec{R}_j(t) = M(\vec{q})\ddot{\vec{q}}(t) + \vec{F}_c - \left( \sum \vec{F}^M(t) + \sum \vec{F}^{ext}(t) + \vec{R}_{j+1}(t) \right)$$

**Equation 2.6**

where  $M$  and  $\vec{F}^M$  are as defined previously and  $\vec{F}_c$ ,  $\vec{F}^{ext}$ ,  $\vec{R}_{j+1}$  and  $\vec{R}_j$  represent any applicable constraint forces, external forces, joint reaction load applied at the distal joint and joint reaction load at the proximal joint.

### 2.5.7 Musculoskeletal Modelling and Simulation in CP

Abnormal gait in CP is mainly influenced by abnormal limb geometry and muscle control and the use of musculoskeletal models allows for the probing of associated factors that would otherwise not be possible except by invasive methods.

With the different models available for carrying out MSK simulations, it is important to choose an approach that has high bio-fidelity and that can produce the most accurate results while minimizing the resources required to achieve such accuracy. This particularly holds true for clinical applications. In this bid, a few studies have investigated how increased personalization or otherwise of these models influence simulation outputs in CP. A primary concern in CP is the change in bone geometries. Generic models are based off cadaveric specimens of healthy adults which do not account for these structural changes in CP and these omissions have been found to influence the estimates obtained from these models when used for children with CP, when compared to subject-specific models incorporating these changes. For instance, muscle tendon length and moment arm length estimates have been found to be different depending on whether a generic or subject-specific model was used [107, 108].

A second issue of concern is with the neuromuscular control of movement. This is affected in CP, with issues of muscle weakness, increased muscle tone and spasticity, different muscle control strategies, etc reported [5, 109]. The generally used approach for solving for muscle forces is via an inverse dynamics approach that assumes optimal control of muscles and thus solves an optimization problem (static optimisation) that was described in a previous section. An alternative to this approach is via a forward dynamics approach known as an EMG driven approach where knowledge of muscle excitations is used to drive model simulation to determine muscle forces and subsequently joint reaction forces. While the latter approach has been reported to produce results consistent with experimental data [110], it is not always feasible as it relies on the ability to collect muscle activation data. Again, this collection is usually limited to superficial muscles. Similarly, there are changes in muscle-tendon dynamics introduced by muscle spasticity (a velocity-dependent resistance to stretch), that affects the force-generation capacity of the affected muscles in CP. These are not captured in the models currently used and are not easily determined for all affected muscles.

The above notwithstanding, several other studies have also investigated different factors leading to the observed gait deviations and potential interventions utilising musculoskeletal models in CP. Steele, et al. [106] investigated the impact of crouch gait on muscle forces and joint contact forces in children with cerebral palsy. Their study identified the contribution of the quadriceps muscle force to an increase in tibiofemoral JCF during crouch gait and its potential association with knee pain in patients. In a related study on crouch gait in CP, Hicks, et al. [111] found a decrease in the ability of the muscles to extend the hip and knee during gait and suggested an association with the increased energy requirements of gait in CP patients. Similarly, Carriero, et al. [112] found that the altered gait patterns associated with cerebral palsy caused the hip joint force magnitude to deviate from normal by up to 30% contributing further to developing bone deformation.

Arnold, et al. [28] investigated the impact of increased femoral anteversion, a feature of cerebral palsy, on hip abduction capacity and found that correcting the excessive anteversion potentially restores the muscle moment arm and hence the abduction capacity. Kainz, et al. [113] also investigated outcomes of a selective dorsal rhizotomy using a musculoskeletal modelling approach and found that the intervention improved muscle forces in children with CP during walking. Similarly, in a recent study by Van Rossom, et al. [114], in which scaled generic models were used to investigate the effect of two different interventions on joint contact forces in children with CP showed that the use of surgical methods in the form of SEMLS provided a higher reduction to joint contact forces than the use of Botulinum Toxin.

The work done by Pitto, et al. [115] comes closest in terms of the prediction of outcomes after an orthopaedic intervention in children with CP. In this study, a simulation platform was developed that permits the evaluation of different treatment plans prior to an actual intervention to select the one with best potential. The platform successfully predicted gait outcomes of a child who had undergone an intervention after the same intervention was simulated with a model.

Although the majority of these studies do not predict subjects to benefit from a prescribed intervention particularly prior to an intervention and from initial assessment, they provide a template of methods and parameters that would be informative for this study as well as justify the potential of using MSK models to provide insights for understanding gait pathology and improving treatment outcomes.

## **2.6 Aim and objectives**

The indeterminate success of an FDO, especially in the long term, behoves an examination of the factors that contribute to successful cases. This would better

inform the selection of likely candidates for a successful intervention. From the available literature, most attempts in this direction have used standard gait analysis techniques and its outputs to try and provide some answers to this issue. While these have provided insights to some predisposing factors for recurrence of internal rotation gait in the long term, pre-intervention prediction of outcomes has not yet been achieved. This study thus seeks to employ a different approach in the form of musculoskeletal modelling. Previous studies have highlighted the phenomenon of diminishing returns where patients who deviate more from normal tend to have greater improvements after intervention [33, 116, 117]. These trends have also been reported when using musculoskeletal models to retrospectively investigate outcomes [21, 118]. Based on these observations, it is hypothesised that patients who have better outcomes after FDO in the long term have kinematic, kinetic and muscle-length and moment-arm characteristics that deviate substantially from the normal population and from those who show a deterioration or recurrence some years after the intervention. Using current approaches such as the clinical gait analysis, studies have reported indicators based on kinematics that could be used to infer outcomes after the FDO, although prediction is still not possible.

The aim of this thesis was to apply a musculoskeletal modelling approach to the prediction of outcome and recurrence of internally rotated gait after FDO in the long term to distinguish positive responders to FDO from non-responders.

To achieve the aim of this exploratory study, data already collected as part of the standard clinical management of the patients was used. Ideally, and from reports from the literature on the performance of musculoskeletal models, the best approach would have been to go with personalised models that provide high bio-fidelity to the features of this population before and after the surgery. However, this would require ad hoc imaging data, which were not available. Additionally, with the intent to investigate long term effects, data availability over the course of the PhD study was a concern leading to the decision of a retrospective analysis. While this choice introduced a constraint on the potential modelling approach that could be used in terms of the nature and depth of data available, it also presented an opportunity to query the level of personalisation and data necessary to achieve clinically relevant information from the musculoskeletal models. These constraints and opportunities were factored into the following objectives set to accomplish the overall aim of the thesis:

**Objective 1:** to investigate the effect of experimental (marker set) and musculoskeletal modelling (generic/subject-specific) choices on the estimate of joint kinematics. Relevant results are reported in chapter 3.

**Objective 2:** to test the consistency and agreement between two kinematic models to predict non-3D clinical data-based judgement of outcomes after FDO surgery. This was to determine the validity or otherwise of using a generic model in quantifying post-surgical changes and outcomes compared to the traditional Plugin gait model. Chapter 4 provides insights into this aspect and suggests the potential of this approach.

**Objective 3:** to explore and determine potential discriminators between responders and non-responders to the FDO in the context of SEMLS. This was the focus of chapter 5.

**Objective 4:** to evaluate the suitability of scaled generic models in predicting longitudinal changes in gait outcomes compared to patient-specific models. Chapter 6 described the relevant achievements.

**Objective 5:** to evaluate the effect of including sparse subject-specific details on model parameters. This is presented in chapter 7.

## 2.7 References

- [1] M. Oskoui, F. Coutinho, J. Dykeman, N. Jette, and T. Pringsheim, "An update on the prevalence of cerebral palsy: a systematic review and meta-analysis," *Dev Med Child Neurol*, vol. 55, no. 6, pp. 509-19, Jun 2013, doi: 10.1111/dmcn.12080.
- [2] M. Bax *et al.*, "Proposed definition and classification of cerebral palsy, April 2005," *Dev Med Child Neurol*, vol. 47, no. 8, pp. 571-6, Aug 2005, doi: 10.1017/s001216220500112x.
- [3] A. Rajab *et al.*, "An autosomal recessive form of spastic cerebral palsy (CP) with microcephaly and mental retardation," (in eng), *Am J Med Genet A*, vol. 140, no. 14, pp. 1504-10, Jul 15 2006, doi: 10.1002/ajmg.a.31288.
- [4] R. Palisano, P. Rosenbaum, S. Walter, D. Russell, E. Wood, and B. Galuppi, "Development and reliability of a system to classify gross motor function in children with cerebral palsy," (in eng), *Dev Med Child Neurol*, vol. 39, no. 4, pp. 214-23, Apr 1997, doi: 10.1111/j.1469-8749.1997.tb07414.x.
- [5] J. R. Gage, M. H. Schwartz, S. E. Koop, and T. F. Novacheck, *The Identification and Treatment of Gait Problems in Cerebral Palsy*. Wiley, 2009.
- [6] S. Armand, G. Decoulon, and A. Bonnefoy-Mazure, "Gait analysis in children with cerebral palsy," *EFORT Open Rev*, vol. 1, no. 12, pp. 448-460, Dec 2016, doi: 10.1302/2058-5241.1.000052.
- [7] G. Molenaers, K. Fagard, A. Van Campenhout, and K. Desloovere, "Botulinum toxin A treatment of the lower extremities in children with cerebral palsy," *J Child Orthop*, vol. 7, no. 5, pp. 383-387, 2013, doi: 10.1007/s11832-013-0511-x.
- [8] H. K. Graham *et al.*, "Recommendations for the use of botulinum toxin type A in the management of cerebral palsy," *Gait & posture*, vol. 11, no. 1, pp. 67-79, 2000.
- [9] E. R. Boyer, Z. B. Novaczyk, T. F. Novacheck, F. J. Symons, and C. C. Burkitt, "Presence and predictors of pain after orthopedic surgery and associated orthopedic outcomes in children with cerebral palsy," *Paediatric and Neonatal Pain*, vol. 4, no. 1, pp. 43-51, 2022, doi: 10.1002/pne2.12067.
- [10] I. Rehbein, V. Teske, I. Pagano, A. Cúneo, M. E. Pérez, and J. von Heideken, "Analysis of orthopedic surgical procedures in children with cerebral palsy," (in eng), *World J Orthop*, vol. 11, no. 4, pp. 222-231, 2020, doi: 10.5312/wjo.v11.i4.222.
- [11] H. M. Horstmann, H. Hosalkar, and M. A. Keenan, "Orthopaedic issues in the musculoskeletal care of adults with cerebral palsy," *Developmental Medicine & Child Neurology*, vol. 51, pp. 99-105, 2009, doi: 10.1111/j.1469-8749.2009.03417.x.
- [12] R. Norlin and H. Tkaczuk, "One-session surgery for correction of lower extremity deformities in children with cerebral palsy," (in eng), *J Pediatr Orthop*, vol. 5, no. 2, pp. 208-11, Mar-Apr 1985.
- [13] J. L. McGinley, F. Dobson, R. Ganeshalingam, B. J. Shore, E. Rutz, and H. K. Graham, "Single-event multilevel surgery for children with cerebral palsy: a systematic review," *Dev Med Child Neurol*, vol. 54, no. 2, pp. 117-128, 2012, doi: 10.1111/j.1469-8749.2011.04143.x.

- [14] P. Steinbok, "Selective dorsal rhizotomy for spastic cerebral palsy: a review," *Child's Nervous System*, vol. 23, no. 9, pp. 981-990, 2007, doi: 10.1007/s00381-007-0379-5.
- [15] E. Boyer, T. F. Novacheck, A. Rozumalski, and M. H. Schwartz, "Long-term changes in femoral anteversion and hip rotation following femoral derotational osteotomy in children with cerebral palsy," *Gait & posture*, vol. 50, pp. 223-228, Oct 2016, doi: 10.1016/j.gaitpost.2016.09.004.
- [16] M. Niklasch, E. R. Boyer, T. Novacheck, T. Dreher, and M. Schwartz, "Proximal versus distal femoral derotation osteotomy in bilateral cerebral palsy," *Dev Med Child Neurol*, vol. 60, no. 10, pp. 1033-1037, Oct 2018, doi: 10.1111/dmcn.13910.
- [17] D. L. Skaggs, S. A. Rethlefsen, R. M. Kay, S. W. Dennis, R. A. Reynolds, and V. T. Tolo, "Variability in gait analysis interpretation," (in eng), *J Pediatr Orthop*, vol. 20, no. 6, pp. 759-64, Nov-Dec 2000, doi: 10.1097/00004694-200011000-00012.
- [18] J. L. Hicks, S. L. Delp, and M. H. Schwartz, "Can biomechanical variables predict improvement in crouch gait?," *Gait & Posture*, vol. 34, no. 2, pp. 197-201, 2011, doi: 10.1016/j.gaitpost.2011.04.009.
- [19] M. C. d. M. Filho, R. Yoshida, W. d. S. Carvalho, H. E. Stein, and N. F. Novo, "Are the recommendations from three-dimensional gait analysis associated with better postoperative outcomes in patients with cerebral palsy?," *Gait & posture*, vol. 28, no. 2, pp. 316-322, 2008/08/01/ 2008, doi: <https://doi.org/10.1016/j.gaitpost.2008.01.013>.
- [20] B. Lofterød, T. Terjesen, I. Skaaret, A. B. Huse, and R. Jahnsen, "Preoperative gait analysis has a substantial effect on orthopedic decision making in children with cerebral palsy: comparison between clinical evaluation and gait analysis in 60 patients," (in eng), *Acta Orthop*, vol. 78, no. 1, pp. 74-80, Feb 2007, doi: 10.1080/17453670610013448.
- [21] A. S. Arnold, M. Q. Liu, M. H. Schwartz, S. Ounpuu, and S. L. Delp, "The role of estimating muscle-tendon lengths and velocities of the hamstrings in the evaluation and treatment of crouch gait," *Gait & posture*, vol. 23, no. 3, pp. 273-81, Apr 2006, doi: 10.1016/j.gaitpost.2005.03.003.
- [22] A. S. Arnold, M. Q. Liu, M. H. Schwartz, S. Ounpuu, L. S. Dias, and S. L. Delp, "Do the hamstrings operate at increased muscle-tendon lengths and velocities after surgical lengthening?," *J Biomech*, vol. 39, no. 8, pp. 1498-506, 2006, doi: 10.1016/j.jbiomech.2005.03.026.
- [23] J. R. Gage and T. F. Novacheck, "An update on the treatment of gait problems in cerebral palsy," *J Pediatr Orthop B*, vol. 10, no. 4, pp. 265-74, Oct 2001. [Online]. Available: <https://www.ncbi.nlm.nih.gov/pubmed/11727367>.
- [24] J. Robin, H. K. Graham, P. Selber, F. Dobson, K. Smith, and R. Baker, "Proximal femoral geometry in cerebral palsy: a population-based cross-sectional study," *The Journal of bone and joint surgery. British volume*, vol. 90, no. 10, pp. 1372-9, Oct 2008, doi: 10.1302/0301-620X.90B10.20733.

- [25] M. T. Cibulka, "Determination and significance of femoral neck anteversion," (in English), *Phys Ther*, vol. 84, no. 6, pp. 550-8, Jun 2004. [Online]. Available: <https://www.ncbi.nlm.nih.gov/pubmed/15161420>.
- [26] J. R. Gage, P. A. Deluca, and T. S. Renshaw, "Gait Analysis - Principles and Applications - Emphasis on Its Use in Cerebral-Palsy," (in English), *J Bone Joint Surg Am*, vol. 77, no. 10, pp. 1607-1623, Oct 1995, doi: Doi 10.2106/00004623-199510000-00017.
- [27] H. Uden and S. Kumar, "Non-surgical management of a pediatric &ldquo;intoed&rdquo; gait pattern &ndash; a systematic review of the current best evidence," *Journal of Multidisciplinary Healthcare*, p. 27, 2012, doi: 10.2147/jmdh.s28669.
- [28] A. S. Arnold, A. V. Komattu, and S. L. Delp, "Internal rotation gait: a compensatory mechanism to restore abduction capacity decreased by bone deformity," (in eng), *Dev Med Child Neurol*, vol. 39, no. 1, pp. 40-4, Jan 1997, doi: 10.1111/j.1469-8749.1997.tb08202.x.
- [29] E. E. Bleck, "Mechanisms and treatment of internal rotation of the hip deformity in cerebral palsy," *Acta Orthopaedica Belgica*, vol. 50, pp. 273-274, 1984.
- [30] P. A. Ruwe, J. R. Gage, M. B. Ozonoff, and P. A. DeLuca, "Clinical determination of femoral anteversion. A comparison with established techniques," (in eng), *J Bone Joint Surg Am*, vol. 74, no. 6, pp. 820-30, Jul 1992. [Online]. Available: <https://www.ncbi.nlm.nih.gov/pubmed/1634572>.
- [31] C. Y. Chung, K. M. Lee, M. S. Park, S. H. Lee, I. H. Choi, and T. J. Cho, "Validity and reliability of measuring femoral anteversion and neck-shaft angle in patients with cerebral palsy," (in eng), *J Bone Joint Surg Am*, vol. 92, no. 5, pp. 1195-205, May 2010, doi: 10.2106/JBJS.I.00688.
- [32] A. M. Kerr, S. J. Kirtley, S. J. Hillman, M. L. van der Linden, M. E. Hazlewood, and J. E. Robb, "The mid-point of passive hip rotation range is an indicator of hip rotation in gait in cerebral palsy," (in English), *Gait & posture*, vol. 17, no. 1, pp. 88-91, Feb 2003, doi: doi: 10.1016/S0966-6362(02)00056-5.
- [33] T. Dreher, S. Wolf, F. Braatz, D. Patikas, and L. Doderlein, "Internal rotation gait in spastic diplegia--critical considerations for the femoral derotation osteotomy," *Gait & posture*, vol. 26, no. 1, pp. 25-31, Jun 2007, doi: 10.1016/j.gaitpost.2006.07.018.
- [34] F. Braatz, S. I. Wolf, A. Gerber, M. C. Klotz, and T. Dreher, "Do changes in torsional magnetic resonance imaging reflect improvement in gait after femoral derotation osteotomy in patients with cerebral palsy?," (in English), *Int Orthop*, vol. 37, no. 11, pp. 2193-8, Nov 2013, doi: 10.1007/s00264-013-2054-7.
- [35] D. E. Westberry, L. I. Wack, R. B. Davis, and J. W. Hardin, "Femoral anteversion assessment: Comparison of physical examination, gait analysis, and EOS biplanar radiography," *Gait & posture*, vol. 62, pp. 285-290, 2018/05/01/ 2018, doi: <https://doi.org/10.1016/j.gaitpost.2018.03.033>.
- [36] Y. Saglam, N. Ekin Akalan, Y. Temelli, and S. Kuchimov, "Femoral derotation osteotomy with multi-level soft tissue procedures in children with cerebral



- palsy: Does it improve gait quality?," *J Child Orthop*, vol. 10, no. 1, pp. 41-48, 2016-02-01 2016, doi: 10.1007/s11832-015-0706-4.
- [37] H. S. Read, M. E. Hazlewood, S. J. Hillman, R. J. Prescott, and J. E. Robb, "Edinburgh visual gait score for use in cerebral palsy," (in eng), *J Pediatr Orthop*, vol. 23, no. 3, pp. 296-301, May-Jun 2003.
- [38] L. T. Staheli, M. Corbett, C. Wyss, and H. King, "Lower-extremity rotational problems in children. Normal values to guide management," (in English), *J Bone Joint Surg Am*, vol. 67, no. 1, pp. 39-47, Jan 1985, doi: Doi 10.2106/00004623-198567010-00006.
- [39] M. H. Schwartz, A. Rozumalski, and T. F. Novacheck, "Femoral derotational osteotomy: surgical indications and outcomes in children with cerebral palsy," *Gait & posture*, vol. 39, no. 2, pp. 778-83, Feb 2014, doi: 10.1016/j.gaitpost.2013.10.016.
- [40] C. Putz, S. I. Wolf, A. Geisbusch, M. Niklasch, L. Doderlein, and T. Dreher, "Femoral derotation osteotomy in adults with cerebral palsy," *Gait & posture*, vol. 49, pp. 290-296, Sep 2016, doi: 10.1016/j.gaitpost.2016.06.034.
- [41] K. H. Sung, S. S. Kwon, C. Y. Chung, K. M. Lee, G. H. Cho, and M. S. Park, "Long-term outcomes over 10 years after femoral derotation osteotomy in ambulatory children with cerebral palsy," *Gait & posture*, vol. 64, pp. 119-125, Jul 2018, doi: 10.1016/j.gaitpost.2018.06.003.
- [42] J. R. Davids, P. Benfanti, D. W. Blackhurst, and B. L. Allen, "Assessment of femoral anteversion in children with cerebral palsy: accuracy of the trochanteric prominence angle test," *J Pediatr Orthop*, vol. 22, no. 2, pp. 173-8, Mar-Apr 2002, doi: 10.1097/00004694-200203000-00007.
- [43] B. A. MacWilliams, M. L. McMulkin, R. B. Davis, D. E. Westberry, G. O. Baird, and P. M. Stevens, "Biomechanical changes associated with femoral derotational osteotomy," *Gait & posture*, vol. 49, pp. 202-206, Sep 2016, doi: 10.1016/j.gaitpost.2016.07.002.
- [44] M. Pirpiris, A. Trivett, R. Baker, J. Rodda, G. R. Nattrass, and H. K. Graham, "Femoral derotation osteotomy in spastic diplegia. Proximal or distal?," (in eng), *The Journal of bone and joint surgery. British volume*, vol. 85, no. 2, pp. 265-72, Mar 2003, doi: 10.1302/0301-620x.85b2.13342.
- [45] C. P. Carty *et al.*, "The effect of femoral derotation osteotomy on transverse plane hip and pelvic kinematics in children with cerebral palsy: a systematic review and meta-analysis," (in eng), *Gait & posture*, vol. 40, no. 3, pp. 333-40, Jul 2014, doi: 10.1016/j.gaitpost.2014.05.066.
- [46] M. H. Schwartz and A. Rozumalski, "The Gait Deviation Index: a new comprehensive index of gait pathology," *Gait & posture*, vol. 28, no. 3, pp. 351-7, Oct 2008, doi: 10.1016/j.gaitpost.2008.05.001.
- [47] R. Baker *et al.*, "The gait profile score and movement analysis profile," *Gait & posture*, vol. 30, no. 3, pp. 265-9, Oct 2009, doi: 10.1016/j.gaitpost.2009.05.020.

- [48] H. Y. Kim, Y. H. Cha, J. Y. Byun, Y. S. Chun, and W. S. Choy, "Changes in gait parameters after femoral derotational osteotomy in cerebral palsy patients with medial femoral torsion," *J Pediatr Orthop B*, vol. 27, no. 3, pp. 194-199, May 2018, doi: 10.1097/BPB.0000000000000467.
- [49] V. Cimolin *et al.*, "The effects of femoral derotation osteotomy in cerebral palsy: a kinematic and kinetic study," *Hip Int*, vol. 21, no. 6, pp. 657-64, Nov-Dec 2011, doi: 10.5301/HIP.2011.8758.
- [50] Boyer, "Corrigendum," *Dev Med Child Neurol*, vol. 60, no. 3, p. 324, Mar 2018, doi: 10.1111/dmcn.13637.
- [51] M. Thielen *et al.*, "Supracondylar femoral rotation osteotomy affects frontal hip kinetics in children with bilateral cerebral palsy," *Dev Med Child Neurol*, vol. 61, no. 3, pp. 322-328, Mar 2019, doi: 10.1111/dmcn.14035.
- [52] C. Church *et al.*, "Persistence and Recurrence Following Femoral Derotational Osteotomy in Ambulatory Children With Cerebral Palsy," *J Pediatr Orthop*, vol. 37, no. 7, pp. 447-453, Oct/Nov 2017, doi: 10.1097/BPO.0000000000000701.
- [53] S. Ounpuu, M. Solomito, K. Bell, and K. Pierz, "Long-term outcomes of external femoral derotation osteotomies in children with cerebral palsy," *Gait & posture*, vol. 56, pp. 82-88, Jul 2017, doi: 10.1016/j.gaitpost.2017.04.029.
- [54] M. Niklasch *et al.*, "Factors associated with recurrence after femoral derotation osteotomy in cerebral palsy," *Gait & posture*, vol. 42, no. 4, pp. 460-5, Oct 2015, doi: 10.1016/j.gaitpost.2015.07.059.
- [55] H. Kim, M. Aiona, and M. Sussman, "Recurrence after femoral derotational osteotomy in cerebral palsy," *J Pediatr Orthop*, vol. 25, no. 6, pp. 739-43, Nov-Dec 2005, doi: 10.1097/01.bpo.0000173304.34172.06.
- [56] M. Niklasch, M. C. Klotz, S. I. Wolf, and T. Dreher, "Long-term development of overcorrection after femoral derotation osteotomy in children with cerebral palsy," *Gait & posture*, vol. 61, pp. 183-187, Mar 2018, doi: 10.1016/j.gaitpost.2018.01.012.
- [57] R. Baker, "Gait analysis methods in rehabilitation," *J Neuroeng Rehabil*, journal article vol. 3, no. 1, p. 4, Mar 2 2006, doi: 10.1186/1743-0003-3-4.
- [58] R. B. Davis, S. Ounpuu, D. Tyburski, and J. R. Gage, "A Gait Analysis Data-Collection and Reduction Technique," (in English), *Hum Movement Sci*, vol. 10, no. 5, pp. 575-587, Oct 1991, doi: Doi 10.1016/0167-9457(91)90046-Z.
- [59] M. P. Kadaba, H. K. Ramakrishnan, and M. E. Wootten, "Measurement of lower extremity kinematics during level walking," *J Orthop Res*, vol. 8, no. 3, pp. 383-92, May 1990, doi: 10.1002/jor.1100080310.
- [60] A. Cappozzo, U. Della Croce, A. Leardini, and L. Chiari, "Human movement analysis using stereophotogrammetry. Part 1: theoretical background," (in English), *Gait & posture*, vol. 21, no. 2, pp. 186-96, Feb 2005, doi: 10.1016/j.gaitpost.2004.01.010.
- [61] H. Kainz and M. H. Schwartz, "The importance of a consistent workflow to estimate muscle-tendon lengths based on joint angles from the conventional

- gait model," *Gait & posture*, vol. 88, pp. 1-9, 2021/07/01/ 2021, doi: <https://doi.org/10.1016/j.gaitpost.2021.04.039>.
- [62] M. Wesseling, E. C. Ranz, and I. Jonkers, "Objectifying Treatment Outcomes Using Musculoskeletal Modelling-Based Simulations of Motion," in *Handbook of Human Motion*, B. Müller *et al.* Eds. Cham: Springer International Publishing, 2018, ch. Chapter 52-1, pp. 1-25.
- [63] B. J. Fregly, "A Conceptual Blueprint for Making Neuromusculoskeletal Models Clinically Useful," *Applied Sciences*, vol. 11, no. 5, p. 2037, 2021. [Online]. Available: <https://www.mdpi.com/2076-3417/11/5/2037>.
- [64] B. H. F. J. M. Koopman, "Dynamics of human movement," (in English), *Technol Health Care*, vol. 18, no. 4-5, pp. 371-385, 2010, doi: 10.3233/Thc-2010-0599.
- [65] S. L. Delp, J. P. Loan, M. G. Hoy, F. E. Zajac, E. L. Topp, and J. M. Rosen, "An interactive graphics-based model of the lower extremity to study orthopaedic surgical procedures," (in English), *Ieee T Bio-Med Eng*, vol. 37, no. 8, pp. 757-67, Aug 1990, doi: 10.1109/10.102791.
- [66] V. Carbone, M. M. van der Krogt, H. F. J. M. Koopman, and N. Verdonshot, "Sensitivity of subject-specific models to errors in musculo-skeletal geometry," *Journal of Biomechanics*, vol. 45, no. 14, pp. 2476-2480, 2012/09/21/ 2012, doi: <https://doi.org/10.1016/j.jbiomech.2012.06.026>.
- [67] L. Scheys, K. Desloovere, P. Suetens, and I. Jonkers, "Level of subject-specific detail in musculoskeletal models affects hip moment arm length calculation during gait in pediatric subjects with increased femoral anteversion," *Journal of Biomechanics*, vol. 44, no. 7, pp. 1346-1353, 2011/04/29/ 2011, doi: <https://doi.org/10.1016/j.jbiomech.2011.01.001>.
- [68] L. Bosmans *et al.*, "Sensitivity of predicted muscle forces during gait to anatomical variability in musculotendon geometry," (in English), *J Biomech*, vol. 48, no. 10, pp. 2116-23, Jul 16 2015, doi: 10.1016/j.jbiomech.2015.02.052.
- [69] D. G. Thelen, "Adjustment of Muscle Mechanics Model Parameters to Simulate Dynamic Contractions in Older Adults," *Journal of biomechanical engineering*, vol. 125, no. 1, pp. 70-77, 2003, doi: 10.1115/1.1531112.
- [70] F. E. Zajac, "Muscle and tendon: properties, models, scaling, and application to biomechanics and motor control," *Crit Rev Biomed Eng*, vol. 17, no. 4, pp. 359-411, 1989. [Online]. Available: <https://www.ncbi.nlm.nih.gov/pubmed/2676342>.
- [71] J. A. Friederich and R. A. Brand, "Muscle fiber architecture in the human lower limb," *Journal of Biomechanics*, vol. 23, no. 1, pp. 91-95, 1990/01/01/ 1990, doi: [https://doi.org/10.1016/0021-9290\(90\)90373-B](https://doi.org/10.1016/0021-9290(90)90373-B).
- [72] W. Vr, "Muscle Architecture of the Human Lower Limb," *Clinical orthopaedics and related research.*, vol. 179, no. 179, pp. 275-283, 1983, doi: info:doi/.
- [73] E. Montefiori, B. M. Kalkman, W. H. Henson, M. A. Paggiosi, E. V. McCloskey, and C. Mazzà, "MRI-based anatomical characterisation of lower-limb muscles in older women," *PLOS ONE*, vol. 15, no. 12, p. e0242973, 2020, doi: 10.1371/journal.pone.0242973.

- [74] J. P. Charles, C.-H. Moon, and W. J. Anderst, "Determining Subject-Specific Lower-Limb Muscle Architecture Data for Musculoskeletal Models Using Diffusion Tensor Imaging," *Journal of biomechanical engineering*, vol. 141, no. 6, 2019, doi: 10.1115/1.4040946.
- [75] A. Erdemir, S. McLean, W. Herzog, and A. J. van den Bogert, "Model-based estimation of muscle forces exerted during movements," *Clinical biomechanics*, vol. 22, no. 2, pp. 131-154, 2007. [Online]. Available: [https://www.clinbiomech.com/article/S0268-0033\(06\)00183-5/fulltext](https://www.clinbiomech.com/article/S0268-0033(06)00183-5/fulltext).
- [76] D. Tsirakos, V. Baltzopoulos, and R. Bartlett, "Inverse optimization: functional and physiological considerations related to the force-sharing problem," (in eng), *Crit Rev Biomed Eng*, vol. 25, no. 4-5, pp. 371-407, 1997, doi: 10.1615/critrevbiomedeng.v25.i4-5.20.
- [77] Y.-C. Lin, T. W. Dorn, A. G. Schache, and M. G. Pandy, "Comparison of different methods for estimating muscle forces in human movement," *Proceedings of the Institution of Mechanical Engineers, Part H: Journal of Engineering in Medicine*, vol. 226, no. 2, pp. 103-112, 2012, doi: 10.1177/0954411911429401.
- [78] L. Modenese, A. T. Phillips, and A. M. Bull, "An open source lower limb model: Hip joint validation," *J Biomech*, vol. 44, no. 12, pp. 2185-93, Aug 11 2011, doi: 10.1016/j.jbiomech.2011.06.019.
- [79] B. A. Garner and M. G. Pandy, "The Obstacle-Set Method for Representing Muscle Paths in Musculoskeletal Models," *Computer Methods in Biomechanics and Biomedical Engineering*, vol. 3, no. 1, pp. 1-30, 2000/01/01 2000, doi: 10.1080/10255840008915251.
- [80] T. A. Correa, R. Baker, H. K. Graham, and M. G. Pandy, "Accuracy of generic musculoskeletal models in predicting the functional roles of muscles in human gait," (in English), *J Biomech*, vol. 44, no. 11, pp. 2096-105, Jul 28 2011, doi: 10.1016/j.jbiomech.2011.05.023.
- [81] E. M. Arnold, S. R. Ward, R. L. Lieber, and S. L. Delp, "A model of the lower limb for analysis of human movement," *Ann Biomed Eng*, vol. 38, no. 2, pp. 269-79, Feb 2010, doi: 10.1007/s10439-009-9852-5.
- [82] S. R. Hamner, A. Seth, and S. L. Delp, "Muscle contributions to propulsion and support during running," *Journal of Biomechanics*, vol. 43, no. 14, pp. 2709-2716, 2010/10/19/ 2010, doi: <https://doi.org/10.1016/j.jbiomech.2010.06.025>.
- [83] S. S. Blemker, D. S. Asakawa, G. E. Gold, and S. L. Delp, "Image-based musculoskeletal modeling: applications, advances, and future opportunities," (in English), *J Magn Reson Imaging*, vol. 25, no. 2, pp. 441-51, Feb 2007, doi: 10.1002/jmri.20805.
- [84] Z. Ding, C. K. Tsang, D. Nolte, A. E. Kedgley, and A. M. J. Bull, "Improving Musculoskeletal Model Scaling Using an Anatomical Atlas: The Importance of Gender and Anthropometric Similarity to Quantify Joint Reaction Forces," *IEEE Transactions on Biomedical Engineering*, vol. 66, no. 12, pp. 3444-3456, 2019, doi: 10.1109/tbme.2019.2905956.

- [85] R. L. Lieber and J. Fridén, "Functional and clinical significance of skeletal muscle architecture," *Muscle & Nerve*, vol. 23, no. 11, pp. 1647-1666, 2000, doi: [https://doi.org/10.1002/1097-4598\(200011\)23:11<1647::AID-MUS1>3.0.CO;2-M](https://doi.org/10.1002/1097-4598(200011)23:11<1647::AID-MUS1>3.0.CO;2-M).
- [86] L. Modenese, E. Montefiori, A. Wang, S. Wesarg, M. Viceconti, and C. Mazza, "Investigation of the dependence of joint contact forces on musculotendon parameters using a codified workflow for image-based modelling," (in English), *J Biomech*, vol. 73, pp. 108-118, May 17 2018, doi: 10.1016/j.jbiomech.2018.03.039.
- [87] R. Hainisch, M. Gfoehler, M. Zubayer-UI-Karim, and M. G. Pandy, "Method for determining musculotendon parameters in subject-specific musculoskeletal models of children developed from MRI data," (in English), *Multibody Syst Dyn*, vol. 28, no. 1-2, pp. 143-156, Aug 2012, doi: 10.1007/s11044-011-9289-0.
- [88] N. Thompson, J. Stebbins, M. Seniorou, and D. Newham, "Muscle strength and walking ability in Diplegic Cerebral Palsy: Implications for assessment and management," *Gait & posture*, vol. 33, no. 3, pp. 321-325, 2011/03/01/ 2011, doi: <https://doi.org/10.1016/j.gaitpost.2010.10.091>.
- [89] M. E. Wiley and D. L. Damiano, "Lower-Extremity strength profiles in spastic cerebral palsy," *Developmental Medicine & Child Neurology*, vol. 40, no. 2, pp. 100-107, 2008, doi: 10.1111/j.1469-8749.1998.tb15369.x.
- [90] M. M. van der Krogt, L. Bar-On, T. Kindt, K. Desloovere, and J. Harlaar, "Neuro-musculoskeletal simulation of instrumented contracture and spasticity assessment in children with cerebral palsy," (in English), *J Neuroeng Rehabil*, vol. 13, no. 1, p. 64, Jul 16 2016, doi: 10.1186/s12984-016-0170-5.
- [91] T. A. Correa and M. G. Pandy, "A mass-length scaling law for modeling muscle strength in the lower limb," (in English), *J Biomech*, vol. 44, no. 16, pp. 2782-9, Nov 10 2011, doi: 10.1016/j.jbiomech.2011.08.024.
- [92] H. Kainz *et al.*, "The influence of maximum isometric muscle force scaling on estimated muscle forces from musculoskeletal models of children with cerebral palsy," (in English), *Gait & posture*, vol. 65, pp. 213-220, Sep 2018, doi: 10.1016/j.gaitpost.2018.07.172.
- [93] M. Wesseling *et al.*, "Subject-specific musculoskeletal modelling in patients before and after total hip arthroplasty," (in English), *Comput Method Biomec*, vol. 19, no. 15, pp. 1683-91, Nov 2016, doi: 10.1080/10255842.2016.1181174.
- [94] R. Akagi, Y. Takai, M. Ohta, H. Kanehisa, Y. Kawakami, and T. Fukunaga, "Muscle volume compared to cross-sectional area is more appropriate for evaluating muscle strength in young and elderly individuals," *Age Ageing*, vol. 38, no. 5, pp. 564-569, 2009, doi: 10.1093/ageing/afp122.
- [95] S. L. Delp and J. P. Loan, "A graphics-based software system to develop and analyze models of musculoskeletal structures," *Computers in Biology and Medicine*, vol. 25, no. 1, pp. 21-34, 1995/01/01/ 1995, doi: [https://doi.org/10.1016/0010-4825\(95\)98882-E](https://doi.org/10.1016/0010-4825(95)98882-E).
- [96] M. Damsgaard, J. Rasmussen, S. T. Christensen, E. Surma, and M. de Zee, "Analysis of musculoskeletal systems in the AnyBody Modeling System,"

- Simulation Modelling Practice and Theory*, vol. 14, no. 8, pp. 1100-1111, 2006/11/01/ 2006, doi: <https://doi.org/10.1016/j.simpat.2006.09.001>.
- [97] S. L. Delp *et al.*, "OpenSim: open-source software to create and analyze dynamic simulations of movement," (in English), *Ieee T Bio-Med Eng*, vol. 54, no. 11, pp. 1940-50, Nov 2007, doi: 10.1109/TBME.2007.901024.
- [98] T. W. Lu and J. J. O'Connor, "Bone position estimation from skin marker coordinates using global optimisation with joint constraints," (in English), *Journal of Biomechanics*, vol. 32, no. 2, pp. 129-134, Feb 1999, doi: Doi 10.1016/S0021-9290(98)00158-4.
- [99] R. D. Crowninshield and R. A. Brand, "The prediction of forces in joint structures; distribution of intersegmental resultants," *Exerc Sport Sci Rev*, vol. 9, pp. 159-81, 1981. [Online]. Available: <https://www.ncbi.nlm.nih.gov/pubmed/6749521>.
- [100] R. D. Crowninshield and R. A. Brand, "A physiologically based criterion of muscle force prediction in locomotion," *J Biomech*, vol. 14, no. 11, pp. 793-801, 1981, doi: 10.1016/0021-9290(81)90035-x.
- [101] F. C. Anderson and M. G. Pandy, "Static and dynamic optimization solutions for gait are practically equivalent," *J Biomech*, vol. 34, no. 2, pp. 153-61, Feb 2001, doi: 10.1016/s0021-9290(00)00155-x.
- [102] M. Wesseling *et al.*, "Muscle optimization techniques impact the magnitude of calculated hip joint contact forces," *Journal of Orthopaedic Research*, vol. 33, no. 3, pp. 430-438, 2015, doi: 10.1002/jor.22769.
- [103] F. De Groote *et al.*, "A physiology based inverse dynamic analysis of human gait: potential and perspectives," *Computer Methods in Biomechanics and Biomedical Engineering*, vol. 12, no. 5, pp. 563-574, 2009, doi: 10.1080/10255840902788587.
- [104] F. De Groote, B. Demeulenaere, J. Swevers, J. De Schutter, and I. Jonkers, "A physiology-based inverse dynamic analysis of human gait using sequential convex programming: a comparative study," *Computer Methods in Biomechanics and Biomedical Engineering*, vol. 15, no. 10, pp. 1093-1102, 2012, doi: 10.1080/10255842.2011.571679.
- [105] F. De Groote, A. L. Kinney, A. V. Rao, and B. J. Fregly, "Evaluation of Direct Collocation Optimal Control Problem Formulations for Solving the Muscle Redundancy Problem," *Annals of Biomedical Engineering*, vol. 44, no. 10, pp. 2922-2936, 2016, doi: 10.1007/s10439-016-1591-9.
- [106] K. M. Steele, M. S. Demers, M. H. Schwartz, and S. L. Delp, "Compressive tibiofemoral force during crouch gait," (in English), *Gait & posture*, vol. 35, no. 4, pp. 556-60, Apr 2012, doi: 10.1016/j.gaitpost.2011.11.023.
- [107] L. Scheys, A. Spaepen, P. Suetens, and I. Jonkers, "Calculated moment-arm and muscle-tendon lengths during gait differ substantially using MR based versus rescaled generic lower-limb musculoskeletal models," (in English), *Gait & posture*, vol. 28, no. 4, pp. 640-8, Nov 2008, doi: 10.1016/j.gaitpost.2008.04.010.

- [108] L. Scheys, A. Van Campenhout, A. Spaepen, P. Suetens, and I. Jonkers, "Personalized MR-based musculoskeletal models compared to rescaled generic models in the presence of increased femoral anteversion: effect on hip moment arm lengths," *Gait & posture*, vol. 28, no. 3, pp. 358-65, Oct 2008, doi: 10.1016/j.gaitpost.2008.05.002.
- [109] K. M. Steele, A. Rozumalski, and M. H. Schwartz, "Muscle synergies and complexity of neuromuscular control during gait in cerebral palsy," *Dev Med Child Neurol*, vol. 57, no. 12, pp. 1176-82, Dec 2015, doi: 10.1111/dmcn.12826.
- [110] D. G. Lloyd and T. F. Besier, "An EMG-driven musculoskeletal model to estimate muscle forces and knee joint moments in vivo," *J Biomech*, vol. 36, no. 6, pp. 765-76, Jun 2003, doi: 10.1016/s0021-9290(03)00010-1.
- [111] J. L. Hicks, M. H. Schwartz, A. S. Arnold, and S. L. Delp, "Crouched postures reduce the capacity of muscles to extend the hip and knee during the single-limb stance phase of gait," (in eng), *J Biomech*, vol. 41, no. 5, pp. 960-7, 2008, doi: 10.1016/j.jbiomech.2008.01.002.
- [112] A. Carriero *et al.*, "Influence of altered gait patterns on the hip joint contact forces," (in English), *Comput Method Biomec*, vol. 17, no. 4, pp. 352-9, Mar 12 2014, doi: 10.1080/10255842.2012.683575.
- [113] H. Kainz *et al.*, "Selective dorsal rhizotomy improves muscle forces during walking in children with spastic cerebral palsy," *Clin Biomech*, vol. 65, pp. 26-33, May 2019, doi: 10.1016/j.clinbiomech.2019.03.014.
- [114] S. Van Rossom *et al.*, "Single-event multilevel surgery, but not botulinum toxin injections normalize joint loading in cerebral palsy patients," *Clin Biomech*, vol. 76, p. 105025, Jun 2020, doi: 10.1016/j.clinbiomech.2020.105025.
- [115] L. Pitto *et al.*, "SimCP: A Simulation Platform to Predict Gait Performance Following Orthopedic Intervention in Children With Cerebral Palsy," (in eng), *Front Neurorobot*, vol. 13, pp. 54-54, 2019, doi: 10.3389/fnbot.2019.00054.
- [116] M. H. Schwartz, A. Rozumalski, and K. M. Steele, "Dynamic motor control is associated with treatment outcomes for children with cerebral palsy," *Developmental Medicine & Child Neurology*, vol. 58, no. 11, pp. 1139-1145, 2016, doi: 10.1111/dmcn.13126.
- [117] T. Dreher *et al.*, "Long-term outcome of femoral derotation osteotomy in children with spastic diplegia," *Gait & posture*, vol. 36, no. 3, pp. 467-70, Jul 2012, doi: 10.1016/j.gaitpost.2012.04.017.
- [118] A. Rajagopal, Ł. Kidziński, A. S. McGlaughlin, J. L. Hicks, S. L. Delp, and M. H. Schwartz, "Pre-operative gastrocnemius lengths in gait predict outcomes following gastrocnemius lengthening surgery in children with cerebral palsy," *PLOS ONE*, vol. 15, no. 6, p. e0233706, 2020, doi: 10.1371/journal.pone.0233706.

### **3 Effect of lower limb marker set on musculoskeletal model predictions of joint kinematics in a juvenile population**



### **3.1 Summary**

This research involves the use of retrospective gait analysis data and this may present a challenge in terms of the level of control of specifications in the data collection process. One such specification is the number and location of retroreflective markers used during the data acquisition. In this chapter, results of a study investigating the effect of reducing the number of markers used in the scaling, pose estimation and kinematic simulation of generic and personalised models are reported. These results serve as a means to understanding the challenges that may be presented going forward with the available research data.

### **3.2 Introduction**

Clinical gait analysis is a process of investigation used in the assessment of human movement disorders such as Cerebral Palsy, usually in the clinical setting with the aim of making suggestions towards treatment [1, 2] and evaluating outcomes following an intervention. While it employs different techniques and tools, a major component of the setup for gait analysis is the stereophotogrammetrical system for capturing the trajectories of reflective markers placed on the body from which the motion of the subject's bones can be reconstructed. From these reconstructions, the joint angles associated with both normal and pathological gait can be extracted.

The number of markers used in an acquisition were previously limited by the available technology, but modern systems are far improved and allow for the use of a large number of markers meaning that other considerations drive this decision particularly the resolution of the motion being captured and the practicability of using those markers. For instance, in children particularly those with pathology, placement of a substantial number of markers can be time consuming and cumbersome and as such a minimal set of markers may be used unless otherwise indicated [3]. Decisions on the choice of the marker sets are also driven by the associated kinematic models which are used to describe the motion of the joints. A kinematic model provides a mathematical description of how the markers are used to define the body segments, intersegmental joints and their degrees of freedom, as well as any constraints from which the desired kinematics can then be obtained. The most common marker set and kinematic model in current use in clinical settings is the PlugIn Gait model (Vicon, Oxford, UK), a variant of the so called conventional gait model proposed by Kadaba, et al. [4] and Davis, et al. [5].

It is well acknowledged that the marker set and kinematic biomechanical model used introduce differences in the estimated biomechanical gait variables with several studies reporting on this. In a study that compared five universally used protocols that

differed for marker set and kinematic model, it was reported that while protocol intra-repeatability was good for each of the protocols, there were also differences observed in estimated non-sagittal plane rotations particularly where the models used were not similar [6]. This was similar to the findings of Schulz and Kimmel [7] who reported limited differences between different configurations of marker sets for sagittal plane motions but also showed that the selection of marker sets was significantly impacting the analysis of non-sagittal motions at the hip and knee. Similarly, Collins, et al. [8] investigated and compared the repeatability of a six degrees of freedom kinematic model and its associated marker set to the conventional model and found comparable performance for the two methods although there were also clear differences between methods in joint angle estimates particularly for the non-sagittal plane movements. In all these studies, joint angles were estimated using unconstrained models and a computational approach known as direct kinematics where the orientation and pose of the body segments are determined directly from the marker locations in three-dimensional space.

An alternative is the use of skeletal kinematic models that permit the estimation of joint kinematics in a similar manner, with the added advantage of being able quantify muscle forces and joint loads when information about muscles is included to create a musculoskeletal model. By their nature of mimicking the physiological function of joints, particularly in terms of the constraints they apply as described in the introductory chapter, they are able to minimise the effect of soft tissue artefact [9] a challenge with the conventional model and the use of direct kinematics. This notwithstanding they also depend on the marker sets from motion capture and are thus susceptible to the influences of marker quantity and placement. While the literature is limited on the subject in musculoskeletal models, Slater, et al. [10] in a recent study, evaluated the effect different numbers of markers on the thigh and shank had on joint angle estimates using a constrained kinematic model with a multibody optimisation approach and found that the estimated kinematics was robust to the placement and quantity of markers and went on to propose a minimal set of markers that could be used to achieve similar performance to a traditionally used marker set configuration. On the other hand, Mantovani and Lamontagne [11] found significant differences between marker sets in their estimates of range of motion as well as clinically relevant values of minimum detectable changes. Both these studies were however limited to using a scaled generic model. It has been suggested that personalising joints as in a personalised constrained kinematic model can help enhance the reduction of soft tissue artefact effects in kinematics obtained with musculoskeletal models and multibody optimisation [12, 13]. What impact this personalisation would have on the relationship between marker quantity and joint

kinematics is however unclear. It would also be of interest to know how this compares to the scaled generic model, given that the personalised models have been shown to increase accuracy and reliability [14-19].

In this light, the primary aim of this study is to verify the hypothesis that marker quantity and placement would have less impact in a personalised constrained kinematic model than in a scaled generic model. Moreover, the impact of quantity and placement of markers during experimental data collection on joint kinematics estimated with a global optimisation approach using personalised and generic musculoskeletal models will be assessed.

### **3.3 Methods**

#### **3.3.1 Participants and data collection**

A subset of available gait analysis and Magnetic Resonance Imaging (MRI) data collected as part of the EU-funded MD-Paedigree project (p. no. 600932) were retrospectively analysed in this study. Briefly, 14 juvenile participants (mass:  $42.3 \pm 17.0$  kg, height:  $1.41 \pm 0.16$  m, age:  $11.0 \pm 3.3$  years) had instrumented gait analysis data collected using a set of 44 markers that consisted of the commonly used Vicon PlugIn gait protocol markers (Vicon, Oxford, UK) and the modified Oxford Foot Model [20, 21]. This full set of markers (44 markers) together with three other configurations were used in the subsequent analysis by reducing the number of markers used for scaling and tracking during inverse kinematics. The four configurations were: (1) the full set of markers (M1), (2) markers on just anatomical and palpable landmarks (M2), (3) PlugIn gait with a Sheffield Foot Model (M3)[22] and (4) the minimal PlugIn gait marker set (M4) as detailed in Table 3.1. Participants had at least three gait trials walking at a self-selected speed collected. Given that the M1 marker set did not include a sacrum (SACR) marker at the pelvis, the midpoint of two experimental markers on the posterior iliac spine (PSIS) were used to approximate its location for use in M3 and M4.

#### **3.3.2 Scaled generic kinematic skeletal model**

A generic lower-limb musculoskeletal model (gait2392 model [23]) comprising a 3 degree of freedom (DoF) hip, hinge knee (1 DoF), and ankle complex (tibiotalar and subtalar, 2 DoF) joint was used. Scaling of the generic model was performed using the static standing trial per participant following recommendation [24]. Scaling of the model to match each subject's anthropometry was achieved by scaling distances between pairs of markers placed on the generic model to replicate corresponding locations on the body in the experimental data collected during motion capture. The

femur and tibia were scaled isotropically whereas the pelvis was scaled nonuniformly in three dimensions for all marker configurations. Scaling of the foot segment was done isotropically using the heel (HEE) and toe (TOE) markers as these were the only markers on the foot present in all four groups. The scaled model was reduced to a mono-lateral right limb for the subsequent analysis.

### **3.3.3 Image-based kinematic skeletal model**

For each participant, Magnetic Resonance Imaging (MRI)-based models constructed as part of a previous study [25] were also evaluated. Briefly, to construct the model, foot and ankle regional MRI (multi-slice multi-echo 3D gradient echo with water only selection, 0.5 mm in-plane resolution and 1 mm slice thickness) were collected at an initial point and six months later lower limb MRI images were obtained using a T1-weighted fat-suppression imaging sequence. Segmented bone geometries from the MRI were combined and used to build the models in NMS Builder [26] following a previously published pipeline [27]. These were also mono-lateral lower-limb models of the right limb with a 3-DoF hip, 1-DoF knee and 2-DoF ankle complex comprising tibiotalar and subtalar joints.

### **3.3.4 Simulation and data analysis**

The above processes yielded 14 sets of models per marker set pipeline and model type. Static pose estimation was subsequently run using the marker placer tool in OpenSim3.3. Joint angles in the static pose were then extracted for each subject for all pipelines and models.

All models were subsequently simulated using the inverse kinematics tool in OpenSim 3.3 to determine the joint angles over the gait cycle. Marker weights (Table 3.1) were based on anatomical location with those on bony landmarks weighted higher. Weights were maintained across all scenarios of marker quantity for inverse kinematics. Additionally, all output kinematic curves were time normalised to 100% of the gait cycle. Two levels of analysis were performed from the outputs of the simulations. The first level of comparison focussed on differences between the marker set outputs for the generic and MRI-based model. For each model, estimated static pose joint angles were compared between the four marker groups using a repeated measures analysis of variance. Joint angles in static pose classed as significantly different between groups were analysed with a post hoc test (paired sample t-tests) with Bonferroni correction. The estimated dynamic joint angles were compared between groups after subtracting the static pose angles (to remove offsets due to differences in anatomical axes definitions between the generic and MRI-based model) to determine curve similarity

using the Root Mean Square Difference (RMSD). The coefficient of determination was also calculated between marker group curves for the same model. To determine phases of the gait cycle where there were differences between marker pipelines, a non-parametric one-way repeated measures analysis of variance (ANOVA) test using the statistical parametric mapping (SPM) package (v0.4.5, [28, 29]) in MATLAB (v2018b, MathWorks). Alpha was set to 0.0056 after a Bonferroni correction for multiple comparisons (9 comparisons). Joint range of motion extracted from the gait kinematics curves were also compared using repeated measures ANOVA and post-hoc tests where significance was observed. To assess the reliability and sensitivity of the ROM estimates to marker set pipeline, the intraclass correlation coefficient (ICC) was used. All statistics were carried out in SPSS v25 (IBM Corp., Armonk, NY).

**Table 3.1 Summary of markers used in static pose estimation and inverse kinematics.**

Segment	Marker	Position	M1	M2	M3	M4	Weight
Pelvis	PSI	Posterior superior iliac spine	✓	✓			10
	ASI	Anterior superior iliac spine	✓	✓	✓	✓	10
	SACR	Sacrum (midpoint of PSI)			✓	✓	10
Femur	TRO	Greater trochanter	✓	✓			5
	THI	Thigh	✓		✓	✓	3
	KNE	Lateral femur condyle	✓	✓	✓	✓	10
	MFC	Medial femur condyle	✓*	✓*			10
Tibia	HFB	Head of fibula	✓	✓			5
	TUB	Tibial tuberosity	✓	✓			5
	SHN	Anterior aspect of shin	✓		✓	✓	3
	ANK	Lateral malleolus	✓	✓	✓	✓	10
	MMA	Medial malleolus	✓*	✓*	✓*	✓*	10
Calcaneus	D1M	Distal first metatarsal	✓*	✓*	✓*		5
	D5M	Distal fifth metatarsal	✓	✓	✓		5
	P1M	Proximal first metatarsal	✓	✓			5
	P5M	Proximal fifth metatarsal	✓	✓			5
	STL	Sustentaculum tali	✓				3
	LCA	Lateral calcaneus	✓				3

	PCA	Posterior medial aspect of heel	✓				1
	CPG	Wand marker on posterior calcaneus	✓				1
	HEE	Heel	✓	✓	✓	✓	10
Toes	TOE	Between 2nd and 3rd metatarsal heads	✓	✓	✓	✓	10
	HLX	Base of hallux	✓				3
No. of markers			22	15	11	9	

\*Not used in dynamic IK

For the between-models comparisons, Pearson's correlations ( $r$ ) were calculated for the static joint angles to determine the agreement between estimates from either model. The ensemble mean kinematic curves from each model were also compared using the non-parametric paired sample t-test package from the SPM toolbox in MATLAB. The alpha level was corrected for multiple comparisons. Additionally, and for each of the marker pipelines, the RMSD was calculated in addition to the coefficient of determination ( $R^2$ ) to assess levels of curve similarity. RMSD between models for each joint angle was assessed for normality and then compared between marker pipelines using a one-way repeated measures ANOVA when normally distributed with Bonferroni-corrected post-hoc tests. Where normality was not met, comparisons were with a Friedman's test and Dunn's correction for multiple comparisons.

### 3.4 Results

Table 3.2 shows the correlations between the generic and MR model estimates of participant static poses for the different joints and markers. Static pose angles for the three pelvis rotations, hip flexion and hip rotation were strongly correlated (Pearson's  $r > 0.7$ ) for all marker pipelines. The correlations decreased in strength for the distal joints especially for ankle dorsiflexion (M1 and M2) and subtalar inversion (all marker pipelines). Additionally, significant inter-model differences in the static pose angles were found for pelvis tilt and hip flexion for all the marker pipelines (Figure 3.1).

Average RMSD of kinematic curves across all joints between MR based and generic models were  $2.5^\circ \pm 0.9^\circ$ ,  $2.5^\circ \pm 1.0^\circ$ ,  $3.5^\circ \pm 1.5^\circ$  and  $3.7^\circ \pm 1.5^\circ$  for M1, M2, M3 and M4, respectively. Figure 3.2 shows the distribution of inter-model RMSD for individual joints, with the largest differences for all marker sets recorded for hip rotation.

**Table 3.2 Correlation between static pose estimates between generic and MR model for the four marker pipelines.**

	Pearson's correlation (r)			
	M1	M2	M3	M4
Pelvis tilt	0.93	0.93	0.90	0.90
Pelvis list	0.94	0.96	0.94	0.95
Pelvis rot	0.95	0.94	0.95	0.94
Hip flexion	0.88	0.89	0.86	0.88
Hip ab/adduction	0.89	0.90	0.91	0.92
Hip rotation	0.67*	0.65*	0.49*	0.38*
Knee flexion	0.72	0.72	0.49*	0.53*
Ankle plantar/dorsiflexion	0.23*	0.21*	0.59*	0.53*
Subtalar inv/eversion	0.15*	0.15*	-0.03*	0.29*

\* non-significant ( $p > 0.0056$ ) correlations

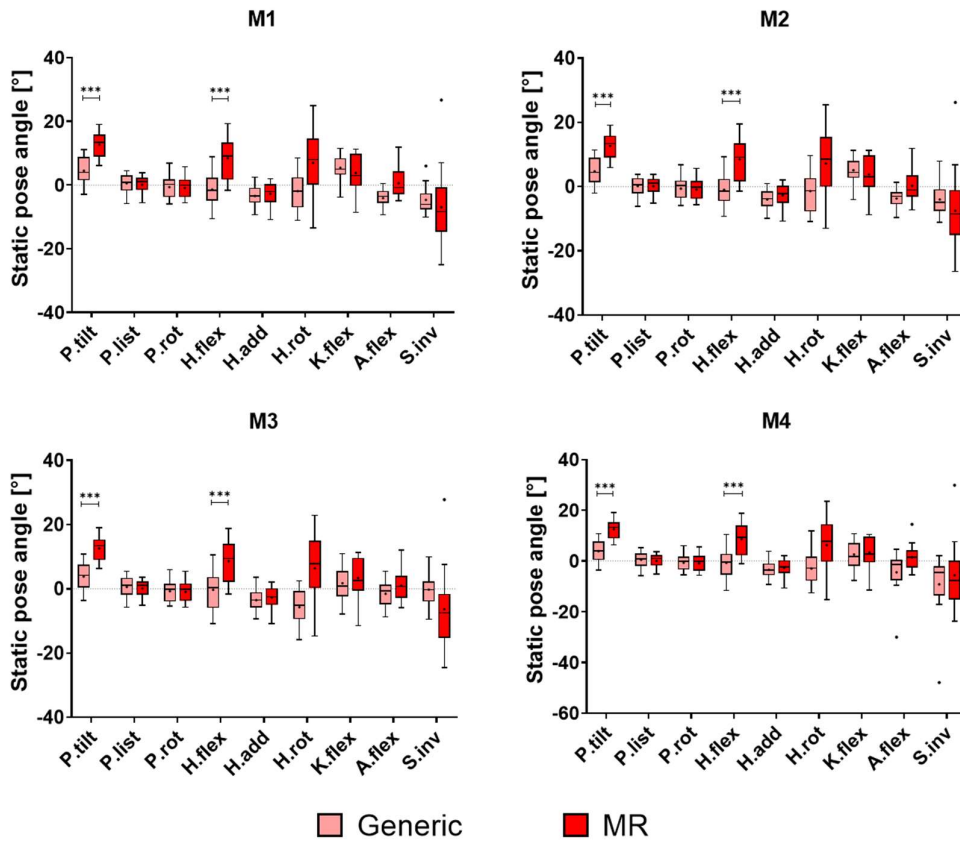


**Figure 3.1 Inter-model comparison of static pose angles for the four marker sets. \*\*\* $p < 0.01$**

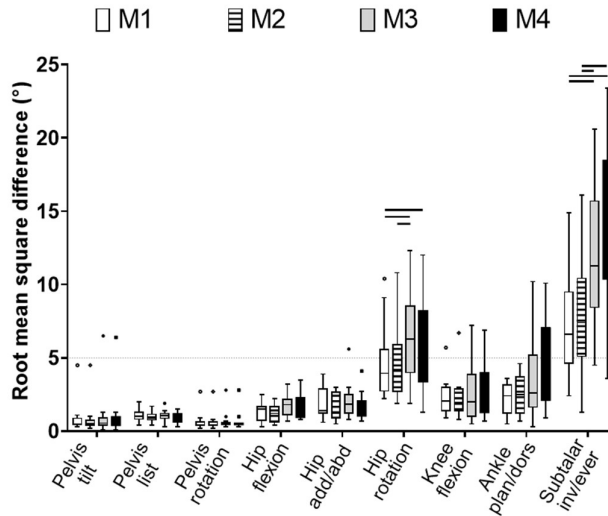


**Figure 3.2 RMSD between MRI-based and Gen models for all four marker set configurations. Horizontal bars indicate significant difference between marker pipelines**

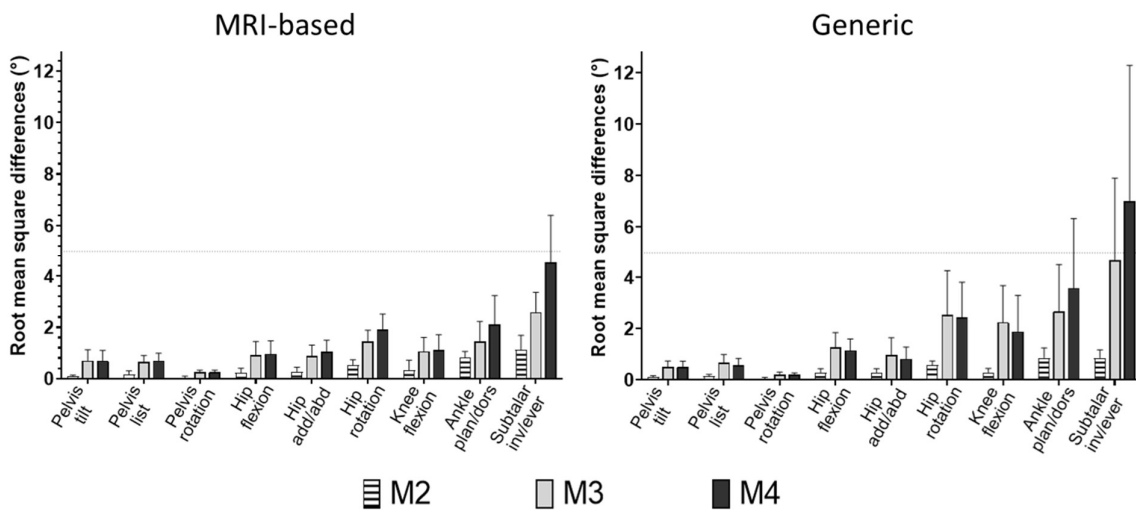


**Figure 3.3 Mean root mean square differences for the comparison of joint kinematics between M1 and three other marker sets (M2, M3, and M4) for the MRI-based and scaled generic models.**

The hip rotation RMSDs between models were also significantly different between the maximal (M1 and M2) marker sets and the least (M3 and M4). Similarly, the coefficient of determination between models averaged across all joints was high (minimum  $R^2 = 0.90 \pm 0.08$ ) for all marker sets. The subtalar joint angle had the lowest  $R^2$  (range: 0.40 - 0.67) of all the joints followed by hip rotation (range: 0.65 - 0.76).



For the MRI-based model, average RMSD in kinematics between M1 and the three other marker pipelines were less than 3° for all the joint angles compared bar the subtalar angle (Figure 3.3). This was similar for all comparisons in the scaled generic model, except for those between M1, M3 and M4 where the RMSDs increased above 3° for hip rotation, knee flexion, ankle plantarflexion and subtalar inversion (Figure 3.3).

The kinematic waveforms for the generic and MR models using the same marker set were not significantly different for pelvic tilt, pelvic list and ankle plantar/dorsiflexion. Knee flexion angles were similar for all markers except M1. Hip rotation was the one that differed the most over the gait cycle, with the generic model tending to estimate more internal rotation than the MR model. This was observed as a positive offset of the generic estimate from the MR estimate. Plots for the inter-model kinematic waveform comparison are shown in Figures 3.4 - 3.7.

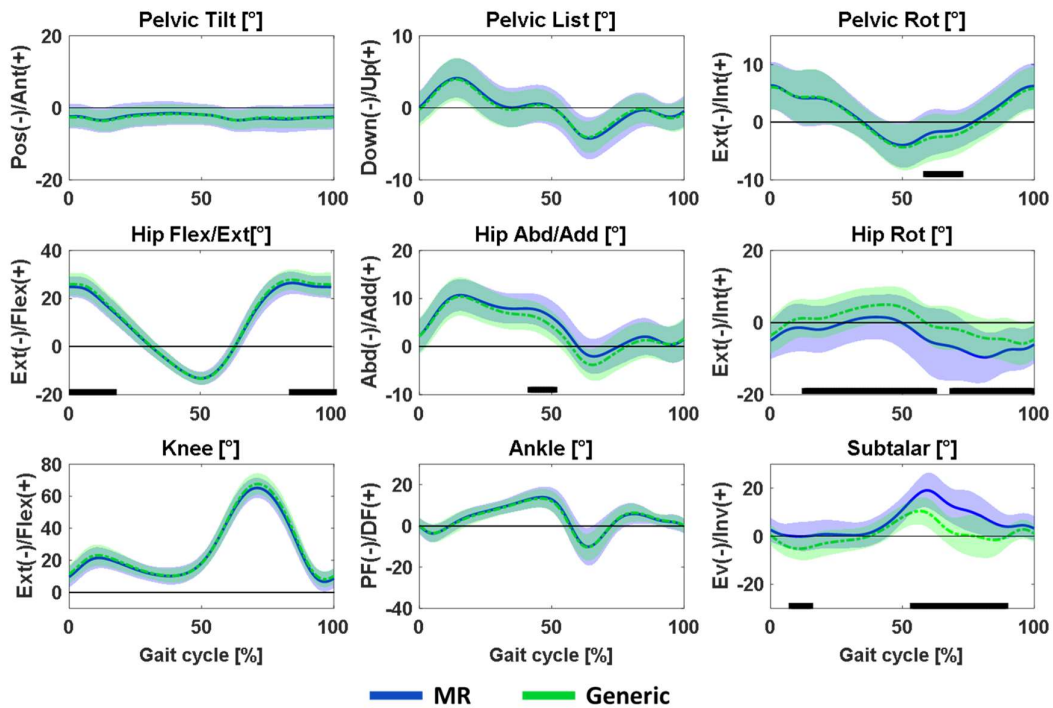


**Figure 3.4 Kinematic waveform comparison between MR and Generic models for the M1 marker set. Black bars indicate significant difference between the two model estimates**

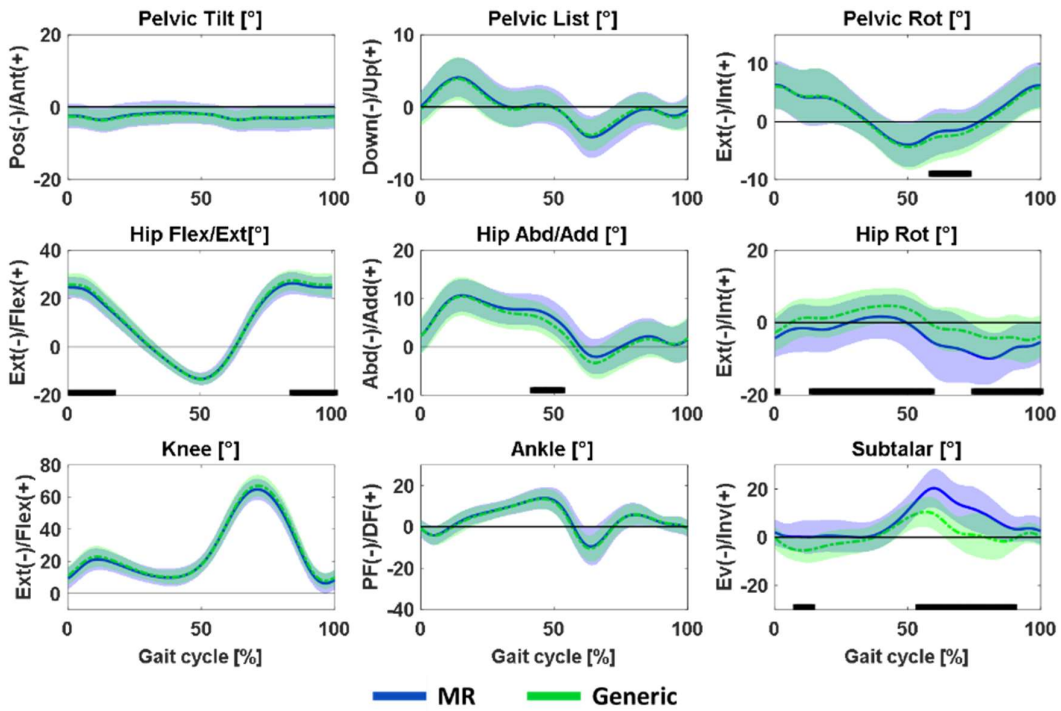


Figure 3.5 Kinematic waveform comparison between MR and Generic models for the M2 marker set. Black bars indicate significant difference between the two model estimates

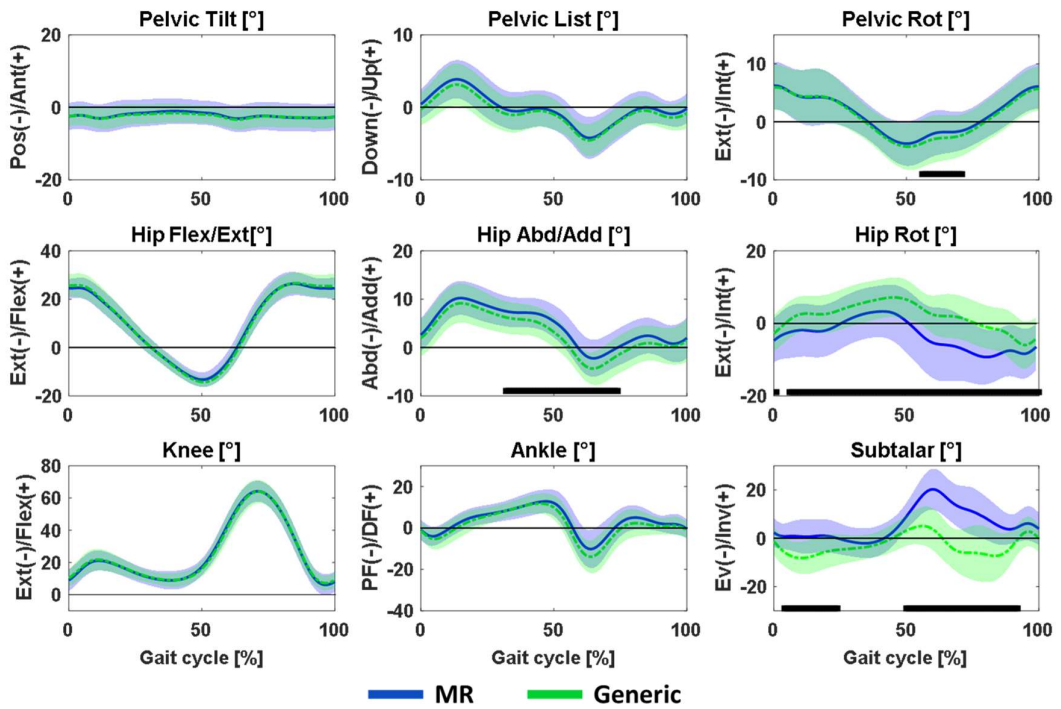
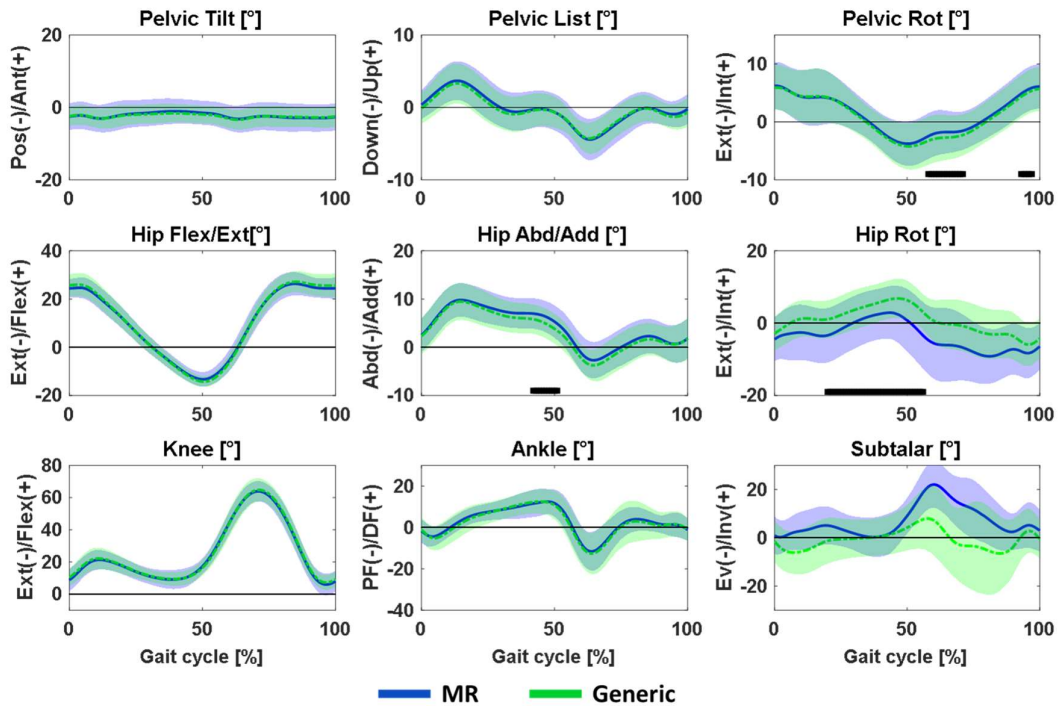


Figure 3.6 Kinematic waveform comparison between MR and Generic models for the M3 marker set. Black bars indicate significant difference between the two model estimates.



**Figure 3.7 Kinematic waveform comparison between MR and Generic models for the M4 pipeline. Black bars indicate significant difference between the two model estimates.**

Kinematics estimated with the four marker pipelines were found to be significantly different over late stance through swing of the gait cycle for both the generic and MRI-based model (Figure 3.8 and Figure 3.9, respectively). Despite differences in amplitude, there were high curve similarity between pairs of marker estimates ( $R^2 > 0.7$ ) for both models. Relations between M1/M2 and M3/M4 pairs were the strongest ( $R^2 > 0.8$ ).

The range of motion (ROM) for all joints estimated by either model were found to be on average within  $2^\circ$  of each other for all the marker pipelines except for the subtalar ( $6^\circ$ ). This value was similar for the intra-model comparisons except for the generic model where M3 and M4 differed from M1 greater than  $2^\circ$  for hip rotation, knee flexion, ankle plantar/dorsiflexion and subtalar angle. Significant differences assessed with a repeated measures ANOVA ( $p$ -value  $< 0.001$ ) between marker sets for the ROM in the MR-based model were for the transverse plane: pelvic rotation and hip rotation. M3 and M4 tended to estimate higher ROM for these rotations. For the generic model, significant differences were found for hip adduction, hip rotation and knee flexion ROMs between the marker pipelines. The ICC for all markers was greater than 0.9 for all joint ROMs in both generic and MR models and are not reported.

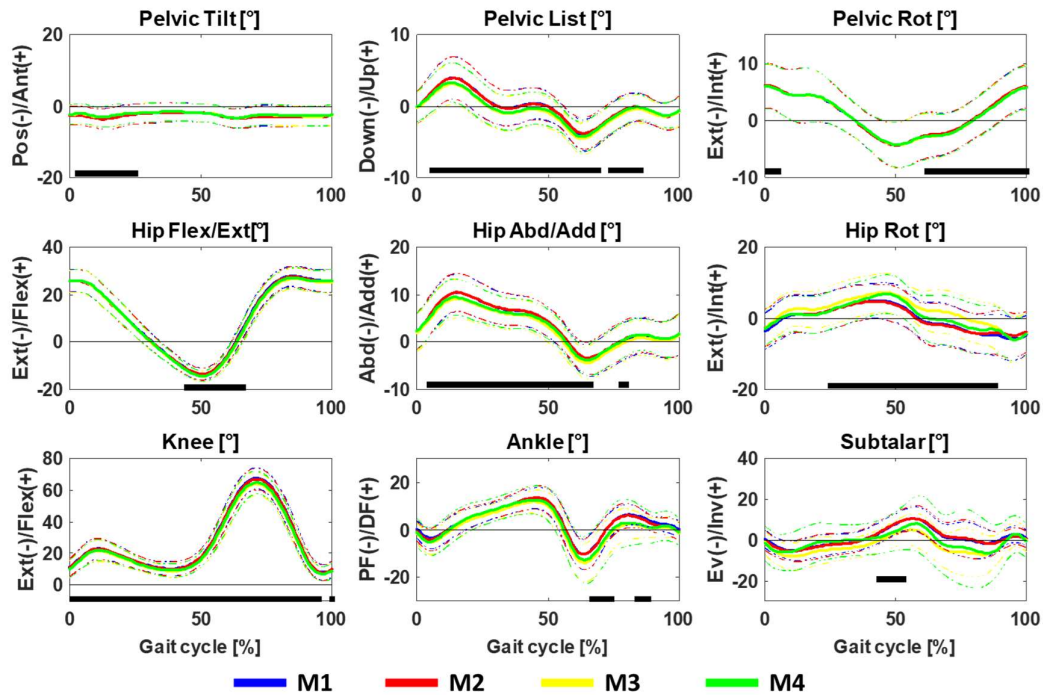


**Figure 3.8 Kinematic curves showing differences due to markers used in IK for the generic model. Black bars indicate statistical significance between marker pipelines.**

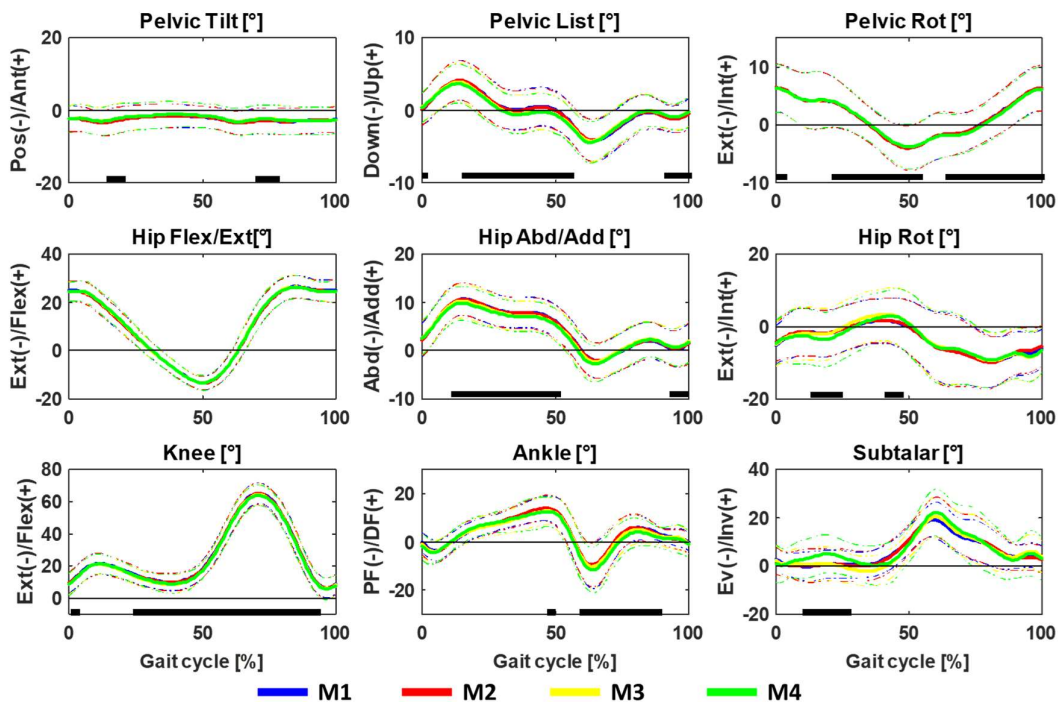


**Figure 3.9 Kinematic curves showing differences due to markers used in IK for the MRI model. Black bars indicate statistical significance between marker pipelines**

### 3.5 Discussion

This study sought to investigate the effect of marker quantity on the estimates of joint kinematics using two musculoskeletal models.

For the static pose angles, significant inter-model differences between estimates of pelvis tilt, hip flexion, hip rotation and ankle plantarflexion were observed for all the marker sets. When the static pose angle values (offsets) were subtracted from the walking kinematics, however, the differences between estimated kinematics by the models were reduced. Previous studies [30, 31] have reported the presence of such offsets in joint angles between different kinematic models particularly where the models have differently defined segment anatomical and joint axis reference frame definitions. The inter-model differences that remained between the walking kinematics after removing the offsets can thus be attributed to the effect of the different number of markers on each model's ability to track participants' motion. Marker set M4, with the least number of markers, produced the largest inter-model differences in joint angles.

The joint kinematics obtained for all marker pipelines and models had similar profiles as those reported in the literature [4, 32]. Inter-model comparison of joint angle curves showed high similarity for each of the marker sets with a minimum  $R^2$  of 0.6 (observed for hip rotation). From the inter-model RMSD results, it was observed that the largest differences between models were observed in the distal joints. This was consistent with the fact that the largest differences in the number of markers used between marker sets was on the distal segments, particularly the foot where the number of markers used reduced to two in M4. Hip rotation, knee flexion/extension and ankle plantar/dorsiflexion tended to have larger differences and variability between the two models for all the marker sets considered, particularly for the M3 and M4 pipelines. These larger differences between models can be explained by the fact that the personalised MRI-based models captured participant geometry (for example femur and tibial torsions) better and hence estimate more accurate joint centres and rotational axes compared to generic models [17]. The generic models on the other hand, were scaled using the skin markers and estimated joint centres and were thus subject to potential mislocation of the joint centres, which could lead to errors in segment dimensions, as shown by Koller, et al. [33] who reported that joint kinematics were altered by up to  $9.4^\circ$  when models were inaccurately scaled.

The reported results also proved the joint kinematics estimates sensitivity to the number of skin-mounted markers, irrespective of the model type used. These differences, however, were generally below the  $5^\circ$  threshold above which there can be an effect on clinical meaning [34]. This was consistent with the findings of Slater, et

al. [10] that constrained models were robust to marker quantities and placements and the use of less markers on a limb increased the error in kinematic estimates. While the differences were within the acceptable limits, they however tended to be higher and more variable in the scaled generic model than in the MRI-based models. The trochanter marker (TRO) used in M1 and M2 appeared to support the estimation of external hip rotation compared to M3 and M4 in the generic model as indicated by the significant difference between markers in midstance to late swing. This marker however had the largest marking tracking errors for M1 and M2 in both models. In M3 and M4, the marker on the anterior aspect of the shin (SHN) had the largest tracking error. Overall, the MR model's estimation of joint kinematics was less sensitive to the changes in the quantities of markers used. For both models however, the marker tracking errors decreased with decreasing marker quantity. This trend can be attributed to the global optimisation approach used in estimating the joint kinematics. A larger number of markers corresponds to a larger number of terms in the objective function to be minimised. The below clinically meaningful threshold RMSD found between models was consistent with the findings of Kainz, et al. [16] who compared an MRI-based and generic model, albeit for a single marker set configuration. Overall, increasing the number of markers increased marker tracking errors during IK but did not substantially change joint kinematic estimates.

Tracking two degrees of motion at the ankle complex with only two markers and the ankle joint centre is not advisable and can lead to errors in the estimates of ankle angles. This was captured by our results as indicated by the magnitude and variability in the RMSD between M4 and M1. The addition of two extra markers on the foot in M3 appeared to reduce the error with respect to M1 in both generic and MR models. The errors for MR were however consistently lower and this may be attributed to the personalised ankle joint centre and axis of the MR model.

The ROM estimated by either model for each marker set were generally similar although differences were observed for transverse plane motion of the pelvis and hip in MR and all but pelvic list and hip flexion in the generic model. In both models, M4 and M3 tended to have slightly higher values of hip rotation ROM compared to the M1 and M2. When comparing the M4 marker set to a larger quantity marker set, Mantovani and Lamontagne [11] found a similar trend although this was for all joints not just hip rotation. Additionally, their finding of lower ICC values when comparing the M4 and large set markers was consistent with the findings in this study. Given that M3 and M4 pipelines differed for only two markers on the foot, their close correspondence in estimates of ROM was expected. Overall, marker quantity had less effect on the dynamic range of motion of the MR models compared to the generic model.

Taken in the context of excessive femoral anteversion and the femoral derotation osteotomy in cerebral palsy where the hip rotation is a key measure of the condition and abnormal gait, the inconsistency between the absolute values of this estimate may be of concern when quantifying the degree of internal or external rotation. The generic model would indicate more internal hip rotation during gait than the MR-based model for the same patient leading to potential erroneous decision-making. Clinical metrics derived from joint kinematics such as the Gait Profile Score [35] are however calculated relative to reference healthy populations, and thus it is expected that by maintaining the same models and procedures for both pathological and healthy groups, this concern would be mitigated. The importance of maintaining a consistent workflow was shown by Kainz and Schwartz [36] when estimating muscle-tendon lengths with musculoskeletal models. Additionally, using a minimal marker set such as M4 may lead to more variable and less reliable estimates of the distal joint angles (subtalar inversion) and potentially the foot progression angle when compared to using a full marker set such as M1 with a generic model.

Limitations of this study are recognised. First the retrospective nature of this study meant that the marker set configuration could not be optimised for all the marker sets considered. For instance, the thigh and shank markers for M4 are wand markers whereas in this dataset, they were directly on the skin. Secondly, the MR model and M1 marker set were considered as ground truths in the comparisons given that gold standards such as the use of bone pin fluoroscopy or dynamic MRI were not available to compare to. Additionally, although kept consistent across models and marker sets, the individual markers were weighted differently, and it is unclear how this might have influenced the results. Weighting the markers uniformly would have meant that each marker's error term would most likely be minimised to a similar extent thereby minimising any potential contribution of differences in marker weights to the variability observed, however the intent was to approximate as close to how inverse kinematics would have been performed.

### **3.6 Conclusion**

The number of markers influenced the estimation of joint kinematics to a lesser extent than the type of model associated to them. The patient-specific model appeared less sensitive to the number of markers than the generic model, which had larger differences and variations between marker sets. The distal joints angle estimates were the most affected by both number of markers and model type. Although in most cases the differences were not clinically relevant, care should still be taken in comparing different studies, particularly when different biomechanical models are used.

### 3.7 References

- [1] R. Baker, A. Esquenazi, M. G. Benedetti, and K. Desloovere, "Gait analysis: clinical facts," *Eur J Phys Rehabil Med*, vol. 52, no. 4, pp. 560-74, Aug 2016. [Online]. Available: <https://www.ncbi.nlm.nih.gov/pubmed/27618499>.
- [2] M. W. Whittle, "Clinical gait analysis: A review," *Hum Movement Sci*, vol. 15, no. 3, pp. 369-387, 1996/06/01/ 1996, doi: [https://doi.org/10.1016/0167-9457\(96\)00006-1](https://doi.org/10.1016/0167-9457(96)00006-1).
- [3] A. Leardini, Z. Sawacha, G. Paolini, S. Inghrosso, R. Nativo, and M. G. Benedetti, "A new anatomically based protocol for gait analysis in children," *Gait & posture*, vol. 26, no. 4, pp. 560-71, Oct 2007, doi: 10.1016/j.gaitpost.2006.12.018.
- [4] M. P. Kadaba, H. K. Ramakrishnan, and M. E. Wootten, "Measurement of lower extremity kinematics during level walking," *J Orthop Res*, vol. 8, no. 3, pp. 383-92, May 1990, doi: 10.1002/jor.1100080310.
- [5] R. B. Davis, S. Ounpuu, D. Tyburski, and J. R. Gage, "A Gait Analysis Data-Collection and Reduction Technique," (in English), *Hum Movement Sci*, vol. 10, no. 5, pp. 575-587, Oct 1991, doi: Doi 10.1016/0167-9457(91)90046-Z.
- [6] A. Ferrari *et al.*, "Quantitative comparison of five current protocols in gait analysis," *Gait & posture*, vol. 28, no. 2, pp. 207-216, 2008/08/01/ 2008, doi: <https://doi.org/10.1016/j.gaitpost.2007.11.009>.
- [7] B. W. Schulz and W. L. Kimmel, "Can hip and knee kinematics be improved by eliminating thigh markers?," (in English), *Clinical Biomechanics*, vol. 25, no. 7, pp. 687-692, Aug 2010, doi: 10.1016/j.clinbiomech.2010.04.002.
- [8] T. D. Collins, S. N. Ghoussayni, D. J. Ewins, and J. A. Kent, "A six degrees-of-freedom marker set for gait analysis: Repeatability and comparison with a modified Helen Hayes set," *Gait & posture*, vol. 30, no. 2, pp. 173-180, 2009/08/01/ 2009, doi: <https://doi.org/10.1016/j.gaitpost.2009.04.004>.
- [9] T. W. Lu and J. J. O'Connor, "Bone position estimation from skin marker coordinates using global optimisation with joint constraints," (in English), *Journal of Biomechanics*, vol. 32, no. 2, pp. 129-134, Feb 1999, doi: Doi 10.1016/S0021-9290(98)00158-4.
- [10] A. A. Slater, T. J. Hullfish, and J. R. Baxter, "The impact of thigh and shank marker quantity on lower extremity kinematics using a constrained model," *BMC Musculoskeletal Disorders*, vol. 19, no. 1, p. 399, 2018/11/13 2018, doi: 10.1186/s12891-018-2329-7.
- [11] G. Mantovani and M. Lamontagne, "How Different Marker Sets Affect Joint Angles in Inverse Kinematics Framework," *Journal of biomechanical engineering*, vol. 139, no. 4, 2017, doi: 10.1115/1.4034708.
- [12] V. Richard, A. Cappozzo, and R. Dumas, "Comparative assessment of knee joint models used in multi-body kinematics optimisation for soft tissue artefact compensation," *Journal of Biomechanics*, vol. 62, pp. 95-101, 2017/09/06/ 2017, doi: <https://doi.org/10.1016/j.jbiomech.2017.01.030>.



- [13] V. Camomilla, R. Dumas, and A. Cappozzo, "Human movement analysis: The soft tissue artefact issue," *Journal of Biomechanics*, vol. 62, pp. 1-4, 2017/09/06/ 2017, doi: <https://doi.org/10.1016/j.jbiomech.2017.09.001>.
- [14] M. Wesseling, E. C. Ranz, and I. Jonkers, "Objectifying Treatment Outcomes Using Musculoskeletal Modelling-Based Simulations of Motion," in *Handbook of Human Motion*, B. Müller *et al.* Eds. Cham: Springer International Publishing, 2018, ch. Chapter 52-1, pp. 1-25.
- [15] S. S. Blemker, D. S. Asakawa, G. E. Gold, and S. L. Delp, "Image-based musculoskeletal modeling: applications, advances, and future opportunities," (in English), *J Magn Reson Imaging*, vol. 25, no. 2, pp. 441-51, Feb 2007, doi: 10.1002/jmri.20805.
- [16] H. Kainz *et al.*, "O 107 – Impact of subject-specific musculoskeletal geometry on estimated joint kinematics, joint kinetics and muscle forces in typically developing children," *Gait & posture*, vol. 65, pp. 223-225, 2018/09/01/ 2018, doi: 10.1016/j.gaitpost.2018.06.142.
- [17] L. Scheys, K. Desloovere, A. Spaepen, P. Suetens, and I. Jonkers, "Calculating gait kinematics using MR-based kinematic models," *Gait & posture*, vol. 33, no. 2, pp. 158-64, Feb 2011, doi: 10.1016/j.gaitpost.2010.11.003.
- [18] L. Scheys, I. Jonkers, D. Loeckx, F. Maes, A. Spaepen, and P. Suetens, "Image based musculoskeletal modeling allows personalized biomechanical analysis of gait," (in English), *Lect Notes Comput Sc*, vol. 4072, pp. 58-66, 2006. [Online]. Available: <Go to ISI>://WOS:000239565100007.
- [19] L. Scheys, A. Van Campenhout, A. Spaepen, P. Suetens, and I. Jonkers, "Personalized MR-based musculoskeletal models compared to rescaled generic models in the presence of increased femoral anteversion: effect on hip moment arm lengths," *Gait & posture*, vol. 28, no. 3, pp. 358-65, Oct 2008, doi: 10.1016/j.gaitpost.2008.05.002.
- [20] J. Stebbins, M. Harrington, N. Thompson, A. Zavatsky, and T. Theologis, "Repeatability of a model for measuring multi-segment foot kinematics in children," (in English), *Gait & posture*, vol. 23, no. 4, pp. 401-10, Jun 2006, doi: 10.1016/j.gaitpost.2005.03.002.
- [21] M. C. Carson, M. E. Harrington, N. Thompson, J. J. O'Connor, and T. N. Theologis, "Kinematic analysis of a multi-segment foot model for research and clinical applications: a repeatability analysis," *Journal of Biomechanics*, vol. 34, no. 10, pp. 1299-1307, 2001/10/01/ 2001, doi: [https://doi.org/10.1016/S0021-9290\(01\)00101-4](https://doi.org/10.1016/S0021-9290(01)00101-4).
- [22] E. J. Pratt, M. L. Reeves, J. M. van der Meulen, B. W. Heller, and T. R. Good, "The development, preliminary validation and clinical utility of a shoe model to quantify foot and footwear kinematics in 3-D," *Gait & posture*, vol. 36, no. 3, pp. 434-438, 2012/07/01/ 2012, doi: <https://doi.org/10.1016/j.gaitpost.2012.04.002>.
- [23] S. L. Delp, J. P. Loan, M. G. Hoy, F. E. Zajac, E. L. Topp, and J. M. Rosen, "An interactive graphics-based model of the lower extremity to study orthopaedic

- surgical procedures," (in English), *Ieee T Bio-Med Eng*, vol. 37, no. 8, pp. 757-67, Aug 1990, doi: 10.1109/10.102791.
- [24] H. Kainz, H. X. Hoang, C. Stockton, R. R. Boyd, D. G. Lloyd, and C. P. Carty, "Accuracy and Reliability of Marker-Based Approaches to Scale the Pelvis, Thigh, and Shank Segments in Musculoskeletal Models," *J Appl Biomech*, vol. 33, no. 5, pp. 354-360, Oct 1 2017, doi: 10.1123/jab.2016-0282.
- [25] E. Montefiori *et al.*, "An image-based kinematic model of the tibiotalar and subtalar joints and its application to gait analysis in children with Juvenile Idiopathic Arthritis," (in English), *J Biomech*, vol. 85, pp. 27-36, Mar 6 2019, doi: 10.1016/j.jbiomech.2018.12.041.
- [26] G. Valente, G. Crimi, N. Vanella, E. Schileo, and F. Taddei, "nmsBuilder: Freeware to create subject-specific musculoskeletal models for OpenSim," (in English), *Comput Methods Programs Biomed*, vol. 152, pp. 85-92, Dec 2017, doi: 10.1016/j.cmpb.2017.09.012.
- [27] L. Modenese, E. Montefiori, A. Wang, S. Wesarg, M. Viceconti, and C. Mazza, "Investigation of the dependence of joint contact forces on musculotendon parameters using a codified workflow for image-based modelling," (in English), *J Biomech*, vol. 73, pp. 108-118, May 17 2018, doi: 10.1016/j.jbiomech.2018.03.039.
- [28] T. C. Pataky, "Generalized n-dimensional biomechanical field analysis using statistical parametric mapping," (in eng), *J Biomech*, vol. 43, no. 10, pp. 1976-82, Jul 20 2010, doi: 10.1016/j.jbiomech.2010.03.008.
- [29] T. C. Pataky, M. A. Robinson, and J. Vanrenterghem, "Vector field statistical analysis of kinematic and force trajectories," *Journal of Biomechanics*, vol. 46, no. 14, pp. 2394-2401, 2013/09/27/ 2013, doi: <https://doi.org/10.1016/j.jbiomech.2013.07.031>.
- [30] H. Kainz *et al.*, "Reliability of four models for clinical gait analysis," (in eng), *Gait & posture*, vol. 54, pp. 325-331, May 2017, doi: 10.1016/j.gaitpost.2017.04.001.
- [31] H. Kainz, L. Modenese, D. G. Lloyd, S. Maine, H. P. J. Walsh, and C. P. Carty, "Joint kinematic calculation based on clinical direct kinematic versus inverse kinematic gait models," *J Biomech*, vol. 49, no. 9, pp. 1658-1669, Jun 14 2016, doi: 10.1016/j.jbiomech.2016.03.052.
- [32] M. H. Schwartz, A. Rozumalski, and J. P. Trost, "The effect of walking speed on the gait of typically developing children," (in English), *J Biomech*, vol. 41, no. 8, pp. 1639-50, 2008, doi: 10.1016/j.jbiomech.2008.03.015.
- [33] W. Koller, A. Baca, and H. Kainz, "Impact of scaling errors of the thigh and shank segments on musculoskeletal simulation results," *Gait & posture*, 2021/02/18/ 2021, doi: <https://doi.org/10.1016/j.gaitpost.2021.02.016>.
- [34] J. L. McGinley, R. Baker, R. Wolfe, and M. E. Morris, "The reliability of three-dimensional kinematic gait measurements: A systematic review," *Gait & posture*, vol. 29, no. 3, pp. 360-369, 2009/04/01/ 2009, doi: <https://doi.org/10.1016/j.gaitpost.2008.09.003>.

- [35] R. Baker *et al.*, "The gait profile score and movement analysis profile," *Gait & posture*, vol. 30, no. 3, pp. 265-9, Oct 2009, doi: 10.1016/j.gaitpost.2009.05.020.
- [36] H. Kainz and M. H. Schwartz, "The importance of a consistent workflow to estimate muscle-tendon lengths based on joint angles from the conventional gait model," *Gait & posture*, vol. 88, pp. 1-9, 2021/07/01/ 2021, doi: <https://doi.org/10.1016/j.gaitpost.2021.04.039>.

## **4 Effectiveness of global optimisation and direct kinematics in predicting surgical outcome in children with cerebral palsy**

### *Acknowledgement of co-authorship*

This chapter comprises a published manuscript titled "Effectiveness of global optimisation and direct kinematics in predicting surgical outcome in children with cerebral palsy " that has been re-formatted for this thesis. This was work done in collaboration with the co-authors listed in the paper.

In this study, I contributed to the conceptualisation, design, implementation of the methods and simulations, analysis of the results and its interpretation. I also led in the writing of the manuscript and production of all figures and tables therein as well as being responsible for the submission and review process.

Student:

Claude Fiifi Hayford



Date 12/01/2022

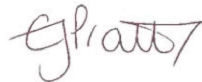
The main co-authors:

Claudia Mazzà



Date 14/01/2022

Emma Pratt



Date 17/01/2022

## 4.1 Abstract

Multibody optimisation approaches have not seen much use in routine clinical applications despite evidence of improvements in modelling through a reduction in soft tissue artifacts compared to the standard gait analysis technique of direct kinematics. To inform clinical use, this study investigated the consistency with which both approaches predicted post-surgical outcomes, using changes in Gait Profile Score (GPS) when compared to a clinical assessment of outcome which did not include the 3D gait data. Retrospective 3-dimensional motion capture data were utilised, from 34 typically developing children, and 26 children with cerebral palsy who underwent femoral derotation osteotomies as part of Single Event Multi Level Surgeries. Results indicated that while, as expected, the GPS estimated from the two methods were numerically different, they were strongly correlated (Spearman's  $\rho = 0.93$ ) and no significant differences were observed between their estimations of change in GPS after surgery. The two scores equivalently classified a worsening or improvement in the gait quality in 93% of the cases. When compared with the clinical classification of responders versus non-responders to the intervention, an equivalent performance was found for the two approaches, with 27/41 and 28/41 cases in agreement with the clinical judgement for multibody optimisation and direct kinematics, respectively. With this equivalent performance to the direct kinematics approach and the benefit of being less sensitive to skin artefact and allowing additional analysis such as estimation of musculotendon lengths and joint contact forces, multibody optimisation has the potential to improve the clinical decision-making process in children with cerebral palsy.

## 4.2 Introduction

Three-dimensional clinical gait analysis (CGA) use is widespread in the diagnosis and treatment of movement abnormalities particularly in people with cerebral palsy, where it forms a part of the clinical decision-making process [1, 2]. When considering surgical interventions, studies report up to 92% agreement between pre-operative CGA recommendations and the actual surgery performed [3, 4], underlying its importance in the clinical setting. CGA produces a variety of kinematic and kinetic output variables, primarily including estimates of joint angles, moments and powers during the gait cycle of a patient.

The most common approach to estimating joint kinematics in CGA is the so-called conventional gait model, based on the Davis protocol [5] and also implemented in the Plug-in-Gait model (PiG, Vicon, Oxford, UK). In this approach, experimental markers are attached to the body and used to determine the orientation of the anatomical

segments and the 3D intersegmental joint kinematics. In the so-called direct kinematics approach, the latter are calculated using Cardan angles, i.e., a sequence of rotations about three different and mutually perpendicular axes, that rotate a distal segment with respect to a proximal segment [5-7]. While this approach enjoys widespread clinical acceptance and use, it has been shown to have limitations, especially in regard to error due to soft tissue artefacts [8]. Additionally, when using this approach bony segment dimensions might vary as a result of being defined by the time variant distances between joint centres [8] arising from the limited marker set of the PiG which uses the same markers to define adjacent segment lengths. This latter issue precludes the subsequent use of the same model when estimating other relevant metrics, such as the muscle length and the internal forces obtainable through musculoskeletal modelling techniques [8]. Multibody optimisation, also referred to as global optimisation, has hence been proposed as an alternative approach for estimating joint kinematics. This method simultaneously determines the orientation of a constrained skeletal model while minimising the distance between experimental markers and their corresponding virtual markers placed on the model. It addresses some of the challenges of the PiG model, in particular minimising skin tissue artefacts [9], and has been shown to provide reliable estimates of gait kinematics [10, 11]. Its successful adoption in routine assessment of pathological gait however, is yet to be determined due to limited implementation in commercial software packages and limitations associated to the simplifications made within the reference joint models, such as the use of minimal degrees of freedom, as well as complexity and time constraints [12, 13]. A comparison between estimates obtained using the direct and global optimisation approaches described above as applied to gait data from both typically developing children and children with cerebral palsy showed that the choice of approach resulted in root mean square differences between the two kinematic outputs of less than 1° when keeping the same anatomical model (i.e. the same degrees of freedoms for the joint models and segments anatomical definitions) [14]. The same study showed that among all factors, 94% of the variations are to be attributed to the anatomical model.

Kinematic outputs from CGA cover multiple joints, anatomical planes, and span across the whole gait cycle. This multiplicity of interdependent information can benefit from being summarised into a single measure to aid interpretation [15]. One such measure is the Gait Profile Score proposed by Baker et al [16] which provides a summary index of overall gait quality or pathology and has been shown to have high clinical validity in terms of its relationship with other clinical measures and the ability to quantify changes in gait patterns and the effects of treatment interventions in pathological populations [17-20]. The formulation of the GPS also allows for identifying the aspect

of the kinematics contributing to the deviation from normal [16]. While use of the GPS is well documented with the PiG model, to the best of our knowledge, no studies have calculated this metric using outputs from other modelling approaches, including global optimisation. Furthermore, independently of the modelling approach, the GPS has not been previously evaluated with respect to its agreement with non-3D data-based clinical judgement of surgical outcome in a pathological population. The aim of this paper is hence to evaluate the agreement between GPS and clinical data-based judgment in estimating surgical post-intervention outcomes, when the GPS is calculated from kinematic outcomes obtained using either the global optimisation or the direct kinematic approach. In particular, as a paradigmatic case where using global optimisation with a generic model could be particularly challenging in terms of uncertainties in joint centre and axis definitions, we focused on investigating the outcome of Femoral Derotation Osteotomy, a surgical procedure aiming at correcting excessive femoral anteversion.

## **4.3 Methods**

### **4.3.1 Data description**

This study retrospectively analysed anonymised data of 26 children with CP (age:  $8.8 \pm 3.0$  years, mass:  $26.1 \pm 9.2$  kg, height:  $1.26 \pm 0.16$  m at pre-intervention observation) from the Sheffield Children's Hospital Gait Laboratory database. Ethics was approved by the South Central – Oxford B Research Ethics Committee (19/SC/0329).

Participants were selected based on the following criteria:

1. Diagnosis of Cerebral Palsy
2. Gross Motor Function Classification System (GMFCS) I-III
3. Femoral Derotation Osteotomy as part of Single Event Multi Level Surgery (FDO-SEMLS)
4. Availability of at least one pre- and post-intervention 3D gait analysis capture

The CP cohort had gait analysis on average  $13.1 \pm 9.1$  months prior to FDO-SEMLS and again  $31.3 \pm 18.5$  months after the surgery. Additionally, retrospective control data of 34 typically developing (TD) participants (age:  $15.9 \pm 9.8$  years, mass:  $47.5 \pm 20.7$  kg, height:  $1.53 \pm 0.22$  m) were analysed. Participants in the TD cohort were divided into three subgroups: children (<10 years), teenagers (<16 years) and young adults ( $\geq 16$  years) as detailed in Table 1. For all groups, CGA was performed using a Vicon system (Vicon, Oxford, UK) and comprised one static and at least three walking trials. Markers were placed on the lower limbs using the Plug-In Gait marker set. A Knee Alignment



Device (KAD) was utilised in the standing trial defining the knee flexion axis and a thigh rotation offset angle relative to the applied thigh wand. The KAD was subsequently replaced by a single lateral knee marker (KNE) in the walking trials.

**Table 4.1 Anthropometric details for the TD cohort subgroups**

TD Groups	Age (years)	Mass (kg)	Height (m)
Young Adults (n=12)	27.8 ± 6.2	68.7 ± 14.6	1.75 ± 0.11
Teenagers (n = 10)	11.8 ± 1.8	44.9 ± 11.9	1.52 ± 0.14
Children (n = 12)	7.5 ± 1.4	28.4 ± 7.6	1.31 ± 0.12

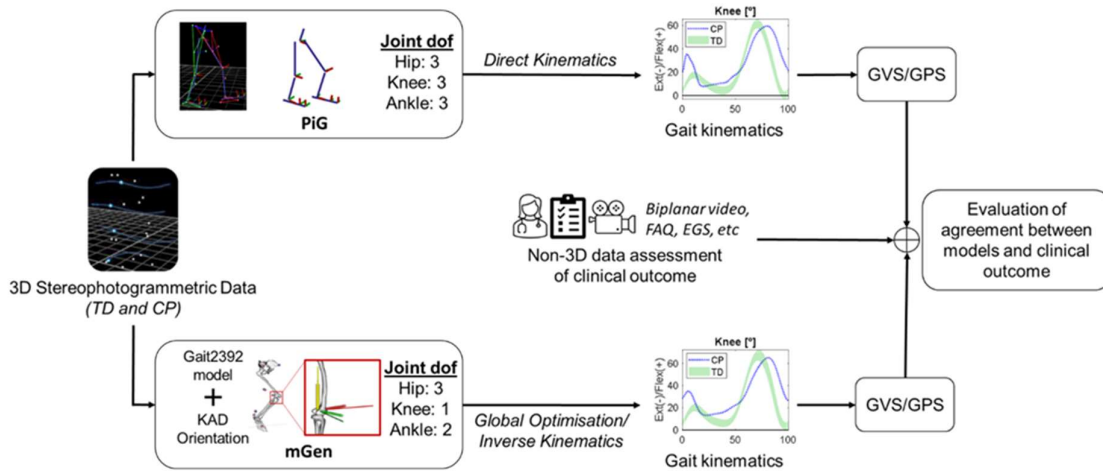


**Figure 4.1 Flowchart showing workflow of analysis**

### 4.3.2 Calculation of the joint kinematics

To achieve the study objective, two workflows (Figure 4.1) were followed. Firstly, the gait2392 lower-limb model bundled with Opensim3.3 [21] was adapted to each participant's characteristics. This model has three degrees of freedom at the hip, one at the knee and hinges for both the tibiotalar joint and subtalar joint. The metatarsophalangeal joint was locked. Prior to scaling the model to each participants anthropometry, the orientation of the knee flexion axis in the transverse plane was modified with custom MATLAB (R2018b, MathWorks, MA, USA) scripts to match the alignment of a KAD placed on the participant during a static trial. The applied rotation to the gait2392 model's knee flexion axis was compared between TD, CP pre- and CP post-surgery with a Kruskal-Wallis test followed by a post-hoc Dunn's multiple comparison test. This modified model was then scaled following recommended procedures [22]. Briefly, scale factors were calculated from surface marker positions and calculated joint centres. The pelvis was scaled anisotropically whereas the femur and tibia were scaled linearly using distances between the hip and knee joint centres

and knee and ankle joint centre, respectively. The modified scaled generic models (mGen) were subsequently used to simulate the participants' gait using the Inverse Kinematics tool in OpenSim3.3 to estimate their joint kinematics over the gait cycle. In addition, the foot progression angle (FPA) over the gait cycle was calculated. To this purpose, the OpenSim "Analyze" tool was used to estimate the model body kinematics, from which the direction of progression was defined as the vector from the pelvis centre of mass position at initial heel strike to its position at end of the gait cycle. The foot vector was defined as the line joining the ankle joint centre to the model TOE marker [23]. The FPA was calculated as the angle between the direction of progression and the foot axis projected in the transverse plane using custom MATLAB scripts.

The second workflow followed the standard clinical protocol of the Sheffield Children's Hospital Gait Laboratory for PiG model data analysis using Nexus (Vicon, Oxford, UK). Post processing with thigh rotation offset adjustment [24] was completed using laboratory standard protocols, to optimise the knee axis alignment where necessary.

#### **4.3.3 Data analysis**

From the output of both workflows, eight joint angles (pelvic tilt, pelvic list/obliquity, pelvic rotation, hip flexion, hip abduction, hip rotation, knee flexion and ankle dorsiflexion) and the FPA were extracted, and time normalised to 100% of the gait cycle using custom scripts in MATLAB. Additionally, for each subject the mean kinematic waveform of the three gait trials for each limb was calculated.

The kinematics estimated with the two workflows were statistically compared using the non-parametric paired sample t-test option of the 1-dimensional statistical parametric package [25] in MATLAB. A Bonferroni correction was applied for multiple comparisons, and  $\alpha$  was set to 0.0056 (9 pairwise comparisons). The root mean square difference (RMSD) was calculated between individual trials kinematic waveform from PiG and mGen for each subject and averaged to quantify the effect of the chosen approach on the joint angle estimates. Similarly, the coefficient of determination ( $R^2$ ) was calculated for individual trials with the linear fit method between PiG and mGen and averaged per subject for each of the nine kinematic variables as a measure of curve similarity.

The GPS was also calculated for all subjects using the data from the age-matched controls and the mean kinematic waveform outputs from both mGen and PiG. The GPS is calculated separately for each limb and is based on the Gait Variable Score (GVS), which is the root mean square (RMS) difference between the gait vector of a patient and the mean gait vector of a non-pathological group. These gait vectors include nine

key kinematic variables: pelvic tilt, pelvic list/obliquity, pelvic rotation, hip flexion, hip abduction, hip rotation, knee flexion, ankle dorsiflexion and foot progression angle. Formally, the GVS and GPS were calculated as described in Equation 4.1 and Equation 4.2, respectively.

$$GVS_i = \sqrt{\frac{1}{T} \sum_{t=1}^T (x_{i,t} - x_{i,t}^{ref})^2} \quad \text{Equation 4.1}$$

where  $GVS_i$  is the Gait Variable Score of the kinematic variable  $i$ ,  $t$  is a specific instance in the gait cycle,  $T$  is the total number of points in the cycle,  $x_{i,t}$  is the value of kinematic variable  $i$  at instance  $t$ , and  $x_{i,t}^{ref}$  is the mean of that variable at the same time point for a reference population.

$$GPS = \sqrt{\frac{1}{N} \sum_{i=1}^N GVS_i^2} \quad \text{Equation 4.2}$$

where  $N$  is the total number of kinematic variables used and  $i$ , the  $i$ th kinematic variable used.

Data were checked for normality and appropriate statistical tests used subsequently. Consistency in GPS estimated with mGen and PiG, was assessed using Spearman's correlation coefficient ( $\rho$ ). A Wilcoxon rank test was performed to determine significant differences between the two groups of GPS estimates. Additionally, the Symmetry Index (SI)[26] was used to calculate left/right limb asymmetry in GPS values for both models and compared using the Pearson's correlation coefficient. To test the agreement between models when estimating changes in GPS ( $\Delta_t$ GPS) after FDO-SEMLS, a Bland-Altman analysis was used.  $\Delta_t$ GPS were normally distributed and a paired sample t-test was used to determine if model estimates of  $\Delta_t$ GPS were significantly different. To understand the contributing factors to any differences in  $\Delta_t$ GPS estimated by both models, the above-described analyses were applied also to the nine components of the GPS.

To determine a classification of improvement (responders) from 3D gait analysis data using both mGen and PiG estimates of GPS, change in GPS ( $\Delta_t$ GPS) from pre- to post-FDO-SEMLS for each model was calculated, after which a criterion of  $\Delta_t$ GPS  $\leq$  -1.6 (minimal clinically important difference for GPS [27]) was applied. This 1.6° threshold reflects the mean difference between GPS values of children classified in adjacent levels of the Functional Assessment Questionnaire measure of functional mobility. Participants with  $\Delta_t$ GPS values not satisfying this criterion were classified as non-responders.

The process for clinically adjudging participants as responders or non-responders to FDO-SEMLS was based on consensus between two consultant orthopaedic surgeons

and the team of gait laboratory staff (including clinical scientists and physiotherapists). This process involved review of clinical examination findings and clinical dictations as well as video recordings looking at components of the Edinburgh Gait Score (EGS) [28], a validated visual analysis scale, that pertained to the desired correction from the FDO. In this regard, the video analysis emphasized on hip rotation (using the knee progression angle in stance with consideration of transverse plane alignment as a surrogate) and the foot progression angle in stance. One clinical scientist completed the classifications, and these decisions were reviewed by the consultant orthopaedic surgeons. The measured kinematics and report from 3D gait analysis were not used in this process. Only the limbs that underwent the surgery were considered for each participant.

#### **4.3.4 Results**

The KAD-based modifications to the knee flexion axis were found to be significantly different between TD and CP groups at both pre- and post-intervention (Figure 4.2). There was also large variation within the CP cohort in terms of the modification that was applied to the generic model although this did not change after the surgery. Figure 4.3 shows the kinematic waveforms estimated by PiG and mGen for the TD participants. Mean inter-trial standard deviation for the kinematics waveforms are shown in Supplementary Figures S3 and S4 for CP and TD, respectively. Joint kinematics over the gait cycle estimated by the two models were highly correlated (minimum average  $R^2$ :  $0.83 \pm 0.10$ ) with the exception of pelvic list/obliquity and hip internal/external rotation (average  $R^2$ :  $0.61 \pm 0.23$  and  $0.55 \pm 0.18$ , respectively). Additionally, the joint kinematics for pelvic tilt, hip flexion and hip rotation had large differences between model estimates ( $RMSD > 5^\circ$ ). These results were similar for the CP group (see supplementary data, Figure S1). The distribution of RMSD quantifying the differences between joint angles estimated by PiG and mGen for the TD participants is shown in Figure 4.4 (data for CP cohort shown in Supplementary Figure S2). The mean RMSD over all analysed joints was  $7.7 \pm 0.9^\circ$  and  $8.0 \pm 1.3^\circ$  for TD and CP, respectively. Hip rotation had the largest variability in RMSD for both TD and CP (IQR =  $10.0^\circ$  and  $7.7^\circ$ , respectively).

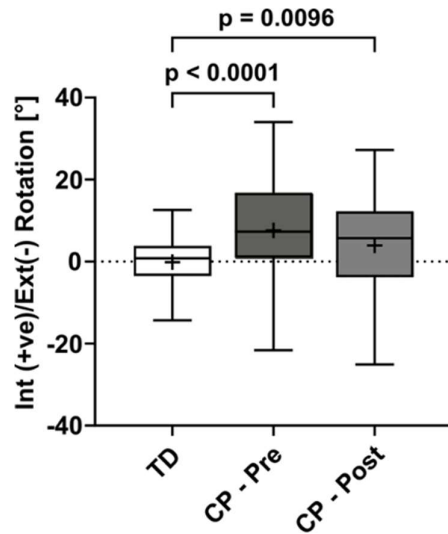


Figure 4.2 Box plot of knee flexion axis corrections estimated from the KAD and applied to mGen for the TD and CP participants. p-values indicate significant differences as highlighted by a post-hoc Dunn's multiple comparison test comparing TD, CP pre and CP post

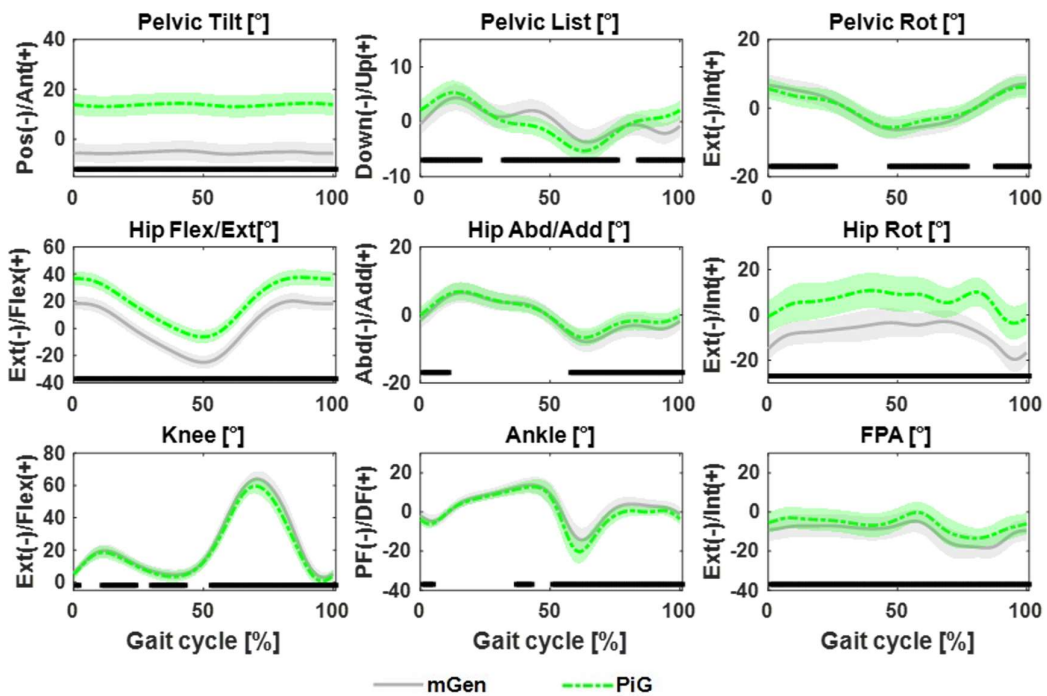
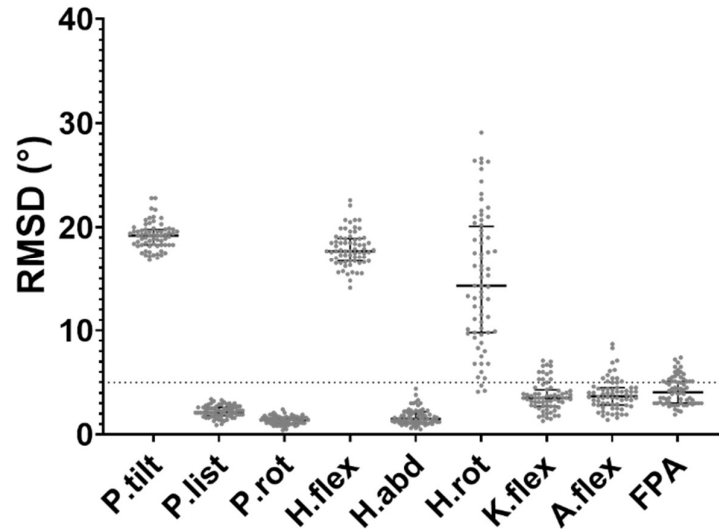


Figure 4.3 Mean joint kinematic waveforms for 68 limbs from 34 TD participants estimated with PiG and mGen models. Shaded bands indicate 1SD with significant difference shown by bottom black bars.



**Figure 4.4 Distribution of RMSD of joint kinematics between PiG and mGen models for TD participants. Bars represent median and interquartile range. Dotted line at 5° represents clinically acceptable threshold of data error [29].**

The comparison of the GPS calculated from the kinematic output of the two approaches indicated agreement in values with a mean absolute difference of 1.1° (range: 0.0° to 4.8°). Figure 4.5 shows the strength of the relationship between PiG and mGen with a Spearman  $\rho$  of 0.93 ( $p$ -value < 0.0001). The GPS estimated by PiG and mGen were however found to be significantly different ( $p$ -value = 0.002) using the Wilcoxon test. Both models reported on average a similar Symmetry Index ( $4.8\% \pm 23.6\%$  and  $3.2\% \pm 24.0\%$  for PiG and mGen, respectively) with a Pearson correlation coefficient  $r$  of 0.90 between the two.

Changes in gait kinematics pre- and post-intervention, as assessed by  $\Delta_t$ GPS, were not significantly different when calculated using the PiG or the mGen ( $p$ -value = 0.14, paired t-test, Supplementary Table S1) although PiG estimated generally higher  $\Delta_t$ GPS than mGen. The Bland Altman analysis (Figure 4.6) showed a bias in estimating  $\Delta_t$ GPS of 0.44° (Limits of Agreement: -3.29° to 4.18°).

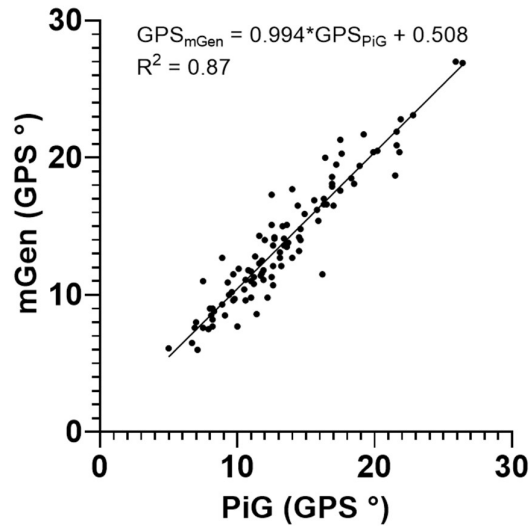


**Figure 4.5 Correlation between the GPS estimated with PiG and mGen for all subject limbs and observations.**

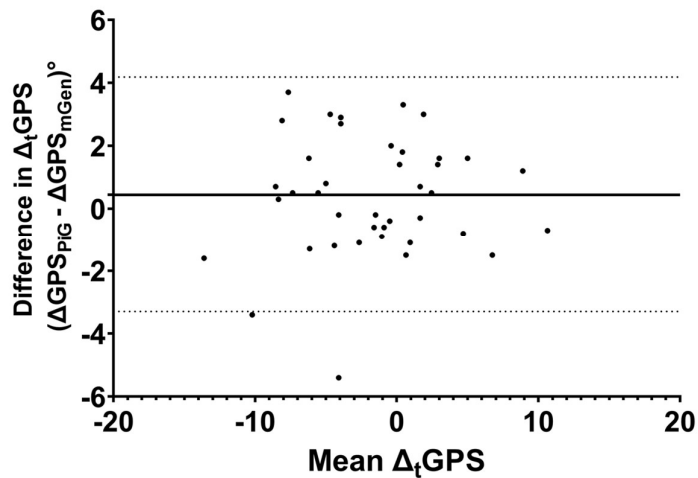


**Figure 4.6 Bland-Altman plot of changes in GPS estimated by PiG and mGen. Solid and dotted lines represent the mean difference and limits of agreement, respectively.**

Results from comparing the clinical judgement with the models' classifications are shown in Figure 4.7. Overall, there was >60% alignment of both PiG and mGen with the clinical judgement. When not considering what the clinical judgement was, both models predicted the same outcome in greater than 90% of cases (38 out of 41 limbs). For the three limbs where the prediction of classification differed between models, differences between model estimates of  $\Delta_tGPS$  were negligible with the exception of one case (0.2°, 0.6° and 5.4°, respectively). Additionally, for these three cases, both

models were consistent in their estimation of post FDO-SEMLS increase/decrease in GPS.

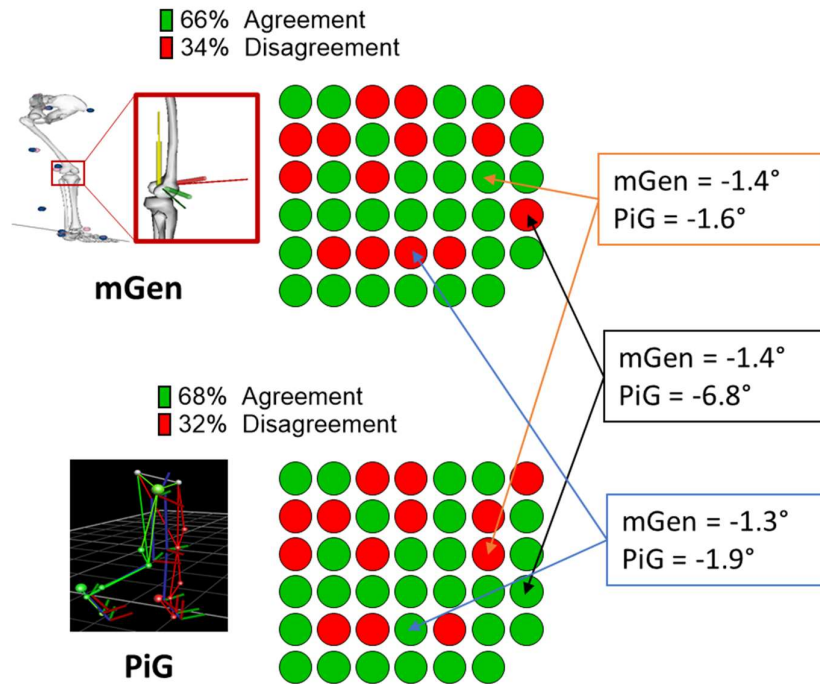


**Figure 4.7 Agreement of clinical classification of CP participants after surgery with PiG and mGen-based classification from GPS values for 41 limbs analysed. The boxes represent the three cases where there was a difference (values within box) between model predictions of outcome with similar coloured arrows pointing to the prediction from mGen and PiG.**

#### 4.4 Discussion

This retrospective study sought to evaluate the agreement between non-3D data-based clinical judgement of surgical outcome and kinematic-based outcomes estimated using either global optimisation or direct kinematics in children with CP after Femoral Derotation Osteotomy as part of Single Event Multi Level Surgery (FDO-SEMLS).

Results showed that joint kinematics estimated by the two modelling approaches were highly correlated, although there existed differences in the values. The main difference between the two approaches were offsets for pelvic tilt, hip flexion and hip rotation. This was consistent with earlier reported studies in children with CP that attributed these offsets to the differences in both the anatomical and joint axes definitions [14]. In the PiG, the pelvis anatomical coordinate system is oriented such that the anteroposterior axis lies in a plane defined by the pelvis markers (sacrum and two



anterior iliac spines) whereas the axis for the mGen is oriented parallel to the horizontal. This led to a RMSD difference of about 10-15°, which was shown to reduce by adjustment of the anatomical and joint reference frames [10, 11]. Similarly in this study a RMSD of  $18^{\circ} \pm 1.5^{\circ}$  in pelvic tilt between the PiG and mGen approaches was found. However, such model differences are not expected to influence the estimation of GPS as the model definitions were kept consistent within each approach and its reference data.

Compared to the other joints, a larger range of values was observed in the hip rotation's RMSD. This is most likely to be attributed to the differences in degrees of freedom observed between the two models. Horsak, et al. [11], in fact, showed in a group of obese children that using three instead of one degree of freedom at the knee joint in mGen reduced the RMSD between mGen and PiG estimates of hip rotation. From their results, it could also be observed that the  $R^2$  improved with a 3-DoF mGen knee. In agreement with their findings, our analysis of these data in the TD cohort showed a significant decrease in the magnitude and variability of hip rotation RMSD when a 3-DoF knee joint was used in the mGen (see Appendix 1 Figure S5). An additional explanation for the observed range of values could be associated to the inaccuracies in the tracking of the thigh marker, which is the main driver of hip rotation when using global optimisation. While still within the recommended limits, this marker had on average the highest tracking root mean square error ( $1.88 \pm 0.77$  cm and  $1.74 \pm 0.62$  cm for right and left thigh markers respectively, Appendix 1 Table S3). In the absence of a gold standard measure of joint kinematics such as that from using intracortical bone pins and fluoroscopy to determine which model was most accurate in estimating the hip rotation, a comparison of the predictions of outcome based on just the hip rotation showed the mGen with better agreement to the clinical judgement of outcome.

From our analysis, mGen and PiG models calculated similar values for the GPS with a mean absolute difference of  $1.1^{\circ}$  observed between the two model estimates which was less than the cut-off for clinical significance. Additionally, estimation of left and right asymmetry in GPS by mGen was captured similarly to the PiG ( $r = 0.90$ , Table S2 in Supplementary Materials). In comparing agreement in predictions of outcome after the FDO-SEMLS, it was shown that in 65.9% (27/41 limbs) of cases, the mGen predicted the same status for the patient as the clinical judgement. A similar agreement (68.3%, 28/41 limbs) was found for the PiG. The observed level of agreement with the clinical judgement for both models is in line with the notion that clinical assessment and CGA are relatively independent sources of information and should be used in tandem [30]. The clinical judgement of post-intervention outcome used in this study was based on clinical measures such as clinical examination, subjective reports (e.g., Gillette

Functional Assessment Questionnaire) and video footage of the gait with no dependence on 3D gait analysis output. Placing this in context, studies have shown that changes in surgical recommendations after including gait analysis data occurred in 52% of cases [31] and the GPS is just one of the outputs from gait analysis. Although both models' agreement with the clinical judgement was less than 70%, the classification of participants as responders or non-responders by mGen and PiG using  $\Delta_t$ GPS aligned in 38 out of 41 limbs compared. This relatively high concordance (92.7%) is important for the purpose of this study because it shows that the mGen is capable of predicting similar changes in gait kinematics after FDO-SEMLS as the PiG, despite different values of GPS. Notably, for the three cases that were not aligned in terms of agreement in predicted outcome, both models predicted the same direction of change in GPS in all cases, and negligible differences between models' estimates in all but one case (0.2°, 0.6° and 5.4°, respectively). Exploring the latter, the PiG was correctly aligned with the clinical judgement and there was a large inter-model difference ( $>10^\circ$ ) between mGen and PiG in the GVS of hip rotation and ankle plantarflexion. This difference was also reflected in the RMSD in those variables between PiG and mGen for that case. Taken together, these results suggest mGen performs similarly to PiG in estimating surgical outcomes when using the GPS.

When looking at the transverse plane components of the GPS, changes in FPA were more likely to agree ( $>70\%$ ) with the clinical judgement for both mGen and PiG and this resonated with the fact that the FPA was one of the main factors used to classify a response as per the criterion for classification. Using a machine learning approach, Schwartz, et al. [32] showed that femoral derotation osteotomies have a causal effect on FPA in CP and this result from our analysis goes to further justify the applied criterion for clinical classification. Interestingly, changes in the hip rotation component of the GPS showed that the mGen performed better (58.5% vs 48.8%) than the PiG in its agreement with the clinical judgement. For these two aspects of importance for FDO-SEMLS, the mGen was marginally better than the PiG when compared to the clinical judgement.

With mGen showing near equivalence to the PiG with respect to the GPS, it can be argued that the use of global optimisation might be preferred if the aim is to provide additional benefit to the clinical decision-making process. This approach, in fact, besides improving the estimate of the joint kinematics [9, 33], allows for the estimation of muscle tendon lengths and forces and joint reaction forces, parameters not directly accessible to the direct kinematics approach. A number of studies have reported using the output of PiG to drive a musculoskeletal model to obtain these variables [13, 34], however as reported by Kainz and Schwartz [13], it is important to ensure consistency

between the mGen and PiG as this influences the estimates of muscle-tendon lengths obtained in this way.

The knee axis modification that was applied using information from the KAD was found to be significantly different between the TD and CP cohort which was expected. On the other hand, there was no significant differences between the pre- and post-modifications made for the CP cohort. This could be attributable to the heterogenous nature of the CP limbs as there were limbs that saw improvement or deterioration and others that were not operated on. Further analysis, requiring additional data, is warranted to investigate how the applied modifications could be used as a surrogate measure for the degree of femoral anteversion in the same manner as the clinical measures, hip passive range of motion and the trochanteric prominence angle test.

The limitations of the current study are acknowledged. Changes in femoral or tibial torsions which were present in the CP participants were not fully captured by the mGen models. Personalisation of musculoskeletal geometry is known to improve estimates of joint kinematics [35] due to the influence on joint centre estimates and axis definitions. Nonetheless, this study attempted to approximate some aspect of personalisation in the mGen model, adapting the model to use the knee axis orientation defined with the KAD. An alternative approach of deforming the generic model using clinical measures of femoral anteversion has been proposed [36-38], however given that this was a retrospective study, these metrics were not available for most participants and control data and thus could not be implemented. It is also recognised that using the consensus clinical judgement with no gait analysis metrics input as a proxy gold standard is by nature subjective, and this may have introduced additional error. In addition, the choice of using the same MCID in GPS of  $1.6^\circ$  for the mGen, could be considered arbitrary, however this was justified as akin to using the  $5^\circ$  threshold for detecting clinically relevant changes in clinical gait analysis kinematics in this and other studies [10, 11, 14, 39].

## **4.5 Conclusion**

In conclusion, the mGen model estimated both GPS and post-intervention change in GPS comparable to the PiG model. Furthermore, non-3D data based clinical judgement of outcome post-intervention aligned similarly to the longitudinal change in GPS calculated from either model. Given that the mGen lends itself to advanced musculoskeletal modelling techniques, such as muscle length modelling and estimation of muscle and joint contact forces, results from this paper constitute a first step towards the use of these techniques in the clinics, with the potential to improve the clinical decision-making process in children with cerebral palsy.

## 4.6 References

- [1] J. R. Gage, P. A. Deluca, and T. S. Renshaw, "Gait Analysis - Principles and Applications - Emphasis on Its Use in Cerebral-Palsy," (in English), *J Bone Joint Surg Am*, vol. 77, no. 10, pp. 1607-1623, Oct 1995, doi: Doi 10.2106/00004623-199510000-00017.
- [2] J. R. Gage and T. F. Novacheck, "An update on the treatment of gait problems in cerebral palsy," *J Pediatr Orthop B*, vol. 10, no. 4, pp. 265-74, Oct 2001. [Online]. Available: <https://www.ncbi.nlm.nih.gov/pubmed/11727367>.
- [3] B. Lofterød, T. Terjesen, I. Skaaret, A. B. Huse, and R. Jahnsen, "Preoperative gait analysis has a substantial effect on orthopedic decision making in children with cerebral palsy: comparison between clinical evaluation and gait analysis in 60 patients," (in eng), *Acta Orthop*, vol. 78, no. 1, pp. 74-80, Feb 2007, doi: 10.1080/17453670610013448.
- [4] T. A. Wren, K. Woolf, and R. M. Kay, "How closely do surgeons follow gait analysis recommendations and why?," (in eng), *J Pediatr Orthop B*, vol. 14, no. 3, pp. 202-5, May 2005, doi: 10.1097/01202412-200505000-00012.
- [5] R. B. Davis, S. Ounpuu, D. Tyburski, and J. R. Gage, "A Gait Analysis Data-Collection and Reduction Technique," (in English), *Hum Movement Sci*, vol. 10, no. 5, pp. 575-587, Oct 1991, doi: Doi 10.1016/0167-9457(91)90046-Z.
- [6] E. S. Grood and W. J. Suntay, "A Joint Coordinate System for the Clinical Description of Three-Dimensional Motions: Application to the Knee," *Journal of biomechanical engineering*, vol. 105, no. 2, pp. 136-144, 1983, doi: 10.1115/1.3138397.
- [7] M. P. Kadaba, H. K. Ramakrishnan, and M. E. Wootten, "Measurement of lower extremity kinematics during level walking," *J Orthop Res*, vol. 8, no. 3, pp. 383-92, May 1990, doi: 10.1002/jor.1100080310.
- [8] R. Baker, F. Leboeuf, J. Reay, and M. Sangeux, "The conventional gait model-success and limitations," *Handbook of human motion*, pp. 489-508, 2018.
- [9] T. W. Lu and J. J. O'Connor, "Bone position estimation from skin marker coordinates using global optimisation with joint constraints," (in English), *Journal of Biomechanics*, vol. 32, no. 2, pp. 129-134, Feb 1999, doi: Doi 10.1016/S0021-9290(98)00158-4.
- [10] H. Kainz *et al.*, "Reliability of four models for clinical gait analysis," (in eng), *Gait & posture*, vol. 54, pp. 325-331, May 2017, doi: 10.1016/j.gaitpost.2017.04.001.
- [11] B. Horsak, B. Pobatschnig, C. Schwab, A. Baca, A. Kranzl, and H. Kainz, "Reliability of joint kinematic calculations based on direct kinematic and inverse kinematic models in obese children," *Gait & posture*, vol. 66, pp. 201-207, Oct 2018, doi: 10.1016/j.gaitpost.2018.08.027.
- [12] S. H. L. Smith, R. J. Coppack, A. J. van den Bogert, A. N. Bennett, and A. M. J. Bull, "Review of musculoskeletal modelling in a clinical setting: Current use in rehabilitation design, surgical decision making and healthcare interventions,"

- Clinical Biomechanics*, vol. 83, p. 105292, 2021/03/01/ 2021, doi: <https://doi.org/10.1016/j.clinbiomech.2021.105292>.
- [13] H. Kainz and M. H. Schwartz, "The importance of a consistent workflow to estimate muscle-tendon lengths based on joint angles from the conventional gait model," *Gait & posture*, vol. 88, pp. 1-9, 2021/07/01/ 2021, doi: <https://doi.org/10.1016/j.gaitpost.2021.04.039>.
- [14] H. Kainz, L. Modenese, D. G. Lloyd, S. Maine, H. P. J. Walsh, and C. P. Carty, "Joint kinematic calculation based on clinical direct kinematic versus inverse kinematic gait models," *J Biomech*, vol. 49, no. 9, pp. 1658-1669, Jun 14 2016, doi: 10.1016/j.jbiomech.2016.03.052.
- [15] V. Cimolin and M. Galli, "Summary measures for clinical gait analysis: a literature review," *Gait & posture*, vol. 39, no. 4, pp. 1005-10, Apr 2014, doi: 10.1016/j.gaitpost.2014.02.001.
- [16] R. Baker *et al.*, "The gait profile score and movement analysis profile," *Gait & posture*, vol. 30, no. 3, pp. 265-9, Oct 2009, doi: 10.1016/j.gaitpost.2009.05.020.
- [17] S. Beynon, J. L. McGinley, F. Dobson, and R. Baker, "Correlations of the Gait Profile Score and the Movement Analysis Profile relative to clinical judgments," *Gait & posture*, vol. 32, no. 1, pp. 129-32, May 2010, doi: 10.1016/j.gaitpost.2010.01.010.
- [18] H. M. Rasmussen, D. B. Nielsen, N. W. Pedersen, S. Overgaard, and A. Holsgaard-Larsen, "Gait Deviation Index, Gait Profile Score and Gait Variable Score in children with spastic cerebral palsy: Intra-rater reliability and agreement across two repeated sessions," *Gait & posture*, vol. 42, no. 2, pp. 133-137, 2015/07/01/ 2015, doi: <https://doi.org/10.1016/j.gaitpost.2015.04.019>.
- [19] L. A. B. Ferreira, V. Cimolin, P. F. Costici, G. Albertini, C. S. Oliveira, and M. Galli, "Effects of gastrocnemius fascia lengthening on gait pattern in children with cerebral palsy using the Gait Profile Score," *Research in Developmental Disabilities*, vol. 35, no. 5, pp. 1137-1143, 2014/05/01/ 2014, doi: <https://doi.org/10.1016/j.ridd.2014.02.001>.
- [20] G. B. Firth *et al.*, "Multilevel surgery for equinus gait in children with spastic diplegic cerebral palsy: medium-term follow-up with gait analysis," *J Bone Joint Surg Am*, vol. 95, no. 10, pp. 931-8, May 15 2013, doi: 10.2106/JBJS.K.01542.
- [21] S. L. Delp *et al.*, "OpenSim: open-source software to create and analyze dynamic simulations of movement," (in English), *Ieee T Bio-Med Eng*, vol. 54, no. 11, pp. 1940-50, Nov 2007, doi: 10.1109/TBME.2007.901024.
- [22] H. Kainz, H. X. Hoang, C. Stockton, R. R. Boyd, D. G. Lloyd, and C. P. Carty, "Accuracy and Reliability of Marker-Based Approaches to Scale the Pelvis, Thigh, and Shank Segments in Musculoskeletal Models," *J Appl Biomech*, vol. 33, no. 5, pp. 354-360, Oct 1 2017, doi: 10.1123/jab.2016-0282.
- [23] M. Simic, T. V. Wrigley, R. S. Hinman, M. A. Hunt, and K. L. Bennell, "Altering foot progression angle in people with medial knee osteoarthritis: the effects of varying toe-in and toe-out angles are mediated by pain and

- malalignment," *Osteoarthritis and Cartilage*, vol. 21, no. 9, pp. 1272-1280, 2013, doi: 10.1016/j.joca.2013.06.001.
- [24] I. Motion Lab Systems, "Knee Alignment Device: User Manual," ed. Baton Rouge, Louisiana: Motion Lab Systems, Inc, 2011.
- [25] T. C. Pataky, "One-dimensional statistical parametric mapping in Python," (in English), *Comput Method Biomec*, vol. 15, no. 3, pp. 295-301, 2012, doi: 10.1080/10255842.2010.527837.
- [26] R. O. Robinson, W. Herzog, and B. M. Nigg, "Use of force platform variables to quantify the effects of chiropractic manipulation on gait symmetry," (in eng), *J Manipulative Physiol Ther*, vol. 10, no. 4, pp. 172-6, Aug 1987.
- [27] R. Baker, J. L. McGinley, M. Schwartz, P. Thomason, J. Rodda, and H. K. Graham, "The minimal clinically important difference for the Gait Profile Score," *Gait & posture*, vol. 35, no. 4, pp. 612-5, Apr 2012, doi: 10.1016/j.gaitpost.2011.12.008.
- [28] H. S. Read, M. E. Hazlewood, S. J. Hillman, R. J. Prescott, and J. E. Robb, "Edinburgh visual gait score for use in cerebral palsy," (in eng), *J Pediatr Orthop*, vol. 23, no. 3, pp. 296-301, May-Jun 2003.
- [29] J. L. McGinley, R. Baker, R. Wolfe, and M. E. Morris, "The reliability of three-dimensional kinematic gait measurements: A systematic review," *Gait & posture*, vol. 29, no. 3, pp. 360-369, 2009/04/01/ 2009, doi: <https://doi.org/10.1016/j.gaitpost.2008.09.003>.
- [30] K. Desloovere, G. Molenaers, H. Feys, C. Huenaearts, B. Callewaert, and P. V. d. Walle, "Do dynamic and static clinical measurements correlate with gait analysis parameters in children with cerebral palsy?," *Gait & posture*, vol. 24, no. 3, pp. 302-313, 2006/11/01/ 2006, doi: <https://doi.org/10.1016/j.gaitpost.2005.10.008>.
- [31] P. A. DeLuca, R. B. Davis, 3rd, S. Ounpuu, S. Rose, and R. Sirkin, "Alterations in surgical decision making in patients with cerebral palsy based on three-dimensional gait analysis," *J Pediatr Orthop*, vol. 17, no. 5, pp. 608-14, Sep-Oct 1997, doi: 10.1097/00004694-199709000-00007.
- [32] M. H. Schwartz, H. Kainz, and A. G. Georgiadis, "Estimating Causal Treatment Effects of Femoral and Tibial Derotational Osteotomies on Foot Progression in Children with Cerebral Palsy," Cold Spring Harbor Laboratory, 2021.
- [33] A. Leardini, C. Belvedere, F. Nardini, N. Sancisi, M. Conconi, and V. Parenti-Castelli, "Kinematic models of lower limb joints for musculo-skeletal modelling and optimization in gait analysis," *Journal of Biomechanics*, vol. 62, pp. 77-86, 2017, doi: 10.1016/j.jbiomech.2017.04.029.
- [34] A. S. Arnold, M. Q. Liu, M. H. Schwartz, S. Ounpuu, and S. L. Delp, "The role of estimating muscle-tendon lengths and velocities of the hamstrings in the evaluation and treatment of crouch gait," *Gait & posture*, vol. 23, no. 3, pp. 273-81, Apr 2006, doi: 10.1016/j.gaitpost.2005.03.003.
- [35] H. Kainz *et al.*, "O 107 – Impact of subject-specific musculoskeletal geometry on estimated joint kinematics, joint kinetics and muscle forces in typically

- developing children," *Gait & posture*, vol. 65, pp. 223-225, 2018/09/01/ 2018, doi: 10.1016/j.gaitpost.2018.06.142.
- [36] K. Veerkamp, H. Kainz, B. A. Killen, H. Jónasdóttir, and M. M. van der Krogt, "Torsion Tool: An automated tool for personalising femoral and tibial geometries in OpenSim musculoskeletal models," *Journal of Biomechanics*, vol. 125, p. 110589, 2021/08/26/ 2021, doi: <https://doi.org/10.1016/j.jbiomech.2021.110589>.
- [37] L. Modenese, M. Barzan, and C. P. Carty, "Dependency of Lower Limb Joint Reaction Forces on Femoral Anteversion," *Gait & posture*, 2021/06/16/ 2021, doi: <https://doi.org/10.1016/j.gaitpost.2021.06.014>.
- [38] A. S. Arnold, S. S. Blemker, and S. L. Delp, "Evaluation of a deformable musculoskeletal model for estimating muscle-tendon lengths during crouch gait," *Ann Biomed Eng*, vol. 29, no. 3, pp. 263-74, Mar 2001, doi: 10.1114/1.1355277.
- [39] A. A. Slater, T. J. Hullfish, and J. R. Baxter, "The impact of thigh and shank marker quantity on lower extremity kinematics using a constrained model," *BMC Musculoskeletal Disorders*, vol. 19, no. 1, p. 399, 2018/11/13 2018, doi: 10.1186/s12891-018-2329-7.

## **5 Role of pre-surgery muscle-tendon lengths on the outcome of femoral derotation osteotomy.**



## 5.1 Introduction

Cerebral Palsy (CP) is the commonest musculoskeletal disorder in children that affects muscular function and skeletal geometry [1]. One structural aberration is the development of an excessive femoral anteversion which leads to deviations from normal gait, the commonest of which is an internal rotation gait characterised by an excessively internally rotated hip [2-4] and intoeing of the lower extremity. Treatment of this bone deformity and by extension the pathologic gait pattern, is by a femoral derotation osteotomy (FDO) [5]. This is usually part of a battery of surgeries to correct other related issues in what is termed a Single Event Multiple Level Surgery (SEMLS). The rationale of SEMLS is to limit the number of surgeries and attendant recuperation periods that can have a negative psychological effect on the children [6].

While outcomes of the FDO are generally reported to be positive [7, 8], recent studies have indicated the incidence of recurrence of the excessive anteversion or abnormal gait and attempted to identify the risk factors that contribute to the recurrence [9-12]. These studies have predominantly focussed on the kinematic measures of gait and met with limited success. In particular, the discrimination of positive responders from non-responders to FDO has not been possible, while this information would be vital for surgical stratification and planning. A probable contributing factor to the limited success is the complexity of the intervention in the context of SEMLS, especially in the simultaneous presence of soft tissue surgeries. The potential impact of the FDO on a soft tissue intervention, in fact, even led to the suggestion that the anteversion should be first corrected and the need for the soft tissue surgery then be reassessed [13].

The FDO is primarily a bony correction, however since the musculature leverages on the bone geometries it certainly impacts also on the function of the muscles in terms of their lengths, moment arms and force-generation capacity during a movement. Numerous studies have investigated and shown the impact of bone geometry and muscle attachments on these muscle parameters and function during gait [14-16]. For instance, when focussing on femoral anteversion which the FDO seeks to correct, Schutte, et al. [17] found that the length of the psoas was sensitive to the degree of femoral anteversion that was present. Additionally, Nyland, et al. [18] reported on differences in the magnitude of activations of the vastus medialis and gluteus medius between groups with different degrees of femoral anteversion. Given that the FDO impacts directly on the degree of femoral anteversion, there exists the potential to also impact on muscle-tendon lengths by altering the lines of action of muscles about the hip. Any length changes produced as a consequence of the FDO could therefore play a role in determining post-SEMLS intervention outcomes, particularly where there are also concomitant muscle lengthening surgeries on the affected muscles.

Three-dimensional gait analysis is an approach that is used in the clinical and research setting to study and diagnose gait deviations based on the analysis of the joint kinematics (joint angles) and kinetics (joint moments) [19-21]. Although this is of high utility [22, 23], it fails to provide insights into other biomechanical parameters that could be highly relevant for surgical predictions, such as changes in muscle length, moment arms or intersegmental forces exerted during gait. Obtaining these parameters would normally require invasive methods, which is not justifiable under both ethical and patient care considerations. Musculoskeletal (MSK) modelling and simulation provides an avenue to query this information as well as perform what-if analyses [4, 24-27]. For instance, using 3D gait analysis, studies have shown that Botulinum Toxin injections and SEMLS are able to improve to an extent, gait patterns in children with CP [28, 29]. In a recent study using MSK models however, it has been shown that despite the observed improvements in gait pattern, the Botulinum injections do not significantly alter muscle force generation or reduce joint loadings, two main contributors to the development of bone deformation and gait deviation, compared to SEMLS [30]. Additionally, Rajagopal, et al. [31] showed with MSK models that knowledge of pre-operative lengths of muscles such as the gastrocnemius can have good predictive value for outcomes from muscle lengthening surgeries. FDO can benefit from such an analysis with MSK models.

The literature is however sparse with regards to the effect of the FDO, on the muscle parameters, particularly in the context of SEMLS. Previous work reported that FDO was unlikely to substantially change the lengths of the adductors, hamstrings and gracilis, muscles that are often lengthened during surgery, using a computer model and verified with an anatomical study [32]. It is however important to note that the measure of the significance of the change observed was with respect to what would have been achieved with a muscle lengthening surgery. Further, the above study was opposed to another study where the adductor longus was reported to shorten by as much as 10% [32]. Aside the contrasting conclusions from these studies, it is important to highlight that these were static studies and did not address outcomes attributed to changes in the muscle-tendon lengths during gait. Moreover, the results were not linked to the effectiveness of the surgery and the potential to discriminate positive responders from non-responders. Last but not least, not all muscles supporting hip ab/adduction, whose moment arms are reported to be affected by the anteversion, were considered.

Muscle-tendon lengths are known to influence the force generating capacity of muscles [33, 34] and changes in muscle-tendon length aside changes in moment arms occasioned by an FDO can either reinforce or negate gains from concurrent muscle lengthening surgeries during SEMLS thereby affecting gait outcomes. The aim of this

study is therefore to investigate the hypothesis that pre-surgery hip muscle-tendon lengths can be a factor affecting outcomes and as such could serve as a potential discriminators to identify responders from non-responders when considering FDO as part of SEMLS.

## **5.2 Methods**

Using the data, models and kinematics from the previous chapter (chapter four), the "Analyze" tool in OpenSim3.3 was used to estimate the muscle-tendon lengths over the gait cycle for both healthy controls and participants with CP.

### **5.2.1 Data and statistical analysis**

To permit comparison and identify potential indicators of outcome within the CP cohort, the participants were classified as responders (RS) and non-responders (NR) to FDO in the context of SEMLS based on a scheme agreed between two consultant orthopaedic surgeons and the gait analysis service including clinical scientists and physiotherapists as in [35]. Briefly, participant classification into the two groups were based on review of clinical examination and dictation notes, as well as video recordings emphasising on hip rotation and foot progression in stance. The classifications were completed by one clinical scientist and reviewed by the surgeons. No aspect of the 3D gait analysis and reports were included in this evaluation.

Joint kinematic profiles and foot progression angles were compared between responders and non-responders using a non-parametric two sample test from the *spm1d* statistical parametric mapping package [36] with alpha set to 0.0056 after Bonferroni correction for multiple comparison.

Analysis of the muscle-tendon lengths focussed on the hip ab/adductor muscles as those were expected to be impacted by the FDO. These were adductor brevis (add.brev), adductor longus (add.long), adductor magnus (add.mag), gluteus medius (glut.med), gluteus minimus (glut.min), gracilis (grac), pectoralis (pect), quadratus femoris (quad.fem) and sartorius (sar). Muscle tendon lengths over the gait cycle for each muscle were normalised to their lengths in anatomical/neutral pose (joint angles set equal to zero) to account for growth and facilitate comparison between groups and participants [37].

The maximum of the normalised MTL over the gait cycle and over all trials ( $MTL_{max}$ ) was extracted for each participant as shown in Figure 5.1. For the muscles whose geometrical paths were represented by three lines (adductor magnus, gluteus medius and gluteus minimus), the average for the 3 segments was calculated. This approach was decided upon using available subject-specific data from the cohort of juveniles

analysed in chapter 3 where it was observed that the mean  $MTL_{max}$  of the three segments of these muscles was similar to the value from the middle line segment. Comparison with generic models generated for the same juvenile cohort showed a similar correlation between the values estimated in this way as shown in Figure 5.2 below.

The first part of the analysis focused on determining whether muscles were longer or shorter at pre and post intervention observations with respect to an age-matched control group (TD). To do this, the extracted  $MTL_{max}$  was compared to that from the controls [37, 38]. Muscles were classified as long when  $MTL_{max}$  was more than two standard deviations higher than the control mean and shorter when less than two standard deviations lower than the control mean (Equation 5.1 - 5.3 and Figure 5.1).

$$\text{Normal: } MTL_{max}^{TD} - 2SD_{MTL_{max}^{TD}} \leq MTL_{max}^{CP} \leq MTL_{max}^{TD} + 2SD_{MTL_{max}^{TD}} \quad \text{(Equation 5.1)}$$

$$\text{Short: } MTL_{max}^{CP} < MTL_{max}^{TD} - 2SD_{MTL_{max}^{TD}} \quad \text{(Equation 5.2)}$$

$$\text{Long: } MTL_{max}^{CP} > MTL_{max}^{TD} + 2SD_{MTL_{max}^{TD}} \quad \text{(Equation 5.3)}$$

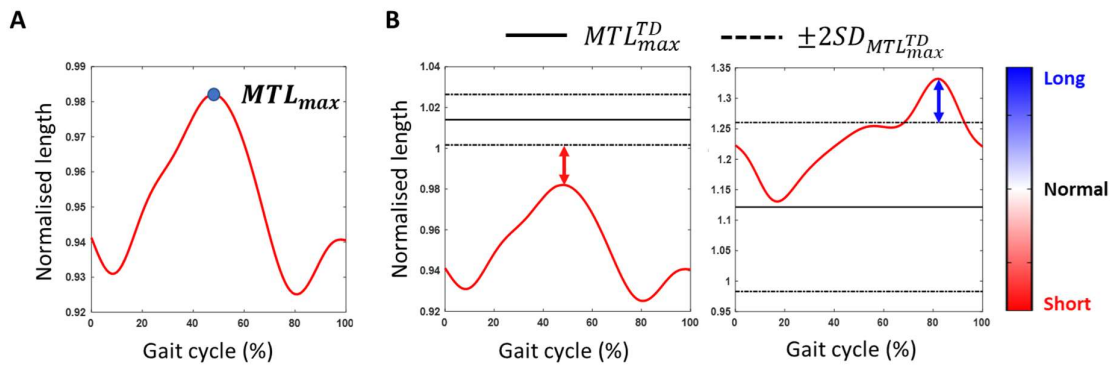


**Figure 5.1 Classification of muscles as long or short with respect to the controls (TD). Maximum MTL achieved over the gait cycle (A). Colour scale indicating the magnitude of deviation of a CP group muscle from the TD maximum values (B).**

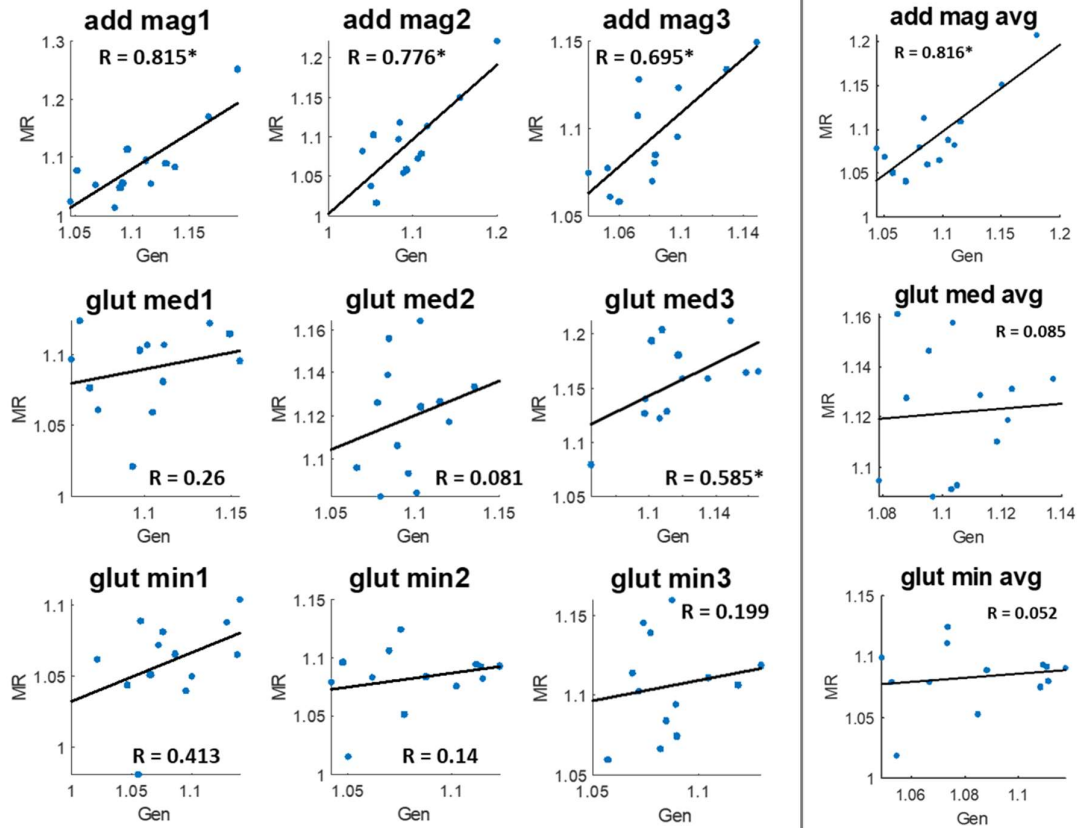


**Figure 5.2 Correlation between generic (Gen) and subject-specific (MR) estimates of  $MTL_{max}$  for each segment per muscle and as the average of muscle segment values.**

The second level of analysis investigated how the muscle lengths compared between responders (RS) and non-responders (NR) at both pre- and post-surgery observations without consideration of the controls.  $MTL_{max}$  were extracted as previously. Following tests for normality, either a two-sample t-test or non-parametric two-sample test was employed to determine if  $MTL_{max}$  were different between RS and NR groups before and after surgery. Similarly, either a paired sample t-test or Wilcoxon sign rank test was used to compare pre- and post-surgery  $MTL_{max}$  for both RS and NR groups.

To determine if the trends observed for FDO in the context of SEMLS was maintained for limbs that received just the FDO, the preceding analysis was repeated for this subgroup of RS and NR although the sample size was reduced. Statistical tests on the MTLs were performed at an alpha of 0.05 to minimise the likelihood of type II errors making it more likely to reject the null hypothesis when a difference exists. Cohen's d is calculated as estimates of effect size for each comparison.

### 5.3 Results

The 26 participants yielded 52 limbs of which 43 had undergone FDO as part of SEMLS (FDO-SEMLS). Of the 43 limbs, 31 had additional soft tissue surgeries to the FDO (responders: 20 and non-responders: 11). Additionally, of the 12 who had only FDO as intervention, 10 were responders and 2, non-responders. Table A2.1 in the appendix summarises the concomitant soft tissue surgeries.

Joint angle and foot progression angle profiles over the gait cycle for responders and non-responders were not significantly different between the two outcome groups and this is presented as Figures A2.1 and A2.2 in the appendix. The RS group however had on average, relatively more anterior pelvic tilt and less internal hip rotation than the NR group at both pre- and post-intervention.

As an example, the MTL profiles of the hip ab/adductor muscles over the gait cycle for one CP participant (7 years, 21.9 kg and 1.20 m, GMFCS level II at pre-surgery) before and after FDO-SEMLS is shown in Figure 5.3.

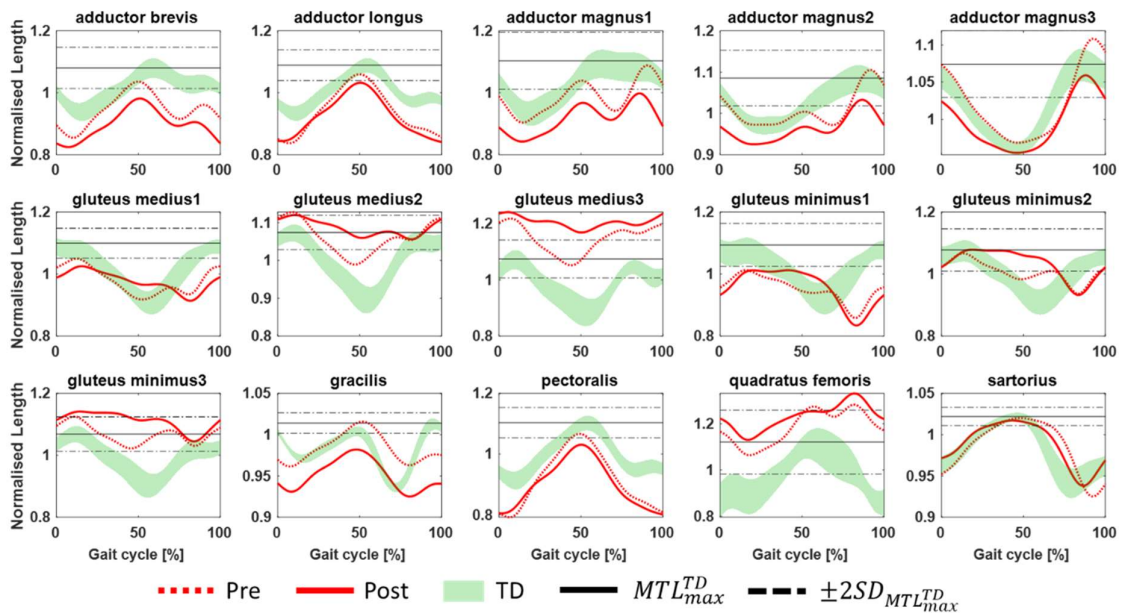


**Figure 5.3 Example of muscle-tendon lengths over the gait cycle for a CP participant before and after FDO-SEMLS**

Figure 5.4, built using the  $MTL_{max}$  values, shows a visual summary of the amount by which the  $MTL_{max}$  of muscles in the CP cohort were longer or shorter with respect to the TD group. Most muscles appeared to deviate from the healthy to a similar extent for both RS and NR. The quadratus femoris muscle was consistently longer than normal in most participants pre-operatively, decreasing in length post-operatively for both RS and NR. Post-operatively however, only the RS group achieved a reduction to

normal levels. The adductor magnus was also consistently longer than normal in the RS group (3±3% longer), whereas in the NR group it was of relatively normal length (1±3% longer), pre-operatively.

When comparing directly MTL<sub>max</sub> between RS and NR, statistically significant differences were observed for 3 muscles (adductor brevis, adductor magnus and gracilis) at pre-surgery observation (Figure 5.5). These muscles were on average longer in the RS group than in the NR group with moderate to strong effect sizes estimated with Cohen's d (0.79, 0.78 and 1.15 for adductor brevis, adductor magnus and gracilis, respectively). Post-operatively, hip ab/adductor MTL<sub>max</sub> were not significantly different between the two groups.

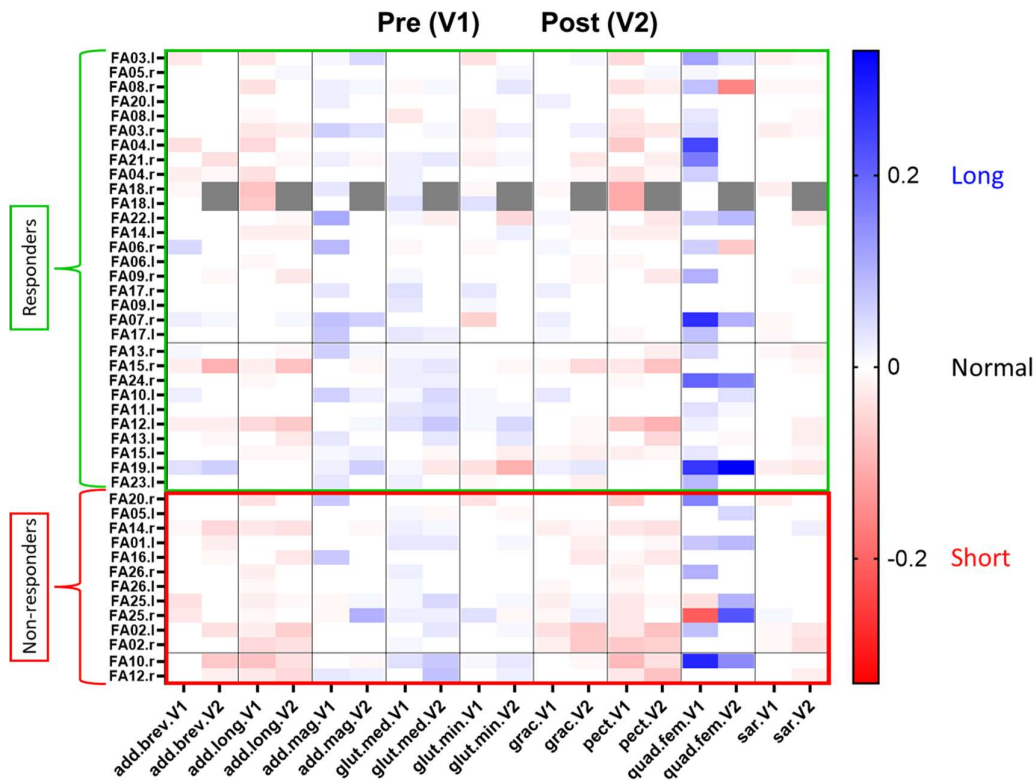


**Figure 5.4 Heatmap showing classification of CP cohort hip ab/adductor muscles as longer or shorter than TD before and after FDO-SEMLS. Muscle abbreviations are adductor brevis (add.brev), adductor longus (add.long), adductor magnus (add.mag), gluteus medius (glut.med), gluteus minimus (glut.min), gracilis (grac), pectoralis (pect), quadratus femoris (quad.fem) and sartorius (sar). FA18 had no 3D data for post-intervention (grey).**

For the comparison between pre- and post-surgery MTL<sub>max</sub>, the RS group tended to attain longer MTL<sub>max</sub> during gait pre-operatively with a decrease in MTL<sub>max</sub> after the intervention in four of the hip ab/adductors considered (Figure 5.5). Effect size

estimate of Cohen's d was greater than 0.5. MTL<sub>max</sub> were similar in the NR group before and after FDO-SEMLS.

Overall, the FDO-SEMLS intervention appeared to have higher impact in the RS group than NR when considering the change in the MTL<sub>max</sub> values as summarised in Table 5.1. The observation for the RS group were maintained when the analysis was limited to those limbs that received only the FDO with no other surgeries (Figure 5.6).

**Table 5.1 Post-surgery change in MTL<sub>max</sub> (mean (SD)) for RS and NR groups**

	add.brev	add.long	add.mag	glut.med	glut.min	grac	pect	quad.fem	sar
RS	-0.02 (0.04)	0.00 (0.04)	-0.05 (0.05)	0.00 (0.04)	0.02 (0.06)	-0.01 (0.02)	0.00 (0.04)	-0.14 (0.14)	0.00 (0.01)
NR	0.00 (0.06)	0.01 (0.04)	-0.02 (0.08)	0.01 (0.05)	0.00 (0.06)	0.00 (0.03)	0.02 (0.05)	0.00 (0.25)	-0.01 (0.02)

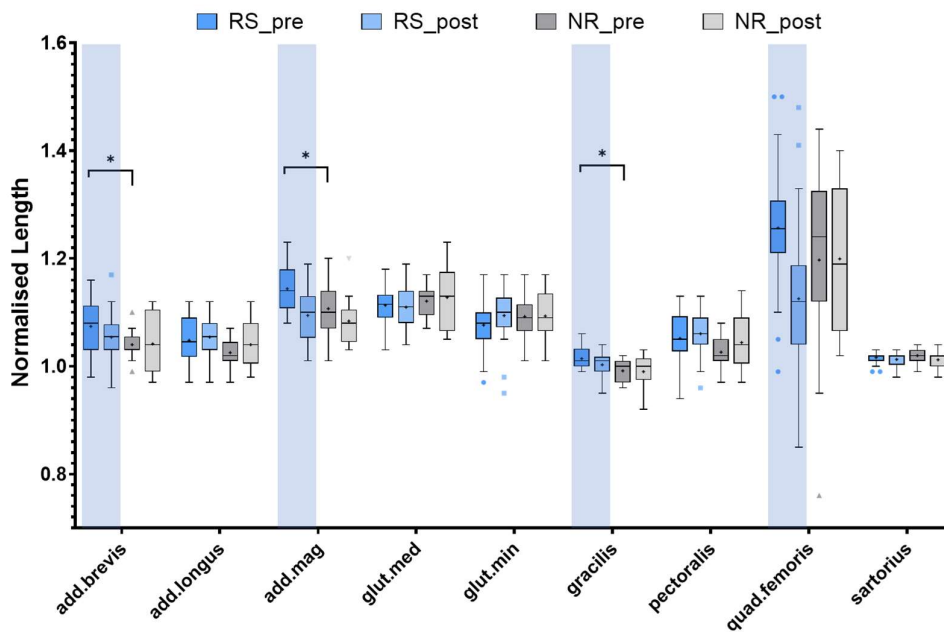


**Figure 5.5 MTL<sub>max</sub> distribution and comparison between RS and NR groups of the CP cohort at pre- and post- FDO-SEMLS. Blue bands indicate statistically significant differences between pre and post lengths for the RS group. \*Significant difference between RS and NR pre-surgery.**



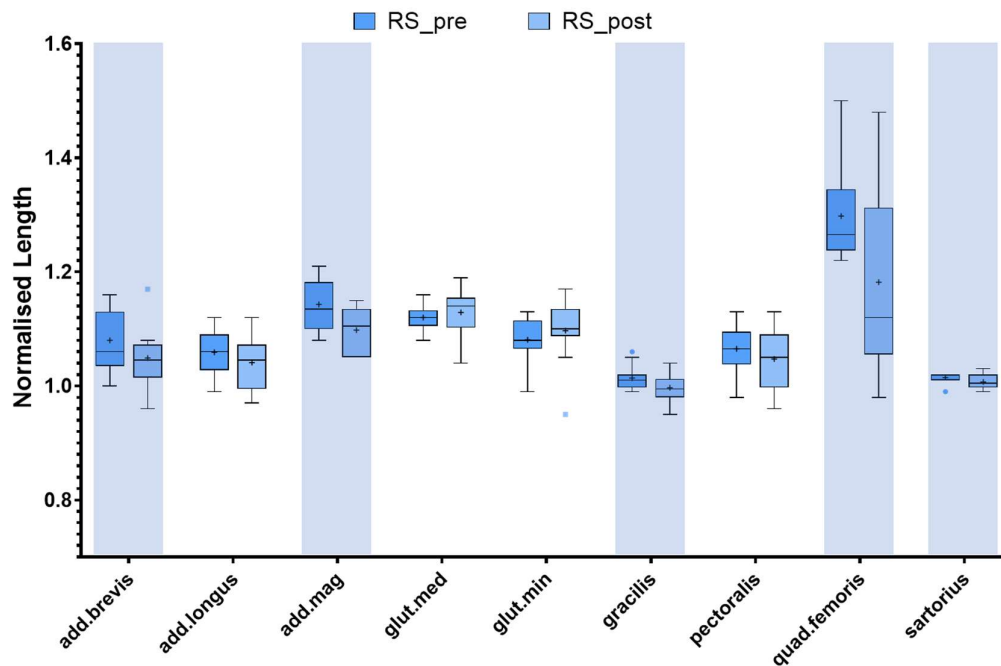


**Figure 5.6 Pre/post-surgery comparison of  $MTL_{max}$  values for RS group who had only the FDO. Plots for NR not shown due to low sample size ( $n=2$ ). Blue bands indicate statistically significant differences between pre and post  $MTL_{max}$ .**

## 5.4 Discussion

The aim of this study was to evaluate the hypothesis that pre-surgical lengths of hip muscles can serve as possible discriminators of outcome after FDO as part of SEMLS. The reported results suggest that three muscles could be of interest for predictive value: adductor brevis, adductor magnus and gracilis. The length of these muscles, in fact, were significantly different between responders and non-responders before surgery, with medium to strong effect size (Cohen's  $d > 0.7$ ), and they were also effectively modified by the surgery in the responder group.

From the reported results, it emerged that the differences between patients and controls did not appear to be informative as discriminators for most muscles. Maximum muscle length achieved over the gait cycle deviated by similar amounts when compared to those of healthy controls for both responders and non-responders at pre- and post-surgery. Although not clear, some trends existed. For instance, the adductor magnus in the RS group tended to be longer pre-operatively and approached normal bounds after the surgery. Those in the NR group were generally within normal bounds pre- and post-operatively bar a few exceptions. Similarly, the quadratus femoris changed from being predominantly long pre-operatively to within normal for the RS group. How longer or shorter than normal the hip ab/adductors were, was

however only informative for the adductor magnus in identifying those who achieved positive outcomes from those who did not. On the contrary, when the  $MTL_{max}$  was compared directly between the two groups in the CP cohort, there were significant differences between the two groups at the pre-surgery observation, and thus providing a basis for identifying additional potential predictors of outcome after the FDO-SEMLS.

Within the patient group, differences between pre-surgical length emerged when comparing responders and non-responders. In particular, three hip ab/adductor muscles were identified (adductor brevis, adductor magnus and gracilis) which were different between the RS and NR groups at the pre-surgery observation. In addition to being significantly different from non-responders pre-operatively, the maximum lengths attained during gait by the responders tended to differ between timepoints (4 out of 9 muscles) indicating a medium to strong effect as calculated with Cohen's d, of the FDO-SEMLS. These muscles comprised the three that were different pre-surgery between groups (adductor brevis, adductor magnus and gracilis) and the quadratus femoris. This effect was maintained for the responders when considering the cohort who received only FDO to the ipsilateral lower limb.

Muscles in the responder group also tended to undergo greater changes after the FDO-SEMLS. Although not directly comparable in terms of the amount of correction that was applied during the FDO, the range of percentage change in  $MTL_{max}$  reported here (0 - 14%) are in line with the muscle length changes after FDO reported by Schmidt, et al. [32]. In discriminating responders from non-responders at the pre-surgery observation, the adductor brevis, adductor magnus and gracilis muscles appeared to be the most informative when considering SEMLS. These muscles showed a longer length during gait than those of the non-responders and tended to be shortened after the intervention to achieve similar lengths in both groups. When considering FDOs without any additional surgeries, the trend for the responders having longer  $MTL_{max}$  pre-surgery were maintained. That for the non-responders, however, could not be determined due to the small number of participants in that cohort who had received only FDO. This entails that further studies would be needed to identify a clear threshold of  $MTL_{max}$  that would separate RS and NR.

Limitations include the heterogenous nature of the dataset used. The limited database meant we could not have a high enough cohort of participants who had only FDO as the intervention. The outcomes reported in this study may be impacted by the additional soft tissue surgeries that were had. A clearer understanding of the impact of the FDO on MTLs could have been had. There was also limited availability to compare the selected hip ab/adductor MTL profiles over the gait cycle for both TD and CP

cohorts to, however comparison of the psoas and hamstrings from our models were found to be consistent with the literature [17, 24, 37, 39]. It is also conceded that the observed  $MTL_{max}$  are a consequence of the kinematics and any strategies the participants adopt during gait and that the findings reported are only suggestive of a predictive value of pre-surgical lengths for discriminating responders from non-responders to FDO-SEMLS. The strategy employed in this study to classify participants deviates slightly from what is normally used as the information from 3D gait analysis forms an intrinsic part of the clinical determination of outcome. This strategy was however kept for consistency with the previous chapter's results. Including this information may change participant classification as responder or non-responder and this is acknowledged. An additional limitation, which the next chapter would seek to address, is that these are not subject specific models and not capturing pre- and post-surgery geometries in the generic model could result in possibly erroneous estimates of the instantaneous muscle-tendon lengths. When comparing a scaled generic model and a subject-specific model, Scheys, et al. [14] showed that although the muscle-tendon lengths computed from either model were highly correlated, absolute values of muscle-tendon lengths were different. While that may be the case, they also showed that estimates of change in MTL corresponded between models for most muscles analysed. Further studies are hence needed to better clarify this point. Finally, the alpha used in the statistical tests is less conservative and may increase the likelihood of finding a significant difference when there is none, however given the exploratory nature of the study and the limitation of model and sample size, this approach was felt appropriate in this study.

## **5.5 Conclusion**

These initial results provide a case to further the question on the role of muscle-tendon lengths on outcomes after FDO and suggest that further investigation would be worth it to establish whether the pre-surgical lengths of the hip muscles should be included as an indicator for femoral derotation osteotomy. Given that the generic models with their known challenges suggest some predictive power, these could be focusing on patient-specific models that allow to account for the effects of simultaneous surgical interventions.

## 5.6 References

- [1] M. Bax *et al.*, "Proposed definition and classification of cerebral palsy, April 2005," *Dev Med Child Neurol*, vol. 47, no. 8, pp. 571-6, Aug 2005, doi: 10.1017/s001216220500112x.
- [2] M. T. Cibulka, "Determination and significance of femoral neck anteversion," (in English), *Phys Ther*, vol. 84, no. 6, pp. 550-8, Jun 2004. [Online]. Available: <https://www.ncbi.nlm.nih.gov/pubmed/15161420>.
- [3] J. Robin, H. K. Graham, P. Selber, F. Dobson, K. Smith, and R. Baker, "Proximal femoral geometry in cerebral palsy: a population-based cross-sectional study," *The Journal of bone and joint surgery. British volume*, vol. 90, no. 10, pp. 1372-9, Oct 2008, doi: 10.1302/0301-620X.90B10.20733.
- [4] A. S. Arnold, A. V. Komattu, and S. L. Delp, "Internal rotation gait: a compensatory mechanism to restore abduction capacity decreased by bone deformity," (in eng), *Dev Med Child Neurol*, vol. 39, no. 1, pp. 40-4, Jan 1997, doi: 10.1111/j.1469-8749.1997.tb08202.x.
- [5] M. H. Schwartz, A. Rozumalski, and T. F. Novacheck, "Femoral derotational osteotomy: surgical indications and outcomes in children with cerebral palsy," *Gait & posture*, vol. 39, no. 2, pp. 778-83, Feb 2014, doi: 10.1016/j.gaitpost.2013.10.016.
- [6] R. Norlin and H. Tkaczuk, "One-session surgery for correction of lower extremity deformities in children with cerebral palsy," (in eng), *J Pediatr Orthop*, vol. 5, no. 2, pp. 208-11, Mar-Apr 1985.
- [7] S. Ounpuu, P. DeLuca, R. Davis, and M. Romness, "Long-term effects of femoral derotation osteotomies: an evaluation using three-dimensional gait analysis," (in eng), *J Pediatr Orthop*, vol. 22, no. 2, pp. 139-45, Mar-Apr 2002.
- [8] V. Saraph, E. B. Zwick, G. Zwick, M. Dreier, G. Steinwender, and W. Linhart, "Effect of derotation osteotomy of the femur on hip and pelvis rotations in hemiplegic and diplegic children," (in eng), *J Pediatr Orthop B*, vol. 11, no. 2, pp. 159-66, Apr 2002, doi: 10.1097/00009957-200204000-00014.
- [9] T. Dreher *et al.*, "Long-term outcome of femoral derotation osteotomy in children with spastic diplegia," *Gait & posture*, vol. 36, no. 3, pp. 467-70, Jul 2012, doi: 10.1016/j.gaitpost.2012.04.017.
- [10] M. Niklasch, M. C. Klotz, S. I. Wolf, and T. Dreher, "Long-term development of overcorrection after femoral derotation osteotomy in children with cerebral palsy," *Gait & posture*, vol. 61, pp. 183-187, Mar 2018, doi: 10.1016/j.gaitpost.2018.01.012.
- [11] C. Church *et al.*, "Persistence and Recurrence Following Femoral Derotational Osteotomy in Ambulatory Children With Cerebral Palsy," *J Pediatr Orthop*, vol. 37, no. 7, pp. 447-453, Oct/Nov 2017, doi: 10.1097/BPO.0000000000000701.
- [12] S. Ounpuu, M. Solomito, K. Bell, and K. Pierz, "Long-term outcomes of external femoral derotation osteotomies in children with cerebral palsy," *Gait & posture*, vol. 56, pp. 82-88, Jul 2017, doi: 10.1016/j.gaitpost.2017.04.029.

- [13] M. S. Orendurff, A. K. Spens, R. A. Pierce, M. A. Aiona, and R. Dorociak, "The effect of femoral derotational osteotomies on kinematics of the lower extremities in gait," *Gait & posture*, vol. 4, no. 2, p. 200, 1996/04/01/ 1996, doi: [https://doi.org/10.1016/0966-6362\(96\)80643-6](https://doi.org/10.1016/0966-6362(96)80643-6).
- [14] L. Scheys, A. Spaepen, P. Suetens, and I. Jonkers, "Calculated moment-arm and muscle-tendon lengths during gait differ substantially using MR based versus rescaled generic lower-limb musculoskeletal models," (in English), *Gait & posture*, vol. 28, no. 4, pp. 640-8, Nov 2008, doi: 10.1016/j.gaitpost.2008.04.010.
- [15] L. Bosmans *et al.*, "Sensitivity of predicted muscle forces during gait to anatomical variability in musculotendon geometry," (in English), *J Biomech*, vol. 48, no. 10, pp. 2116-23, Jul 16 2015, doi: 10.1016/j.jbiomech.2015.02.052.
- [16] T. A. Correa, R. Baker, H. K. Graham, and M. G. Pandy, "Accuracy of generic musculoskeletal models in predicting the functional roles of muscles in human gait," (in English), *J Biomech*, vol. 44, no. 11, pp. 2096-105, Jul 28 2011, doi: 10.1016/j.jbiomech.2011.05.023.
- [17] L. M. Schutte, S. W. Hayden, and J. R. Gage, "Lengths of hamstrings and psoas muscles during crouch gait: effects of femoral anteversion," (in eng), *J Orthop Res*, vol. 15, no. 4, pp. 615-21, Jul 1997, doi: 10.1002/jor.1100150419.
- [18] J. Nyland, S. Kuzemchek, M. Parks, and D. N. M. Caborn, "Femoral anteversion influences vastus medialis and gluteus medius EMG amplitude: composite hip abductor EMG amplitude ratios during isometric combined hip abduction-external rotation," *Journal of Electromyography and Kinesiology*, vol. 14, no. 2, pp. 255-261, 2004/04/01/ 2004, doi: [https://doi.org/10.1016/S1050-6411\(03\)00078-6](https://doi.org/10.1016/S1050-6411(03)00078-6).
- [19] S. Armand, G. Decoulon, and A. Bonnefoy-Mazure, "Gait analysis in children with cerebral palsy," *EFORT Open Rev*, vol. 1, no. 12, pp. 448-460, Dec 2016, doi: 10.1302/2058-5241.1.000052.
- [20] R. Baker, "Gait analysis methods in rehabilitation," *J Neuroeng Rehabil*, journal article vol. 3, no. 1, p. 4, Mar 2 2006, doi: 10.1186/1743-0003-3-4.
- [21] R. Baker, A. Esquenazi, M. G. Benedetti, and K. Desloovere, "Gait analysis: clinical facts," *Eur J Phys Rehabil Med*, vol. 52, no. 4, pp. 560-74, Aug 2016. [Online]. Available: <https://www.ncbi.nlm.nih.gov/pubmed/27618499>.
- [22] T. A. L. Wren, G. E. Gorton, S. Öunpuu, and C. A. Tucker, "Efficacy of clinical gait analysis: A systematic review," *Gait & posture*, vol. 34, no. 2, pp. 149-153, 2011/06/01/ 2011, doi: <https://doi.org/10.1016/j.gaitpost.2011.03.027>.
- [23] T. A. L. Wren, C. A. Tucker, S. A. Rethlefsen, G. E. Gorton, and S. Öunpuu, "Clinical efficacy of instrumented gait analysis: Systematic review 2020 update," *Gait & posture*, vol. 80, pp. 274-279, 2020/07/01/ 2020, doi: <https://doi.org/10.1016/j.gaitpost.2020.05.031>.
- [24] A. S. Arnold, S. S. Blemker, and S. L. Delp, "Evaluation of a deformable musculoskeletal model for estimating muscle-tendon lengths during crouch gait," *Ann Biomed Eng*, vol. 29, no. 3, pp. 263-74, Mar 2001, doi: 10.1114/1.1355277.

- [25] A. S. Arnold, M. Q. Liu, M. H. Schwartz, S. Ounpuu, and S. L. Delp, "The role of estimating muscle-tendon lengths and velocities of the hamstrings in the evaluation and treatment of crouch gait," *Gait & posture*, vol. 23, no. 3, pp. 273-81, Apr 2006, doi: 10.1016/j.gaitpost.2005.03.003.
- [26] K. M. Steele, M. S. Demers, M. H. Schwartz, and S. L. Delp, "Compressive tibiofemoral force during crouch gait," (in English), *Gait & posture*, vol. 35, no. 4, pp. 556-60, Apr 2012, doi: 10.1016/j.gaitpost.2011.11.023.
- [27] K. M. Steele, M. M. van der Krogt, M. H. Schwartz, and S. L. Delp, "How much muscle strength is required to walk in a crouch gait?," *J Biomech*, vol. 45, no. 15, pp. 2564-9, Oct 11 2012, doi: 10.1016/j.jbiomech.2012.07.028.
- [28] J. Wissel *et al.*, "Gait analysis to assess the effects of botulinum toxin type A treatment in cerebral palsy: an open-label study in 10 children with equinus gait pattern," *European Journal of Neurology*, vol. 6, no. S4, pp. s63-s67, 1999, doi: <https://doi.org/10.1111/j.1468-1331.1999.tb00037.x>.
- [29] R. P. Lamberts, M. Burger, J. du Toit, and N. G. Langerak, "A Systematic Review of the Effects of Single-Event Multilevel Surgery on Gait Parameters in Children with Spastic Cerebral Palsy," (in eng), *PLoS One*, vol. 11, no. 10, p. e0164686, 2016, doi: 10.1371/journal.pone.0164686.
- [30] S. Van Rossom *et al.*, "Single-event multilevel surgery, but not botulinum toxin injections normalize joint loading in cerebral palsy patients," *Clin Biomech*, vol. 76, p. 105025, Jun 2020, doi: 10.1016/j.clinbiomech.2020.105025.
- [31] A. Rajagopal, Ł. Kidziński, A. S. McGlaughlin, J. L. Hicks, S. L. Delp, and M. H. Schwartz, "Pre-operative gastrocnemius lengths in gait predict outcomes following gastrocnemius lengthening surgery in children with cerebral palsy," *PLOS ONE*, vol. 15, no. 6, p. e0233706, 2020, doi: 10.1371/journal.pone.0233706.
- [32] D. J. Schmidt, A. S. Arnold, N. C. Carroll, and S. L. Delp, "Length changes of the hamstrings and adductors resulting from derotational osteotomies of the femur," (in eng), *J Orthop Res*, vol. 17, no. 2, pp. 279-85, Mar 1999, doi: 10.1002/jor.1100170218.
- [33] A. V. Hill, "The mechanics of active muscle," (in eng), *Proc R Soc Lond B Biol Sci*, vol. 141, no. 902, pp. 104-17, Mar 11 1953, doi: 10.1098/rspb.1953.0027.
- [34] E. M. Arnold, S. R. Hamner, A. Seth, M. Millard, and S. L. Delp, "How muscle fiber lengths and velocities affect muscle force generation as humans walk and run at different speeds," *Journal of Experimental Biology*, vol. 216, no. 11, pp. 2150-2160, 2013, doi: 10.1242/jeb.075697.
- [35] C. F. Hayford, E. Pratt, J. P. Cashman, O. G. Evans, and C. Mazza, "Effectiveness of Global Optimisation and Direct Kinematics in Predicting Surgical Outcome in Children with Cerebral Palsy," *Life (Basel)*, vol. 11, no. 12, p. 1306, Nov 27 2021, doi: 10.3390/life11121306.
- [36] T. C. Pataky, "Generalized n-dimensional biomechanical field analysis using statistical parametric mapping," (in eng), *J Biomech*, vol. 43, no. 10, pp. 1976-82, Jul 20 2010, doi: 10.1016/j.jbiomech.2010.03.008.

- [37] S. L. Delp, A. S. Arnold, R. A. Speers, and C. A. Moore, "Hamstrings and psoas lengths during normal and crouch gait: Implications for muscle-tendon surgery," *Journal of Orthopaedic Research*, vol. 14, no. 1, pp. 144-151, 1996, doi: <https://doi.org/10.1002/jor.1100140123>.
- [38] H. Kainz and M. H. Schwartz, "The importance of a consistent workflow to estimate muscle-tendon lengths based on joint angles from the conventional gait model," *Gait & posture*, vol. 88, pp. 1-9, 2021/07/01/ 2021, doi: <https://doi.org/10.1016/j.gaitpost.2021.04.039>.
- [39] A. S. Arnold, M. Q. Liu, M. H. Schwartz, S. Ounpuu, L. S. Dias, and S. L. Delp, "Do the hamstrings operate at increased muscle-tendon lengths and velocities after surgical lengthening?" *J Biomech*, vol. 39, no. 8, pp. 1498-506, 2006, doi: 10.1016/j.jbiomech.2005.03.026.

**6 Predicting longitudinal changes in joint contact forces  
in a juvenile population: scaled generic versus subject-  
specific musculoskeletal models**



### *Acknowledgement of co-authorship*

This chapter comprises a published manuscript titled "Predicting longitudinal changes in joint contact forces in a juvenile population: scaled generic versus subject-specific musculoskeletal models". This was work done in collaboration with the co-authors listed in the paper.

In this study, I contributed to the conceptualisation, design, implementation of the methods and simulations, analysis of the results and its interpretation. I also led in the drafting of the manuscript and production of all figures and tables therein as well as being responsible for the submission and review process.

Student:

Claude Fiifi Hayford



Date 12/01/2022

The main co-authors:

Claudia Mazzà



Date 14/01/2022

Emma Pratt



Date 17/01/2022

Erica Montefiori



Date 17/01/2022

## **6.1 Abstract**

Subject-specific musculoskeletal model use in clinical settings is limited due to development-associated time and effort burdens together with potential medical imaging unavailability. As an alternative, this study investigated consistency in estimating longitudinal changes in joint contact forces (JCF) between scaled generic and subject-specific models. For 11 children, joint kinematics and JCF were calculated using subject-specific and scaled generic models. Longitudinal changes in JCF in the absence of musculoskeletal interventions estimated by both models were strongly correlated for the hip and knee although JCF estimates varied between models. Findings suggest that within specified limits of accuracy, scaled generic models are sensitive enough to detect JCF changes consistent with subject-specific models.

## **6.2 Introduction**

Three-dimensional gait analysis (3DGA), based on optoelectronic and force platform data, has become a mainstay in the study of human movement musculoskeletal disorders, providing useful information to guide treatment planning and rehabilitation[1, 2]. Most recent literature has shown that the utility of conventional 3DGA can be further augmented with musculoskeletal models (MSK)[3, 4]. These are mathematical representations of the body as a system of rigid bodies linked in a chain by joints and constraints and actuated by muscle forces. This formulation lends itself to rigid multibody dynamics and simulation that provides information such as estimates of changes in muscle length, muscle force and joint contact force that are not available using conventional 3DGA or would require the use of some instrumented prosthesis.

Most commonly used MSK models, typically referred to as scaled generic models, are based on data extrapolated from cadaveric specimens of healthy adults[5-7] which are scaled based on markers or anthropometry to match a subject. This poses a challenge when dealing with different populations, such as children and those with pathologic conditions[8-10]. Imaging modalities such as Computed Tomography (CT) and Magnetic Resonance Imaging (MRI) have been used to address this challenge by allowing for the increase in personalisation of these models through the inclusion of subject-specific details like bone geometry[11], muscle paths and attachment[10, 12], as well as estimates of musculotendon parameters[13, 14]. This personalisation has been proven to increase the accuracy and reliability of these MSK models[11, 15]. Nonetheless, subject-specific models created in this way have cost and time burdens which limit their use in clinical settings [16]. In addition, medical imaging may not be feasible or available, especially when conducting retrospective studies. In such

instances, if sensitive enough to detect changes that are bigger than their expected limits of accuracy, generic models might represent a relatively easily implementable substitute.

A number of studies have compared the performance between generic models and image-based subject-specific models and concur that differences exist between the biomechanical measures estimated. When investigating a normal and a pathologic gait condition, Scheys et al.[17] found that differences existed between the moment arms and muscle-lengths estimated by the two types of models for 16 major muscles of the lower limb for each gait condition. For most of the muscles however, the changes in muscle length and moment arm estimates was found to be similar for the two approaches, for both normal and pathologic gait. Similarly, Correa et al.[18] found significant differences in muscle moment arms when comparing generic and subject-specific models but also reported that both models were consistent in their predictions of muscle action. Muscle forces contribute to the magnitude of joint contact forces (JCFs) and differences are therefore expected to be observed in JCF estimates between the two models. However, it remains unclear to what extent these differences impact on longitudinal estimates of changes in the biomechanical variables predicted by generic models and how they differ from those predicted from subject-specific models. The aim of this study was to examine the suitability of using scaled generic models to predict longitudinal changes in biomechanical measures and how these predictions differ from those obtained from subject-specific models in a juvenile population. We hypothesised that despite differences in instantaneous estimates of JCFs, there would be no difference in the change in calculated JCF over time between models. If this hypothesis holds true, scaled generic models could be used to infer clinically meaningful information where interest is in change over time as opposed to absolute estimates such as in predicting or evaluating surgical outcomes, hence suggesting the feasibility of using them as alternative to the more accurate subject-specific models.

## **6.3 Materials and methods**

### **6.3.1 Data collection**

Data from 11 participants (age at initial observation: mean 11.5 (SD 3.2) years) were extracted from a dataset collected during the MD-PAEDIGREE project, which aimed at investigating disease progression in children with Juvenile Idiopathic Arthritis (JIA)[3]. Subject anthropometry was recorded at an initial observation (mass:  $46.5 \pm 18.0$  kg, height:  $1.4 \pm 0.2$  m) and at twelve months follow-up (mass:  $51.4 \pm 20.5$  kg, height:  $1.5 \pm 0.2$  m). Approval was obtained from the research ethics committees of the hospitals

from which the data was collected. Gait data were collected over two observations (M0 and M12, 12 months apart) and across two laboratories, one using a 6-camera setup (BTS, SmartDX, 100Hz) with two force plates (Kistler, 1 kHz) and the other, an 8-camera system (Vicon, MX, 200Hz) with two force plates (AMTI, OR6, 1 kHz). The Vicon Plug in gait protocol (Vicon Motion Systems, 2008) augmented with the modified Oxford Foot Model [19] formed the set of forty-four markers used. Regional MRI of the foot and ankle was acquired for each participant at the two observations (M0 and M12) using a multi-slice multi-echo 3D Gradient Echo (mFFE) with water only selection (0.5 mm in plane resolution and 1 mm slice thickness). MRI was also used to acquire entire lower limb images at an intermediate timepoint (six months from initial observation) using a 3D T1-weighted fat-suppression sequence. In-plane resolution was 1 mm with a slice thickness of 1 mm. These images were used to clinically evaluate bone erosion and cartilage damage [20].

### **6.3.2 Modelling approaches**

Subject-specific bone geometries for the two timepoints were obtained by a single expert operator segmenting MRI images of the full lower-limb together with the regional foot and ankle images from each observation point, respectively. The full lower-limb geometries for each participant were subsequently coupled with the regional geometries to build subject-specific models (SubS) for each observation using NMSBuilder [21]. For each SubS model, the hip was modelled as an ideal ball-and-socket joint, with ideal hinges for the knee, ankle and subtalar joints. The joint axes were defined by morphological fitting of articular surfaces isolated from the bone geometries, using a least square difference minimization approach. A sphere was fitted to the femoral head to determine the hip joint centre with cylinders fitted to the femur condyles and talus to determine the knee flexion/extension axis, ankle plantar/dorsi-flexion axis and subtalar inversion/eversion axis, respectively. A supervised atlas registration procedure with a reference generic model [5] was used to estimate muscle attachments and via points, with manual adjustment against the MRI when needed. The maximum isometric force for each muscle in the SubS model was linearly scaled from the generic model value using the ratio of participant lower-limb mass and the lower limb mass of the generic model as in [3]. The participant lower-limb mass was calculated as the product of the soft tissue volume and bone volume and their respective densities from the literature [22]. Further details for generating the SubS are provided in Modenese, et al. [23] and Montefiori, et al. [20].

The cadaver-based generic gait2392 model [5] formed the basis of the scaled generic models (Gen). The gait2392 model was scaled by each subject's mass and anthropometry based on experimental markers placed on anatomical landmarks and

estimated joint centres using the Scale tool in OpenSim 3.3 [5, 24]. Scaling was based on literature recommendations [25, 26] using Harrington regression equation estimates of the hip joint centre [27], midpoint of medial and lateral epicondyle and malleolus markers for the knee and ankle joint centres, respectively. The pelvis was scaled anisotropically using the markers on the pelvis and the two hip joint centre markers. Pelvis height was defined as the average of the distance between marker pairs (RASI/RHJC and LASI/LHJC) and pelvis depth as the average of distance between marker pairs (RASI/RPSI and LASI/LPSI). Maximum isometric force of each muscle was scaled by the mass of the subject divided by the mass of the gait2392 model. Optimal fibre length was scaled to preserve the muscle-tendon length ratio in the gait2392 model. The Gen models consisted of a single lower limb model with 12 degrees of freedom (DoF) for consistency with the SubS which were unilateral.

Simulations were subsequently performed in OpenSim 3.3 using a minimum of three collected experimental gait trials for each participant. The OpenSim simulation pipeline included inverse kinematics, inverse dynamics, static optimisation and joint reaction analysis [28]. For each model and observation, joint angles, joint moments, muscle forces and JCFs were obtained. In line with best practice, maximum root mean square tracking error and peak marker tracking error between experimental marker trajectories and virtual markers for each model were kept below the recommended 20 mm and 40 mm thresholds [25], respectively for inverse kinematics. Static posture joint angles were considered as a zero reference in comparing kinematic outputs between the two models. Joint powers were calculated as the product of joint moment and angular velocity. The muscle force-length-velocity relationship was ignored for both models during the estimation of muscle activation and force during static optimisation. Simulated joint moments and JCFs were normalised by participant body weight (BW). The value of reserve actuators applied to the models were checked and these were less than 1 N from the output of static optimisation.

### **6.3.3 Differences between Gen and SubS models**

Group mean and standard deviation for each estimated variable were determined as the average of ensemble means of subject trials for all subjects for both models. Joint angles, joint moments, joint power, JCF and differences in JCF ( $\Delta$ JCF) at the hip, knee and ankle were compared between models and observations using the nonparametric one sample paired t-tests from the *spm1d* statistical parametric mapping (SPM) package [29] in MATLAB (v9.5.0, R2018b, MathWorks, USA). Significance was evaluated at  $\alpha < 0.05$ .

For the JCFs, total waveform variability or goodness of fit was assessed using the Root Mean Square Deviation (RMSD) [30] between Gen and SubS for each subject at each observation. The percentage difference (*%Diff*) in JCF estimates was calculated as the ratio of RMSD to range of JCF predicted by the SubS model for each participant.

The coefficient of determination ( $R^2$ ) was calculated using the Linear Fit Method to assess waveform shape similarity [31] of JCF estimates over the gait cycle between Gen and SubS for each participant. This method can be used as a robust measure of curve similarity in the analysis of gait data [32]. Peak values of JCF during the loading response (P1, indicated as occurring within the first 20% of the gait cycle) and push off (P2, indicated as occurring between 40 to 60% of the gait cycle) for both models were extracted for each participant and analysed. Area under the JCF curves (AUC) were also calculated as measures of overall loading of the joint throughout the gait cycle and compared between the two models. A graphical representation of the different indices used is presented in the supplementary materials.

#### **6.3.4 Consistency in longitudinal predictions**

Inter-observation differences ( $\Delta_t$ ) between the values of JCFs, AUC and JCF peak 1 and peak 2 were calculated for each participant's Gen and SubS model to assess their agreement in estimating longitudinal changes. Inter-model differences ( $\Delta_m$ ) for these metrics at each observation were similarly calculated for each participant. Gen and SubS were judged as in agreement in predicting longitudinal changes in JCFs if the coefficient of determination  $R^2$  calculated between  $\Delta_t(\text{JCF}_{\text{Gen}})$  and  $\Delta_t(\text{JCF}_{\text{SubS}})$  was greater than or equal to 0.6.

It has been previously reported that SubS output is affected by repeatability errors associated to operator input [3]. In order to account for this when assessing the differences between the two models, ad-hoc thresholds were calculated for hip (H), knee (K) and ankle (A) joints using publicly available data [3]:  $\Delta_m(\text{AUC}_H) = 29.17$ ,  $\Delta_m(\text{AUC}_K) = 7.88$ ,  $\Delta_m(\text{AUC}_A) = 4.42$ ,  $\Delta_m(\text{P1}_H) = 0.45$  BW,  $\Delta_m(\text{P2}_H) = 1.27$  BW,  $\Delta_m(\text{P1}_K) = 0.36$  BW,  $\Delta_m(\text{P2}_K) = 0.64$  BW and  $\Delta_m(\text{P1}_A) = 0.94$  BW. If corresponding  $\Delta_m(\text{JCF peaks})$  and  $\Delta_m(\text{AUC})$  were lower than these thresholds at both observations, then the longitudinal output from the two models were considered to be in agreement for that participant. If the differences between the two models were bigger than these thresholds for at least one of the observations, then the differences ( $\Delta_t$ ) obtained for the two models were considered as being in agreement if consistent in signs.

Finally, significance of inter-model and inter-observation differences in estimates of RMSD, JCF peak values and area under JCF curve were assessed with the Wilcoxon signed-rank test in MATLAB. Effect size statistics for these estimates was also

calculated using Cohen's d estimate with a pooled standard deviation from SubS and Gen. All statistical tests were conducted at  $\alpha < 0.05$ .

## 6.4 Results

Assessment of MRI images of the ankle did not highlight any clinically meaningful changes in bone erosion and cartilage damage between the two time points, evidencing no relevant bone deformities at this joint.

Estimates of joint kinematics, moments and power in the sagittal plane at all observations and for all participants are presented as supplementary figures. Profile shapes of these estimates over the whole gait cycle were overall similar between the models, although there existed significant ( $P < 0.05$ ) differences at instances in the gait cycle. The JCFs estimated by the two models showed similar waveform profile (Figure 6.1).

The Gen tended to have lower estimates (average difference of 0.8 BW) of hip JCF during the loading response. This difference was found to be significant at both observed timepoints ( $P < 0.001$  at both M0 and M12). JCF estimates were generally similar at the ankle with some significant differences reported during the swing phase of the gait cycle. The Gen also estimated higher JCF at the knee during push off (P2); this was however found to be not significant. The higher P2 prediction at the knee by the Gen was coincident with the prediction of a higher gastrocnemius medialis muscle force and knee flexion moment (see supplementary material) by the Gen in the same phase of the gait cycle.

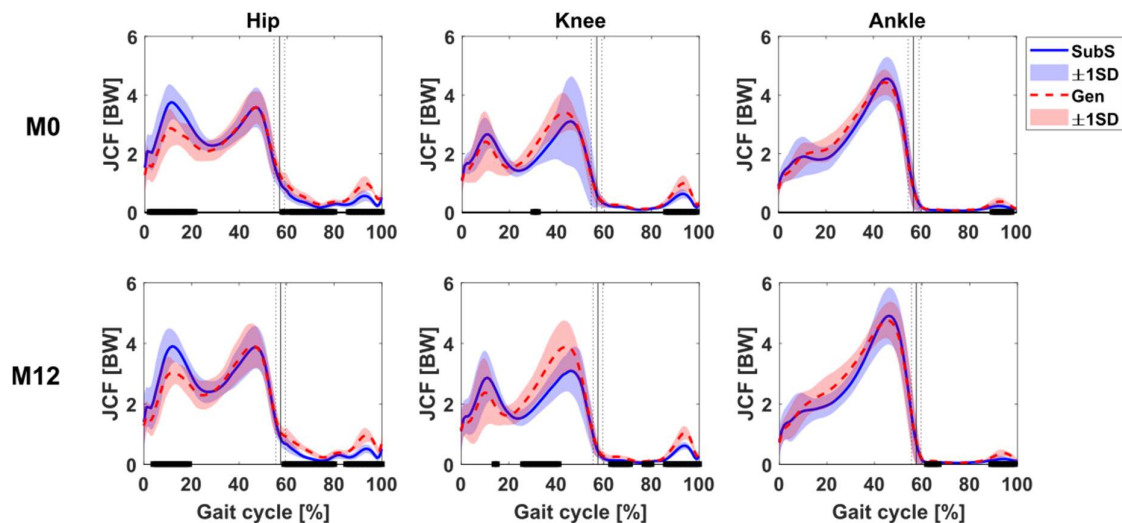


**Figure 6.1 Comparison between Gen (red) and SubS (blue) model estimations of joint contact forces at observations M0 and M12. Black bars indicate region of gait cycle with significant statistical difference between the two models at  $P < 0.01$ .**

Differences in JCF between the Gen and SubS were then analysed for each of the three joints (Table 6.1). Group median RMSD results ranged from 0.30 to 0.60. These values were similar for M0 and M12 with no statistical difference between RMSD values recorded at the two timepoints. The largest mean RMSD was recorded at the knee with a value of 0.59. The knee also had the largest variability between participants' RMSD as indicated by its standard deviation. Similar trends were observed when looking at %Diff, where the knee values doubled those at the ankle.

**Table 6.1 Inter-model analysis of gait waveform profile at M0 and M12**

	M0			M12		
	RMSD (IQR)	%Diff (SD)	R <sup>2</sup> (range)	RMSD (IQR)	%Diff (SD)	R <sup>2</sup> (range)
Hip	0.38 (0.17)	11 (3)	0.87 - 0.97	0.40 (0.18)	10 (2)	0.77 - 0.98
Knee	0.43 (0.27)	17 (6)	0.74 - 0.98	0.63 (0.41)	17 (7)	0.71 - 0.98
Ankle	0.32 (0.15)	8 (3)	0.93 - 0.99	0.29 (0.22)	8 (5)	0.95 - 0.99

Median RMSD, interquartile range (IQR) and range of JCF curve similarity (correlation) between Gen and SubS model estimates for the hip, knee and ankle joints of 11 participants. %Diff is the mean RMSD expressed as a percentage of the range of normalised JCF estimated by SubS.

The coefficient of determination values (Table 6.1) were greater than 0.7 for all participants, with the highest correlations observed at the ankle (higher than 0.9) indicating a very strong linear relationship between JCF predictions between the Gen and SubS. Again, estimates at the knee showed the widest range of values. The comparison of selected peaks highlighted a large inter-subject variability in differences between the two models, however the hip loading response peak, P1, was consistently and significantly lower in the Gen than in the SubS ( $P(M0) = 0.006$ ,  $P(M12) = 0.002$ , Figure 6.2). Further, Cohen's d values (-1.31 and -1.48 for P1 and P2, respectively) suggested a high relevance of this difference.



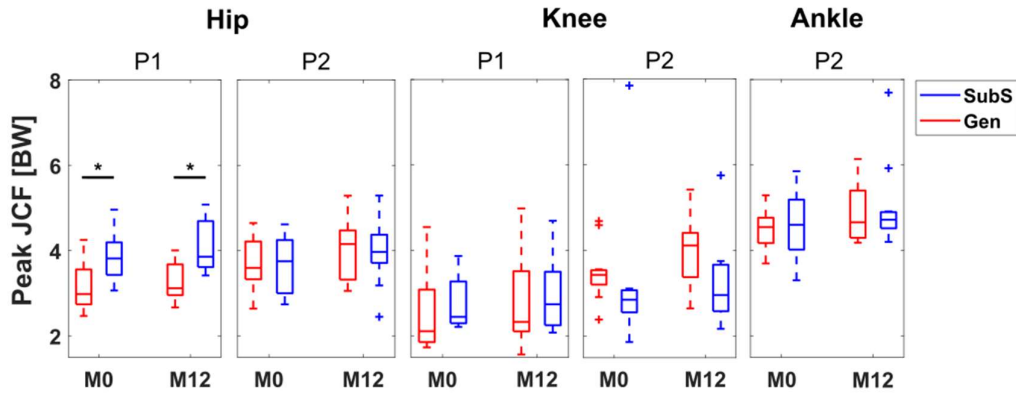


**Figure 6.2** Boxplot distribution of P1 and P2 JCF estimates for scaled generic and subject-specific models at two observations, M0 and M12. \* indicates significant difference at  $P < 0.05$ .

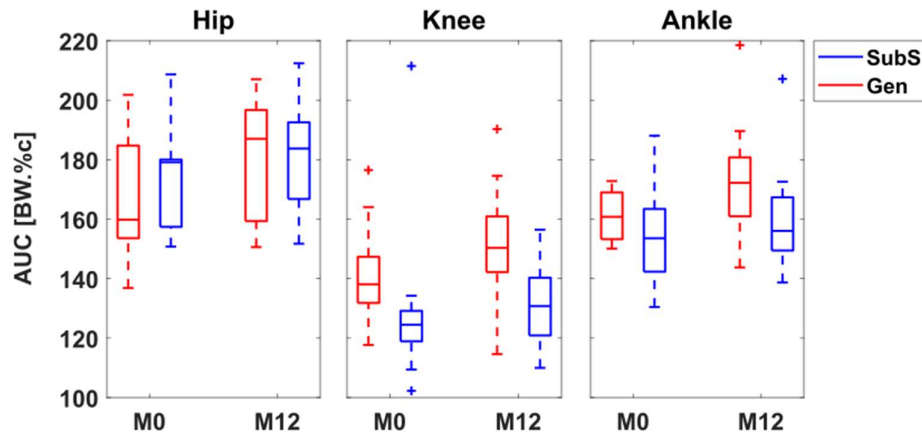


**Figure 6.3** Boxplot distribution of overall joint loading estimates calculated as area under BW-normalised JCF curve. AUC expressed as BW\*%Gait Cycle (BW.%c)

Comparison of longitudinal differences in JCF,  $\Delta_t(\text{JCF})$  estimates for each model revealed that the Gen reported mean differences that were not significantly higher than the SubS for the hip and ankle joint. Peak  $\Delta_t(\text{JCF})$  was lower at the hip for the Gen compared to the SubS. Both models showed an overall increase going from M0 to M12 in maximum values of  $\Delta_t(\text{JCF})$  for all joints (hip: 0.9 (0.3) BW, 1.0 (0.3) BW; knee: 0.8 (0.3) BW, 0.7 (0.3) BW; ankle: 1.0 (0.8) BW, 0.9 (0.6) BW for Gen and SubS, respectively).

**Table 6.2 Inter-model differences in participant estimates at M0**

	$\Delta_m(\text{AUC})$  [BW.%c]			$\Delta_m(\text{Peak})$  [BW]					$R^2[\Delta_m(\text{JCF})]$		
	H	K	A	P1 <sub>H</sub>	P2 <sub>H</sub>	P1 <sub>K</sub>	P2 <sub>K</sub>	P2 <sub>A</sub>	H	K	A
S1	9.1	<b>14.1</b>	<b>11.0</b>	0.4	0.3	<b>0.8</b>	0.6	0.5	<b>0.94</b>	<b>0.75</b>	<b>0.96</b>
S2	0.1	<b>13.6</b>	0.8	0.3	0.2	0.2	0.6	<b>0.9</b>	<b>0.93</b>	<b>0.90</b>	<b>0.93</b>
S3	3.2	<b>15.7</b>	<b>10.5</b>	<b>0.9</b>	0.1	<b>0.5</b>	<b>0.7</b>	0.6	<b>0.89</b>	<b>0.85</b>	<b>0.99</b>
S4	6.9	<b>39.5</b>	0.7	<b>1.2</b>	0.1	<b>0.5</b>	<b>1.6</b>	0.6	<b>0.92</b>	<b>0.94</b>	<b>0.98</b>
S5	7.7	<b>42.2</b>	<b>16.4</b>	0.4	0.6	<b>0.7</b>	<b>1.7</b>	0.3	<b>0.94</b>	<b>0.94</b>	<b>0.99</b>
S6	9.0	<b>22.4</b>	1.0	<b>0.8</b>	0.7	0.3	<b>1.2</b>	0.9	<b>0.87</b>	<b>0.74</b>	<b>0.93</b>
S7	21.5	<b>12.1</b>	<b>17.9</b>	<b>1.2</b>	0.5	0.4	<b>0.7</b>	0.4	<b>0.96</b>	<b>0.88</b>	<b>0.96</b>
S8	12.1	<b>20.1</b>	<b>13.3</b>	<b>0.5</b>	0.2	<b>0.8</b>	0.4	0.6	<b>0.92</b>	<b>0.98</b>	<b>0.98</b>
S9	6.2	<b>14.4</b>	<b>30.3</b>	0.1	0.5	0.3	0.3	0.6	<b>0.97</b>	<b>0.92</b>	<b>0.98</b>
S10	17.5	<b>15.4</b>	<b>29.9</b>	<b>1.0</b>	0.2	0.2	0.5	0.6	<b>0.95</b>	<b>0.89</b>	<b>0.99</b>
S11	<b>37.3</b>	<b>91.5</b>	0.3	<b>1.5</b>	1.0	<b>1.1</b>	<b>4.9</b>	0.0	<b>0.91</b>	<b>0.86</b>	<b>0.99</b>
n	10	0	4	4	11	5	5	10	11	11	11

Absolute values of inter-model differences ( $\Delta_m$ ) at M0. Values in bold indicate greater than applied thresholds. [n] is the number of participants for which Gen and SubS were considered to be in agreement based on  $\Delta_m$ . AUC expressed as BW\*%Gait Cycle (BW.%c).

**Table 6.3 Inter-model differences in participant estimates at M12**

	$\Delta_m(\text{AUC})$  [BW.%c]			$\Delta_m(\text{Peak})$  [BW]					$R^2[\Delta_m(\text{JCF})]$		
	H	K	A	P1 <sub>H</sub>	P2 <sub>H</sub>	P1 <sub>K</sub>	P2 <sub>K</sub>	P2 <sub>A</sub>	H	K	A
S1	19.5	<b>41.6</b>	<b>75.1</b>	0.4	0.4	0.2	<b>1.8</b>	<b>1.3</b>	<b>0.91</b>	<b>0.78</b>	<b>0.95</b>
S2	9.5	<b>29.6</b>	<b>27.0</b>	0.0	0.4	0.3	<b>1.3</b>	0.1	<b>0.95</b>	<b>0.91</b>	<b>0.96</b>
S3	11.3	<b>25.2</b>	<b>7.3</b>	<b>0.6</b>	0.9	<b>0.6</b>	<b>1.6</b>	0.9	<b>0.90</b>	<b>0.81</b>	<b>0.98</b>
S4	4.8	<b>38.7</b>	<b>26.0</b>	<b>1.4</b>	0.5	0.1	<b>1.7</b>	<b>1.9</b>	<b>0.90</b>	<b>0.95</b>	<b>0.98</b>
S5	1.9	<b>34.3</b>	3.1	<b>1.1</b>	0.4	0.3	<b>1.4</b>	0.1	<b>0.92</b>	<b>0.95</b>	<b>0.99</b>
S6	1.1	<b>26.3</b>	<b>9.9</b>	<b>1.3</b>	0.6	<b>0.9</b>	<b>1.6</b>	0.6	<b>0.77</b>	<b>0.71</b>	<b>0.95</b>
S7	0.1	<b>16.2</b>	2.0	<b>0.9</b>	0.2	<b>0.7</b>	<b>1.1</b>	0.2	<b>0.95</b>	<b>0.82</b>	<b>0.97</b>
S8	12.4	<b>16.9</b>	<b>24.5</b>	0.3	0.5	0.2	0.4	0.7	<b>0.98</b>	<b>0.98</b>	<b>0.99</b>
S9	5.4	<b>10.0</b>	<b>18.7</b>	<b>0.6</b>	0.0	0.1	0.6	0.1	<b>0.98</b>	<b>0.92</b>	<b>0.98</b>
S10	9.8	<b>10.4</b>	<b>5.4</b>	<b>0.6</b>	0.5	0.4	0.5	0.5	<b>0.98</b>	<b>0.88</b>	<b>0.97</b>
S11	20.3	<b>41.9</b>	<b>5.1</b>	<b>1.5</b>	0.6	<b>1.0</b>	<b>3.1</b>	0.1	<b>0.95</b>	<b>0.85</b>	<b>0.99</b>
n	11	0	2	3	11	7	3	9	11	11	11

Absolute values of inter-model differences at M12. Values in bold indicate greater than applied thresholds. [n] is the number of participants for which Gen and SubS were considered to be in agreement based on  $\Delta_m$ . AUC expressed as BW\*%Gait Cycle (BW.%c).

**Table 6.4 Agreement in longitudinal changes (M12 - M0) in selected metrics between Gen and SubS predictions of JCF for each of 11 participants.**

	$\Delta_t(\text{AUC})$			$\Delta_t(\text{Peak})[\text{BW}]$					$R^2[\Delta_t(\text{JCF})]$			Tot <sub>s</sub>
	H	K	A	P1 <sub>H</sub>	P2 <sub>H</sub>	P1 <sub>K</sub>	P2 <sub>K</sub>	P2 <sub>A</sub>	H	K	A	
S1	✓	✓	x	✓	✓	x	✓	x	✓	✓	x	7
S2	✓	✓	✓	✓	✓	✓	✓	x	✓	✓	x	9
S3	✓	x	x	x	✓	✓	x	✓	✓	x	✓	6
S4	✓	✓	✓	x	✓	✓	✓	✓	✓	✓	✓	10
S5	✓	✓	x	x	✓	✓	✓	✓	✓	✓	x	8
S6	✓	✓	✓	✓	✓	✓	✓	✓	x	x	✓	9
S7	✓	✓	✓	✓	✓	✓	✓	✓	✓	✓	x	10
S8	✓	x	✓	✓	✓	x	✓	✓	✓	✓	✓	9
S9	✓	✓	✓	✓	✓	✓	✓	✓	✓	x	✓	10
S10	✓	✓	x	x	✓	✓	✓	✓	x	✓	x	7
S11	x	✓	✓	✓	✓	✓	✓	✓	x	x	x	7
Tot <sub>g</sub>	10	9	7	7	11	9	10	9	8	7	5	

Change ( $\Delta_t$ ) in area under JCF curve (AUC), peak 1 (P1) and peak 2 (P2) and coefficient of determination for Gen against SubS  $\Delta$ JCF. Subscripts represent hip (H), knee (K) and ankle (A). (✓) agreement, (x) disagreement. Tot<sub>g</sub> and Tot<sub>s</sub> refer to the number of participants with agreement for a particular metric and number of metrics in agreement per participant, respectively.

A large within group variability (maximum SD: 28.5 BW.%c) was observed for the overall joint loading (AUC, Figure 6.3) measures, particularly at the hip and at the ankle, for both Gen and SubS. No group differences were found for these values, even if a tendency was observed at the knee, where SubS predictions of JCF at both time points tended to be on average, 10% lower than that of Gen, with higher estimates (>40%) from SubS observed only for one subject (still true at both time points).

Inter-model differences ( $\Delta_m$ ) at the knee were observed for the majority of participants at both time points when considering the AUC and JCF peaks whereas the opposite was true for all joints, looking at the waveform correlation between model predictions of JCF (Table 6.2 and Table 6.3).

The matrix in Table 6.4 shows an overall good agreement between predictions from the two models for most of the subjects, except for the  $R^2$  that at the ankle showed a disagreement for about half of the participants.

## 6.5 Discussion

The aim of this study was to evaluate the consistency in measures of JCF and JCF changes over time, using subject-specific (SubS) and scaled generic (Gen) MSK

models applied to 3D gait data from a group of children with Juvenile Idiopathic Arthritis.

Several indices have been used by different authors to analyse the temporal curves usually obtained from gait data, with some looking into distinct parameters such as the mean value at a specified event, while others look at how a parameter of interest changes over the whole cycle [30, 32-34]. These different approaches yield complementary information associated to changes in peak values, amplitudes and phases of the curves which can all be of interest, depending on the outcome (e.g. maximum force vs impulse). For this reason, in this study indices from both groups were used to capture the salient features of the subject gait as well as any time-dependent patterns in the data.

Within sessions, the outputs of the two models were similar in terms of range of motion and waveform profiles of joint angles, net joint moments and powers, despite the significant differences observed when looking at individual time instances between models over the gait cycle. Kainz, et al. [35] also found similarities when comparing joint kinematics and kinetics between scaled generic and MRI-based models of typically developing children. As expected in this study, differences were likewise observed in the JCF profiles and estimates between the two models, in line with what has generally been reported in the literature [16, 17, 36, 37]. In particular, the range of JCF estimates observed for both models were comparable to values reported by other studies for the hip [38], knee [16] and ankle [39]. The mean JCF peaks were also comparable to previous independent work conducted on a subset of children from the same cohort at a different time point observation [23]. Differences observed between the models likely originate from the personalisation of muscle origin and insertion points as well as joint centre and axis locations, both in children [35] and adults [17]. An assessment of some selected muscle forces estimated by both models showed a general concurrence in timing of activity and magnitude during the gait cycle for most muscles (see supplementary data). As per the JCFs, the differences in calculated muscle forces between the two models remained similar across observations for all muscles, which was unsurprising, since muscle forces are known to be the main contributors to JCF [40] predictions.

When looking at specific points on the JCF loading profiles (Figure 6.1), lower hip loading response peaks (P1) were predicted by the Gen compared to the SubS. This is in contrast with what was reported by Wesseling, et al. [41], in a sample of adult subjects. An explanation for this disagreement could be the different methods used to calculate the maximal isometric force for Gen and SubS models in this study, this was kept the same for both models by Wesseling et al. However, it has been previously

suggested that this should not have a significant influence on output muscle force and JCF estimates [16, 23, 42]. Differences in moment arms between models could also account for this contrast. Further study would be needed to further explore this specific aspect.

A large variability between subjects was observed for the JCFs at all the joints, particularly at the knee when using SubS models. This high between-subject variability was in line with what was previously found when looking at joint kinematics, moments and knee JCF in a larger group from the same cohort [3, 20]. This may be attributable to participants adopting a variety of loading strategies to attenuate pain or discomfort resulting from swelling or inflammation of their joints [3]. This variability was partially masked by the scaled model with a reduced between subject variability indicating its less sensitive inter-subject nature. We similarly observed larger between model differences in AUC at the knee (Table 6.2 and Table 6.3), but these were expected since the SubS was implemented to have a simplified knee joint (extension/flexion) compared to the Gen which had an additional prescription of tibial translation as a function of knee joint angle leading to inter-model differences in kinematics and moments at the knee. Despite these inter-model differences in AUC, the Gen was able to capture longitudinal changes at individual level consistently with the subject specific model for the hip and knee especially, as suggested by the results of the agreement matrix (Table 6.4). Taking the knee for example, although predictions of AUC were different between models at each observation, a majority of participants had  $\Delta_t(\text{AUC})$  in agreement in terms of whether there was an increase or decrease.

Comparing the differences between the JCF profiles estimated at the two time points for each of the models, it was observed that Gen and SubS provided consistent information in terms of increased or decreased JCFs between different phases of the gait cycle going from M0 to M12, even if these changes were of different magnitude. The difference in magnitude was particularly prominent at the ankle, which also explains why the number of participants with between model agreement ( $\text{Tot}_g$ ) for  $R^2[\Delta_t(\text{JCF})]$  (Table 6.4) was the lowest for this joint. This was despite the observation that predictions of JCFs at the ankle had the most highly correlated waveforms between models at each observation. At group level, no statistically significant difference in longitudinal change in JCFs between Gen and SubS was observed. Overall, these results indicate that both models were able to account for changes in the JCFs likely attributable to changes in the patient's condition and gait over time.

The sample size involved in this study is small, although larger than other studies comparing generic and image-based subject-specific models [10, 18, 35, 41]. Moreover, the investigated group is a good representation of a very heterogeneous patient

population [3], as also indicated by the reported between subject variability in calculated JCF, which may be considered an advantage in terms of applicability of the reported results. It must be acknowledged, however, that even if Juvenile Idiopathic Arthritis might cause bone deformities, these were not evident in the investigated group of children and no clinically meaningful longitudinal changes emerged from the analysis of their ankle MRIs. This does of course limit the generalisability of the reported results to populations with large bony deformities. The inability of scaled generic models to account for significant anatomical alterations, such as increased femoral anteversion or tibial torsion, have been reported to impact significantly on predictions of moment arm lengths [12].

The SubS was considered as the gold standard in this study as it is assumed to be more representative of the subject's anatomy than the generic models. This assumption of course has its limitations such as errors in operator input but was the only one possible due to the unavailability of longitudinal data from instrumented prosthesis, especially for children.

## **6.6 Conclusion**

In conclusion, this study evaluated the consistency between scaled generic and subject-specific model estimates of longitudinal changes in JCF for a population of children with JIA. By using different metrics for reporting JCF, it was shown that even if the estimates of JCF can be highly different at a single timepoint, the two models showed agreement when calculating the longitudinal difference in joint contact forces, particularly at the hip. It is hence suggested, albeit with caution, that scaled generic models can be used as an initial and easily implementable modelling approach when interest is in trends rather than exact estimates.

## **6.7 Acknowledgements**

This research was supported by the European Commission under Grant MD-PAEDIGREE FP7 (p. no. 600932); the NIHR Sheffield Biomedical Research Centre (BRC) under Grant (p. no. IS-BRC-1215-20017); and the UK-EPSRC under Grant Multisim (p. no. EP/K03877X/1 & EP/SO32940/1).

## 6.8 References

- [1] R. Baker, A. Esquenazi, M. G. Benedetti, and K. Desloovere, "Gait analysis: clinical facts," *Eur J Phys Rehabil Med*, vol. 52, no. 4, pp. 560-74, Aug 2016. [Online]. Available: <https://www.ncbi.nlm.nih.gov/pubmed/27618499>.
- [2] M. Wesseling, E. C. Ranz, and I. Jonkers, "Objectifying Treatment Outcomes Using Musculoskeletal Modelling-Based Simulations of Motion," in *Handbook of Human Motion*, B. Müller *et al.* Eds. Cham: Springer International Publishing, 2018, ch. Chapter 52-1, pp. 1-25.
- [3] E. Montefiori *et al.*, "Linking Joint Impairment and Gait Biomechanics in Patients with Juvenile Idiopathic Arthritis," *Ann Biomed Eng*, vol. 47, no. 11, pp. 2155-2167, Nov 2019, doi: 10.1007/s10439-019-02287-0.
- [4] H. Kainz *et al.*, "Selective dorsal rhizotomy improves muscle forces during walking in children with spastic cerebral palsy," *Clin Biomech*, vol. 65, pp. 26-33, May 2019, doi: 10.1016/j.clinbiomech.2019.03.014.
- [5] S. L. Delp, J. P. Loan, M. G. Hoy, F. E. Zajac, E. L. Topp, and J. M. Rosen, "An interactive graphics-based model of the lower extremity to study orthopaedic surgical procedures," (in English), *Ieee T Bio-Med Eng*, vol. 37, no. 8, pp. 757-67, Aug 1990, doi: 10.1109/10.102791.
- [6] L. Modenese, A. T. Phillips, and A. M. Bull, "An open source lower limb model: Hip joint validation," *J Biomech*, vol. 44, no. 12, pp. 2185-93, Aug 11 2011, doi: 10.1016/j.jbiomech.2011.06.019.
- [7] E. M. Arnold, S. R. Ward, R. L. Lieber, and S. L. Delp, "A model of the lower limb for analysis of human movement," *Ann Biomed Eng*, vol. 38, no. 2, pp. 269-79, Feb 2010, doi: 10.1007/s10439-009-9852-5.
- [8] G. N. Duda, D. Brand, S. Freitag, W. Lierse, and E. Schneider, "Variability of femoral muscle attachments," *J Biomech*, vol. 29, no. 9, pp. 1185-90, Sep 1996, doi: 10.1016/0021-9290(96)00025-5.
- [9] L. Bosmans, K. Jansen, M. Wesseling, G. Molenaers, L. Scheys, and I. Jonkers, "The role of altered proximal femoral geometry in impaired pelvis stability and hip control during CP gait: A simulation study," (in English), *Gait & posture*, vol. 44, pp. 61-7, Feb 2016, doi: 10.1016/j.gaitpost.2015.11.010.
- [10] L. Bosmans *et al.*, "Sensitivity of predicted muscle forces during gait to anatomical variability in musculotendon geometry," (in English), *J Biomech*, vol. 48, no. 10, pp. 2116-23, Jul 16 2015, doi: 10.1016/j.jbiomech.2015.02.052.
- [11] G. Lenaerts *et al.*, "Subject-specific hip geometry and hip joint centre location affects calculated contact forces at the hip during gait," (in English), *J Biomech*, vol. 42, no. 9, pp. 1246-51, Jun 19 2009, doi: 10.1016/j.jbiomech.2009.03.037.
- [12] L. Scheys, A. Van Campenhout, A. Spaepen, P. Suetens, and I. Jonkers, "Personalized MR-based musculoskeletal models compared to rescaled generic models in the presence of increased femoral anteversion: effect on hip moment arm lengths," *Gait & posture*, vol. 28, no. 3, pp. 358-65, Oct 2008, doi: 10.1016/j.gaitpost.2008.05.002.

- [13] R. Hainisch, M. Gfoehler, M. Zubayer-UI-Karim, and M. G. Pandy, "Method for determining musculotendon parameters in subject-specific musculoskeletal models of children developed from MRI data," (in English), *Multibody Syst Dyn*, vol. 28, no. 1-2, pp. 143-156, Aug 2012, doi: 10.1007/s11044-011-9289-0.
- [14] T. A. Correa and M. G. Pandy, "A mass-length scaling law for modeling muscle strength in the lower limb," (in English), *J Biomech*, vol. 44, no. 16, pp. 2782-9, Nov 10 2011, doi: 10.1016/j.jbiomech.2011.08.024.
- [15] S. S. Blemker, D. S. Asakawa, G. E. Gold, and S. L. Delp, "Image-based musculoskeletal modeling: applications, advances, and future opportunities," (in English), *J Magn Reson Imaging*, vol. 25, no. 2, pp. 441-51, Feb 2007, doi: 10.1002/jmri.20805.
- [16] G. Valente *et al.*, "Are subject-specific musculoskeletal models robust to the uncertainties in parameter identification?," (in English), *PLoS One*, vol. 9, no. 11, p. e112625, Nov 12 2014, doi: 10.1371/journal.pone.0112625.
- [17] L. Scheys, A. Spaepen, P. Suetens, and I. Jonkers, "Calculated moment-arm and muscle-tendon lengths during gait differ substantially using MR based versus rescaled generic lower-limb musculoskeletal models," (in English), *Gait & posture*, vol. 28, no. 4, pp. 640-8, Nov 2008, doi: 10.1016/j.gaitpost.2008.04.010.
- [18] T. A. Correa, R. Baker, H. K. Graham, and M. G. Pandy, "Accuracy of generic musculoskeletal models in predicting the functional roles of muscles in human gait," (in English), *J Biomech*, vol. 44, no. 11, pp. 2096-105, Jul 28 2011, doi: 10.1016/j.jbiomech.2011.05.023.
- [19] J. Stebbins, M. Harrington, N. Thompson, A. Zavatsky, and T. Theologis, "Repeatability of a model for measuring multi-segment foot kinematics in children," (in English), *Gait & posture*, vol. 23, no. 4, pp. 401-10, Jun 2006, doi: 10.1016/j.gaitpost.2005.03.002.
- [20] E. Montefiori *et al.*, "An image-based kinematic model of the tibiotalar and subtalar joints and its application to gait analysis in children with Juvenile Idiopathic Arthritis," (in English), *J Biomech*, vol. 85, pp. 27-36, Mar 6 2019, doi: 10.1016/j.jbiomech.2018.12.041.
- [21] G. Valente, G. Crimi, N. Vanella, E. Schileo, and F. Taddei, "nmsBuilder: Freeware to create subject-specific musculoskeletal models for OpenSim," (in English), *Comput Methods Programs Biomed*, vol. 152, pp. 85-92, Dec 2017, doi: 10.1016/j.cmpb.2017.09.012.
- [22] D. R. White, H. Q. Woodard, and S. M. Hammond, "Average soft-tissue and bone models for use in radiation dosimetry," *Br J Radiol*, vol. 60, no. 717, pp. 907-13, Sep 1987, doi: 10.1259/0007-1285-60-717-907.
- [23] L. Modenese, E. Montefiori, A. Wang, S. Wesarg, M. Viceconti, and C. Mazza, "Investigation of the dependence of joint contact forces on musculotendon parameters using a codified workflow for image-based modelling," (in English), *J Biomech*, vol. 73, pp. 108-118, May 17 2018, doi: 10.1016/j.jbiomech.2018.03.039.



- [24] S. L. Delp *et al.*, "OpenSim: open-source software to create and analyze dynamic simulations of movement," (in English), *Ieee T Bio-Med Eng*, vol. 54, no. 11, pp. 1940-50, Nov 2007, doi: 10.1109/TBME.2007.901024.
- [25] J. L. Hicks, T. K. Uchida, A. Seth, A. Rajagopal, and S. L. Delp, "Is my model good enough? Best practices for verification and validation of musculoskeletal models and simulations of movement," (in English), *Journal of biomechanical engineering*, vol. 137, no. 2, p. 020905, Feb 1 2015, doi: 10.1115/1.4029304.
- [26] H. Kainz, H. X. Hoang, C. Stockton, R. R. Boyd, D. G. Lloyd, and C. P. Carty, "Accuracy and Reliability of Marker-Based Approaches to Scale the Pelvis, Thigh, and Shank Segments in Musculoskeletal Models," *J Appl Biomech*, vol. 33, no. 5, pp. 354-360, Oct 1 2017, doi: 10.1123/jab.2016-0282.
- [27] M. E. Harrington, A. B. Zavatsky, S. E. Lawson, Z. Yuan, and T. N. Theologis, "Prediction of the hip joint centre in adults, children, and patients with cerebral palsy based on magnetic resonance imaging," *J Biomech*, vol. 40, no. 3, pp. 595-602, 2007, doi: 10.1016/j.jbiomech.2006.02.003.
- [28] K. M. Steele, M. S. Demers, M. H. Schwartz, and S. L. Delp, "Compressive tibiofemoral force during crouch gait," (in English), *Gait & posture*, vol. 35, no. 4, pp. 556-60, Apr 2012, doi: 10.1016/j.gaitpost.2011.11.023.
- [29] T. C. Pataky, "One-dimensional statistical parametric mapping in Python," (in English), *Comput Method Biomec*, vol. 15, no. 3, pp. 295-301, 2012, doi: 10.1080/10255842.2010.527837.
- [30] P. Picerno, A. Cereatti, and A. Cappozzo, "Joint kinematics estimate using wearable inertial and magnetic sensing modules," (in English), *Gait & posture*, vol. 28, no. 4, pp. 588-95, Nov 2008, doi: 10.1016/j.gaitpost.2008.04.003.
- [31] M. Iosa, A. Cereatti, A. Merlo, I. Campanini, S. Paolucci, and A. Cappozzo, "Assessment of waveform similarity in clinical gait data: the linear fit method," (in English), *Biomed Res Int*, vol. 2014, p. 214156, 2014, doi: 10.1155/2014/214156.
- [32] R. Di Marco, E. Scalona, A. Pacilli, P. Cappa, C. Mazzà, and S. Rossi, "How to choose and interpret similarity indices to quantify the variability in gait joint kinematics," *International Biomechanics*, vol. 5, no. 1, pp. 1-8, 2018/01/01 2018, doi: 10.1080/23335432.2018.1426496.
- [33] M. P. Kadaba, H. K. Ramakrishnan, M. E. Wootten, J. Gainey, G. Gorton, and G. V. Cochran, "Repeatability of kinematic, kinetic, and electromyographic data in normal adult gait," *J Orthop Res*, vol. 7, no. 6, pp. 849-60, 1989, doi: 10.1002/jor.1100070611.
- [34] T. Chau, "A review of analytical techniques for gait data. Part 1: Fuzzy, statistical and fractal methods," (in English), *Gait & posture*, vol. 13, no. 1, pp. 49-66, Feb 2001, doi: 10.1016/s0966-6362(00)00094-1.
- [35] H. Kainz *et al.*, "O 107 – Impact of subject-specific musculoskeletal geometry on estimated joint kinematics, joint kinetics and muscle forces in typically developing children," *Gait & posture*, vol. 65, pp. 223-225, 2018/09/01/ 2018, doi: 10.1016/j.gaitpost.2018.06.142.

- [36] K. Song, A. E. Anderson, J. A. Weiss, and M. D. Harris, "Musculoskeletal models with generic and subject-specific geometry estimate different joint biomechanics in dysplastic hips," (in English), *Comput Method Biomec*, vol. 22, no. 3, pp. 259-270, Feb 2019, doi: 10.1080/10255842.2018.1550577.
- [37] G. Lenaerts *et al.*, "Subject-specific hip geometry affects predicted hip joint contact forces during gait," *J Biomech*, vol. 41, no. 6, pp. 1243-52, 2008/01/01/2008, doi: 10.1016/j.jbiomech.2008.01.014.
- [38] A. Carriero *et al.*, "Influence of altered gait patterns on the hip joint contact forces," (in English), *Comput Method Biomec*, vol. 17, no. 4, pp. 352-9, Mar 12 2014, doi: 10.1080/10255842.2012.683575.
- [39] J. A. Prinold *et al.*, "A Patient-Specific Foot Model for the Estimate of Ankle Joint Forces in Patients with Juvenile Idiopathic Arthritis," *Ann Biomed Eng*, vol. 44, no. 1, pp. 247-57, Jan 2016, doi: 10.1007/s10439-015-1451-z.
- [40] T. A. Correa, K. M. Crossley, H. J. Kim, and M. G. Pandy, "Contributions of individual muscles to hip joint contact force in normal walking," *J Biomech*, vol. 43, no. 8, pp. 1618-22, May 28 2010, doi: 10.1016/j.jbiomech.2010.02.008.
- [41] M. Wesseling *et al.*, "Subject-specific geometrical detail rather than cost function formulation affects hip loading calculation," (in English), *Comput Method Biomec*, vol. 19, no. 14, pp. 1475-88, Nov 2016, doi: 10.1080/10255842.2016.1154547.
- [42] M. Wesseling *et al.*, "Subject-specific musculoskeletal modelling in patients before and after total hip arthroplasty," (in English), *Comput Method Biomec*, vol. 19, no. 15, pp. 1683-91, Nov 2016, doi: 10.1080/10255842.2016.1181174.

**7 Effects of statistical shape modelling-based personalisation of musculoskeletal models on muscle-tendon length and moment arm length estimates during gait.**

## 7.1 Summary

This chapter presents a method to personalise subject bone geometry using sparse imaging data. A comparison between Magnetic Resonance Imaging bone segmentations and bone geometries derived from this approach is also reported. The chapter concludes with an investigation into the impact of these model refinements on biomechanical simulation outputs. Part of this work was done in collaboration with the Human Movement Biomechanics Research Group at KU Leuven in Belgium (Prof. I. Jonkers, Dr Bryce Killen), with support of an Insigneo Institute for *in silico* Medicine Travel Bursary.

## 7.2 Introduction

Image-based musculoskeletal modelling has gained traction over the years in research and in most instances is considered a gold standard for musculoskeletal modelling due to their increased accuracy and reliability [1]. That notwithstanding, these models require effort and time expenditures which are not always feasible in clinical settings, thereby limiting their use [2]. Another challenge to the use of these image-based models is the non-availability or dearth of imaging data. The erstwhile common and traditional scaling of generic models developed from cadaver specimens and anatomical values from literature are also being called into question due to their poor capture of subject bone geometry and morphology, particularly in pathologic populations [3-5]. These models are also subject to operator-dependent modelling decisions (bone and muscle geometry definition, model scaling) which can lead to errors in kinematic and kinetic estimates and decreased repeatability [6-8].

Exploiting the gap between these two modelling extremes, mathematical methods are being used to generate geometric bone models from sparse or unavailable subject imaging data. One such approach is statistical shape modelling (SSM) which permits the reconstruction of geometric bone models from the characterization and analysis of population variations in bone anatomy and shape. Using this knowledge of anatomical variance, subject-specific shapes can be morphed along some principal components of variance while decreasing the deviation from a set of reference measurements. The reference measurements could be from available segmentations of imaging data or anthropometric values. A number of studies employing SSMs have shown that these methods are able to reconstruct subject bone geometries and anatomical features to a high level of accuracy [9-11]. These studies however did not evaluate the downstream effect of using these bone geometries in the generation and simulation of musculoskeletal models. In a further study using bone geometries derived from SSM-based methods, Bakke and Besier [12] developed a workflow for

customizing a generic model and reported that compared to scaled generic models, SSM-derived models had increased repeatability in their estimates of joint kinematics and kinetics and reduced inter-operator variability. This study however did not evaluate the accuracy with respect to subject-specific models of the parameters estimated and did not employ any subject-specific imaging data in the generation of the SSM-derived models. Bahl, et al. [13] who included imaging data of the hip from computed tomography, reported reduction in hip joint centre location errors of at least 2cm and improved to a lesser extent, moment arm estimates when using an SSM approach in a population with hip osteoarthritis when compared with linear scaling methods and reference hip joint centre from the computed tomography.

Despite the increased bio-fidelity shown with SSM models by the above-mentioned studies, it is still unclear how these gains in accuracy transfer to estimates of biomechanical parameters during gait. It has been suggested that the use of these models would reduce errors associated with non-representative bone morphology and dimensions, as well as improve estimates of muscle associated parameters (moment arm lengths, muscle-tendon lengths and muscle forces). This is of particular interest for the clinical cohort of CP where it may not be possible to have children stay immobile for the duration of the times required for a full lower-limb imaging assessment from magnetic resonance imaging, computed tomography or other imaging modalities. In this context, the MAP-Client [14], an open-source tool developed as part of the Musculoskeletal Atlas Project, provides a platform for rapidly deriving personalized models based on SSM for use in simulations. Although results were influenced by the size of the participant, this approach of reconstructing lower limb bones has been shown to generally outperform the linear scaling method used with generic models when applied to children's datasets [11], reducing hip joint centre location errors and improving accuracy of the reconstruction.

In this chapter, I investigated these gaps in the literature and compared model and simulation outcomes during gait derived from SSM-based models and those from image-based personalised models. It was hypothesised that SSM-based estimates would be more accurate than scaled generic model estimates.

## **7.3 Materials and methods**

### **7.3.1 Participants**

Thirteen individuals (age:  $11.5 \pm 3.0$  years, mass:  $44.8 \pm 15.9$  kg, height:  $1.43 \pm 0.17$  m) with Juvenile Idiopathic Arthritis (JIA) for which medical imaging MRI data was available were selected from a larger cohort of participants recruited from two hospitals during the MD-PAEDIGREE project (FP7-ICT Programme, Project ID: 600932)[15, 16]. Approval

was sought from the ethical committees of the hospitals from which data was collected.

### **7.3.2 Motion capture and magnetic resonance imaging**

Participants underwent 3D gait analysis. Gait data was collected using a 6-camera setup (BTS, SmartDX, 100Hz) with two force plates (Kistler, 1kHz) at one centre and an 8-camera system (Vicon, MX, 200 Hz) with two force plates (AMTI, OR6, 1kHz) at a second centre. A set of 44 markers were used at both centres and consisted of a combination of the standard Vicon PlugIn gait protocol markers (Vicon Motion Systems) and the modified Oxford Foot Model [17]. At least three gait trials were collected per participant walking at self-selected speed. EMG data was collected for all participants during the dynamic gait trials for five muscles: biceps femoris, medial and lateral gastrocnemius, tibialis anterior and the vastus medialis. Each participant also underwent MR imaging of the lower limb using a 3D T1-weighted fat-suppression sequence with an in-plane resolution of 1mm and slice thickness of 1 mm. Regional MRI of the foot and ankle was also acquired using a multi-slice multi-echo 3D Gradient Echo (mFFE) with water only selection (slice thickness: 1 mm; in-plane resolution: 0.5 mm).

### **7.3.3 Musculoskeletal modelling**

#### *MRI-based models*

The development of the MRI-based models was as described by [15, 18]. A single expert operator segmented MRI images of the full lower-limbs as well as the regional MRIs to obtain subject-specific bone geometries. The full lower-limb geometries were subsequently coupled with the regional geometries to build each subject-specific model (MRb) using NMSBuilder [19]. The 7 segment MRb had the hip modelled as a ball and socket joint with the knee and ankle as ideal hinges. Using articular surfaces isolated from the segmented bone geometries, a least square difference minimization approach was employed to define joint axes by morphological fitting. The femoral head of the femur was fitted with a sphere to define the hip joint, the condyles of the femur with a cylinder to define the hinge knee joint, the trochlear dome of the tibia with a cylinder and the subtalar joint defined as the axis connecting the centre of two spheres fitted to the two facets of the talus respectively. Muscle attachment and via points were estimated with a supervised atlas registration using the commonly used and validated generic gait2392 model [20] as reference. These were manually adjusted against the MRI when required. Lower limb mass for the MRb was calculated as the product of soft tissue and bone tissue volumes and their appropriate densities culled

from the literature [21], and used to linearly scale muscle maximum isometric force as a ratio to the lower limb mass of the generic model.

#### *Shape modelling-based models*

The shape modelling used was an atlas-based approach utilizing joint scans from MRI and free form deformation techniques. Joint scans were approximated by manually selecting joint regions from the fully segmented MRI images in MeshLab as illustrated in Figure 7.1. Processing was for just the right lower limb. Shape modelling-based model creation involved the use of the open-source plugin-based software MAP-Client [14]. Two pipelines were utilized in the creation of each model. In the first instance, lower limb bone segments were reconstructed using marker data from the static trial and the simulated joint scan geometries. Marker data was initially used to linearly scale mean statistical shape lower limb bone models according to recommendations by [22], following which the joint scans (Figure 7.1) were used to guide bone reconstruction from the scaled mean SSM models via a morphing process utilizing host mesh fitting (HMF) and local mesh fitting (LMF) techniques. HMF was used as a global refinement to improve the overall bone shape, whereas LMF was used in a local refinement manner to morph nodal points already present in the reference SSM to the target MRI joint scan segmentations. Details of the construction of the reference SSM included with the MAP-Client are as described in [14]. Both steps ensured a minimisation of the distance errors between nodal points in the SSM bone models and the user-supplied segmentations. Secondly, the reconstructed bone segments were fed into a gait2392 model customization step. Generated models (SMb) were subsequently passed through a custom python script to optimise muscle path and moment arms using the generic model and literature values as reference based on the work by Killen, et al. [23]. The muscles optimised were those with via points and wrapping surfaces namely, the three vasti, rectus femoris, gastrocnemius, semitendinosus, semimembranosus, biceps femoris, gracilis, sartorius, iliacus, psoas and gluteus maximus. This optimisation has been shown not to produce statistically significant worse results with improvements in muscle tendon pathways and kinematics in some comparisons [23] although this was for only muscles with wrapping surfaces and not via points. Maximum isometric force for each muscle in the model was determined by linearly scaling generic model values by the ratio of participant mass to generic model mass raised to the power  $2/3$  [24].



**Figure 7.1 Joint scans for SMb model generation. Green shaded regions indicate the bone sections selected from the complete MRI image and used.**

### *Scaled generic model generation*

For comparison, the generic gait2392 model was scaled in OpenSim 3.3 [25] using participant mass and experimental markers placed on anatomical landmarks. Scaling factors were calculated as ratios of distances between experimental or calculated marker positions and their corresponding virtual counterparts following recommendations by [22]. Scaled generic model (SGn) muscle maximum isometric force was determined as for the SMb models.

### **7.3.4 Data processing**

#### *Reconstructed bone mesh similarity*

Bone geometry meshes generated with the MAP-Client were compared with segmented geometries from the MRI using the Jaccard Index, a volume overlap measure for mesh volume similarity and also the Hausdorff Distance for maximal surface to surface distance error [26, 27].

#### *Joint centre location and segment length errors*

To determine the joint hip and knee joint centres, the acetabular cap, femoral head and femoral condyles of MAP-Client generated bone geometries were isolated and fitted to a sphere and cylinder respectively, from which the centres were estimated. From these measures, the inter-hip joint centre was calculated as the Euclidean distance between the left and right hip joint centre, and the femur length as the Euclidean distance between the hip joint centre and knee joint centre. Similar measures were calculated using the virtual hip joint centres estimated from the Harrington regression equations [28] and the static marker trajectories of each participant. These were used to assess the differences in estimate between the MAP and their corresponding values determined directly from the MRI segmentations.

#### *Muscle attachment locations*



Generated models (SGn, MRb and SMb) were then analysed with a custom script through the OpenSim API in MATLAB for the muscle attachment points. Muscle origin and insertion coordinates (in segment reference frames) were extracted for each model from which location errors in 3D space were calculated as the distance between attachment point location in MRb and the two other models. Differences in anterior-posterior, superior-inferior and medial-lateral directions were also calculated with respect the origins of the segments of attachment (i.e., pelvis, femur, tibia and foot (calcaneus)).

#### *Dynamic simulation*

Joint angles, muscle-tendon lengths (MTL) and moment arm lengths (MAL) during walking were subsequently determined using tools available in OpenSim 3.3 namely, Inverse Kinematics and Muscle Analysis. Simulations were run using at least three experimental gait trials per participant and ensuring best practice [29]. Due to bone and joint differences between subjects and differences in anatomical frame definitions between models, there exist some biases in the estimate of joint kinematic angles, and this was accounted for by calculating an offset which is then subtracted from absolute angles from the dynamic trials. This offset was calculated as the static posture angle of the joints and pelvic rotations.

#### **7.3.5 Data and statistical analysis**

Inter-HJC and femur length estimates were compared between models with repeated measures analysis of variance (ANOVA) after tests of normality. Where statistical significance was determined, post-hoc t-tests with Bonferroni correction was performed. Static posture angles (offsets) were compared with the same approach to quantify any biases associated with segment anatomical frame definitions.

All joint angles, MTLs and MALs were time-normalised to 100% of the gait cycle and averaged over the number of trials for each participant. The joint angles were compared between models using the coefficient of determination value to describe the waveform similarity. Differences between model predictions of joint angles were quantified using the root mean square difference (RMSD) between MRb and SGn or SMb. In addition to this, differences over the gait cycle between waveforms of joint angles were compared using a repeated measures ANOVA test within the statistical parametric mapping (SPM) package [30] in MATLAB (v9.5.0, R2018b, MathWorks, USA). Where significance was observed, non-parametric paired t-tests from the same package was carried out with Bonferroni correction for multiple comparisons. Significance was evaluated at  $\alpha < 0.05$  for all tests.

Additionally, for each participant and model, the dynamic MTL was normalised to the length in neutral pose after which the maximum ( $MTL_{max}$ ) over the gait cycle was extracted. The difference from the MRb model in  $MTL_{max}$  were calculated for SGn and SMb models. The average MAL over the gait cycle was calculated. Similarly, differences in MALs for SGn and SMb were calculated as the maximum absolute difference from the MRb values. The RMSE between MRb MALs and SGn and SMb was also calculated.  $MTL_{max}$  and average MAL were compared between the three models with a Friedman test and where significance was observed, pairwise comparisons with Bonferroni correction for multiple comparison was performed. The degree of difference between the models was also assessed using Kendall's coefficient of concordance (Kendall's W). To facilitate discussion with respect to the chapter on pre-surgical MTL potential to predict surgical outcomes, the subset of 15 hip adductor muscles were selected and reported in the results. Results for all muscles are presented in the appendix.

## 7.4 Results

### 7.4.1 Bone geometry similarity

Mesh similarity metrics used to evaluate the reconstruction accuracy of the lower limb bones were acceptable for the SSM derived bone geometries. As shown in Figure 7.2, the geometries of the femur and tibia better matched the MRb geometries compared to those of the pelvis ( $HD = 27.48 \pm 5.31$  mm,  $JI = 0.38 \pm 0.12$ ).

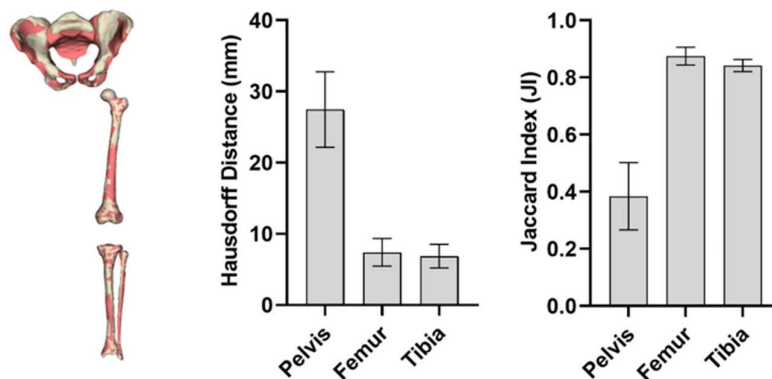
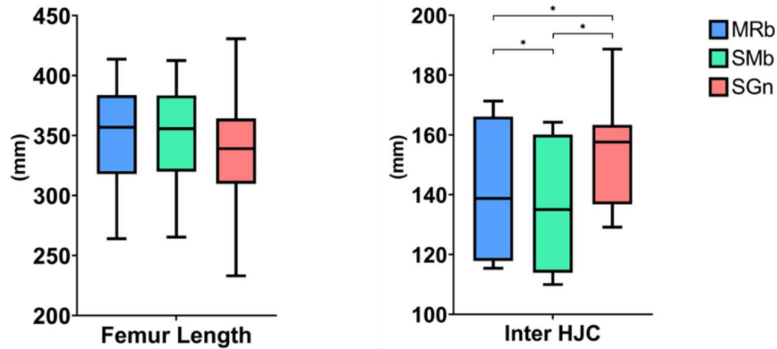


Figure 7.2 Body segment similarity between MR and SM derived bone geometries.

### 7.4.2 Segment length and inter-HJC

Comparison of inter-HJC estimates indicated statistically significant differences:  $F(1.1,13.2) = 14.2$ ,  $p$ -value = 0.002, between the models as shown in Figure 7.3, with a strong effect size (Cohen's  $d = 0.78$ ). Average percentage differences from the MRb model of about -4% and 9% which corresponded to an average underestimation of

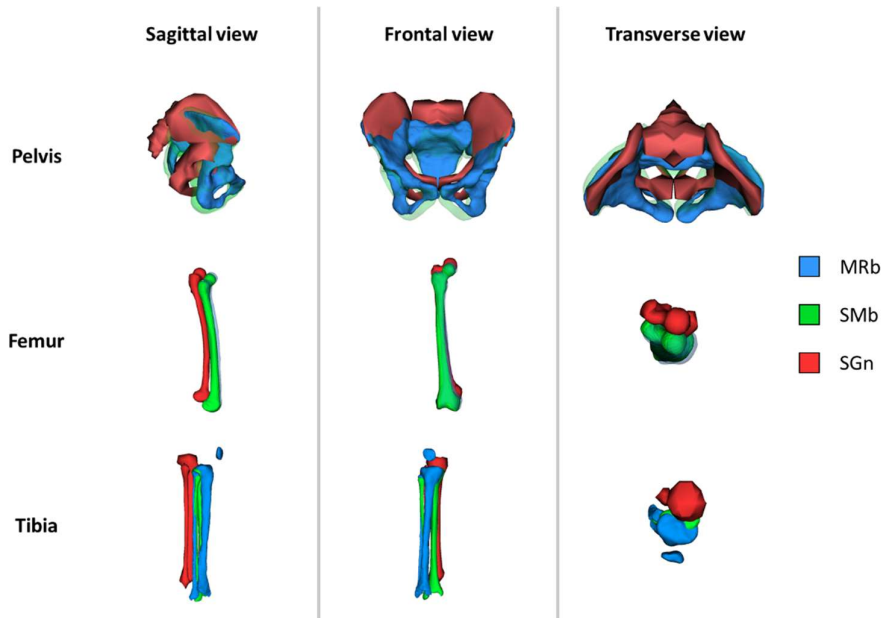
6mm and overestimation of 12mm for SMb and SGn, respectively. SGn estimated bigger inter-HJC than SMb and MRb. For the estimates of femur length, there were no significant differences between the models, although a maximum difference in length of  $3.74 \pm 5.12\%$  was found between SGn and MRb.



**Figure 7.3 Comparison of the femur length and inter-HJC measurements between SMb, SGn and MRb**

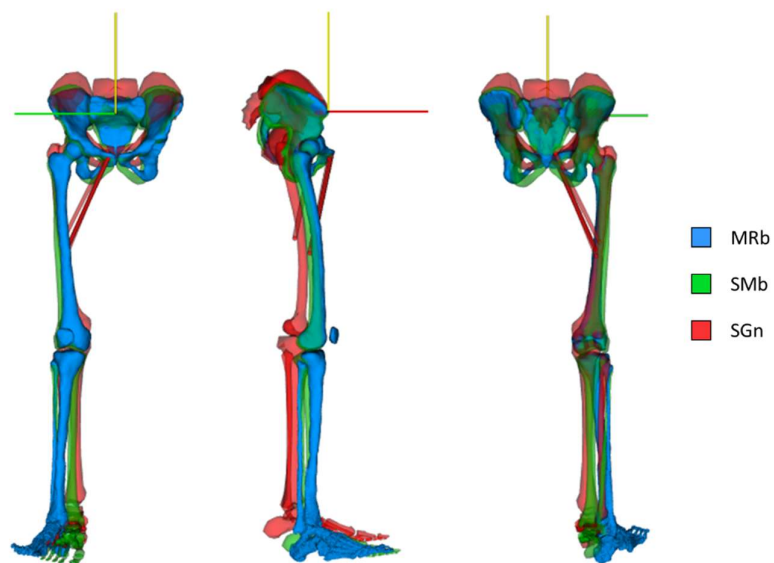
#### 7.4.3 Muscle attachments' location

Figure 7.4 and Figure 7.5 show the inter-model bone geometry and muscle point location differences observable for one participant when all three models for that participant are aligned at the pelvis origin. Differences in 3D locations of origin and insertion points of SGn and SMb models compared to the MRb for all muscles in the model are presented in Appendix 3, Table A3.1. For the hip ab/adduction muscles (Figure 7.6), the differences in 3D location of muscle point ranged from a maximum mean value of 5.3 cm (origin of add\_mag3) to a minimum of 0.6 cm (insertion of pectoralis). Overall, errors in insertion location were lower (<2 cm for both SGn and SMb) compared to those of origin location. SMb models tended to match the MRb models reporting lower differences than the SGn. The largest errors were in the anterior-posterior and superior-inferior directions and in the origin locations for both SMb and SGn (Appendix 3, Figure A3.1).



**Figure 7.4 Example of MRb, SMB and SGn bone geometries for one participant model.**

**Models were aligned at the pelvis origin**



**Figure 7.5 Anterior, lateral and posterior views of aligned SMB, SGn and MRb models of a participant highlighting bone and muscle geometry differences**

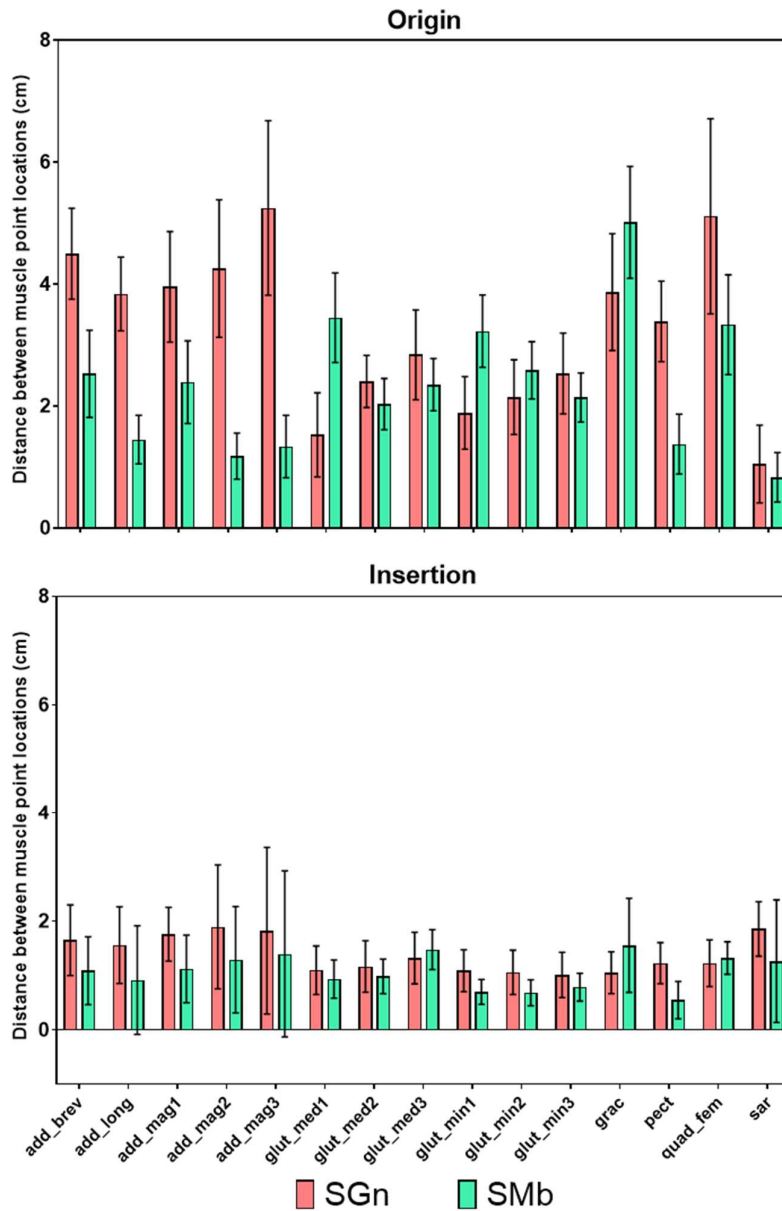


**Figure 7.6** Difference in 3D location of origin and insertion points for hip adductors in SGn and SMb with respect to MRb.

#### 7.4.4 Muscle-tendon length and moment arm length

For the 15 hip ab/adduction muscles considered, the Friedman's test indicated significant differences in  $MTL_{max}$  and average MAL between the three models for 10 and 8 muscles, respectively. Effect size of these differences were ranged from moderate to large (Kendall's  $W > 0.5$ , Table A4.3 in appendix). For those muscles where  $MTL_{max}$  and average MAL were significantly different between the three models, these differences were frequently found between SMb and MRb, with less differences

between SGn and MRb (Table 7.1). The average difference in  $MTL_{max}$  between SGn and MRb were lower and less variable than that between SMb and MRb as shown in Figure 7.7 below.

**Table 7.1 Comparison of MTL<sub>max</sub> and average MAL between MRb, SGn and SMb for muscles with hip ab/adduction function**

Muscle	MTL <sub>max</sub> – Mean (SD)			Average MAL – Mean (SD)			Pairwise significant difference between models (MRb-SGn/MRb-SMb/ SGn-SMb)
	MRb	SGn	SMb	MRb	SGn	SMb	
add_brev	1.05 (0.04)	1.08 (0.03)	1.12 (0.07)	6.05 (1.12)	5.09 (0.61)	5.15 (0.63)	**/*/-
add_long	1.03 (0.03)	1.07 (0.02)	1.09 (0.05)	6.02 (1.22)	5.39 (0.70)	5.27 (0.74)	-/*/-
add_mag1	1.09 (0.06)	1.11 (0.04)	1.13 (0.08)	6.00 (0.98)	5.65 (0.68)	5.83 (0.72)	
add_mag2	1.09 (0.05)	1.10 (0.04)	1.10 (0.06)	5.04 (0.84)	5.15 (0.70)	5.95 (1.06)	-/**/*
add_mag3	1.10 (0.03)	1.08 (0.03)	1.08 (0.03)	2.67 (0.66)	2.77 (0.40)	3.09 (0.95)	
glut_med1	1.09 (0.03)	1.10 (0.03)	1.06 (0.04)	-3.57 (0.56)	-3.55 (0.47)	-4.18 (0.77)	-/*/-
glut_med2	1.12 (0.03)	1.10 (0.02)	1.06 (0.04)	-2.98 (0.47)	-3.37 (0.42)	-3.05 (0.62)	
glut_med3	1.16 (0.04)	1.12 (0.03)	1.05 (0.04)	-2.16 (0.41)	-2.77 (0.36)	-1.97 (0.48)	**/*-****
glut_min1	1.06 (0.03)	1.08 (0.04)	1.04 (0.03)	-2.84 (0.40)	-3.03 (0.37)	-3.53 (0.64)	-/**/*-
glut_min2	1.08 (0.03)	1.08 (0.03)	1.04 (0.03)	-2.78 (0.37)	-3.11 (0.36)	-3.12 (0.58)	/*/*-
glut_min3	1.11 (0.03)	1.09 (0.02)	1.05 (0.03)	-2.45 (0.32)	-2.89 (0.34)	-2.44 (0.50)	**/*-****
grac	1.02 (0.02)	1.02 (0.01)	1.04 (0.03)	4.50 (0.81)	4.56 (0.65)	5.19 (0.91)	-/**/*
pect	1.03 (0.03)	1.08 (0.02)	1.11 (0.06)	3.19 (0.95)	2.75 (0.35)	3.17 (0.42)	-/*/*
quad_fem	1.16 (0.11)	1.12 (0.05)	1.19 (0.13)	3.72 (0.77)	2.96 (0.46)	2.53 (0.67)	/*/*/*-
sar	1.00 (0.01)	1.02 (0.01)	1.01 (0.00)	-1.51 (0.54)	-2.36 (0.36)	-1.97 (0.90)	***/*-/**

Pairwise significant differences between models presented for muscles where there existed significant systematic differences between estimates of MTL<sub>max</sub> and average MAL between the three models based on a Friedman test. Significant differences are presented as a/b/c where a, b and c are the p-values for the pairwise comparisons between MRb/SGn, MRb/SMb and SGn/SMb, respectively. Symbols used are p > 0.05; \*p < 0.05; \*\*p < 0.01; \*\*\*p < 0.001.

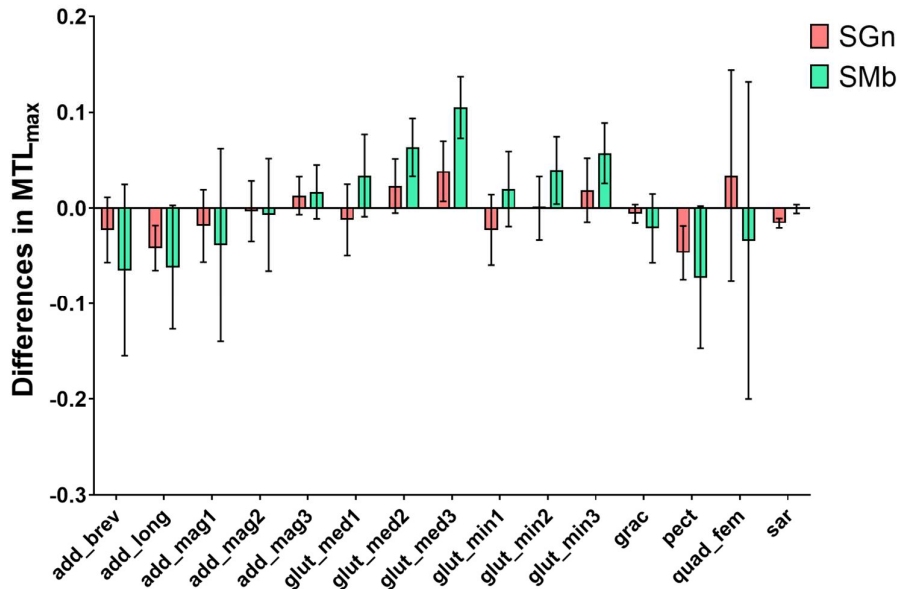


**Figure 7.7 MTL differences between models for hip ab/adduction muscles**

Average RMSD in MAL between the MRb model and SGn and SMb models for all muscles are reported in the appendix. For the hip ab/adduction muscles, average RMS differences from the MRb model were larger for the SMb than the SGn (0.74 cm and 0.63cm, respectively) when considering all the muscles together. When considering the maximum absolute difference in MAL between MRb and the other models, for all the joints, the SGn tended to have smaller differences than the SMb (Table 7.2). The SGn had differences in MAL that were consistently below 2 cm and less variable than the differences for the SMb.

#### 7.4.5 Joint kinematics

For all the joints considered, the SGn and SMb matched in their estimates of the static pose joint angles for participants although there was a higher spread in the values for SMb than SGn (Appendix 3, Figure A3.2). When considering the dynamic joint angles, RMSD were lower for the SGn than SMb in three out of the five joints considered although this was only significant for hip abduction (RMSD = 1.2°, for SGn and RMSD = 1.9°, for SMb, P = 0.02). Similarly, R<sup>2</sup> values for the joint angles were greater than 0.8 except for hip rotation in SMb which was 0.6. Comparing this between SMb and SGn however yielded an R<sup>2</sup> of 0.8 indicating closer waveform similarity between SMb and SGn rather than MRb for this aspect.



**Table 7.2 Maximum absolute difference (Mean (SD)) in MAL between estimates from SMb and SGn with respect to MRb.**

	Hip flexion/extension		Hip ab/adduction		Hip rotation		Knee flexion/extension		Ankle dorsi/plantarflexion	
	SGn	SMb	SGn	SMb	SGn	SMb	SGn	SMb	SGn	SMb
add_brev			1.22 (0.57)	1.45 (0.93)	0.39 (0.16)	0.34 (0.16)				
add_long			1.02 (0.64)	1.05 (0.89)	0.21 (0.09)	0.19 (0.10)				
add_mag1	0.87 (0.44)	3.14 (1.07)	0.78 (0.43)	1.14 (0.64)	0.47 (0.19)	0.35 (0.12)				
add_mag2	0.92 (0.51)	2.05 (1.41)	0.75 (0.45)	1.22 (0.57)	0.23 (0.13)	0.24 (0.10)				
add_mag3	1.27 (0.65)	1.68 (1.19)	0.77 (0.30)	1.07 (0.78)	0.14 (0.07)	0.19 (0.11)				
bifemlh	1.13 (0.57)	1.57 (1.28)					1.23 (0.33)	2.67 (0.67)		
gem					0.75 (0.40)	1.22 (0.49)				
glut_max1	0.94 (0.47)	2.15 (0.61)			1.06 (0.55)	1.73 (0.94)				
glut_max2	0.69 (0.33)	2.08 (1.16)			0.95 (0.52)	1.69 (0.98)				
glut_max3	1.52 (1.00)	4.04 (1.78)			0.96 (0.73)	1.41 (0.85)				
glut_med1			0.94 (0.34)	1.26 (0.69)						
glut_med2			0.80 (0.29)	0.81 (0.43)						
glut_med3			0.81 (0.21)	0.80 (0.40)						
glut_min1			0.73 (0.28)	1.18 (0.63)	0.86 (0.46)	1.74 (1.04)				
glut_min2			0.70 (0.26)	0.85 (0.48)	0.73 (0.37)	1.47 (0.92)				
glut_min3			0.67 (0.24)	0.73 (0.34)	0.56 (0.25)	1.32 (0.79)				
grac			0.70 (0.50)	1.22 (0.64)			1.02 (0.56)	2.58 (1.10)		
iliacus	0.81 (0.68)	2.13 (0.70)								
pect	0.66 (0.35)	0.80 (0.50)	0.78 (0.49)	0.77 (0.43)						

peri								0.65 (0.28)	0.92 (0.43)				
psoas	0.59 (0.39)	1.01 (0.38)											
quad_fem			1.08 (0.28)	1.58 (0.59)	0.99 (0.40)	0.78 (0.50)							
rect_fem							0.91 (0.27)	4.35 (0.66)					
sar	1.29 (0.52)	1.47 (1.35)	1.02 (0.47)	1.20 (0.88)	0.24 (0.12)	0.38 (0.22)	1.01 (0.49)	1.60 (0.66)					
semimem	1.04 (0.63)	1.11 (0.81)					1.06 (1.42)	1.76 (1.39)					
semiten	1.17 (0.62)	1.32 (0.70)					1.30 (0.46)	3.64 (1.94)					
tfl													
bifemsh							1.35 (0.30)	2.96 (0.49)					
lat_gas							1.14 (0.44)	1.57 (0.68)	0.88 (0.32)	0.94 (0.46)			
med_gas							1.02 (0.49)	1.06 (0.38)	0.89 (0.32)	1.01 (0.43)			
vas_int							1.03 (0.33)	4.12 (0.54)					
vas_lat							1.10 (0.32)	3.24 (0.75)					
vas_med							1.11 (0.32)	3.68 (1.24)					
ext_dig									0.57 (0.34)	0.57 (0.37)			
ext_hal									0.86 (0.72)	1.17 (0.43)			
flex_dig									0.41 (0.26)	0.41 (0.25)			
flex_hal									0.60 (0.24)	2.18 (0.90)			
per_brev									0.98 (0.26)	1.02 (0.18)			
per_long									0.82 (0.28)	0.79 (0.20)			
soleus									0.74 (0.30)	0.81 (0.42)			
tib_ant									0.88 (0.35)	0.88 (0.35)			
tib_post									1.15 (0.29)	1.18 (0.32)			

## 7.5 Discussion

This study aimed to evaluate the extent personalisation of a musculoskeletal model with an intermediate level of subject-specific detail would have on model properties like segment lengths, muscle origin and insertion and estimates of joint angles, muscle-tendon lengths and moment arm lengths during walking in a group of children. The personalisation which was achieved using an imaging-informed statistical shape modelling approach, SMb, produced lower average absolute errors than the SGn in inter-HJC estimates and lower hip muscle point location average errors when compared to the MRb model. The SMb was however worse when estimating maximum muscle-tendon lengths and moment arm lengths.

The pelvis volume similarity ( $Jl = 0.38 \pm 0.12$ ) achieved by the SMb when compared to the MRb was lower than that reported by Suwarganda, et al. [9] ( $Jl = 0.62 \pm 0.06$ ). This difference can be attributed to the smaller section of pelvis (Figure 7.1) used in the registration and mesh fitting operation in our study. Indeed, in their study, it was shown that increasing the level of completeness of the body segment used improved the resulting volume similarity scores. Femur and tibia volume similarity values were similar to those reported in [9].

Distances of muscle point locations in SMb and SGn from their locations in the MRb were generally lower for SMb than SGn. They were on average however, still larger than the 1 cm variability associated with creating MRI-based models [31]. In the case of the hip adductors this corresponded to 76.7% of the muscle point locations. The poor pelvis similarity of the SMb when compared to the MRb appeared to translate to the differences in the location of muscle points particularly, the insertion points on the iliac and ischial surfaces of the pelvis. The larger differences for the SGn highlight the deficiency in using the generic model without personalisation for pathological populations such as CP. The range of 3D location differences observed in this study (0.73 - 5.25 cm) for the SGn were within the range (0.79 - 6.48 cm) reported by Wesseling, et al. [32]. In their study, where a non-rigid deformation approach for generating subject-specific models of children with CP was also evaluated, the SMb values were similarly within the ranges reported, with the exception of the insertion points for four of the foot muscles. Although they used complete MRI bone geometries in their deformation approach, the differences were comparable. Further investigation into whether increasing the completeness of the pelvis segment would minimise these differences in muscle point location further is warranted. The pelvis has one of the morphologically complex shapes of the lower limb and being able to capture this with minimal imaging data would enhance the attractiveness of using the SMb approach. An SSM atlas based on a representative population of children may help in this regard.

Contrary to expectation, the  $MTL_{max}$  and MAL differences were larger between SMb and MRb than between SGn and MRb for the degrees of freedom considered. Muscle moment arms contribute most to muscle force generation and comparison of SGn and SMb model estimates of MAL with respect to those from the MRb using the maximum absolute difference showed the SMb performing worse than the SGn (Table 7.2). The knee joint had the worst estimates of muscle moment arms for the SMb with respect to the MRb. Via points which are used to define muscle-tendon pathways are known to produce discontinuities in MAL estimates when they become active or deactivate [33], however these were kept to maintain consistency between the models instead of implementing wrapping surfaces which limit these discontinuities [23]. In the case of the SMb knee MALs, there existed less smoothness and more inter-subject variability of the MAL estimates over the joint range of motion in most muscles compared to the SGn and MRb. This could be attributed to the fact that the via point activations were not optimised by the algorithm, maintaining the same as the generic model template even though their locations were changed. The larger differences in MTL and MAL for the SMb may be caused by the muscle path optimisation that was performed. By its nature, muscle via points and wrapping surface parameters in the SMb were adjusted by the algorithm to prevent the occurrence of muscle paths penetrating the bone segments. Bahl, et al. [13] investigated an SSM without the optimisation performed in this study and observed root mean square differences in hip muscle MAL less than 0.5 mm. Although not currently investigated, it would be notable if these differences between the models persist to their estimates of longitudinal changes in  $MTL_{max}$  and the MAL.

A limitation of using an adult, healthy population-based SSM as implemented in the MAPClient for children is acknowledged. Increased errors have been reported in the geometries obtained for children below a certain size when using this SSM particularly when imaging data is unavailable [27]. Additionally, the sensitivity of the output of the muscle path and moment arm optimisation algorithm part of which is based on particle swarm optimisation to changes in input settings was not investigated and thus it is unclear if better or worse outcomes from what has been reported is possible. Killen, et al. [23] reported using a high-performance cluster in this operation but did not also report settings or a sensitivity analysis for the muscle path optimisation. Furthermore, it is unclear how these results would transfer to populations with increased bone deformities. Compared to other methods for automated personalisation of muscle-tendon paths [15, 31, 34], the approach used in this study does not require muscle imaging data. This would make it a viable alternative for rapid and easy personalisation of musculoskeletal models for the population of interest if the accuracy can be improved. Further studies to improve the optimisation and that

factor in the activations and permit the inclusion of additional via points would be of interest.

## **7.6 Conclusion**

Statistical modelling-based models aided by sparse imaging data were able to capture bone geometries, segment lengths and muscle point locations of participants better than the scaled generic models when compared to subject-specific models. They however struggled to match muscle tendon lengths and moment arm lengths which can affect downstream estimates of generated muscle forces and joint reaction forces. Further work is needed to improve the automated and non-image-based optimisation of the muscle parameters before it can serve as an alternative to image-based personalisation techniques and implemented into clinical pipelines.

## 7.7 References

- [1] S. S. Blemker, D. S. Asakawa, G. E. Gold, and S. L. Delp, "Image-based musculoskeletal modeling: Applications, advances, and future opportunities," (in English), *Journal of Magnetic Resonance Imaging*, vol. 25, no. 2, pp. 441-451, Feb 2007, doi: 10.1002/jmri.20805.
- [2] G. Valente *et al.*, "Are subject-specific musculoskeletal models robust to the uncertainties in parameter identification?," (in English), *PLoS One*, vol. 9, no. 11, p. e112625, Nov 12 2014, doi: 10.1371/journal.pone.0112625.
- [3] G. Lenaerts *et al.*, "Subject-specific hip geometry and hip joint centre location affects calculated contact forces at the hip during gait," (in English), *J Biomech*, vol. 42, no. 9, pp. 1246-51, Jun 19 2009, doi: 10.1016/j.jbiomech.2009.03.037.
- [4] G. Lenaerts *et al.*, "Subject-specific hip geometry affects predicted hip joint contact forces during gait," *J Biomech*, vol. 41, no. 6, pp. 1243-52, 2008/01/01/2008, doi: 10.1016/j.jbiomech.2008.01.014.
- [5] L. Scheys, A. Van Campenhout, A. Spaepen, P. Suetens, and I. Jonkers, "Personalized MR-based musculoskeletal models compared to rescaled generic models in the presence of increased femoral anteversion: effect on hip moment arm lengths," *Gait & posture*, vol. 28, no. 3, pp. 358-65, Oct 2008, doi: 10.1016/j.gaitpost.2008.05.002.
- [6] H. Kainz, C. P. Carty, S. Maine, H. P. J. Walsh, D. G. Lloyd, and L. Modenese, "Effects of hip joint centre mislocation on gait kinematics of children with cerebral palsy calculated using patient-specific direct and inverse kinematic models," *Gait & posture*, vol. 57, pp. 154-160, Sep 2017, doi: 10.1016/j.gaitpost.2017.06.002.
- [7] W. Koller, A. Baca, and H. Kainz, "Impact of scaling errors of the thigh and shank segments on musculoskeletal simulation results," *Gait & posture*, 2021/02/18/2021, doi: <https://doi.org/10.1016/j.gaitpost.2021.02.016>.
- [8] H. Kainz *et al.*, "The influence of maximum isometric muscle force scaling on estimated muscle forces from musculoskeletal models of children with cerebral palsy," (in English), *Gait & posture*, vol. 65, pp. 213-220, Sep 2018, doi: 10.1016/j.gaitpost.2018.07.172.
- [9] E. K. Suwarganda *et al.*, "Minimal medical imaging can accurately reconstruct geometric bone models for musculoskeletal models," *PLoS One*, vol. 14, no. 2, p. e0205628, 2019, doi: 10.1371/journal.pone.0205628.
- [10] J. Zhang, D. Malcolm, J. Hislop-Jambrich, C. D. L. Thomas, and P. M. F. Nielsen, "An anatomical region-based statistical shape model of the human femur," *Computer Methods in Biomechanics and Biomedical Engineering: Imaging & Visualization*, vol. 2, no. 3, pp. 176-185, 2014/07/03 2014, doi: 10.1080/21681163.2013.878668.
- [11] G. Davico *et al.*, "Best methods and data to reconstruct paediatric lower limb bones for musculoskeletal modelling," *Biomech Model Mechanobiol*, Nov 5 2019, doi: 10.1007/s10237-019-01245-y.

- [12] D. Bakke and T. Besier, "Shape model constrained scaling improves repeatability of gait data," *Journal of Biomechanics*, vol. 107, p. 109838, 2020/06/23/ 2020, doi: <https://doi.org/10.1016/j.jbiomech.2020.109838>.
- [13] J. S. Bahl *et al.*, "Statistical shape modelling versus linear scaling: Effects on predictions of hip joint centre location and muscle moment arms in people with hip osteoarthritis," *J Biomech*, vol. 85, pp. 164-172, Mar 6 2019, doi: 10.1016/j.jbiomech.2019.01.031.
- [14] J. Zhang *et al.*, "The MAP Client: User-Friendly Musculoskeletal Modelling Workflows," (in English), *Biomedical Simulation*, vol. 8789, pp. 182-192, 2014. [Online]. Available: <Go to ISI>://WOS:000345576600021.
- [15] L. Modenese, E. Montefiori, A. Wang, S. Wesarg, M. Viceconti, and C. Mazza, "Investigation of the dependence of joint contact forces on musculotendon parameters using a codified workflow for image-based modelling," (in English), *J Biomech*, vol. 73, pp. 108-118, May 17 2018, doi: 10.1016/j.jbiomech.2018.03.039.
- [16] E. Montefiori *et al.*, "An image-based kinematic model of the tibiotalar and subtalar joints and its application to gait analysis in children with Juvenile Idiopathic Arthritis," (in English), *J Biomech*, vol. 85, pp. 27-36, Mar 6 2019, doi: 10.1016/j.jbiomech.2018.12.041.
- [17] J. Stebbins, M. Harrington, N. Thompson, A. Zavatsky, and T. Theologis, "Repeatability of a model for measuring multi-segment foot kinematics in children," (in English), *Gait & posture*, vol. 23, no. 4, pp. 401-10, Jun 2006, doi: 10.1016/j.gaitpost.2005.03.002.
- [18] E. Montefiori *et al.*, "Linking Joint Impairment and Gait Biomechanics in Patients with Juvenile Idiopathic Arthritis," *Ann Biomed Eng*, vol. 47, no. 11, pp. 2155-2167, Nov 2019, doi: 10.1007/s10439-019-02287-0.
- [19] G. Valente, G. Crimi, N. Vanella, E. Schileo, and F. Taddei, "nmsBuilder: Freeware to create subject-specific musculoskeletal models for OpenSim," (in English), *Comput Methods Programs Biomed*, vol. 152, pp. 85-92, Dec 2017, doi: 10.1016/j.cmpb.2017.09.012.
- [20] S. L. Delp, J. P. Loan, M. G. Hoy, F. E. Zajac, E. L. Topp, and J. M. Rosen, "An interactive graphics-based model of the lower extremity to study orthopaedic surgical procedures," (in English), *Ieee T Bio-Med Eng*, vol. 37, no. 8, pp. 757-67, Aug 1990, doi: 10.1109/10.102791.
- [21] D. R. White, H. Q. Woodard, and S. M. Hammond, "Average soft-tissue and bone models for use in radiation dosimetry," *Br J Radiol*, vol. 60, no. 717, pp. 907-13, Sep 1987, doi: 10.1259/0007-1285-60-717-907.
- [22] H. Kainz, H. X. Hoang, C. Stockton, R. R. Boyd, D. G. Lloyd, and C. P. Carty, "Accuracy and Reliability of Marker-Based Approaches to Scale the Pelvis, Thigh, and Shank Segments in Musculoskeletal Models," *J Appl Biomech*, vol. 33, no. 5, pp. 354-360, Oct 1 2017, doi: 10.1123/jab.2016-0282.
- [23] B. A. Killen *et al.*, "Automated creation and tuning of personalised muscle paths for OpenSim musculoskeletal models of the knee joint," *Biomechanics and*

- Modeling in Mechanobiology*, 2020/10/24 2020, doi: 10.1007/s10237-020-01398-1.
- [24] M. M. van der Krogt, L. Bar-On, T. Kindt, K. Desloovere, and J. Harlaar, "Neuro-musculoskeletal simulation of instrumented contracture and spasticity assessment in children with cerebral palsy," (in English), *J Neuroeng Rehabil*, vol. 13, no. 1, p. 64, Jul 16 2016, doi: 10.1186/s12984-016-0170-5.
- [25] S. L. Delp *et al.*, "OpenSim: open-source software to create and analyze dynamic simulations of movement," (in English), *Ieee T Bio-Med Eng*, vol. 54, no. 11, pp. 1940-50, Nov 2007, doi: 10.1109/TBME.2007.901024.
- [26] A. A. Taha and A. Hanbury, "Metrics for evaluating 3D medical image segmentation: analysis, selection, and tool," *BMC Med Imaging*, vol. 15, p. 29, Aug 12 2015, doi: 10.1186/s12880-015-0068-x.
- [27] G. Davico *et al.*, "Best methods and data to reconstruct paediatric lower limb bones for musculoskeletal modelling," *Biomech Model Mechanobiol*, vol. 19, no. 4, pp. 1225-1238, Aug 2020, doi: 10.1007/s10237-019-01245-y.
- [28] M. E. Harrington, A. B. Zavatsky, S. E. Lawson, Z. Yuan, and T. N. Theologis, "Prediction of the hip joint centre in adults, children, and patients with cerebral palsy based on magnetic resonance imaging," *J Biomech*, vol. 40, no. 3, pp. 595-602, 2007, doi: 10.1016/j.jbiomech.2006.02.003.
- [29] J. L. Hicks, T. K. Uchida, A. Seth, A. Rajagopal, and S. L. Delp, "Is my model good enough? Best practices for verification and validation of musculoskeletal models and simulations of movement," (in English), *Journal of biomechanical engineering*, vol. 137, no. 2, p. 020905, Feb 1 2015, doi: 10.1115/1.4029304.
- [30] T. C. Pataky, "Generalized n-dimensional biomechanical field analysis using statistical parametric mapping," (in eng), *J Biomech*, vol. 43, no. 10, pp. 1976-82, Jul 20 2010, doi: 10.1016/j.jbiomech.2010.03.008.
- [31] L. Scheys, D. Loeckx, A. Spaepen, P. Suetens, and I. Jonkers, "Atlas-based non-rigid image registration to automatically define line-of-action muscle models: A validation study," *Journal of Biomechanics*, vol. 42, no. 5, pp. 565-572, 2009/03/26/ 2009, doi: <https://doi.org/10.1016/j.jbiomech.2008.12.014>.
- [32] M. Wesseling, L. Bosmans, C. Van Dijck, J. Vander Sloten, R. Wirix-Speetjens, and I. Jonkers, "Non-rigid deformation to include subject-specific detail in musculoskeletal models of CP children with proximal femoral deformity and its effect on muscle and contact forces during gait," *Comput Method Biomec*, vol. 22, no. 4, pp. 376-385, Mar 2019, doi: 10.1080/10255842.2018.1558216.
- [33] B. A. Garner and M. G. Pandy, "The Obstacle-Set Method for Representing Muscle Paths in Musculoskeletal Models," *Computer Methods in Biomechanics and Biomedical Engineering*, vol. 3, no. 1, pp. 1-30, 2000/01/01 2000, doi: 10.1080/10255840008915251.
- [34] L. Modenese and J. Kohout, "Automated Generation of Three-Dimensional Complex Muscle Geometries for Use in Personalised Musculoskeletal Models," *Annals of Biomedical Engineering*, vol. 48, no. 6, pp. 1793-1804, 2020/06/01 2020, doi: 10.1007/s10439-020-02490-4.



## **8 General discussion**

## 8.1 Summary

The overarching aim of this thesis was to investigate the use of musculoskeletal models in quantifying and predicting outcomes from surgical interventions to aid in clinical decision-making for children with cerebral palsy. The results and discourse presented in this body of work support the achievement of the objectives specified at the beginning of this thesis.

The first part of the thesis (chapter 3) evaluated the constraints associated with the decision to use a retrospective approach. It provided an understanding of the limits of the data and model to be used in achieving the aims of the thesis. Previous studies have highlighted the impact of experimental marker sets on kinematics estimated by unconstrained and constrained kinematic models, with most effect seen in the non-sagittal estimates of these angles [1-5]. What was not clear however, was how the marker sets affected similarly constrained but morphologically different models. The results from this chapter highlighted that although the kinematic profiles obtained from the two model types (generic and subject-specific models) were generally similar, generic model outputs were more subject to variability and most affected by the marker set used. Although between model differences particularly at the hip and distal joints were of concern, the differences were below what would be considered a critical threshold of error affecting clinical interpretation.

Informed by the above results, a modified generic model was used to investigate the Gait Profile Score, a clinical measure of overall gait quality, and how it changes after FDO surgery in a cohort of children with CP in chapter 4. This chapter allowed to compare the generic model estimates with the prevalent method used in the clinic to estimate this measure. The results showed that both methods estimated similar values for the Gait Profile Score ( $R^2 = 0.87$ ) and agreed at least 90% of the time in the changes they predicted [6]. Nonetheless, this analysis also highlighted the challenge in estimating the hip rotation component, a kinematic variable that is predominantly affected in this cohort due to the femoral anteversion present and which the surgery aims to correct. The implementation of a modification that aimed to capture the degree of femoral anteversion would need to be tested for clinical validity particularly with other clinical measurements that have previously been used as surrogates for the degree of anteversion, such as the midpoint of hip passive range of motion or the trochanteric prominence angle test. The data in our cohort were not rich enough to permit such an analysis. This should form a focus of a future prospective study where imaging data can be included.

In chapter 5, the analysis was extended to investigate muscle-tendon lengths and their predictive value for identifying within the CP cohort, those who were most likely to

have positive outcomes from undergoing the FDO as part of SEMLS. Three hip ab/adduction muscles (adductor brevis, adductor magnus and gracilis) were identified as likely candidates for this role, being significantly different between response and non-response groups and also being significantly changed after the surgery only in the response group. These are novel findings and given that these were with a generic model that did not permit a capturing of changes effected by the surgery, further studies to confirm and validate using personalised models is warranted.

The final part of this thesis sought to focus on the effects of personalisation and how closely generic models matched estimates obtained from more personalised models. In chapter 6, the ability of generic models to predict longitudinal changes in joint contact forces that were consistent with predictions from an MRI-based model was analysed. The generic model was found to be able to predict changes that were in line with predictions by the MRI-based model [7]. That notwithstanding, the differences in instantaneous estimates made by both types of models raises concerns for use of the generic model. In chapter 7, a means to personalise a generic model with minimal imaging resources was pursued. The results from this effort showed an improvement in the model bone and muscle segment parameters but not muscle function estimates.

## **8.2 Discussion**

Kinematics and kinetic measurements and outputs derived from three-dimensional gait analysis has been shown to help clinicians better understand normal and abnormal gait in cerebral palsy, particularly when compared with visual assessment [8], with impact on the choice of surgical procedures performed [9, 10]. When recommendations from pre-operative gait analysis were followed, patients also had improved outcomes [11, 12]. Similarly, the ability to estimate details associated with gait not easily measurable with non-invasive means such as muscle and joint contact forces, muscle lengths and moment arms afforded by the use of musculoskeletal models provides insights that can inform clinical decision making and orthopaedic interventions [13-15].

As a whole, the findings from the different chapters of this thesis lend support to the utility of musculoskeletal models in such an application and highlights the challenges in doing this. First off, in CP gait analysis, a minimal marker set such as the widely used PlugIn Gait markers is employed to minimise the time of application and discomfort to the patient. The findings in this thesis showed that although this minimal marker set produced kinematic outputs that were different from those output with many markers, these differences fell below the clinical threshold of concern. This in line with

the findings of Kainz, et al. [16] which suggested that differences in the anatomical model contributed most to differences observed in joint kinematics than either the computational approach or quantity of markers used. A minimal change which can be implemented to reduce the largest differences when using these musculoskeletal models as part of the clinical pipeline, is the addition of two extra markers on the foot as employed in the Sheffield Foot Model, which reduced the differences in joint angles particularly for the distal ankle joint complex for both generic and subject-specific models. Although not investigated in this thesis, for patients with substantial foot deformities, it is suggested to use an increased number of markers on the foot with a more complex foot model as has previously been reported [17-19]. It is expected that these results pertaining to marker sets would still be relevant to the musculoskeletal modelling of gait pathological populations other than CP. The similarity in results from estimating gait deviations of persons with CP from normal populations and changes after the FDO also shows concurrent validity of the musculoskeletal modelling approach and global optimisation with respect to the traditional gait analysis method.

Previous research has reported on the use of musculoskeletal models to aid in the clinical decision-making process for other interventions in cerebral palsy. For instance, when investigating outcomes after muscle lengthening surgery, it was shown with musculoskeletal models that patients who had muscles that tended to be shorter or operated at slower velocities than normal [14, 20]. The literature is however sparse in relation to the use of musculoskeletal models in such an analysis on the FDO. That notwithstanding, this thesis reports significant differences in muscle-tendon lengths between patients with improvement and those without, after the FDO, as well as significant changes after the FDO for the improvers. The observation of similar trends when taken in the context of SEMLS lends strength to the suggestion that the pre-surgery lengths of muscles that are around the hip and can be affected by the FDO play a role in outcomes. The identification of muscle-tendon length thresholds or an index to discriminate patients at the pre-surgery timepoint would have permitted true prediction of outcome. Also, given that the models used in this analysis did not capture the deformities and the effected corrections, there is the likelihood that the differences and changes observed may be driven solely by changes in the kinematics. Nevertheless, the identification of these muscles highlights the usefulness of these musculoskeletal models for providing insights for aiding the clinical decision-making process.

The benefits of Increasing model personalisation have been largely reported in literature, with the MRI-based models the current state of the art approach [21, 22]. The challenges of time, resources and expertise necessary to achieve full personalisation have pushed the need for alternatives methods for developing subject-

specific models to achieve adequate levels of accuracy. The findings from this thesis looking at increasing the level of personalisation using the statistical shape modelling approach with sparse imaging data was in line with what has been reported in particularly in terms of the reconstruction accuracy. When examining the gains in terms of the errors in kinematics when compared to a fully MRI-based model, there were not significant improvements when compared to the generic model to warrant the extra effort in this case. This was despite the observation of better reconstruction accuracy of the bone segments from the statistical shape modelling approach. Given that imaging, albeit sparse may not always be available, recent development of tools [23, 24] that permit the deformation generic models using measures such as the degree of femoral anteversion that are routinely collected as part of clinical assessment provide alternatives to achieving model personalisation.

Overall, the findings from this thesis highlighted the utility of using musculoskeletal models as a means to probe information that could be used to aid the clinical decision-making process in the specific intervention of femoral derotation osteotomy as part of single event multilevel surgery in cerebral palsy.

### **8.3 Limitations**

Limitations of the different components of work undertaken as part of this thesis have been outlined in the relevant chapters. Here I take a global view.

The general concern about the accuracy of estimates obtained from scaled generic models particularly in pathological populations is justified and acknowledged. However, data that permits the build and use of subject-specific models are not always available and this thesis aimed to explore the bounds of this limitation. Their utility as a first line to identify parameters that can be probed further cannot be overemphasised, particularly when resources are not available to pursue the necessary personalisation.

A limitation of both chapter 3 and 4 was the inability to directly compare the hip rotation component of the joint kinematics. Firstly, the cohort used in chapter 1 were of reasonably sound participants with assumedly no excessive anteversion. A modified generic model as used in in chapter 4 would have permitted to determine what impact the modification had on the hip rotation estimates in chapter 3. This was not possible as the marker set used did not account for the KAD in the static trial. That notwithstanding, the RMSD between PiG and mGen for hip rotation in the TD was quite similar to the CP cohort ( $14.9 \pm 6.4$  vs  $12.9 \pm 7.8$ ).

In most cases, we used either the output from the MRI-based model or the clinically used PiG as our gold standard with no substantive assessment of their accuracy. A

true gold standard would have required the use of invasive methods such as the use of bone pin-mounted markers or fluoroscopy [25, 26] which may pose ethical concerns especially for the cohort we deal with in this thesis. The choices of the PiG and the MRI-based model in this role are however justified in the context of surgical prediction, where the PiG is what is the standard currently used and trusted in the clinic and the MRI-based models form the state-of-the-art approach for musculoskeletal modelling.

One aspect of human movement not touched upon by this thesis is the neuromuscular control of movement. Neuromuscular control forms an important aspect of movement, providing the stimulus that drives the performance of any activity. This is particularly affected in cerebral palsy and thus the control strategies exercised by persons with CP are different from healthy populations [27, 28]. Indeed, the selective motor control of children with CP has been found to affect the gross motor function of this group more than other impairments such as spasticity [29, 30]. These different motor control strategies affect outcomes with suggestions that the motor control is important for predicting treatment outcomes [31-33]. Although motor control strategies appear not to change significantly after treatment [34, 35] in persons with CP, their deviation from normal can be informative as reports indicate patients with strategies closer to normal tend to have improvements in their gait kinematics after single event multilevel surgery and thus could be included in pre-operative predictions of outcome simulations [36]. Studies have also looked into methods to incorporate individuals' unique motor control in the simulation with the use of electromyography data as the control signals for the muscles in the musculoskeletal model [37]. The muscles of persons with CP are also characterised by spasticity and contractures which affect their lengthening and force generation capacities. These nuances between different CP participants and the healthy cohort were not accounted for in the models used in this thesis. These variations could influence the changes in muscle-tendon lengths and the lengthening velocities estimated by the models. Although applied to passive stretches, van der Krogt, et al. [38] developed a conceptual model that could explain muscle stretch behaviour and included subject-specific parameters for spasticity and contracture. Their approach could be extended and applied in these musculoskeletal models to reflect the effects of the spasticity and contractures during dynamic gait of patients with CP.

## **8.4 Future work**

Extension of this work in the future would focus on:

- i. Establishing the face validity of the knee axis correction applied as a surrogate for the measure of femoral anteversion and midpoint of hip PROM. Previous

studies of surrogate clinical measures to the degree of femoral anteversion have shown poor to moderate correlations with the more accurate imaging-based measurement. A more accurate surrogate can only go to improve decision-making and this approach would not impact on the time or resource requirements for the normal clinical gait analysis procedure.

- ii. Expanding the comparative analysis of muscle-tendon length properties between subject-specific and generic models briefly mentioned in chapter 5 to a larger and different cohort to inform the generalisability of the approach to determining the maximum MTL for muscles with multi-segment representations in the musculoskeletal models.
- iii. Validating the identified muscles with predictive value for FDO outcomes in a prospective study or with a more restrictive dataset with minimal confounding from soft tissue surgeries.
- iv. Investigation of the sensitivity of the muscle-tendon path and kinematics optimisation to input parameters. The statistical shape modelling approach with sparse imaging data improved model geometry accuracy however the personalisation of the muscle path parameters failed to improve on the generic model and was worse in cases based on the settings we used. Unfortunately, the dependence of the algorithm output on its settings has not been reported. This information would be beneficial for establishing the reliability and validity of this approach as well as establish the limits of accuracy.

## **8.5 Conclusion**

Overall, the findings of this thesis showed that musculoskeletal models can produce results that are consistent with traditional clinical gait analysis techniques when considering longitudinal changes over time and outcomes after surgical intervention. The potential of providing additional information for the decision-making process was also highlighted by novel findings of muscle-tendon pre-operative lengths of hip muscles that discriminate candidates for the FDO who are most probable of reporting positive outcomes after the intervention. Finally, the results showed that minimal personalisation improves some estimates from generic models, although additional efforts are required to achieve parity with fully personalised models for some measures. It is the long-term goal to achieve musculoskeletal models of sufficient bio-fidelity and accuracy for integration into clinical care practice for improving outcomes in CP and this thesis contributes to the growing body of work in this direction.

## 8.6 References

- [1] A. A. Slater, T. J. Hullfish, and J. R. Baxter, "The impact of thigh and shank marker quantity on lower extremity kinematics using a constrained model," *BMC Musculoskeletal Disorders*, vol. 19, no. 1, p. 399, 2018/11/13 2018, doi: 10.1186/s12891-018-2329-7.
- [2] A. Ferrari *et al.*, "Quantitative comparison of five current protocols in gait analysis," *Gait & posture*, vol. 28, no. 2, pp. 207-216, 2008/08/01/ 2008, doi: <https://doi.org/10.1016/j.gaitpost.2007.11.009>.
- [3] B. W. Schulz and W. L. Kimmel, "Can hip and knee kinematics be improved by eliminating thigh markers?", (in English), *Clinical Biomechanics*, vol. 25, no. 7, pp. 687-692, Aug 2010, doi: 10.1016/j.clinbiomech.2010.04.002.
- [4] T. D. Collins, S. N. Ghousayni, D. J. Ewins, and J. A. Kent, "A six degrees-of-freedom marker set for gait analysis: Repeatability and comparison with a modified Helen Hayes set," *Gait & posture*, vol. 30, no. 2, pp. 173-180, 2009/08/01/ 2009, doi: <https://doi.org/10.1016/j.gaitpost.2009.04.004>.
- [5] G. Mantovani and M. Lamontagne, "How Different Marker Sets Affect Joint Angles in Inverse Kinematics Framework," *Journal of biomechanical engineering*, vol. 139, no. 4, 2017, doi: 10.1115/1.4034708.
- [6] C. F. Hayford, E. Pratt, J. P. Cashman, O. G. Evans, and C. Mazza, "Effectiveness of Global Optimisation and Direct Kinematics in Predicting Surgical Outcome in Children with Cerebral Palsy," *Life (Basel)*, vol. 11, no. 12, p. 1306, Nov 27 2021, doi: 10.3390/life11121306.
- [7] C. F. Hayford, E. Montefiori, E. Pratt, and C. Mazza, "Predicting longitudinal changes in joint contact forces in a juvenile population: scaled generic versus subject-specific musculoskeletal models," *Comput Method Biomec*, pp. 1-12, Jun 26 2020, doi: 10.1080/10255842.2020.1783659.
- [8] D. E. Krebs, J. E. Edelstein, and S. Fishman, "Reliability of Observational Kinematic Gait Analysis," *Physical Therapy*, vol. 65, no. 7, pp. 1027-1033, 1985, doi: 10.1093/ptj/65.7.1027.
- [9] T. A. L. Wren, G. E. Gorton, S. Öunpuu, and C. A. Tucker, "Efficacy of clinical gait analysis: A systematic review," *Gait & posture*, vol. 34, no. 2, pp. 149-153, 2011/06/01/ 2011, doi: <https://doi.org/10.1016/j.gaitpost.2011.03.027>.
- [10] B. Lofteørd, T. Terjesen, I. Skaaret, A. B. Huse, and R. Jahnsen, "Preoperative gait analysis has a substantial effect on orthopedic decision making in children with cerebral palsy: comparison between clinical evaluation and gait analysis in 60 patients," (in eng), *Acta Orthop*, vol. 78, no. 1, pp. 74-80, Feb 2007, doi: 10.1080/17453670610013448.
- [11] B. Lofteørd and T. Terjesen, "Results of treatment when orthopaedic surgeons follow gait-analysis recommendations in children with CP," *Developmental Medicine & Child Neurology*, vol. 50, no. 7, pp. 503-509, 2008, doi: 10.1111/j.1469-8749.2008.03018.x.



- [12] T. A. L. Wren, C. Lening, S. A. Rethlefsen, and R. M. Kay, "Impact of gait analysis on correction of excessive hip internal rotation in ambulatory children with cerebral palsy: a randomized controlled trial," *Developmental Medicine & Child Neurology*, vol. 55, no. 10, pp. 919-925, 2013, doi: 10.1111/dmcn.12184.
- [13] A. S. Arnold, D. J. Asakawa, and S. L. Delp, "Do the hamstrings and adductors contribute to excessive internal rotation of the hip in persons with cerebral palsy?," *Gait & posture*, vol. 11, no. 3, pp. 181-190, 2000/06/01/ 2000, doi: [https://doi.org/10.1016/S0966-6362\(00\)00046-1](https://doi.org/10.1016/S0966-6362(00)00046-1).
- [14] A. S. Arnold, M. Q. Liu, M. H. Schwartz, S. Ounpuu, L. S. Dias, and S. L. Delp, "Do the hamstrings operate at increased muscle-tendon lengths and velocities after surgical lengthening?," *J Biomech*, vol. 39, no. 8, pp. 1498-506, 2006, doi: 10.1016/j.jbiomech.2005.03.026.
- [15] S. L. Delp, A. S. Arnold, R. A. Speers, and C. A. Moore, "Hamstrings and psoas lengths during normal and crouch gait: Implications for muscle-tendon surgery," *Journal of Orthopaedic Research*, vol. 14, no. 1, pp. 144-151, 1996, doi: <https://doi.org/10.1002/jor.1100140123>.
- [16] H. Kainz, L. Modenese, D. G. Lloyd, S. Maine, H. P. J. Walsh, and C. P. Carty, "Joint kinematic calculation based on clinical direct kinematic versus inverse kinematic gait models," *J Biomech*, vol. 49, no. 9, pp. 1658-1669, Jun 14 2016, doi: 10.1016/j.jbiomech.2016.03.052.
- [17] J. McCahill, J. Stebbins, B. Koning, J. Harlaar, and T. Theologis, "Repeatability of the Oxford Foot Model in children with foot deformity," (in English), *Gait & posture*, vol. 61, pp. 86-89, Mar 2018, doi: 10.1016/j.gaitpost.2017.12.023.
- [18] J. Stebbins, M. Harrington, N. Thompson, A. Zavatsky, and T. Theologis, "Repeatability of a model for measuring multi-segment foot kinematics in children," (in English), *Gait & posture*, vol. 23, no. 4, pp. 401-10, Jun 2006, doi: 10.1016/j.gaitpost.2005.03.002.
- [19] A. Leardini, M. G. Benedetti, L. Berti, D. Bettinelli, R. Natio, and S. Giannini, "Rear-foot, mid-foot and fore-foot motion during the stance phase of gait," *Gait & posture*, vol. 25, no. 3, pp. 453-462, 2007/03/01/ 2007, doi: <https://doi.org/10.1016/j.gaitpost.2006.05.017>.
- [20] A. S. Arnold, M. Q. Liu, M. H. Schwartz, S. Ounpuu, and S. L. Delp, "The role of estimating muscle-tendon lengths and velocities of the hamstrings in the evaluation and treatment of crouch gait," *Gait & posture*, vol. 23, no. 3, pp. 273-81, Apr 2006, doi: 10.1016/j.gaitpost.2005.03.003.
- [21] L. Scheys, K. Desloovere, A. Spaepen, P. Suetens, and I. Jonkers, "Calculating gait kinematics using MR-based kinematic models," *Gait & posture*, vol. 33, no. 2, pp. 158-64, Feb 2011, doi: 10.1016/j.gaitpost.2010.11.003.
- [22] L. Scheys, K. Desloovere, P. Suetens, and I. Jonkers, "Level of subject-specific detail in musculoskeletal models affects hip moment arm length calculation during gait in pediatric subjects with increased femoral anteversion," *Journal of Biomechanics*, vol. 44, no. 7, pp. 1346-1353, 2011/04/29/ 2011, doi: <https://doi.org/10.1016/j.jbiomech.2011.01.001>.

- [23] L. Modenese, M. Barzan, and C. P. Carty, "Dependency of Lower Limb Joint Reaction Forces on Femoral Anteversion," *Gait & posture*, 2021/06/16/ 2021, doi: <https://doi.org/10.1016/j.gaitpost.2021.06.014>.
- [24] K. Veerkamp, H. Kainz, B. A. Killen, H. Jónasdóttir, and M. M. van der Krogt, "Torsion Tool: An automated tool for personalising femoral and tibial geometries in OpenSim musculoskeletal models," *Journal of Biomechanics*, vol. 125, p. 110589, 2021/08/26/ 2021, doi: <https://doi.org/10.1016/j.jbiomech.2021.110589>.
- [25] D. L. Benoit, D. K. Ramsey, M. Lamontagne, L. Xu, P. Wretenberg, and P. Renström, "Effect of skin movement artifact on knee kinematics during gait and cutting motions measured in vivo," *Gait & posture*, vol. 24, no. 2, pp. 152-164, 2006/10/01/ 2006, doi: <https://doi.org/10.1016/j.gaitpost.2005.04.012>.
- [26] N. M. Fiorentino, P. R. Atkins, M. J. Kutschke, J. M. Goebel, K. B. Foreman, and A. E. Anderson, "Soft tissue artifact causes significant errors in the calculation of joint angles and range of motion at the hip," *Gait & posture*, vol. 55, pp. 184-190, 2017/06/01/ 2017, doi: <https://doi.org/10.1016/j.gaitpost.2017.03.033>.
- [27] K. M. Steele, A. Rozumalski, and M. H. Schwartz, "Muscle synergies and complexity of neuromuscular control during gait in cerebral palsy," *Dev Med Child Neurol*, vol. 57, no. 12, pp. 1176-82, Dec 2015, doi: 10.1111/dmcn.12826.
- [28] A. Bekius, M. M. Bach, M. M. van der Krogt, R. de Vries, A. I. Buizer, and N. Dominici, "Muscle Synergies During Walking in Children With Cerebral Palsy: A Systematic Review," (in eng), *Front Physiol*, vol. 11, p. 632, 2020, doi: 10.3389/fphys.2020.00632.
- [29] S. Ostensjø, E. B. Carlberg, and N. K. Vøllestad, "Motor impairments in young children with cerebral palsy: relationship to gross motor function and everyday activities," (in eng), *Dev Med Child Neurol*, vol. 46, no. 9, pp. 580-9, Sep 2004, doi: 10.1017/s0012162204000994.
- [30] J. M. Voorman, A. J. Dallmeijer, D. L. Knol, G. J. Lankhorst, and J. G. Becher, "Prospective Longitudinal Study of Gross Motor Function in Children With Cerebral Palsy," *Archives of Physical Medicine and Rehabilitation*, vol. 88, no. 7, pp. 871-876, 2007, doi: 10.1016/j.apmr.2007.04.002.
- [31] E. J. Goldberg, E. G. Fowler, and W. L. Oppenheim, "Case Reports: The Influence of Selective Voluntary Motor Control on Gait After Hamstring Lengthening Surgery," *Clinical Orthopaedics & Related Research*, vol. 470, no. 5, pp. 1320-1326, 2012, doi: 10.1007/s11999-011-2028-2.
- [32] M. H. Schwartz, A. Rozumalski, and K. M. Steele, "Dynamic motor control is associated with treatment outcomes for children with cerebral palsy," *Developmental Medicine & Child Neurology*, vol. 58, no. 11, pp. 1139-1145, 2016, doi: 10.1111/dmcn.13126.
- [33] L. M. Oudenhoven *et al.*, "Factors Associated With Long-Term Improvement of Gait After Selective Dorsal Rhizotomy," *Archives of Physical Medicine and Rehabilitation*, vol. 100, no. 3, pp. 474-480, 2019, doi: 10.1016/j.apmr.2018.06.016.

- [34] B. R. Shuman, M. Goudriaan, K. Desloovere, M. H. Schwartz, and K. M. Steele, "Muscle synergies demonstrate only minimal changes after treatment in cerebral palsy," *Journal of NeuroEngineering and Rehabilitation*, vol. 16, no. 1, 2019, doi: 10.1186/s12984-019-0502-3.
- [35] D. Patikas, S. I. Wolf, W. Schuster, P. Armbrust, T. Dreher, and L. Döderlein, "Electromyographic patterns in children with cerebral palsy: Do they change after surgery?," *Gait & posture*, vol. 26, no. 3, pp. 362-371, 2007/09/01/ 2007, doi: <https://doi.org/10.1016/j.gaitpost.2006.10.012>.
- [36] L. Pitto *et al.*, "Pre-treatment EMG can be used to model post-treatment muscle coordination during walking in children with cerebral palsy," *PLOS ONE*, vol. 15, no. 2, p. e0228851, 2020, doi: 10.1371/journal.pone.0228851.
- [37] B. R. Shuman, M. Goudriaan, K. Desloovere, M. H. Schwartz, and K. M. Steele, "Muscle Synergy Constraints Do Not Improve Estimates of Muscle Activity From Static Optimization During Gait for Unimpaired Children or Children With Cerebral Palsy," (in eng), *Front Neurobot*, vol. 13, pp. 102-102, 2019, doi: 10.3389/fnbot.2019.00102.
- [38] M. M. van der Krogt, L. Bar-On, T. Kindt, K. Desloovere, and J. Harlaar, "Neuro-musculoskeletal simulation of instrumented contracture and spasticity assessment in children with cerebral palsy," (in English), *J Neuroeng Rehabil*, vol. 13, no. 1, p. 64, Jul 16 2016, doi: 10.1186/s12984-016-0170-5.

## APPENDIX 1 - CHAPTER 4 SUPPLEMENTAL MATERIAL

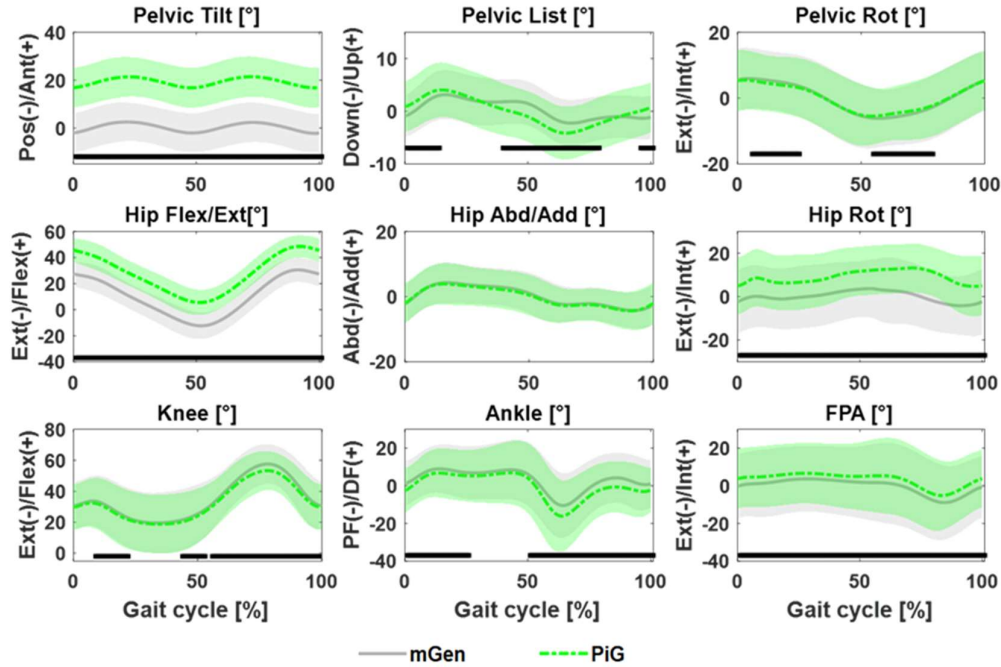


Figure S1. Mean joint kinematic waveforms for 26 CP participants estimated with PiG and mGen models. Shaded bands indicate 1SD with significant difference shown by bottom black bars.

Table S1. Changes in GPS ( $\Delta_t$ GPS) estimated by mGen and PiG for CP cohort.

SUBJECT	RIGHT		LEFT	
	PiG	mGen	PiG	mGen
	$\Delta$ GPS	$\Delta$ GPS	$\Delta$ GPS	$\Delta$ GPS
01	1.3	0.0	-1.6	-1.4
02	9.5	8.3	4.3	5.1
03	-3.2	-6.2	-2.6	-5.3
04	2.7	2.2	-5.4	-7.0
05	5.8	4.2	-0.7	-0.3
06	-5.3	-5.8	-8.2	-8.5
07	-6.7	-9.5	-3.7	-5.3
08	2.1	-1.2	-2.5	-5.4
09	-1.5	-0.6	-4.6	-5.4
10	-7.1	-7.6	-6.8	-1.4
11	2.2	2.1	-5.0	-3.8
12	10.3	11.0	6.0	7.5
13	0.9	-0.5	3.8	2.2
14	0.6	-1.4	-1.9	-1.3
15	2.0	1.3	3.6	2.2
16	1.1	-0.6	1.3	-0.5

<b>17</b>	-11.9	-8.5	-8.2	-8.9
<b>18</b>				
<b>19</b>	0.1	-2.9	-3.2	-2.1
<b>20</b>	-5.8	-9.5	-2.5	-5.4
<b>21</b>	-4.2	-4.0	-1.9	-1.5
<b>22</b>	-2.9	-2.0	-6.8	-5.5
<b>23</b>	1.2	2.0	-14.4	-12.8
<b>24</b>	1.5	1.8	-1.9	-2.2
<b>25</b>	3.4	0.4	-0.1	1.4
<b>26</b>	0.4	1.5	-1.2	-0.6

**Table S2. Right-Left Asymmetry calculated as difference between right and left limb GPS values for CP cohort.**

<b>RIGHT-LEFT ASYMMETRY</b>				
	<b>Pre-FDO-SEMLS</b>		<b>Post-FDO-SEMLS</b>	
	PiG	mGen	PiG	mGen
	R-L Delta	R-L Delta	R-L Delta	R-L Delta
<b>01</b>	-8.0	-10.4	-5.2	-9.1
<b>02</b>	-4.7	-3.3	0.5	-0.1
<b>03</b>	1.0	-0.3	0.4	-1.2
<b>04</b>	-6.2	-7.8	1.9	1.4
<b>05</b>	-4.5	-4.2	2.1	0.2
<b>06</b>	2.0	1.5	4.9	4.2
<b>07</b>	5.5	7.2	2.5	3.0
<b>08</b>	0.0	-2.2	4.6	2.0
<b>09</b>	-1.9	-1.8	1.1	3.0
<b>10</b>	5.4	9.4	5.1	3.2
<b>11</b>	-6.3	-8.9	0.9	-3.0
<b>12</b>	-3.3	-3.3	0.9	0.2
<b>13</b>	3.3	3.3	0.5	0.6
<b>14</b>	4.5	4.8	7.0	4.7
<b>15</b>	2.0	2.2	0.4	1.4
<b>16</b>	-1.8	-2.5	-1.9	-2.5
<b>17</b>	5.0	2.1	1.4	2.5
<b>18</b>	3.0	3.3	0.0	0.0
<b>19</b>	-4.2	-1.9	-1.0	-2.7
<b>20</b>	-0.3	1.2	-3.7	-2.8
<b>21</b>	10.6	10.0	8.3	7.5
<b>22</b>	-5.7	-6.2	-1.7	-2.7
<b>23</b>	-11.3	-10.9	4.3	4.0
<b>24</b>	-2.3	1.2	1.0	5.2
<b>25</b>	-0.6	3.5	2.9	2.5
<b>26</b>	1.4	0.3	3.0	2.4

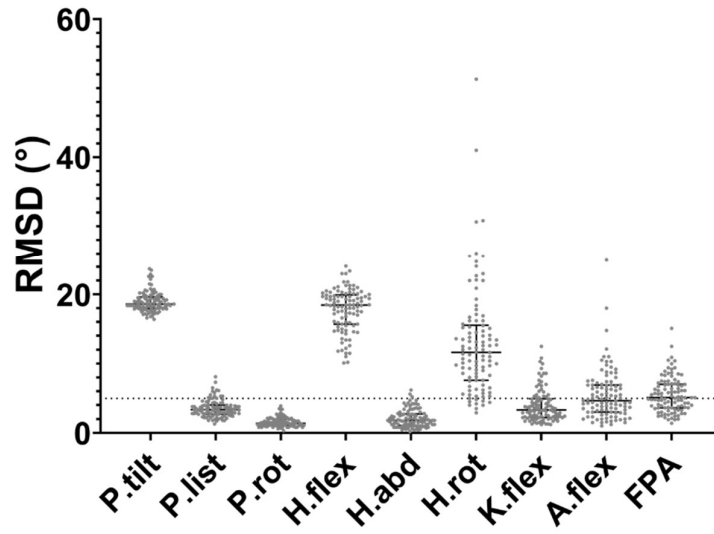


Figure S2. Distribution of RMSD between mGen and PiG for CP cohort.

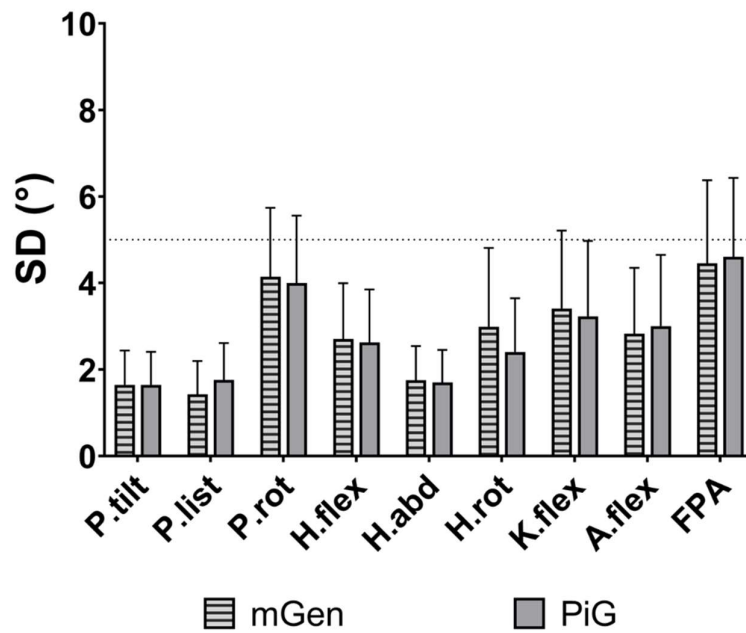


Figure S3. Mean inter-trial (within session) standard deviation for kinematic waveforms from mGen and PiG for CP cohort.

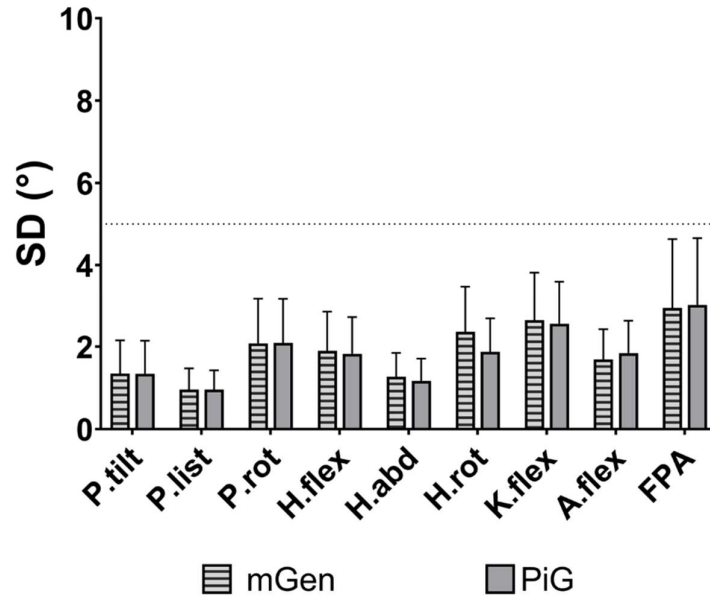


Figure S4. Mean inter-trial standard deviation for kinematic waveforms from mGen and PiG for TD cohort.

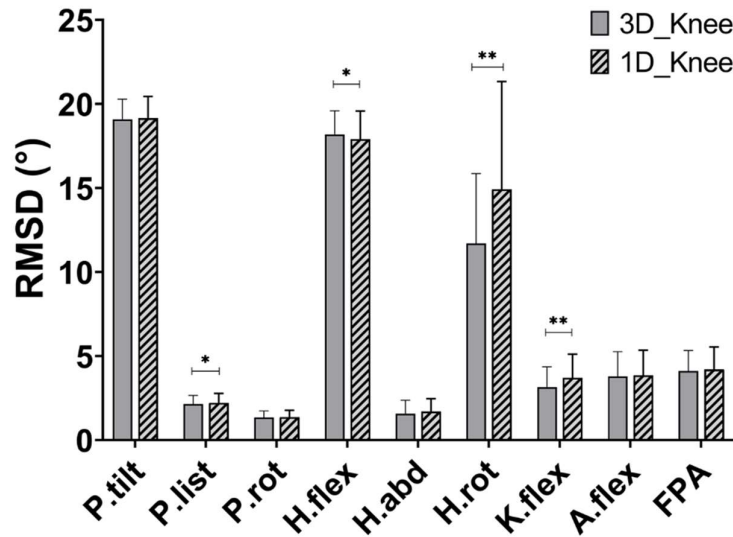
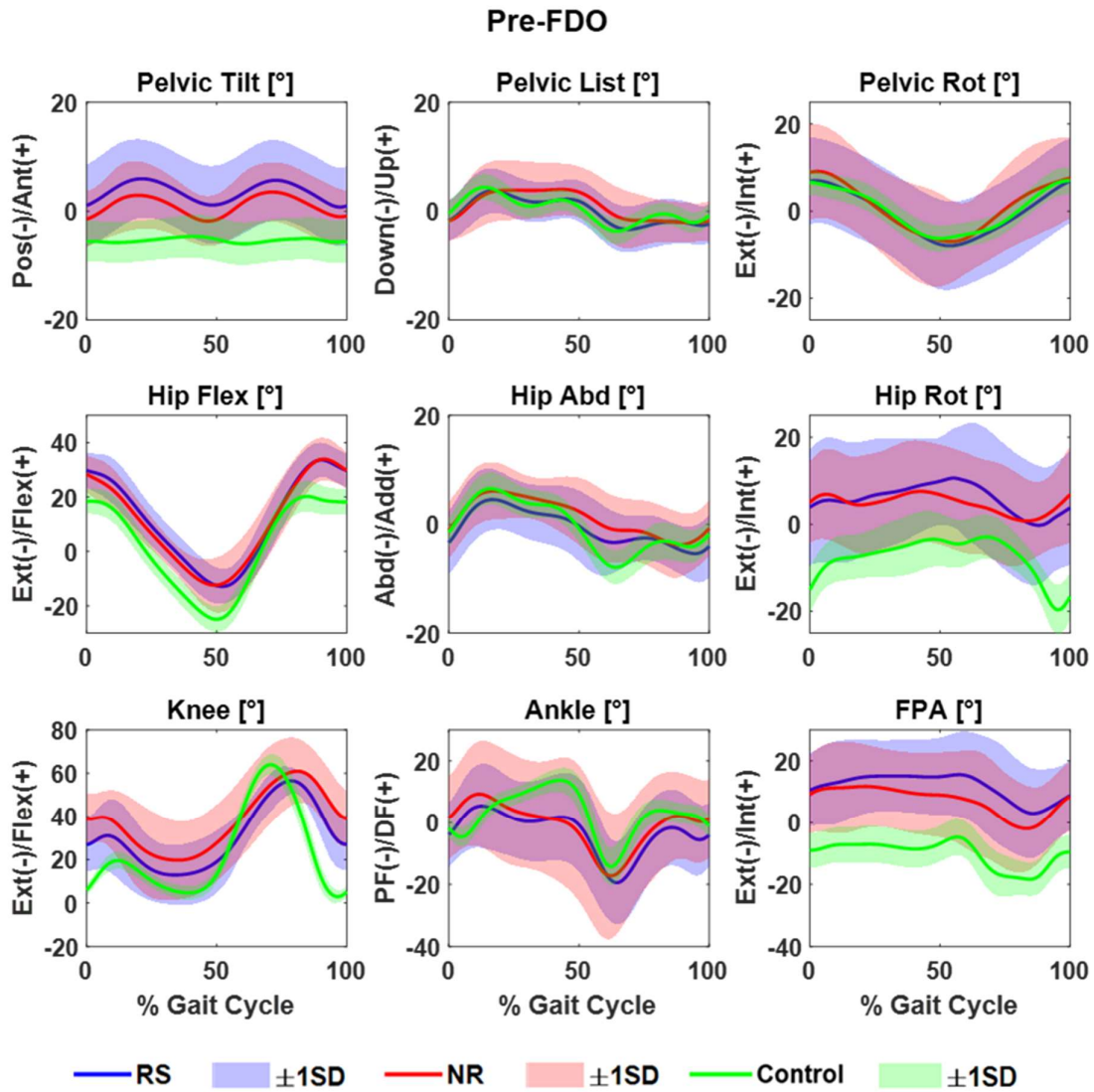


Figure S5. Comparison of RMSD between mGen and PiG for two implementations of the mGen knee joint (3DoF and 1DoF). \*p < 0.01 \*\*p < 0.001.

Table S3. Maximum marker tracking errors.

Marker	LASI	RASI	SACR	THI	KNE	TIB	ANK	HEE	TOE
Right limb	0.39 ± 0.18	0.64 ± 0.30	0.58 ± 0.25	1.88 ± 0.77	1.30 ± 0.71	1.29 ± 0.58	0.86 ± 0.35	0.96 ± 0.42	0.85 ± 0.38
Left limb	0.56 ± 0.23	0.44 ± 0.18	0.54 ± 0.24	1.74 ± 0.62	1.23 ± 0.42	1.20 ± 0.40	0.83 ± 0.30	1.04 ± 0.34	0.73 ± 0.20

## Appendix 2 - Chapter 5 supplemental material



**Figure A2.1 Joint kinematic profiles for responders (RS, blue) and non-responders (NR, red) before FDO-SEMLS compared with healthy controls (green). FPA is foot progression angle**



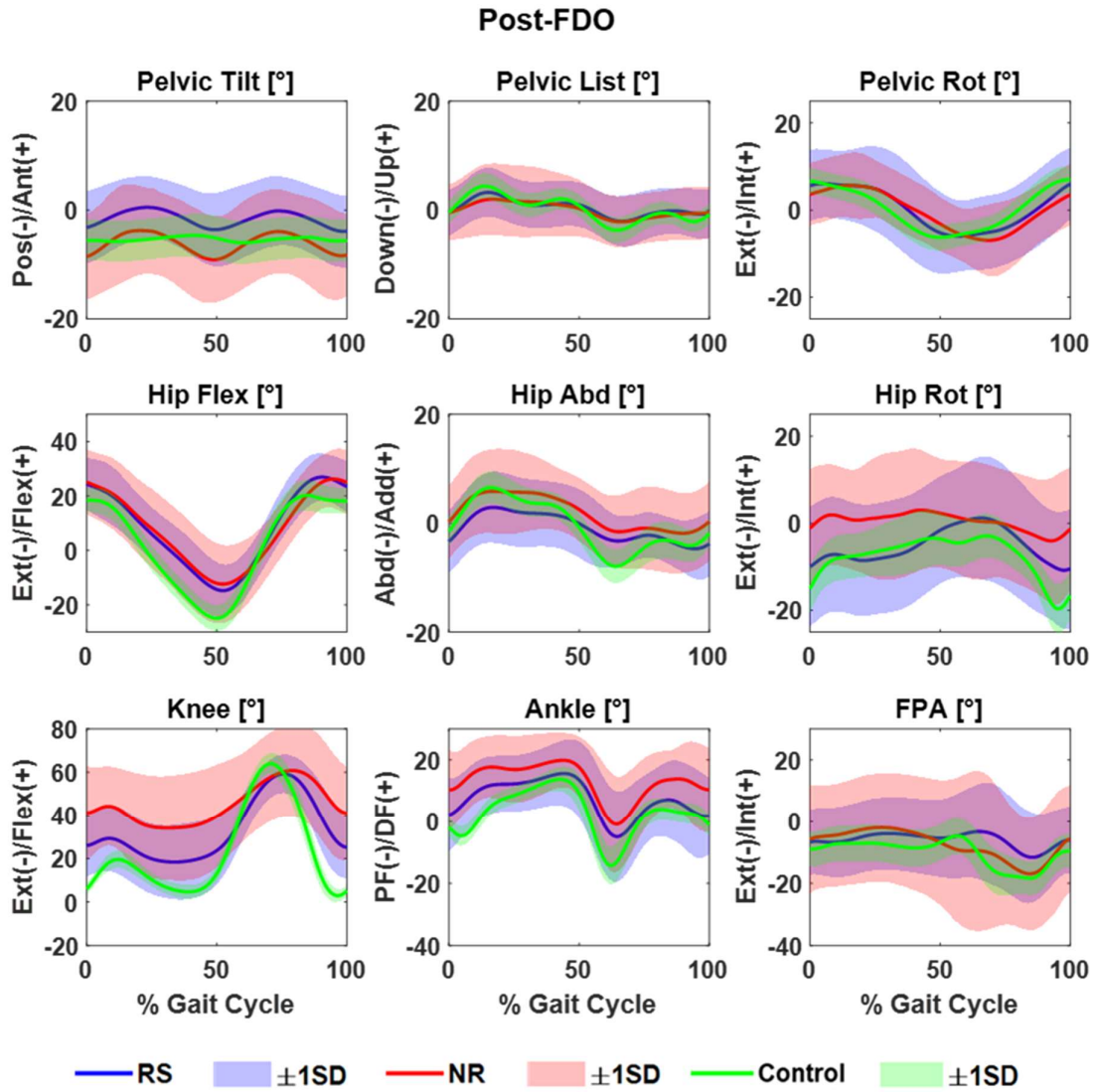


**Figure A2.2** Joint kinematic profiles for responders (RS, blue) and non-responders (NR, red) after FDO-SEMLS compared with healthy controls (green). FPA is foot progression angle

**Table A2.1 Summary of surgeries included as part of SEMLS**

No. of limbs	Concomitant Surgeries
43	FDO
16	Adductor release/lengthening
12	Hamstring lengthening
4	Psoas release/lengthening
13	Gastrocnemius release/lengthening
4	Rectus transfer
2	Patella tendon advancement
1	Tibial osteotomy
3	Tibialis anterior release/transfer
3	Tibialis posterior release/transfer
2	Peroneus transfer

## APPENDIX 3 - CHAPTER 6 SUPPLEMENTAL MATERIAL

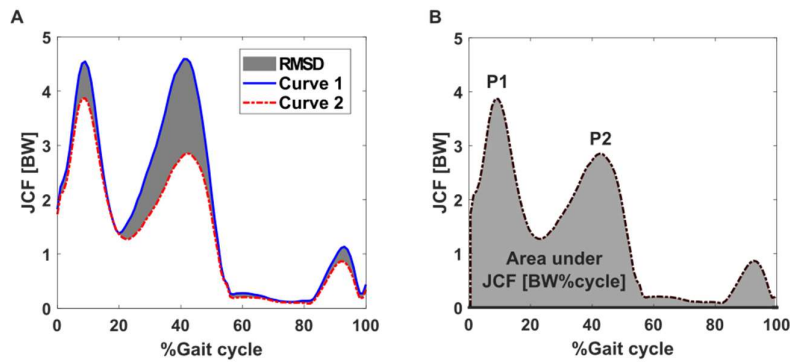


**Figure A3.1** Different indices for the description and analysis of the simulation results.  
**A:** Goodness of fit was assessed with the RMSD. **B:** Joint loading during the loading response (P1) and push off (P2) phases were analysed using the peak values and overall joint loading by the area under JCF/BW curve

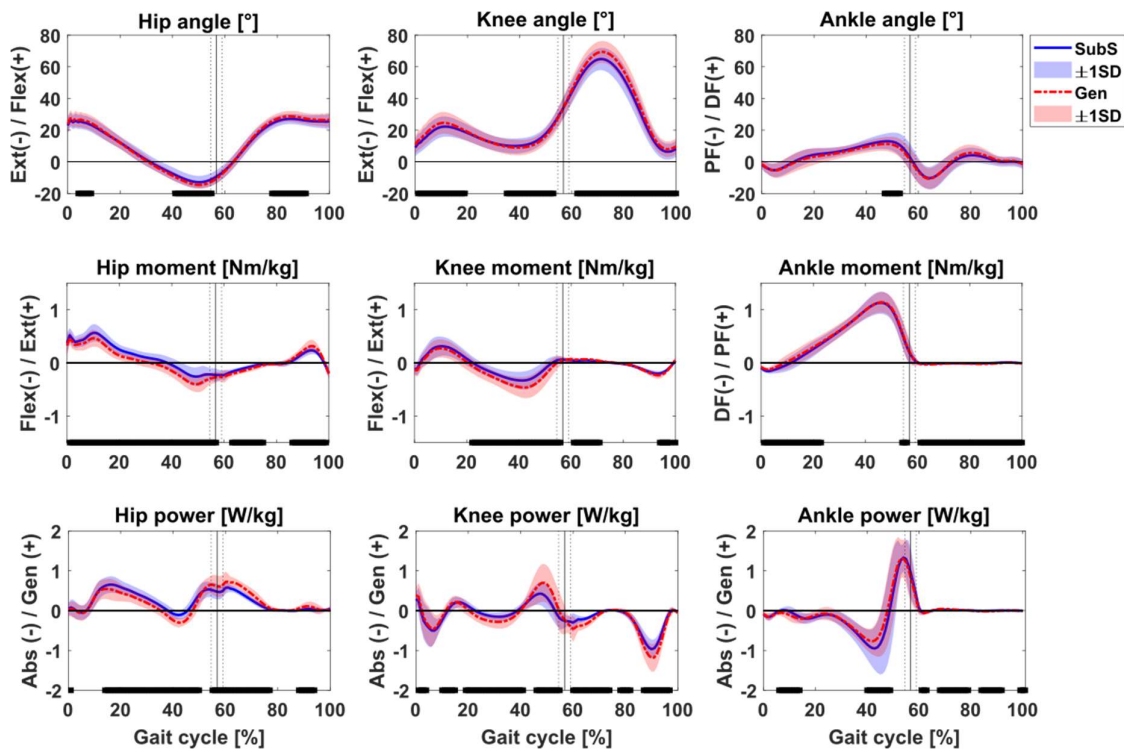


**Figure A3.2** Comparison between Gen (red) and SubS (blue) model estimations of sagittal plane joint angles, moments and powers at all observations for 11 juvenile participants. Joint moments and powers normalised by body mass. Black bars indicate significance at  $P < 0.05$  according to the non-parametric one-sample paired t-test.

**Extension/Flexion (Ext/Flex), Plantarflexion/Dorsiflexion (PF/DF) and  
Absorption/Generation (Abs/Gen).**

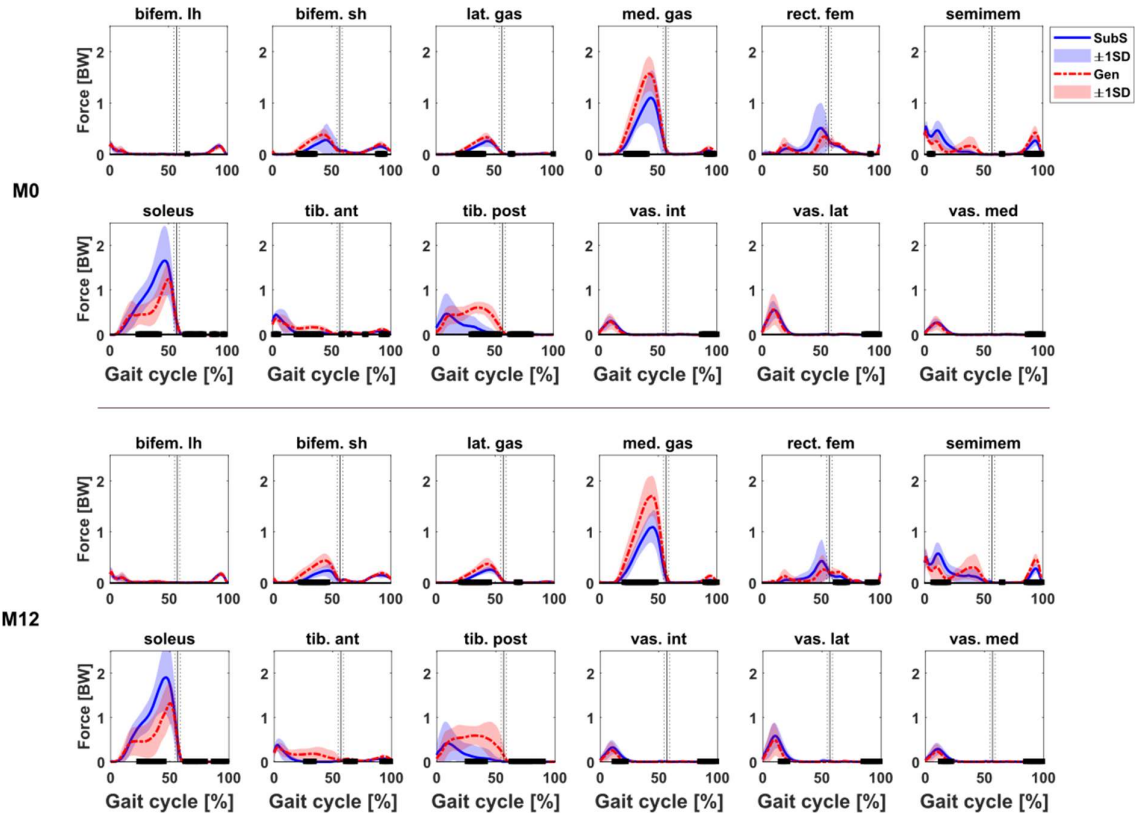


**Figure A3.3. Muscle forces estimated by the Gen (red) and SubS (blue) models for 12 selected muscles at M0 and M12. Black bars indicate statistical significance at  $P < 0.05$  between models. Selected muscles are biceps femoris long head, biceps femoris short head, gastrocnemius lateralis, gastrocnemius medialis, rectus femoris, semimembranosus, soleus, tibialis anterior, tibialis posterior, vastus intermedius, vastus lateralis and vastus medialis.**

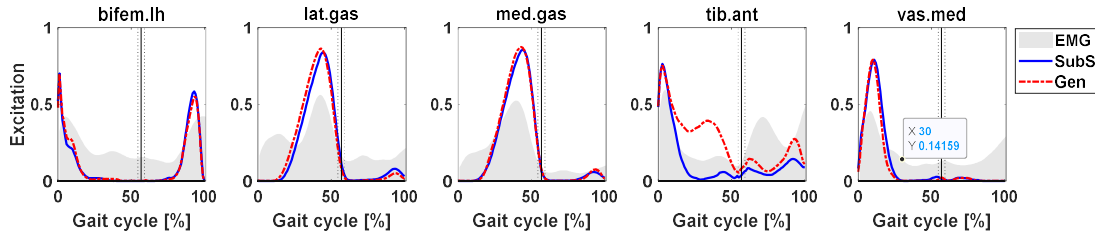


**Figure A3.4. Qualitative comparison of predicted muscle excitations from SubS and Gen to average EMG for each of five muscles at M0 showing timings of muscle activity during the gait cycle. EMG and activations were normalised to maximum over all trials for each participant.**

**Table A3.1. p-values for Wilcoxon sign ranked test between M0 and M12 for  $\Delta_m$ (RMSD)**

	Hip	Knee	Ankle
p-value	0.929	0.285	0.959
Effect size (Cohen's d)	0.069	-0.037	-0.302

**Table A3.2. p-values for Wilcoxon sign ranked test between Gen and SubS for  $\Delta_t$ (RMSD)**

	Hip	Knee	Ankle
p-value	0.965	0.779	0.859
Effect size (Cohen's d)	-0.043	-0.156	0.092

**Table A3.3. p-values for Wilcoxon sign ranked test between Gen and SubS estimates of AUC(JCF)**

	M0			M12		
	Hip	Knee	Ankle	Hip	Knee	Ankle
p-value	0.286	0.050	0.182	0.424	0.050	0.091
Effect size (Cohen's d)	-0.320	0.454	0.541	-0.072	1.009	0.648

## Appendix 4 - Chapter 7 supplemental material

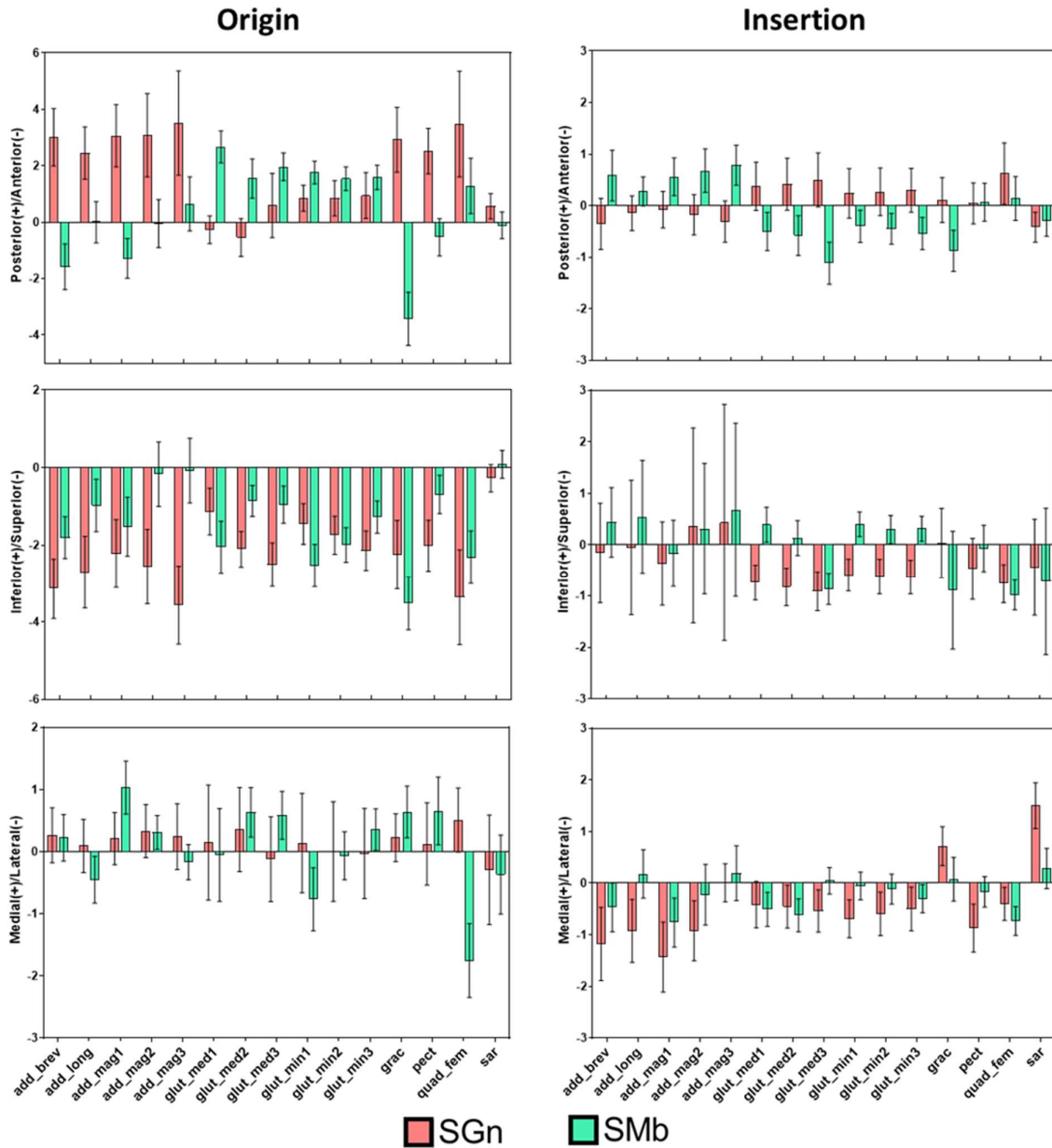


**Figure A4.1** Differences in muscle point location (origin and insertion) in anterior-posterior, superior-inferior and medial-lateral directions for SGn and SMb with respect to MRb models.

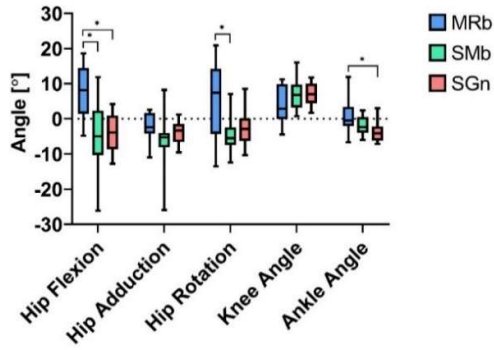


**Figure A4.2** Joint angles estimated by models in the static pose. \* indicates statistically significant difference

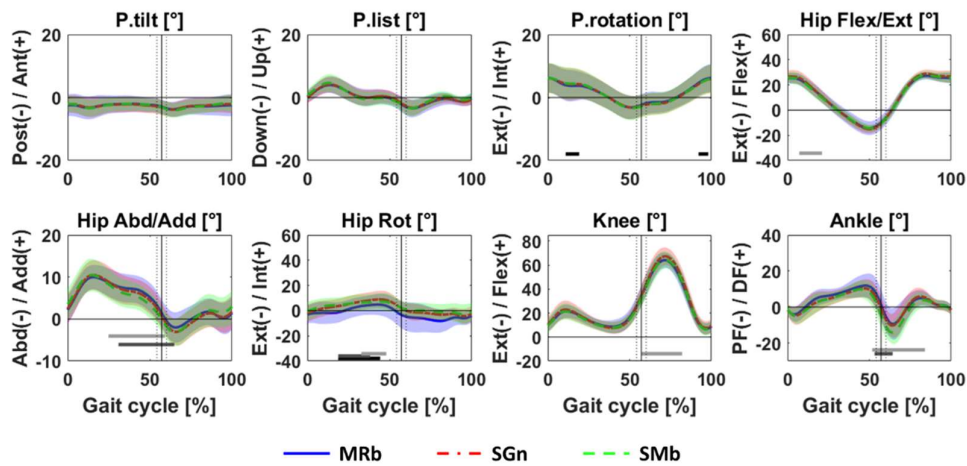


**Figure A4.3** Joint angles estimated by three models presented as group mean values. Coloured bands are  $\pm 1SD$ . Dark horizontal lines are significant differences between models: MRb/SGn (black), MRb/SMb (grey) and SGn/SMb (light grey)

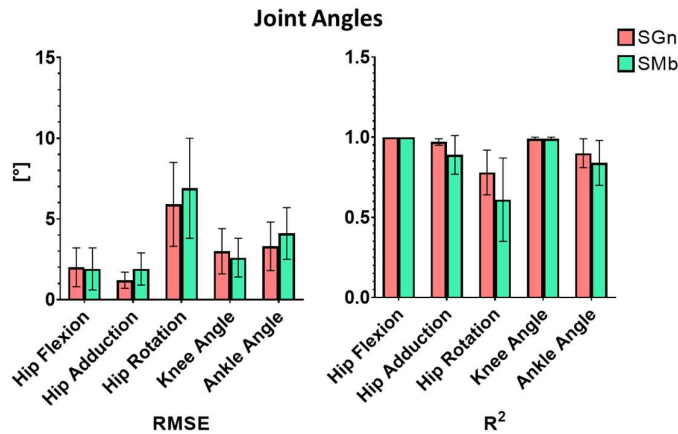


**Figure A4.4** Differences in joint angle estimates for SGn and SMb with respect to the MRb

**Table A4.1 Average (standard deviation) differences between MRb and SGn/SMb in muscle-tendon point locations and MTL**

Muscle	Differences in muscle point location (cm)				Difference in MTL <sub>max</sub>		RMS difference in MTL		No. of muscle points		
	Origin		Insertion		SGn	SMb	SGn	SMb	MRb	SMb	SGn
	SGn	SMb	SGn	SMb							
add_brev	4.50 (0.75)	2.53 (0.71)	1.65 (0.65)	1.09 (0.63)	-0.02 (0.03)	-0.06 (0.09)	0.06 (0.02)	0.09 (0.07)	2	2	2
add_long	3.84 (0.60)	1.45 (0.40)	1.56 (0.70)	0.92 (1.00)	-0.04 (0.02)	-0.06 (0.06)	0.05 (0.01)	0.06 (0.06)	2	2	2
add_mag1	3.95 (0.91)	2.39 (0.68)	1.76 (0.49)	1.12 (0.62)	-0.02 (0.04)	-0.04 (0.10)	0.05 (0.02)	0.10 (0.06)	2	2	2
add_mag2	4.26 (1.13)	1.18 (0.38)	1.90 (1.14)	1.29 (0.98)	0.00 (0.03)	-0.01 (0.06)	0.02 (0.01)	0.05 (0.04)	2	2	2
add_mag3	5.25 (1.43)	1.34 (0.51)	1.82 (1.53)	1.40 (1.53)	0.01 (0.02)	0.02 (0.03)	0.02 (0.01)	0.02 (0.01)	2	2	2
bifemlh	5.00 (1.71)	1.09 (0.52)	1.03 (0.33)	2.30 (0.43)	0.01 (0.01)	0.02 (0.02)	0.01 (0.01)	0.03 (0.01)	3	3	3
gem	4.55 (1.70)	3.50 (1.16)	1.17 (0.70)	1.30 (0.45)	0.05 (0.09)	0.02 (0.07)	0.07 (0.05)	0.07 (0.03)	2	2	2
glut_max1	2.92 (0.60)	2.99 (0.65)	1.38 (0.52)	0.96 (0.45)	0.05 (0.03)	0.02 (0.05)	0.06 (0.02)	0.06 (0.04)	4	4	4
glut_max2	3.02 (0.82)	1.46 (0.51)	1.43 (0.50)	0.81 (0.51)	0.06 (0.02)	0.02 (0.06)	0.06 (0.02)	0.07 (0.04)	4	4	4
glut_max3	4.44 (0.76)	1.03 (0.39)	1.54 (0.60)	4.15 (0.95)	0.07 (0.03)	0.01 (0.07)	0.06 (0.02)	0.06 (0.03)	4	4	4
glut_med1	1.53 (0.69)	3.45 (0.73)	1.10 (0.45)	0.93 (0.35)	-0.01 (0.04)	0.03 (0.04)	0.04 (0.01)	0.05 (0.05)	2	2	2
glut_med2	2.40 (0.43)	2.03 (0.42)	1.16 (0.47)	0.98 (0.32)	0.02 (0.03)	0.06 (0.03)	0.05 (0.02)	0.07 (0.04)	2	2	2
glut_med3	2.84 (0.74)	2.35 (0.43)	1.32 (0.48)	1.47 (0.37)	0.04 (0.03)	0.11 (0.03)	0.06 (0.02)	0.09 (0.03)	2	2	2
glut_min1	1.89 (0.60)	3.23 (0.59)	1.09 (0.38)	0.70 (0.23)	-0.02 (0.04)	0.02 (0.04)	0.04 (0.01)	0.05 (0.04)	3	2	2
glut_min2	2.15 (0.61)	2.58 (0.47)	1.06 (0.41)	0.68 (0.24)	0.00 (0.03)	0.04 (0.04)	0.04 (0.01)	0.05 (0.04)	2	2	2
glut_min3	2.53 (0.66)	2.14 (0.40)	1.01 (0.42)	0.79 (0.26)	0.02 (0.03)	0.06 (0.03)	0.04 (0.02)	0.06 (0.04)	2	2	2
grac	3.87 (0.96)	5.01 (0.92)	1.05 (0.39)	1.56 (0.87)	-0.01 (0.01)	-0.02 (0.04)	0.01 (0.00)	0.04 (0.02)	4	4	4
iliacus	1.88 (0.57)	1.68 (0.65)	1.04 (0.64)	1.06 (0.26)	-0.04 (0.01)	-0.05 (0.04)	0.03 (0.01)	0.04 (0.03)	5	4	5
pect	3.39 (0.66)	1.37 (0.49)	1.23 (0.38)	0.55 (0.34)	-0.05 (0.03)	-0.07 (0.07)	0.07 (0.02)	0.08 (0.08)	2	2	2
peri	3.56 (0.57)	1.83 (0.40)	1.10 (0.54)	1.39 (0.45)	0.04 (0.04)	0.07 (0.04)	0.04 (0.03)	0.05 (0.03)	3	3	3
psoas	3.29 (1.27)	2.87 (1.19)	0.96 (0.60)	0.91 (0.26)	-0.03 (0.01)	-0.05 (0.03)	0.03 (0.01)	0.04 (0.03)	5	4	5
quad_fem	5.11 (1.60)	3.33 (0.82)	1.23 (0.43)	1.32 (0.30)	0.03 (0.11)	-0.03 (0.17)	0.08 (0.06)	0.13 (0.09)	2	2	2
rect_fem	1.92 (0.70)	0.73 (0.34)	1.23 (0.45)	3.62 (1.08)	0.00 (0.01)	0.06 (0.01)	0.01 (0.00)	0.03 (0.01)	2	3	3



sar	1.05 (0.64)	0.83 (0.41)	1.86 (0.50)	1.26 (1.13)	-0.02 (0.00)	0.00 (0.00)	0.02 (0.00)	0.02 (0.01)	5	5	5
semimem	4.79 (1.59)	1.57 (0.66)	1.09 (0.53)	2.53 (0.72)	0.01 (0.01)	0.01 (0.03)	0.02 (0.01)	0.02 (0.01)	3	3	3
semiten	5.12 (1.72)	2.07 (0.79)	0.95 (0.36)	1.70 (0.77)	0.01 (0.01)	0.02 (0.02)	0.02 (0.01)	0.03 (0.02)	5	5	5
tfl	1.44 (0.57)	1.46 (0.83)	1.68 (0.47)	2.44 (0.61)	-0.01 (0.01)	0.00 (0.01)	0.01 (0.01)	0.02 (0.01)	5	4	4
bifemsh	1.31 (0.69)	1.22 (0.77)	1.02 (0.33)	2.30 (0.44)	0.00 (0.01)	0.00 (0.01)	0.02 (0.01)	0.06 (0.01)	3	3	3
lat_gas	2.05 (1.43)	1.76 (1.44)	3.23 (0.59)	3.11 (0.88)	0.00 (0.01)	0.00 (0.01)	0.01 (0.00)	0.01 (0.00)	5	3	3
med_gas	2.00 (1.32)	1.36 (1.56)	3.60 (0.45)	3.46 (0.83)	0.00 (0.01)	0.00 (0.01)	0.01 (0.00)	0.01 (0.00)	5	3	3
vas_int	1.41 (0.71)	1.10 (0.58)	0.96 (0.40)	3.28 (1.13)	0.04 (0.03)	0.24 (0.04)	0.03 (0.01)	0.11 (0.02)	3	4	4
vas_lat	1.24 (0.67)	2.80 (0.51)	1.02 (0.45)	3.65 (1.04)	0.03 (0.03)	0.18 (0.03)	0.02 (0.01)	0.08 (0.02)	3	5	5
vas_med	1.56 (0.68)	1.31 (0.89)	1.65 (0.48)	3.72 (1.06)	0.05 (0.02)	0.24 (0.05)	0.03 (0.01)	0.11 (0.02)	3	5	5
ext_dig	1.93 (0.38)	5.83 (1.41)	1.30 (0.68)	1.69 (0.73)	0.01 (0.01)	0.01 (0.01)	0.01 (0.00)	0.01 (0.00)	8	6	6
ext_hal	1.85 (0.42)	7.54 (1.41)	1.43 (0.83)	1.39 (0.74)	0.00 (0.01)	0.00 (0.01)	0.01 (0.00)	0.01 (0.00)	9	7	7
flex_dig	0.98 (0.55)	2.07 (0.82)	1.38 (0.68)	1.83 (0.76)	0.00 (0.01)	0.00 (0.01)	0.01 (0.01)	0.01 (0.00)	9	8	8
flex_hal	1.58 (0.57)	15.82 (2.12)	1.69 (0.90)	1.67 (0.76)	0.00 (0.01)	-0.01 (0.01)	0.01 (0.00)	0.01 (0.01)	9	7	7
per_brev	2.00 (0.74)	10.75 (1.89)	3.81 (0.56)	4.02 (0.63)	0.02 (0.02)	0.03 (0.02)	0.03 (0.01)	0.03 (0.01)	6	5	5
per_long	2.01 (0.45)	7.02 (1.59)	1.35 (0.57)	1.79 (0.84)	0.02 (0.01)	0.02 (0.01)	0.02 (0.01)	0.02 (0.01)	8	7	7
soleus	0.73 (0.43)	3.57 (1.19)	3.41 (0.53)	3.28 (0.84)	0.00 (0.01)	0.01 (0.01)	0.01 (0.01)	0.01 (0.01)	3	2	2
tib_ant	1.21 (0.50)	3.15 (1.27)	1.91 (0.61)	2.38 (0.81)	-0.01 (0.02)	-0.01 (0.02)	0.02 (0.01)	0.02 (0.01)	6	3	3
tib_post	0.85 (0.40)	3.19 (0.59)	1.49 (0.63)	1.67 (0.82)	-0.01 (0.01)	-0.01 (0.01)	0.02 (0.01)	0.02 (0.01)	5	4	4

**Table A4.2 RMS differences in MAL for SGn and MRb with respect to MRb**

Muscle	RMS difference in MALs with respect to MRb for all muscles (cm)									
	Hip Flexion		Hip Adduction		Hip Rotation		Knee Flexion		Ankle Flexion	
	SGn	SMB	SGn	SMB	SGn	SMB	SGn	SMB	SGn	SMB
add_brev	0.77	2.11	1.01	1.02	0.25	0.22				
add_long	0.53	0.73	0.80	0.79	0.15	0.14				
add_mag1	0.57	2.34	0.58	0.66	0.26	0.18				
add_mag2	0.63	1.59	0.56	0.96	0.15	0.17				
add_mag3	0.78	1.14	0.52	0.72	0.09	0.13				
bifemlh	0.76	1.01	0.37	1.14	0.11	0.42	0.96	1.99		
gem	0.56	0.78	0.70	0.87	0.48	0.72				
glut_max1	0.52	1.46	0.65	2.47	0.64	1.36				
glut_max2	0.49	1.43	0.52	1.62	0.55	1.05				
glut_max3	0.85	2.83	0.76	2.76	0.73	1.07				
glut_med1	0.62	0.75	0.53	0.80	0.83	1.71				
glut_med2	0.63	0.48	0.51	0.49	0.46	1.25				
glut_med3	0.58	0.99	0.63	0.46	0.38	0.79				
glut_min1	0.55	0.57	0.43	0.80	0.65	1.42				
glut_min2	0.50	0.48	0.44	0.55	0.52	1.21				
glut_min3	0.47	0.41	0.47	0.43	0.35	1.12				
grac	0.46	4.56	0.57	0.76	0.15	0.66	0.51	1.53		
iliacus	0.54	1.68	0.66	0.79	0.31	0.32				
pect	0.51	0.52	0.67	0.58	0.14	0.14				
peri	0.51	0.59	0.41	0.85	0.45	0.55				
psoas	0.37	0.70	0.51	1.00	0.23	0.25				
quad_fem	0.72	1.03	0.88	1.22	0.69	0.47				
rect_fem	0.65	0.77	0.30	0.56	0.06	0.08	0.64	2.67		

sar	0.95	1.13	0.86	0.86	0.17	0.25	0.78	0.98		
semimem	0.71	0.74	0.41	0.46	0.08	0.21	0.55	0.79		
semiten	0.76	0.81	0.43	0.46	0.13	0.38	0.75	2.29		
tfl	0.76	1.27	0.63	1.18	0.54	1.16	0.55	1.42		
bifemsh							1.03	2.24		
lat_gas							0.68	0.64	0.43	0.47
med_gas							0.65	0.54	0.41	0.49
vas_int							0.79	2.84		
vas_lat							0.72	2.09		
vas_med							0.86	2.73		
ext_dig									0.34	0.33
ext_hal									0.46	0.83
flex_dig									0.32	0.31
flex_hal									0.50	0.67
per_brev									0.82	0.91
per_long									0.68	0.69
soleus									0.36	0.37
tib_ant									0.44	0.45
tib_post									1.01	1.04

**Table A4.3 Effect size estimates indicating the level of agreement between MRb, SGn and SMB models for the average MAL and MTL<sub>max</sub>**

Muscle	Average MAL		MTL <sub>max</sub>	
	p-value	Kendall's W	p-value	Kendall's W
add_brev	<0.001	0.55	0.018	0.308
add_long	0.008	0.373	<0.001	0.538
add_mag1	0.052	0.228	0.092	0.183
add_mag2	0.002	0.467	0.584	0.041
add_mag3	0.199	0.124	0.146	0.148
glut_med1	0.008	0.373	0.023	0.29
glut_med2	0.05	0.231	<0.001	0.609
glut_med3	<0.001	0.763	<0.001	0.929
glut_min1	<0.001	0.538	0.012	0.337
glut_min2	0.005	0.412	0.003	0.45
glut_min3	<0.001	0.645	<0.001	0.574
grac	<0.001	0.55	0.116	0.166
pect	0.025	0.285	<0.001	0.639
quad_fem	<0.001	0.787	0.232	0.112
sar	<0.001	0.609	<0.001	0.751